

**Revisiting Self-cycling Fermentation – New Characterization, Scheme, and
Application**

by

Yusheng Tan

A thesis submitted in partial fulfillment of the requirement of the degree of

Doctor of Philosophy

in

Chemical Engineering

Department of Chemical and Materials Engineering

University of Alberta

© Yusheng Tan, 2022

Abstract

Self-cycling fermentation (SCF) is an advanced, automated, semi-continuous fermentation strategy that is used to improve the volumetric productivity of bioproduction. Typically, a microbial culture is grown in a reactor and half the reactor contents are harvested once a limiting nutrient is depleted; the reactor is then replenished with the same amount of fresh medium, initiating a new cycle. Nutrient depletion is sensed by control parameters, such as dissolved oxygen and carbon dioxide evolution rate. Thereby, cycling is not dictated by a pre-set cycle time but rather by cell growth itself – hence the name “self-cycling” fermentation. A direct result of implementing this feedback control system is great stability, even when encountering perturbations and nutrient heterogeneity. In addition, by eliminating the lag and stationary phases, SCF presents greatly improved productivity compared to conventional batch reactor (BR) operation. Due to the nutrient cycle, synchrony is observed in many SCF studies, a characteristic feature of SCF.

In this work, the feasibility and impact of SCF operation was investigated for one yeast and two bacteria: *Saccharomyces cerevisiae*, *Escherichia coli*, and *Methylovium burlingii* 5GB1C.

In the first study, the effects of SCF operation on *S. cerevisiae* engineered to overproduce shikimic acid – a valuable compound that can be used as precursor to many aromatic compounds – were assessed. Yield, volumetric productivity, and specific productivity of shikimic acid were all found to be greatly improved compared to BR operation (4-fold, 4-fold, and 3-fold greater, respectively). Global gene regulation patterns, elucidated through transcriptomic analysis,

provided insights into the regulatory mechanisms leading to these significant improvements. They also led to the first demonstration of synchrony in SCF from a gene regulation perspective.

In the second study, SCF long and short cycle schemes implemented for *Escherichia coli* and *Saccharomyces cerevisiae* cultures were investigated to uncover patterns in glucose consumption, carbon dioxide evolution rate, and cell replication during SCF operation. SCF Short cycles significantly improved biomass productivity compared to long cycles and helped identified the relation between doubling time and SCF cycle time. Stemming from these results and previous SCF articles, three trends in the co-occurrence of characteristic events during SCF cycles were identified and summarized: 1) three key events of SCF (i.e., the depletion of a plateau of the limiting nutrient, the completion of synchronized cell replication, and characteristic points of control parameters) occur concomitantly; 2) cell replication ends prior to the concurrence of the other two events; and 3) the limiting nutrient is depleted or reaches a plateau later than the joint occurrence of the other two events. This work uncovers the potential of SCF as a research tool to explore microbial physiological properties (e.g., nutrient uptake, proliferation, and respiration intensity) and highlights the enhanced performance of the short cycle scheme. Moreover, a novel description of SCF was established thoroughly, together with the revealed key trends providing a solid framework for further SCF development and applications.

In the third study, SCF and fed-batch strategies were successfully implemented to cultivate *Methylovium buriatense* 5GB1C, a methanotrophic bacterium, using methanol as the carbon source. A new control parameter, culture reflectance, was used to establish stable SCF operation, leading to a 3-fold or 10-fold increase in volumetric biomass productivity (depending on the SCF scheme implemented) as compared to BR. On the other hand, the fed-batch operation,

when compared to BR, resulted in a 26-fold improvement in biomass density. These results provide an important initiative for exploring methanotroph-mediated methanol bioconversion.

Overall, the present work broadens our understanding of SCF operation, its properties, and its effects on cells. In terms of novelty, these works include: 1) the first characterization of SCF at a transcriptomic level; 2) the first study distinguishing the impacts of short and long SCF cycle schemes on cell cultures; 3) the first in-depth survey of SCF characteristic events and corresponding trends; 4) a new definition of SCF; 5) the first study that incorporated culture reflectance as control parameter leading to stable SCF operation; and 6) the implementation of fed-batch and SCF schemes in cultures of methanotrophic bacteria using methanol as carbon source. These advances in knowledge will help researchers and bioprocessing engineers adopt and adapt this advanced semi-continuous operation.

Preface

Part of this thesis has been submitted for publication, and other chapters will soon be submitted for publication. Additional acknowledgments can be found at the end of each chapter.

Chapter 3 will be submitted for publication as Tan, Y., Stein, L. Y., Sauvageau, D. “An Overview of Yeast Cell Synchronization”. As the primary author, I was responsible for conceptualization, literature review, summary and comparison, and original draft writing. Dr. Lisa Stein contributed to funding acquisition, supervision, and manuscript editing. Dr. Dominic Sauvageau (supervisor) contributed to all stages from conceptualization, funding acquisition, supervision, project administration, and manuscript review and editing.

Chapter 4 has been published as Tan, Y., Agustin, R. V. C., Stein, L. Y., Sauvageau, D. “Transcriptomic Analysis of Synchrony and Productivity in Self-cycling Fermentation of Engineered Yeast Producing Shikimic Acid” on Biotechnology Reports (2021), e00691, DOI: 10.1016/j.btre.2021.e00691. As the primary author, I was responsible for the conceptualization, experimental design and operation (SCF operation and Transcriptomics), data collection, analysis, interpretation, and visualization (SCF operation and Transcriptomics), and original draft writing. Roman Vincent C. Agustin contributed to experimental design and operation (SCF operation and shikimic acid analysis), data collection, analysis, and visualization (SCF operation and shikimic acid analysis), and manuscript editing. This part of Roman Vincent C. Agustin’s work is also included in his M.Sc. thesis (2015, University of Alberta). Dr. Lisa Stein contributed to funding acquisition, supervision, project administration, and manuscript editing. Dr. Dominic Sauvageau (supervisor) contributed to all stages from conceptualization, funding acquisition, supervision, project administration, and manuscript review and editing.

Chapter 5 will be submitted for publication as Tan, Y., Stein, L. Y., Sauvageau, D. “The Influence of Long and Short Cycle Schemes of Self-cycling Fermentation on the Growth of *E. coli* and *S. cerevisiae*” (a preprint available with DOI:10.21203/rs.3.rs-1139754/v1). As the primary author, I was responsible for conceptualization, experimental design and operation, data collection and analysis, data interpretation, visualization of results, literature review, and original draft writing. Dr. Lisa Stein contributed to funding acquisition, supervision, data interpretation, and

manuscript editing. Dr. Dominic Sauvageau (supervisor) contributed to all stages from conceptualization, funding acquisition, supervision, project administration, design of experiment, data interpretation, and manuscript review and editing.

Chapter 6 will be submitted for publication as Tan, Y., Stein, L. Y., Sauvageau, D. “Methanol Bioconversion in *Methyloviumicrobium buryatense* 5GB1C through Self-cycling Fermentation”. As the primary author, I was responsible for conceptualization, experimental design and operation, data collection and analysis, visualization of results, and original draft writing. Dr. Lisa Stein contributed to conceptualization, supervision, project administration, improvement in design of experiment, and manuscript editing. Dr. Dominic Sauvageau (supervisor) contributed to all stages from conceptualization, funding acquisition, supervision, project administration, improvement in design of experiment, and manuscript review and editing.

Acknowledgments

Many thanks to my supervisor Dr. Dominic Sauvageau. I am always grateful for your accepting me into the group, especially when the previously proposed supervisor left the university unpredictably. I was lucky to be able to start my doctoral study in this interdisciplinary field that applies both chemical engineering and microbiology under your supervision. You always give brilliant and constructive advice, from which I have learned very much. For instance, it is so important to make progress “step by step”, which is just wisdom that allows for patience, confidence, and resilience. You always supportively point out the future directions, favorably provide encouragement, and mindfully maintain a supportive group working environment. You commented that I could become a professor in the future even though I saw little possibility given such competitive academia currently. You are generally such a great model as an enthusiastic scientific research leader who is constantly eager to learn more, understand more, and explore more.

Many thanks to Dr. Lisa Y. Stein. Such many pieces of priceless advice and help you have given me, though you do not officially supervise me on the paperwork. As both groups are profoundly collaborating, I enjoy working with people from both sides very much. More importantly, you show me how enthusiastic a talented scientist would be, how helpful, patient, and friendly a supervisor could be, and how proud a mom can be.

Many thanks to Dr. Natalia Semagina. It has been a real privilege to have you as a supervisory committee member throughout my study. Not only did I receive your precious instructions during supervisory meetings and the Heterogeneous Catalysis course, but also be touched and motivated by your passion for teaching and mentoring and your care for the students.

To all the professors and instructors who instructed the valuable courses taken by me during the study, Dr. David Bressler, Dr. Paul Stothard and Dr. Kirill Krivushin, Dr. Hasan Uludag, Dr. Michael Ellison, Dr. Natalia Semagina, Dr. Ravin Narain, and Dr. Dominic Sauvageau, I cannot thank you more for your carefully designed and very well-delivered courses. I am so appreciative that I was able to know you and some of your work, assimilate numerous trunks of knowledge related to a variety of advanced topics, and foster relative skills that benefited my own

research projects. Also, I would like to thank the department technicians, Les Dean and Walter Boddez, for helping with my experimental equipment. I appreciate your contributions.

The collaborative working environment of our research group has been significantly supportive during the work and study. I would like to thank folks in our group, Melissa Harrison, Ana Arvizu, Mark Lawley, Diana Martinez Tobon, Miranda Stahn, Aurelija Grigonyte, Beatriz Iara Cabral E Pacheco, Kieran McDonald, Fatemeh Bakhtiari Ziabari, Catherine Tays, and summer/coop students, Ethan Agena and David Boon, who helped and supported me a lot during the study. Also, I want to thank people in the collaborated groups, Dr. Anastasia Elias, Sim Yee Chen, Phillip Sun, Mariah Hermary, Peyman Derik Vand, Cerrise Weiblen, Sujani Gomes, Marc Waddingham, Hem Sharma, Marina Lazic, Shibashis Das, Yueh-Hao Hung, Jie Wang, and Yadong Fan. I really appreciate the help and suggestions ever from you. It was totally a privilege to have been working alongside each of you.

As an international student, the journey here at UofA frequently leads me to contemplate the consensuses and differences between the east and west based on plenty of perspectives. For instance, I have been intensively thinking about the cultural differences and both achievements in social sciences and natural sciences. These are important and substantially beneficial to the development of my worldview and values. I thank my home country and Tianjin University, who had empowered me to build a relatively solid academic background. Also, in specific, I would love to thank my family, especially my mom and dad. Your selfless care and concern support me all the way. I am so thankful for you. As both of you are retiring from the contributive electrical engineering positions, I hope you enjoy your wonderful post-retirement life. Also, I thank all my friends here in Canada or back in China. I cannot imagine life without your company, either in person or remotely.

Moreover, I would like to thank Dr. Wendy Shen, who opened the door for my studying abroad when I was about to complete the M.Sc. program, even though we, unfortunately, have not been able to really work together.

Finally, I would acknowledge our funding sponsors Natural Sciences and Engineering Research Council of Canada (NSERC) Discovery Grant and CGS-M programs, the Canada First Research Excellence Fund – Future Energy Systems, the Canada Foundation for Innovation – John R. Evans Leaders Fund, the Government of Alberta – Ministry of Economic Development and

Trade Small Equipment Grant, the Climate Change Innovation and Technology Framework (CCITF) – Clean Technology Development (CTD) program, and the University of Alberta Faculty of Engineering. Thank you for making the present work possible.

Table of Contents

1. Introduction.....	1
1.1 Motivation and context.....	1
1.2 Scope of this thesis	3
1.3 Thesis structure.....	3
1.4 References	4
2. Literature Review	8
2.1 Self-cycling fermentation	8
2.1.1 Continuous phasing and SCF.....	9
2.1.2 SCF applications	10
2.1.3 SCF properties	12
2.1.4 SCF hardware configuration	14
2.2 Transcriptomic Analysis.....	15
2.2.1 RNA-Seq.....	16
2.2.2 qPCR.....	20
2.3 <i>Saccharomyces cerevisiae</i>	25
2.3.1 Life Cycle of <i>S. cerevisiae</i>	25
2.3.2 Cell Cycle of <i>S. cerevisiae</i>	26
2.3.3 <i>S. cerevisiae</i> Growth in Batch Reactors.....	28
2.4 Shikimic Acid.....	29
2.4.1 Yeast Producing Shikimic Acid.....	31
2.5 <i>Escherichia coli</i>	33
2.6 <i>Methylotuvimicrobium buryatense</i> 5GB1C	34
2.7 References	37
3. An Overview of Yeast Cell Synchronization	55
3.1 Abstract.....	55
3.2 Introduction	55
3.3 Methods to Assess Cell Synchrony	57
3.4 Methods for Cell Synchrony.....	59
3.4.1 Physical Selection	59

3.4.2 Physical Induction.....	62
3.4.3 Chemical Blockage.....	63
3.4.4 Nutrient Deprivation.....	64
3.4.5 Nutrient Cycle.....	65
3.5 Comparative Analysis.....	66
3.6 Conclusions	68
3.7 Acknowledgments	68
3.8 References	68
4. Transcriptomic Analysis of Synchrony and Productivity in Self-cycling Fermentation of Engineered Yeast Producing Shikimic Acid.....	76
4.1 Abstract.....	76
4.2 Introduction	76
4.3 Materials and Methods	79
4.3.1 Yeast Strain and Medium.....	79
4.3.2 Reactor Operation.....	80
4.3.3 Optical Density and Cell Count.....	81
4.3.4 Measurement of Shikimic Acid, Glucose, and Ethanol.....	82
4.3.5 Production Parameters	82
4.3.6 RNA-Seq Analysis.....	83
4.3.7 qPCR Analysis.....	84
4.4 Results	86
4.4.1 BR and SCF Operation.....	86
4.4.2 Cellular Regulation.....	90
4.5 Discussion.....	99
4.5.1 Impact of SCF Operation.....	99
4.5.2 Production of Shikimic Acid	101
4.6 Conclusions	107
4.7 Supplementary Materials.....	108
4.8 Acknowledgments	109
4.9 References	110
5. The Influence of Long and Short Cycle Schemes of Self-cycling Fermentation on the Growth of <i>E. coli</i> and <i>S. cerevisiae</i>.....	117
5.1 Abstract.....	117

5.2 Introduction	117
5.3 Materials and Methods	120
5.3.1 Strains, Media, and Pre-cultures	120
5.3.2 SCF Configuration and Operation	120
5.3.3 Batch Reactor Configuration and Operation.....	122
5.3.4 Measurement of Optical Density, Glucose, Ammonium, and Nitrate & Nitrite	122
5.3.5 Calculation of Yield and Productivity for Biomass Production	123
5.3.6 qPCR Experiments for <i>S. cerevisiae</i>	123
5.4 Results	125
5.4.1 <i>E. coli</i> grown in BR and SCF operation	125
5.4.2 <i>S. cerevisiae</i> grown in SCF operation.....	129
5.4.3 Relative expression levels of selected cyclin genes in <i>S. cerevisiae</i>	130
5.5 Discussion.....	133
5.5.1 <i>E. coli</i> BR Operation.....	133
5.5.2 SCF Long Cycle and Short Cycle Operation.....	133
5.5.3 An Overview of Characteristic Events in SCF	137
5.6 Conclusions	142
5.7 Supplementary Materials.....	143
5.8 Acknowledgements	143
5.9 References	144
6. Methanol Bioconversion in <i>Methylotheobacterium buryatense</i> 5GB1C through Self-cycling Fermentation.....	149
6.1 Abstract.....	149
6.2 Introduction	149
6.3 Methods and Materials	151
6.3.1 Strains and Media	151
6.3.2 Bioreactor operation.....	152
6.4 Results	154
6.4.1 Methanol Inhibition Assessment.....	154
6.4.2 Fed-batch Operation.....	155
6.4.3 First SCF Feeding Scheme.....	156
6.4.4 Second SCF Feeding Scheme	160

6.5 Discussion.....	162
6.6 Conclusions	166
6.7 Acknowledgement.....	166
6.8 References	167
7. Summary, Conclusion, and Future Directions.....	172
7.1 Summary and conclusion.....	172
7.2 Future directions	176
7.3 References	179
Unified Bibliography.....	182
Appendix A. Supplementary Materials for Chapter 4	209
A.1 Continued Discussion	209
A.2 References for Appendix A	233
Appendix B Supplementary Materials for Chapter 5.....	236

List of Figures

Figure 2.1 Schematic of the cycling sequence during SCF operation.	9
Figure 2.2 Schematic of continuous phased culture (continuous phasing)	10
Figure 2.3 Schematic of SCF configuration used for an investigation of bioproduction using an engineered yeast	15
Figure 2.4 Schematic of RNA-Seq experiments	17
Figure 2.5 Schematic of one-step and two-step RT-qPCR experiments.....	23
Figure 2.6 Schematic of the life cycle of <i>S. cerevisiae</i>	26
Figure 2.7 Schematic for the cell cycle of <i>S. cerevisiae</i>	27
Figure 2.8 The chemical structures of shikimic acid and Oseltamivir.....	30
Figure 2.9 Schematic of metabolic engineering of a <i>S. cerevisiae</i> strain to overproduce shikimic acid.	33
Figure 2.10 Central carbon metabolic pathways of <i>M. buryatense</i> 5GB1 grown on methanol ...	36
Figure 3.1 Schematic of experimental procedures of centrifugal elutriation.....	60
Figure 3.2 Schematic of a baby machine	61
Figure 4.1 Schematic of the SCF configuration.....	81
Figure 4.2 SCF operation of engineered <i>S. cerevisiae</i> for 25 cycles	87
Figure 4.3 Yield, productivity, and integrated specific productivity of shikimic acid during SCF operation.....	89
Figure 4.4 Relative expression levels ($\log_2(\text{FC})$) of genes related to DNA replication at different time points during BR and SCF cycle 23, with growth curves to show these time points.	92
Figure 4.5 Relative expression levels ($\log_2(\text{FC})$) of genes related to the cell cycle at different time points during BR and SCF cycle 23.....	93
Figure 4.6 Relative expression levels ($\log_2(\text{FC})$) of genes related to proteasome at different time points during BR and SCF cycle 23.....	94
Figure 4.7 Relative expression levels ($\log_2(\text{FC})$) of genes related to the citrate cycle at different time points during BR and SCF cycle 23.....	95
Figure 4.8 Relative expression levels ($\log_2(\text{FC})$) of genes related to oxidative phosphorylation at different time points during BR and SCF cycle 23.	96

Figure 4.9 Reactions and up-regulation of genes related to shikimic acid production in SCF operation.....	98
Figure 5.1 Growth of <i>E. coli</i> MG1655 in extended batch operation.....	127
Figure 5.2 <i>E. coli</i> grown in SCF long cycle and short cycle schemes.	128
Figure 5.3 <i>S. cerevisiae</i> grown in SCF long and short cycle strategies.	131
Figure 5.4 Relative expression levels of selected <i>S. cerevisiae</i> cyclin genes	132
Figure 5.5 Schematic of the conceptual trends in characteristic events during SCF.	139
Figure 6.1 Simplified schematic of the bioreactor system incorporating a reflectance sensor for monitoring	153
Figure 6.2 Optical density during fed-batch operation of <i>M. buryatense</i> 5GB1C growing on methanol.....	156
Figure 6.3 Monitored parameters during SCF operation of <i>M. buryatense</i> 5GB1C grown on methanol using the first feeding scheme.	158
Figure 6.4 Intracycle cell count, OD ₆₀₀ , reflectance, and CER in SCF cycles 32 (A) and 40 (B) during SCF operation of <i>M. buryatense</i> 5GB1C growing on methanol using the first feeding scheme.....	159
Figure 6.5 Monitored parameters during SCF operation of <i>M. buryatense</i> 5GB1C grown on methanol using the second feeding scheme.	161
Figure 6.6 Intracycle cell count, OD ₆₀₀ , reflectance, and CER in cycle 16 during SCF operation of <i>M. buryatense</i> 5GB1C growing on methanol using the second feeding scheme.....	162
Figure A1 Relative expression levels (fold changes) of selected cyclin genes during SCF cycles 21 and 23.	214
Figure A2 Relative expression levels (fold changes) for <i>CLB1</i> , <i>CLB3</i> , and <i>CLN1</i> during BR late-log phase and diauxic shift.....	215
Figure A3 Glucose and ethanol concentration during SCF cycle 21	216
Figure A4 Intra-cycle normalized cell density during SCF cycles 11 (A) and 21 (B).....	217
Figure A5 Total RNA concentration (after extraction) during SCF cycle 21	218
Figure A6 Relative expression levels (log ₂ (FC)) of genes related to the ribosome at different time points during BR and SCF cycle 23.....	219
Figure A7 Relative expression levels (log ₂ (FC)) of genes related to ribosome biogenesis at different time points during BR and SCF cycle 23	220

Figure A8	Relative expression levels ($\log_2(\text{FC})$) of genes related to glycolysis and gluconeogenesis at different time points during BR and SCF cycle 23.....	221
Figure A9	Shikimic acid, glucose, and ethanol concentration during extended BR operation..	222
Figure A10	Ethanol concentration measured at the start and the end of the cycles during SCF operation.....	222
Figure A11	Productivity and integrated specific productivity of shikimic acid during extended BR operation.....	223
Figure A12	Relative expression levels ($\log_2(\text{FC})$) for genes related to the ribosome at different time points during late-log phase and diauxic shift in BR.....	224
Figure A13	Relative expression levels ($\log_2(\text{FC})$) for genes related to ribosome biogenesis at different time points during late-log phase and diauxic shift in BR.....	225
Figure A14	Relative expression levels ($\log_2(\text{FC})$) for genes related to RNA polymerase at different time points during late-log phase and diauxic shift in BR.....	226
Figure A15	Relative expression levels ($\log_2(\text{FC})$) for genes related to ubiquitin-mediated proteolysis at different time points during late-log phase and diauxic shift in BR.....	227
Figure A16	Relative expression levels ($\log_2(\text{FC})$) for genes related to glycolysis and gluconeogenesis at different time points during late-log phase and diauxic shift in BR.....	228
Figure A17	Relative expression levels ($\log_2(\text{FC})$) for genes related to the citrate cycle at different time points during late-log phase and diauxic shift in BR.....	229
Figure A18	Relative expression levels ($\log_2(\text{FC})$) for genes related to oxidative phosphorylation at different time points during late-log phase and diauxic shift in BR..	230
Figure A19	Relative expression levels ($\log_2(\text{FC})$) of genes related to RNA polymerase at different time points during BR and SCF cycle 23.....	231
Figure A20	Relative expression levels ($\log_2(\text{FC})$) of genes related to pentose phosphate pathway at different time points during BR and SCF cycle 23.....	232
Figure A21	Relative expression levels ($\log_2(\text{FC})$) of genes related to phenylalanine, tyrosine, and tryptophan biosynthesis at different time points during BR and SCF cycle 23.....	233
Figure B1	Schematic of the batch reactor configuration used for this study.....	236
Figure B2	Relative expression levels of selected <i>S. cerevisiae</i> cyclin genes in replicated experiments.....	237

List of Tables

Table 4.1	Primer sequences, amplicon sizes, and efficiencies for qPCR experiments.	85
Table 5.1	Primer sequences, amplicon sizes, and efficiencies for qPCR experiments	125
Table 5.2	Yield and volumetric productivity in cellular biomass production during SCF long and short cycle operation	134
Table 6.1	Final OD ₆₀₀ and further growth after methanol addition of 5 mM for batch cultures initiated at different concentrations of methanol.....	155
Table A1	Sampling time points in BR and SCF cycle 23 for RNA-Seq analyses.....	212
Table A2	Sampling time points in SCF cycle 21 for qPCR experiments.	213
Table A3	Information about the plasmid used by the engineered yeast strain in this study	213

List of Abbreviations

BR	Batch reactor
<i>CDC</i>	Cell division cycle
CDKs	Cyclin-dependent kinases
CER	Carbon dioxide evolution rate
CO ₂	Carbon dioxide
C _q	Quantification cycle
DAPI	4',6-diamidino-2-phenylindole
dCER	First derivative of carbon dioxide evolution rate
DE	Differential expression
DEGs	Differentially expressed genes
DNA	Deoxyribonucleic acid
DNS	Dinitrosalicylic acid
dNTPs	Deoxynucleotide triphosphates
DO	Dissolved oxygen
dsDNA	Double-stranded deoxyribonucleic acid
DTT	Dithiothreitol
ED pathway	Entner-Doudoroff pathway
EDTA	Ethylenediaminetetraacetic acid
EMP pathway	Embden-Meyerhof-Parnas pathway
FRET	Fluorescence resonance energy transfer
GEO	Genomic run-on
GO	Gene Ontology
HPLC	High-performance liquid chromatography
KEGG	Kyoto Encyclopedia of Genes and Genomes
MDH	Methanol dehydrogenase

MIQE	Minimum Information for Publication of Quantitative Real-Time PCR Experiments
MMO	Methane monooxygenase
OD	Optical density
OD ₆₀₀	Optical density measured at a wavelength of 600 nm
ORP	Oxidation-reduction potential
PCA	Principal Component Analysis
PHB	Poly- β -hydroxybutyrate
qPCR	Quantitative polymerase chain reaction
RNA	Ribonucleic acid
RT	Reverse transcription
RuMP cycle	Ribulose monophosphate cycle
SBR	Sequential batch reactor
SCF	Self-cycling fermentation
TE	Trace element
YNB	Yeast nitrogen base
AU	absorbance unit
bp	base pair
g	gram
h	hour
L	litre
mg	milligram
min	minute
mL	millilitre
mM	micromole per millilitre
mol	mole
nm	nanometer
°C	degree Celsius
ppm	part per million

rpm	rotation per minute
F	Synchrony index
N	Final cell number
N_0	Initial cell number
t (Chapter 3)	Time interval required for the increase in cell number
g	Generation Time
$Y_{P/S}$	Yield of shikimic acid to glucose
r_P (Chapter 4)	(Intra-cycle) productivity of shikimic acid
\bar{r}_P	(Intra-cycle) integrated specific productivity of shikimic acid
t_{norm}	Normalized cycle time
N_P	Amount of the product (mol of shikimic acid)
N_S	Amount of the substrate (mol of glucose)
V	Working volume
t (Chapters 4, 5)	Operation time or in-cycle time
c_X	Cell density
t_{cycle}	Cycle time
$Y_{X/S}$	Yield of cellular biomass
c_S	Substrate concentration
r_P (Chapter 5)	Volumetric biomass productivity

1. Introduction

1.1 Motivation and context

Fermentation accompanies the history of human civilization. Ancient Egyptians started to ferment bread and beer using baker's yeast several thousand years ago (Heitmann et al. 2018), while the earliest fermented food in human history may trace back to 13,000-year old Near Eastern Natufian cultures (Hayden et al. 2013; Liu et al. 2019). Nowadays, fermented products are intrinsic parts of our lives, in the form of food, fuel, cosmetics, medicines, etc. In fact, bioproducts (including fermented products) are a rapidly growing sector of the economy representing a global market of 586.8 billion USD in 2020 and projected to reach 867.7 billion USD in 2025 (2021). Fermentation processes, in general, consist of batch, continuous, and semi-continuous approaches. A batch reactor (BR) is the most conventional method used in industrial fermentation due to its simplicity (Liu 2017). However, lag phase and stationary phase always demand considerable operational time, which can handicap production and economic viability. Downtime between two batches of operation is required to harvest products, clean and sterilize the fermenter, decreasing the overall productivity and increasing the cost of human power. Continuous operation adopts a fixed dilution rate at which substrates and products flow in and out of the reactor continuously. Compared to BR, continuous reactors eliminate downtime, lag, and stationary phases after reaching a steady state, thereby significantly improving productivity. However, considering the dilution effects encountered in continuous reactors, the concentrations of bioproducts are generally lower, making downstream processing more difficult and costly. Semi-continuous fermentation approaches, combining some of the benefits of both BR and continuous operations, show promise towards more efficient bioproduction.

Self-cycling fermentation (SCF) is an advanced semi-continuous fermentation process in which automated cycling relies on a feedback control system (Dawson 1965, 1972; Sheppard and Cooper 1990, 1991). Cycling, triggered after the depletion of a limiting nutrient, consists of harvesting one-half of the working volume and then replenishing the fermenter with the same amount of fresh medium (Brown and Cooper 1991; Sauvageau et al. 2010). Control parameters, such as carbon dioxide evolution rate (CER), dissolved oxygen (DO), and oxidation-reduction

potential (ORP), are used to monitor the growth status of the microbial population, indirectly sensing the exhaustion of the limiting nutrient, and provide the feedback signal to the control system (Brown 2001). Some of the important SCF features are briefly summarized here. (1) The exchange of half the working volume results in most cells in the fermenter double once during each SCF cycle. In many cases, cycle time has been found to be reflective of the doubling time of the microorganisms (Brown 2001). For a number of physiological studies (Sheppard and Cooper 1991; Brown and Cooper 1991; Sarkis and Cooper 1994; Zenaitis and Cooper 1994), SCF cycle time has been used to evaluate the impact of different nutrients on the studied microbes; a shorter cycle time indicates a more beneficial condition. (2) SCF operation has led to significantly improved productivity of a large variety of biomolecules – including surfactin (Sheppard and Cooper 1991; Sheppard 1993; van Walsum and Cooper 1993), sophorolipid (McCaffrey and Cooper 1995), citric acid (Wentworth and Cooper 1996), poly- β -hydroxybutyrate (PHB) (Marchessault and Sheppard 1997), ethanol (Wang et al. 2020, 2021), bacteriophage (Sauvageau and Cooper 2010), recombinant protein (Storms et al. 2012), etc. – compared to production in conventional BR. (3) Depletion of the limiting nutrient within each SCF cycle guarantees complete removal of the pollutants that were used as carbon or nitrogen sources in a handful of environmental studies (Brown and Cooper 1992; Sarkis and Cooper 1994; Hughes and Cooper 1996; Brown et al. 1999, 2000); the degradation rates shown are generally greater than those seen in other types of processes. (4) Synchrony is often observed for cell populations undergoing SCF; cells divide approximately at the same moment in a given cycle (Brown and Cooper 1991; McCaffrey and Cooper 1995; Wentworth and Cooper 1996; Sauvageau et al. 2010; Sauvageau and Cooper 2010). Easy and efficient production of a large volume of synchronized cells – which can act as proxy for single-cell behaviour – using this non-disruptive method facilitates investigations of intracellular mechanisms.

Despite multiple SCF studies showing increased productivity and synchrony, the metabolic regulation behind these phenomena has yet to be explored. Also, the trends in the timing of the depletion of the limiting nutrient, the end of synchronized cell replication, and the trends in control parameters during SCF cycles have not been systematically analyzed and discussed. Moreover, SCF has not been applied to methanotrophic bacteria.

1.2 Scope of this thesis

The overall objective of this work was to provide an enhanced understanding of SCF and broaden SCF's operational strategies, applications, and control parameters.

Specific aims of this work were: 1) to understand the effects of SCF on transcriptional regulation, synchrony and shikimic acid production in an engineered *Saccharomyces cerevisiae*; 2) to investigate the impact of different SCF cycling schemes on operation and production; and 3) to implement SCF operation for the cultivation of a methanotroph using methanol as the carbon source.

1.3 Thesis structure

Chapter 2 first provides a literature review on SCF, its applications, and its properties, and then elaborates on transcriptomics methods, including RNA-Seq and qPCR. Moreover, overviews are provided focusing on the physiology of *S. cerevisiae* (life cycle, cell cycle, and BR operation), shikimic acid and its production in yeast, *Escherichia coli* and *Methylovium buriatense 5GB1C*.

Chapter 3 provides a minireview on yeast synchronization methods. This topic plays an important role in the investigation of cellular behaviors of both yeast and higher eukaryotes. Cell synchronization methods can be classified in a variety of categories: physical selection, physical induction, chemical inhibition, starvation, and nutrient cycling. Comparative analysis of these methods, including SCF which falls within the nutrient cycling category, was then performed.

Chapter 4 presents transcriptomic analyses of a strain of *S. cerevisiae*, engineered to overproduce shikimic acid, undergoing batch and SCF operation. Regulatory patterns related to DNA replication, the cell cycle, proteasome, the citrate cycle, oxidative phosphorylation, shikimic acid synthesis pathways, among others, were highlighted. These results informed a better understanding of two SCF characteristic features: synchrony and increased productivity.

Chapter 5 consists of an exploration of different implementations of SCF strategies (short and long cycles) and their impact on physiological and processing parameters during operation.

SCF short cycle operation of *E. coli* and *S. cerevisiae* was shown to be viable and stable, even though nutrient depletion did not occur by the end of the cycles. The stability and reproducibility of SCF short cycles suggested that cell doubling ended within the time carbon dioxide evolution rate reached a maximum. In addition, expression patterns of selected cyclin genes of *S. cerevisiae* were investigated during SCF short cycle operation, suggesting partial synchrony and inter-cycle cell replication. Finally, a comparative analysis of the major trends in the timing of SCF characteristic events (including the depletion or a plateau of the limiting nutrient, characteristic points of control parameters, and the end of cell replication) observed in this and other SCF studies was performed. A new description of SCF was proposed based on these findings.

Chapter 6 is dedicated to the implementation of SCF to cultures of *M. buryatense* 5GB1C, a methanotrophic bacterium, growing on methanol and using culture reflectance as control parameter. Significant improvements in biomass productivity were observed compared to BR. A fed-batch operation was also investigated, substantially improving final biomass density.

This thesis concludes with Chapter 7, which summarizes the findings and contributions of previous chapters (Chapters 3, 4, 5, and 6) and highlights their potential impacts. This section also presents a description of the future developments (16 future directions) that could stem from this work.

1.4 References

- Brown WA (2001) The self-cycling fermentor – development, applications, and future opportunities. In: Recent Research and Developments in Biotechnology and Bioengineering. pp 4: 61-90
- Brown WA, Cooper DG (1991) Self-cycling fermentation applied to *Acinetobacter calcoaceticus* RAG-1. Appl Environ Microbiol 57:2901–2906. <https://doi.org/10.1128/aem.57.10.2901-2906.1991>
- Brown WA, Cooper DG (1992) Hydrocarbon degradation by *Acinetobacter calcoaceticus* RAG-1 using the self-cycling fermentation technique. Biotechnol Bioeng 40:797–805. <https://doi.org/10.1002/bit.260400707>

- Brown WA, Cooper DG, Liss SN (2000) Toluene removal in an automated cyclical bioreactor. *Biotechnol Prog* 16:378–384. <https://doi.org/10.1021/bp0000149>
- Brown WA, Cooper DG, Liss SN (1999) Adapting the self-cycling fermentor to anoxic conditions. *Environ Sci Technol* 33:1458–1463. <https://doi.org/10.1021/es980856s>
- Dawson PSS (1965) Continuous phased growth, with a modified chemostat. *Can J Microbiol* 11:893–903. <https://doi.org/10.1139/m65-119>
- Dawson PSS (1972) Continuously synchronised growth. *J Appl Chem Biotechnol* 22:79–103. <https://doi.org/10.1002/jctb.2720220112>
- Hayden B, Canuel N, Shanse J (2013) What Was Brewing in the Natufian? An Archaeological Assessment of Brewing Technology in the Epipaleolithic. *J Archaeol Method Theory* 20:102–150. <https://doi.org/10.1007/S10816-011-9127-Y/FIGURES/3>
- Heitmann M, Zannini E, Arendt E (2018) Impact of *Saccharomyces cerevisiae* metabolites produced during fermentation on bread quality parameters: A review. *Crit Rev Food Sci Nutr* 58:1152–1164. <https://doi.org/10.1080/10408398.2016.1244153>
- Hughes SM, Cooper DG (1996) Biodegradation of phenol using the self-cycling fermentation (SCF) process. *Biotechnol Bioeng* 51:112–119. [https://doi.org/10.1002/\(SICI\)1097-0290\(19960705\)51:1<112::AID-BIT13>3.0.CO;2-S](https://doi.org/10.1002/(SICI)1097-0290(19960705)51:1<112::AID-BIT13>3.0.CO;2-S)
- Liu L, Wang J, Rosenberg D, et al (2019) Response to comments on archaeological reconstruction of 13,000-y old Natufian beer making at Raqefet Cave, Israel. *J Archaeol Sci Reports* 28:101914. <https://doi.org/10.1016/J.JASREP.2019.101914>
- Liu S (2017) Batch Reactor. In: *Bioprocess Engineering*. Elsevier, pp 139–178
- Marchessault P, Sheppard JD (1997) Application of self-cycling fermentation technique to the production of poly- β -hydroxybutyrate. *Biotechnol Bioeng* 55:815–820. [https://doi.org/10.1002/\(SICI\)1097-0290\(19970905\)55:5<815::AID-BIT12>3.0.CO;2-A](https://doi.org/10.1002/(SICI)1097-0290(19970905)55:5<815::AID-BIT12>3.0.CO;2-A)
- McCaffrey WC, Cooper DG (1995) Sophorolipids production by *Candida bombicola* using self-cycling fermentation. *J Ferment Bioeng* 79:146–151. [https://doi.org/10.1016/0922-338X\(95\)94082-3](https://doi.org/10.1016/0922-338X(95)94082-3)
- Sarkis BE, Cooper DG (1994) Biodegradation of aromatic compounds in a self-cycling

- fermenter (SCF). *Can J Chem Eng* 72:874–880. <https://doi.org/10.1002/cjce.5450720514>
- Sauvageau D, Cooper DG (2010) Two-stage, self-cycling process for the production of bacteriophages. *Microb Cell Fact* 9:1–10. <https://doi.org/10.1186/1475-2859-9-81>
- Sauvageau D, Storms Z, Cooper DG (2010) Synchronized populations of *Escherichia coli* using simplified self-cycling fermentation. *J Biotechnol* 149:67–73. <https://doi.org/10.1016/J.JBIOTECH.2010.06.018>
- Sheppard JD (1993) Improved volume control for self-cycling fermentations. *Can J Chem Eng* 71:426–430. <https://doi.org/10.1002/cjce.5450710312>
- Sheppard JD, Cooper DG (1990) Development of computerized feedback control for the continuous phasing of *Bacillus subtilis*. *Biotechnol Bioeng* 36:539–545. <https://doi.org/10.1002/bit.260360514>
- Sheppard JD, Cooper DG (1991) The response of *Bacillus subtilis* ATCC 21332 to manganese during continuous-phased growth. *Appl Microbiol Biotechnol* 35:72–76. <https://doi.org/10.1007/BF00180639>
- Storms ZJ, Brown T, Sauvageau D, Cooper DG (2012) Self-cycling operation increases productivity of recombinant protein in *Escherichia coli*. *Biotechnol Bioeng* 109:2262–2270. <https://doi.org/10.1002/bit.24492>
- van Walsum GP, Cooper DG (1993) Self-cycling fermentation in a stirred tank reactor. *Biotechnol Bioeng* 42:1175–1180. <https://doi.org/10.1002/bit.260421007>
- Wang J, Chae M, Beyene D, et al (2021) Co-production of ethanol and cellulose nanocrystals through self-cycling fermentation of wood pulp hydrolysate. *Bioresour Technol* 330:124969. <https://doi.org/https://doi.org/10.1016/j.biortech.2021.124969>
- Wang J, Chae M, Bressler DC, Sauvageau D (2020) Improved bioethanol productivity through gas flow rate-driven self-cycling fermentation. *Biotechnol Biofuels* 13:1–14. <https://doi.org/10.1186/s13068-020-1658-6>
- Wentworth SD, Cooper DG (1996) Self-cycling fermentation of a citric acid producing strain of *Candida lipolytica*. *J Ferment Bioeng* 81:400–405. [https://doi.org/10.1016/0922-338X\(96\)85140-3](https://doi.org/10.1016/0922-338X(96)85140-3)

Zenaitis MG, Cooper DG (1994) Antibiotic production by *Streptomyces aureofaciens* using self-cycling fermentation. *Biotechnol Bioeng* 44:1331–1336.

<https://doi.org/10.1002/bit.260441109>

(2021) Global Bioproduct Market Size, Share & Growth Analysis Report. In: Jan.

<https://www.bccresearch.com/market-research/energy-and-resources/biorefinery-products-markets-report.html>. Accessed 31 Oct 2021

2. Literature Review

2.1 Self-cycling fermentation

Self-Cycling Fermentation (SCF) is an advanced fermentation method used to improve the productivity of valuable chemicals in microbial systems and to facilitate the investigation of biological processes (Sauvageau and Cooper 2010; Storms et al. 2012; Agustin 2015; Wang et al. 2017). It is a semi-continuous, unsteady-state, cyclical process, in which, following an initial batch growth, SCF cycles are triggered when the depletion of the limiting nutrient and/or the cessation of growth-related cellular metabolism occurs (Brown and Cooper 1991; Sauvageau et al. 2010).

Dissolved oxygen (DO), carbon dioxide evolution rate (CER), exit gas mass flowrate, and oxidation-reduction potential (ORP) along with their derivatives have been used as monitoring parameters to fulfill the feedback control system in SCF (Brown 2001; Wang et al. 2020). Lately, CER combined with its first derivative (dCER) were shown to serve as robust control parameters, enabling stable and repeatable SCF cycles (Sauvageau et al. 2010; Sauvageau and Cooper 2010; Storms et al. 2012; Agustin 2015). This approach is advantageous as it avoids the use of intrusive DO or ORP probes, and consequently, prevents potential issues such as sensor fouling and contamination.

When the monitoring parameters reach pre-established threshold values, cycling is triggered. In detail, as shown in Figure 2.1, cycling is completed by draining exactly one-half the working volume of the reactor and then replenishing with the same amount of fresh medium (Sauvageau et al. 2010). This procedure introduces a forcing function (Wincure et al. 1995; Hughes and Cooper 1996; Pinchuk et al. 2000) to the cell cultures, which leads to distinct SCF features, such as synchrony (Brown and Cooper 1991; McCaffrey and Cooper 1995; Wentworth and Cooper 1996; Sauvageau et al. 2010; Sauvageau and Cooper 2010).

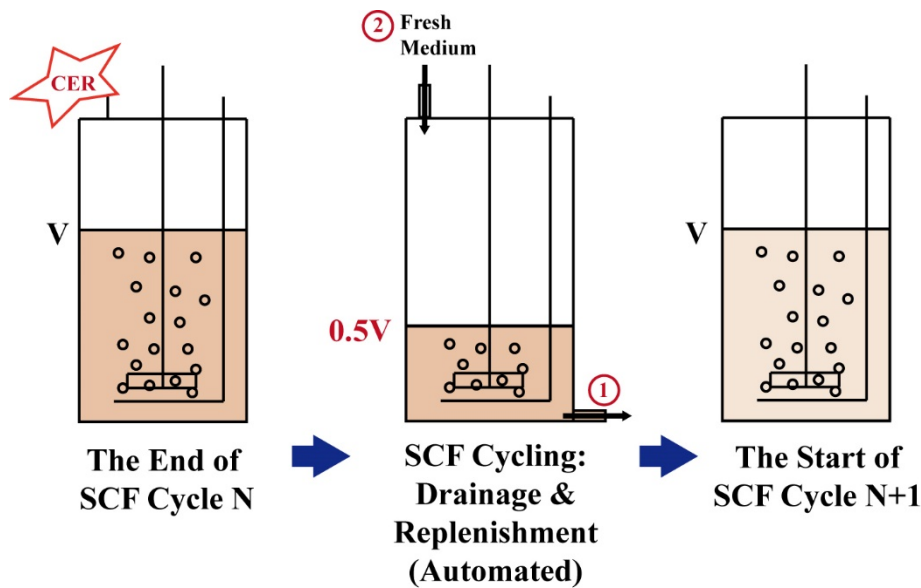


Figure 2.1 Schematic of the cycling sequence during SCF operation. A stirred-tank bioreactor is representative of vessels used in SCF studies. Carbon dioxide evolution rate (CER) is representative of monitoring parameters during SCF.

2.1.1 Continuous phasing and SCF

Continuous phasing, devised in the 1960s, is the precursor to SCF (Dawson 1965, 1970, 1972). The fundamental concept and operation of these two processes are very similar. Figure 2.2 highlights the experimental procedure of continuous phasing (Dawson 1965), whose cycling concept is similar to SCF's (Figure 2.1). Nevertheless, they do have differences. In the context of continuous phasing, the inventor stated that cell doubling time of yeast in each cycle could be forced by imposing a specific cycle time (Dawson 1972). However, washout could occur when the imposed cycle time was too short (Sheppard and Cooper 1990; Brown 2001). The extended cycle strategy could also be implemented by setting a cycle time longer than the doubling time (McCaffrey and Cooper 1995; Wentworth and Cooper 1996; Crosman et al. 2002). Further, since continuous phasing does not implement an automated feedback control system but rather uses a set cycling time, this approach is less amenable to reproducible cycling resilient to perturbations; so it is closer to a sequential batch reactor (SBR) that utilizes 50 % v/v inocula for each batch. SCF, in comparison, could be described as feedback control-integrated SBR with 50 % v/v inocula implemented. Consequently, SCF helps avoid the risk of washout and provides the cycle-to-cycle

stability based on monitoring metabolic events. The greater control over cycling during SCF operation ensures process outcomes and facilitates the implementation of tailored operational/cycling strategies – e.g., the extended cycle strategy (McCaffrey and Cooper 1995; Wentworth and Cooper 1996; Crosman et al. 2002) and two-stage strategy (van Walsum and Cooper 1993; McCaffrey and Cooper 1995; Wentworth and Cooper 1996; Sauvageau and Cooper 2010; Storms et al. 2012).

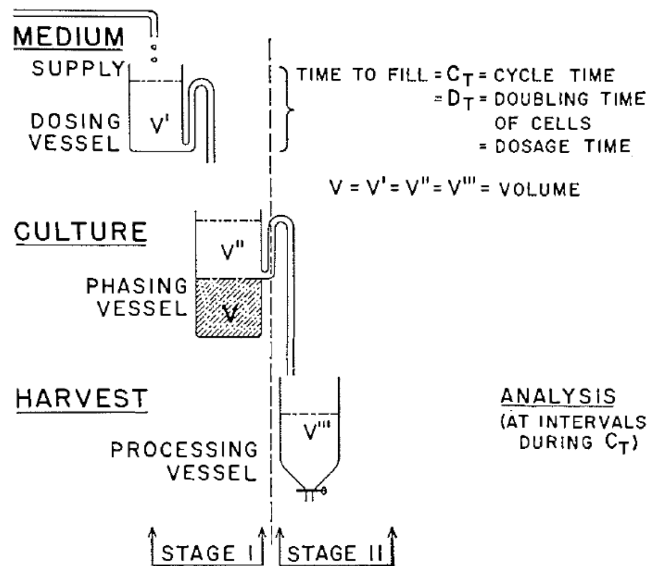


Figure 2.2 Schematic of continuous phased culture (continuous phasing) (Dawson 1965). (Original figure reuse with permission from Canadian Science Publishing)

2.1.2 SCF applications

SCF has been utilized for a wide variety of purposes with different organisms (Brown 2001); generally, these can fit in the following three categories.

(1) Cell physiology studies. Synchronized populations and the inherent cell-directed stability of the repeatable SCF cycles led to the determination of physiological properties for a number of microbes. These include: the effect of the nutrients (manganese, iron, and nitrogen) on the growth of a surfactin-producing *Bacillus subtilis* (Sheppard and Cooper 1991); the suppressing effect of trace amounts of iron on tetracycline production by *Streptomyces aureofaciens* (Zenaitis

and Cooper 1994); and the metabolic stalling due to the accumulation of intermediates exhibited by dissolved oxygen profiles during emulsan production by *Acinetobacter calcoaceticus* (Brown and Cooper 1991) and during degradation of *p*-anisaldehyde by *Pseudomonas putida* (Sarkis and Cooper 1994).

(2) Biodegradation studies. The complete removal of pollutants used as limiting nutrients within SCF cycles is facilitated by the SCF feedback control scheme. Pollutant degradation rates were generally found to be much greater in SCF than in other reactor systems. Such studies include: the degradation of water-soluble aromatics, such as benzoate, *p*-anisaldehyde, and 4-methoxybenzylidene-4-*n*-butylaniline (MBBA) by *Pseudomonas putida* and *Pseudomonas fluorescens* (Sarkis and Cooper 1994), and phenol by *Pseudomonas putida* (Hughes and Cooper 1996); the degradation of water-insoluble aromatics, such as toluene and *p*-xylene by *Pseudomonas putida* containing a TOL plasmid (Brown et al. 2000), and alkanes by *Acinetobacter calcoaceticus* (Brown and Cooper 1992); and the assimilation and removal of soluble inorganic compounds, such as oxidized nitrogen by *Pseudomonas denitrificans* in anoxic conditions (Brown et al. 1999).

(3) Production studies. Generally, productivity is greater in SCF operation than in other bioreactor operation strategies for bioproduction. Different conformations and strategies have been explored. For instance, two-stage SCF schemes, which allows to decouple production from growth, have been utilized in (van Walsum and Cooper 1993; McCaffrey and Cooper 1995; Wentworth and Cooper 1996; Sauvageau and Cooper 2010; Storms et al. 2012) to provide great yields without compromising throughput. Also, controlled extended SCF cycle strategies have been used to achieve great yields and/or productivity (McCaffrey and Cooper 1995; Wentworth and Cooper 1996; Crosman et al. 2002). Bioproduction studies encompassing SCF operation include: the production of secondary metabolites, such as surfactin by *Bacillus subtilis* (Sheppard and Cooper 1991; Sheppard 1993; van Walsum and Cooper 1993), sophorolipid by *Candida bombicola* (McCaffrey and Cooper 1995), poly- β -hydroxybutyrate (PHB) by *Alcaligenes eutrophus* (Marchessault and Sheppard 1997), tetracycline by *Streptomyces aureofaciens* (Zenaitis and Cooper 1994), phospholipid biosurfactant by *Corynebacterium alkanolyticum* (Crosman et al. 2002), and citric acid by *Candida lipolytica* (a secondary metabolite in this organism) (Wentworth and Cooper 1996); the production of growth-associated products, such as emulsan by

Acinetobacter calcoaceticus (Brown and Cooper 1991, 1992), shikimic acid by *Saccharomyces cerevisiae* (Agustin 2015), and ethanol by *Saccharomyces cerevisiae* (Wang et al. 2017, 2020, 2021); and also the production of other types of bioproducts, such as bacteriophage (Sauvageau and Cooper 2010) and recombinant protein (Storms et al. 2012) by *Escherichia coli*.

2.1.3 SCF properties

The distinct features of SCF act as the foundation for the applications listed above. Several significant properties of SCF are introduced here briefly.

(1) Self-cycling. Firstly, SCF cycling is dictated by the cell population itself. There is no pre-set, fixed time for the duration of cycles, but rather a relatively flexible cycle time determined by growth and nutrient use during every cycle. As a consequence, SCF can be very tolerant and resistant to perturbations. For instance, when cycling was disrupted for a cycle or when the carbon source was changed, the SCF system has shown great ability in re-establishing a stable growth pattern within the few cycles following the perturbation (van Walsum and Cooper 1993; Sauvageau et al. 2010). Moreover, SCF cycle time can be used to evaluate the health of cultures or effectiveness of nutrient environments. For example, if a nutritional condition is beneficial to cell growth, the cycle time, which is reflecting the doubling time, should be shorter (Brown 2001). More specific and detailed examples can be found in articles referenced by the “Cell physiology studies” section above.

(2) Increased productivity. Secondly, a large number of studies (Zenaitis and Cooper 1994; Wentworth and Cooper 1996; Sauvageau and Cooper 2010; Storms et al. 2012; Agustin 2015; Wang et al. 2017) have shown SCF has the ability to increase volumetric productivity when used for bioproduction. Greater specific productivity has also been observed (Sauvageau and Cooper 2010; Agustin 2015), meaning SCF can lead to greater product concentrations with fewer cells. SCF eliminates the long lag phase that usually occurs in BR after inoculation and that consumes considerable fermentation time but produces only small amounts of products. A reduction in the ratio of downtime to production time is another significant benefit offered by SCF (Wang et al. 2017). The extended cycle mode of SCF operation (McCaffrey and Cooper 1995; Wentworth and Cooper 1996; Crosman et al. 2002), for which the cycle time is extended beyond the depletion of

the limiting nutrient, is a beneficial strategy for producing stationary phase-associated metabolites. Two-stage SCF strategy can also be used for this purpose, decoupling production from growth and further increasing productivity (van Walsum and Cooper 1993; McCaffrey and Cooper 1995; Wentworth and Cooper 1996; Sauvageau and Cooper 2010; Storms et al. 2012). In general, SCF shows promise in replacing many other types of reactor operation currently being used for bioproduction, at least in terms of productivity (Brown 2001).

(3) Synchrony of cell populations. Thirdly, population synchronization can be achieved during SCF operation (Brown and Cooper 1991; McCaffrey and Cooper 1995; Wentworth and Cooper 1996; Sauvageau et al. 2010; Sauvageau and Cooper 2010). As half the working volume is drained and then replenished, cells double only once during each SCF cycle based on material balance. During an SCF cycle, while the optical density (OD) of the culture (generally used as a proxy for cell density) increases relatively linearly, the cell count of the population only rises in a narrow time frame. Markedly, synchronization of cell populations can be established after 5-10 cycles (Brown and Cooper 1992; Hughes and Cooper 1996; Sauvageau et al. 2010). The Synchrony Index is a metric that can be used to quantify the level of synchrony – $F = N/N_0 - 2^{t/g}$, where F is the synchrony index; N represents cell number; t is the required time interval by an increase in cell number from N_0 to N . g represents the generation time (or doubling time) of an organism (Blumenthal and Zahler 1962). If a cell population were to replicate precisely and completely in unison, the synchrony index would be 1. Conversely, the synchrony index achieved during a BR operation will be close to 0, since cells in this mode of operation grow in a random and asynchronous fashion, demonstrating the “average cell” properties. The synchrony index observed during SCF operation typically ranges from 0.66 to 0.82 (Brown 2001), meaning a significant degree of synchrony is achieved. Other methods used to produce microbial synchronized populations include the “baby machine” (Bates et al. 2005), “famine and feast” strategies (Hirsch and Vondrejs 1971; Chan and Cheng 1977), temperature cycling (Cho et al. 1998), and addition of growth inhibitors (Ferullo et al. 2009). However, these methods are either inefficient at large volumes or disruptive to cellular mechanisms. In contrast, SCF can easily, efficiently, and non-disruptively produce a large volume of synchronized population (based on entrainment mechanism (Sheppard and Dawson 1999)). Thus, as an efficient way to produce synchronized cultures, SCF presents significant advantages.

2.1.4 SCF hardware configuration

SCF hardware configurations have been modified and improved quite extensively over the years. Once, a cyclone reactor was predominantly used as the fermenter vessel (Sheppard and Cooper 1990, 1991; Brown and Cooper 1991; Sheppard 1993). However, in this configuration, the replacement of the half volume was hard to establish precisely. A balance measuring the weight of cultures (Sheppard and Cooper 1990, 1991; Brown and Cooper 1991; Sheppard 1993) and a differential pressure transducer (Brown et al. 1999) were used for this purpose. After two decades of development, a stirred-tank bioreactor equipped with level sensors have become the preferred SCF setup (Sauvageau et al. 2010; Sauvageau and Cooper 2010).

The SCF hardware used for an investigation of bioproduction using an engineered yeast (Agustin 2015) is shown in Figure 2.3. It comprised of a feed system (fresh medium, a peristaltic pump, a solenoid valve, and a glass isolator), a harvesting system (a solenoid valve and a harvest carboy), an air supply line (sterilized water bottle, a rotameter, and a HEPA filter), an outlet for exit gas (a condenser, a HEPA filter, and a CO₂ sensor), tubing connections, a sampling port with glass sampling tubes, a stirred-tank bioreactor (including high- and low-level sensors, a Rushton impeller, an air sparger, a thermocouple, and a heater cartridge), a data acquisition and control system, and a computer with LabView programs. The same setup was used for works presented in this thesis.

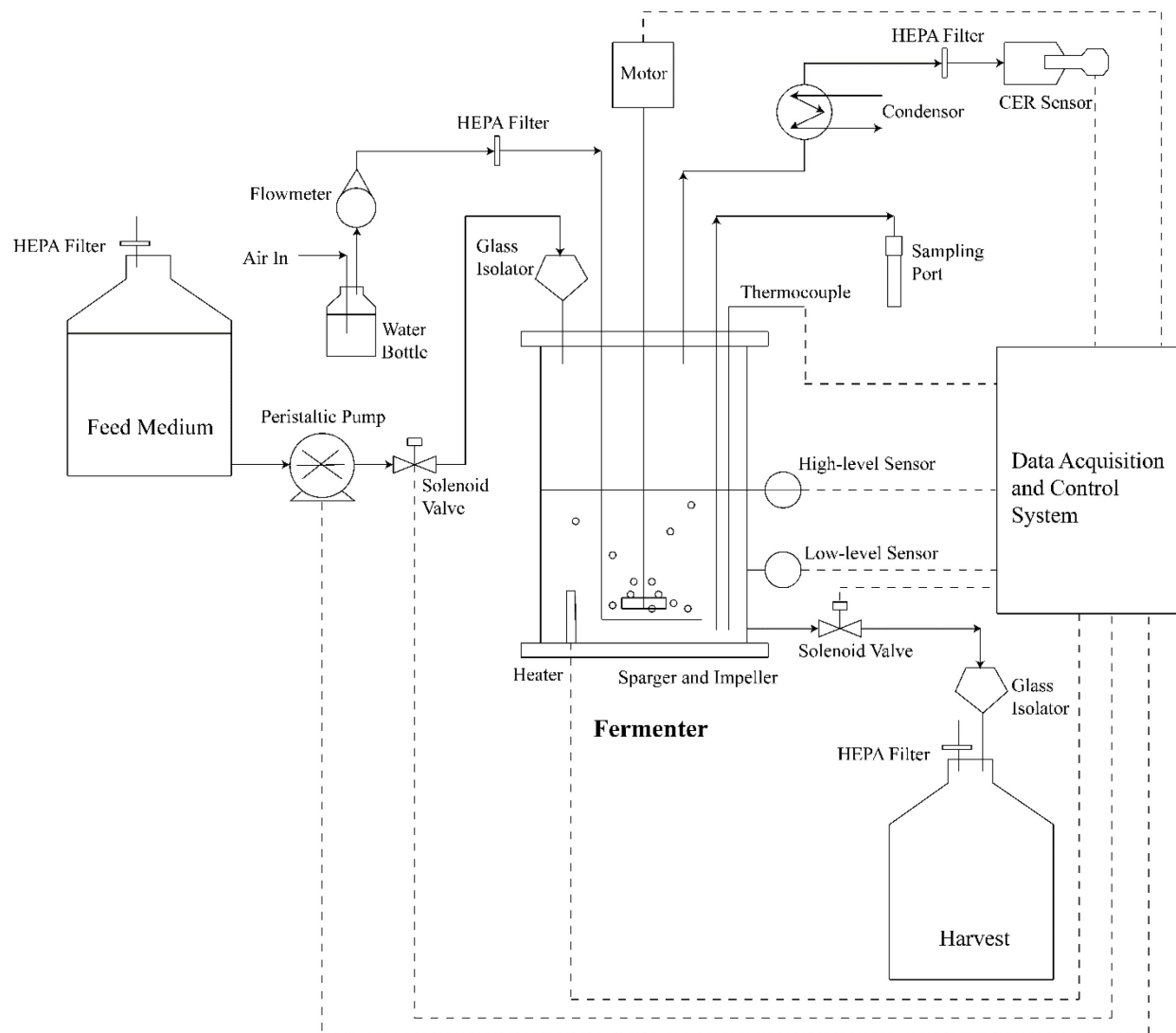


Figure 2.3 Schematic of SCF configuration used for an investigation of bioproduction using an engineered yeast. (Adapted based on an original figure in (Agustin 2015), also presented in (Tan et al. 2021))

2.2 Transcriptomic Analysis

Transcriptome, or global gene regulation patterns, of an organism can be determined through an analysis of either the complete set of RNA molecules (transcripts) or only the mRNA profile (Ishii 2014). This can be done for one single cell or a population of cells. Transcriptome profiles are utilized to estimate global gene expression levels. Significant changes in these levels, also called differential expression (DE), are thus measured through transcriptomic analysis, and

are used to better understand the roles and regulation of various genes under conditions in which the cells are treated or in processes that cells are undergoing. Genes with significantly different expressions between different conditions – referred to as differentially expressed genes (DEGs) – and the associated regulated pathways and ontology enrichment groups provide information on cellular mechanisms and metabolic regulation corresponding to specific conditions or processes.

The hybridization-based DNA microarray approach, which incubates fluorescently labeled cDNA with immobilized microarray chips, was widely used for transcriptomic studies before the rise of sequencing-based methods. Several drawbacks limit the utilization of DNA microarray, including limited detection relying only on genes that were previously identified, high background levels due to cross-hybridization, signal saturation, and complicated normalization across different batches of experiments (Wang et al. 2009). Recently, the sequencing-based approach RNA-Seq has become more standard to carry out transcriptomic analysis (Wang et al. 2009).

A large number of transcriptomic analyses have been performed with yeast and, specifically, *S. cerevisiae* – one of the most studied eukaryotic model organisms. These analyses helped elucidate transcriptional regulation associated with cellular responses under certain conditions (e.g., under chemical treatments (Yu et al. 2010; Zhu et al. 2017)) and physiological processes (such as the cell cycle (Cho et al. 1998), rates of mRNA synthesis and decay (Miller et al. 2011), regulation of protein abundance (Vogel and Marcotte 2012), etc.). A previous study illustrated the regulation of cell cycle-related genes during yeast mitotic cell replication (Cho et al. 1998), in which synchronized yeast cells were obtained through temperature cycles and the transcriptome analysis was fulfilled by the microarray technique.

2.2.1 RNA-Seq

RNA-Seq, also known as whole transcriptome shotgun sequencing, is now the primary and most popular method used to obtain transcriptome profiles (Chu and Corey 2012). It is based on next-generation sequencing. Usually, RNA isolation (see methods in following qPCR section), mRNA selection, fragmentation, cDNA synthesis, adaptor ligation, and amplification are the preparatory steps prior to sequencing (Figure 2.4) (Wang et al. 2009).

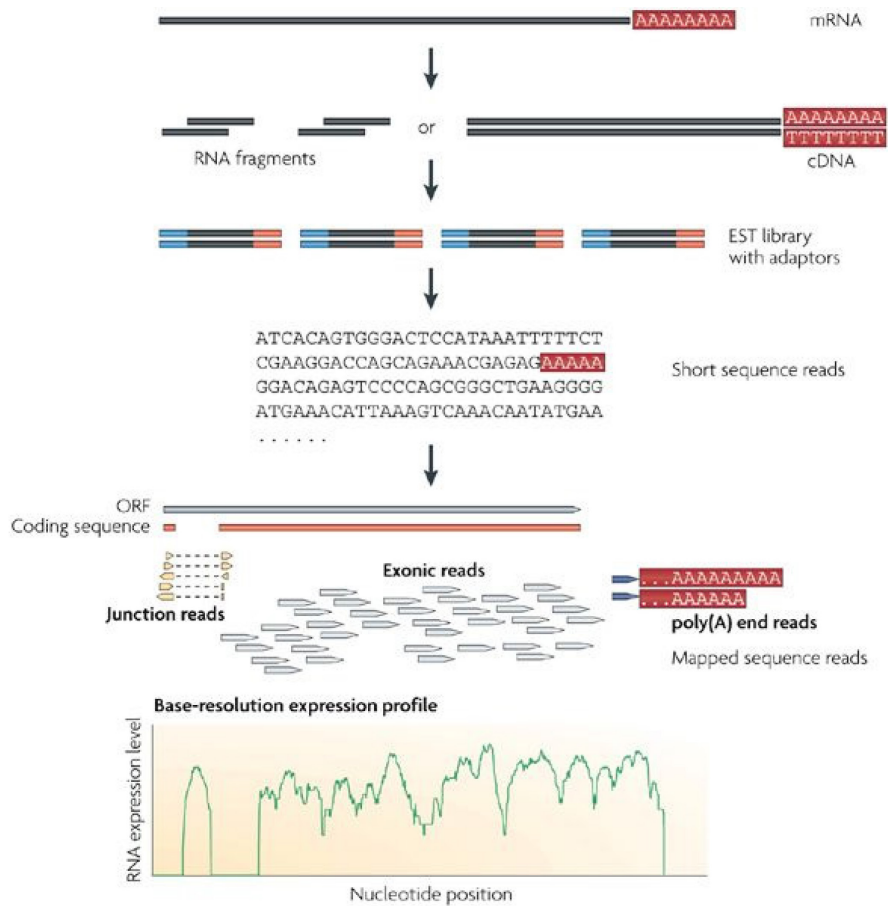


Figure 2.4 Schematic of RNA-Seq experiments (Wang et al. 2009). (Original figure reuse with permission from Springer Nature)

Many bioinformatics tools based on Python and R programming languages have been created to process and analyze RNA-Seq data (Conesa et al. 2016). Remarkably, continuous development is seen regarding many of these RNA-Seq tools. For example, TopHat (developed based on Bowtie (Langmead and Salzberg 2012)), Cufflinks package (including Cufflinks, Cuffcompare, Cuffmerge, Cuffdiff), and CummeRbund for visualization together account for “Tuxedo” (Trapnell et al. 2012). A couple of years after contributing to the release of Tuxedo, Dr. Steven L Salzberg’s team at Johns Hopkins University continued their work and developed a “new Tuxedo”, which is comprised of HISAT, StringTie, and Ballgown (Pertea et al. 2016). These tools, incorporated in either the original or new Tuxedo workflow, have been designed to conduct transcriptomic analysis for both readily annotated genes/transcripts and novel genes/transcripts. In

fact, for many RNA-Seq studies, genome sequence and annotation files are readily available and relatively complete. Also, the scope of these analyses primarily focuses on DE analysis, but not on novel gene detection or novel transcripts/splicing detection. In these cases, workflows relying on genome annotation files (commonly in GFF3 or GTF format) are used and *de novo* transcriptome assembly was skipped. This allows for short data-processing time and rapid data analysis, with solid results generated for comparisons of global gene expression, especially for well-studied organisms.

Similarly, since finding new transcripts or novel splicing has not been a priority for the transcriptomics part of this thesis, *de novo* assembly was not performed herein. Instead, RNA-Seq workflows guided by genome sequence and annotation files were applied, and some of the RNA-Seq programs mentioned below were incorporated.

In detail, after RNA-Seq raw data is deposited, the main steps in compact RNA-Seq workflows are: read quality examination, trimming, second quality examination, read alignment, aligned read quantification, aligned read count (feature) normalization, and finally, DE analysis and DEGs detection. The RNA-Seq programs involved include, but are not limited to, Trimmomatic (Bolger et al. 2014) and Trim Galore (Krueger 2017) for reads trimming, FastQC (Anders 2010) for reads quality examination, TopHat (Trapnell et al. 2009), HISAT (Kim et al. 2015) and STAR (Dobin et al. 2013) for reads alignment, HTSeq-count (Anders et al. 2015) and featureCounts (Liao et al. 2014) for mapped reads quantification, and Cuffdiff (Trapnell et al. 2012), DESeq (Love et al. 2014), and edgeR (Robinson et al. 2010) for normalization and DE analysis (Cuffdiff also provides the function of read quantification).

FastQC is likely the most popular tool to perform quality control for raw and post-trimming datasets. The trimming process is popularly done using Trimmomatic or Trim Galore, which removes any adaptor sequences and trims low-quality regions from the reads. These steps together ensure all reads to be aligned in the next step meet an acceptable quality threshold. TopHat and HISAT (second versions) are popular tools to perform read alignment, which map the reads to the genome sequence. Genome sequence and gene annotation information (in FASTA and GFF/GTF formats, respectively) are referenced during the alignment step. HISAT2 is substantially faster and requires less computational power than TopHat2 due to a different algorithm used (Kim et al. 2015). Despite the difference in computational speed, they tend to result in equivalent high-quality

alignments, and sometimes HISAT2 even prevails (Kim et al. 2015). There are many other relatively new and emerging alignment tools, but improvements regarding data-processing speed and mapping quality, compared to HISAT2, seem limited.

The quantification step can be processed by HTSeq-count or featureCounts, which generates the counting results of the aligned reads based on the features of the genome (features can be genes or transcripts). However, these counts cannot be directly used for the comparison of expression levels, as they contain biases from different sources. Thereby, in the last step, Cuffdiff from the original Tuxedo suite (second version), DESeq (second version), and edgeR can be used to normalize the feature counts, analyze DE, and detect DEGs based on statistics (Cuffdiff also does the quantification). Different normalization algorithms incorporated in these tools eliminate biases produced from different gene/transcript lengths, varying sequencing depth, or different RNA compositions.

Cuffdiff also incorporates the quantification of aligned features, so it directly follows read aligners; it uses their resulting alignment output (bam format files) without requiring mapped reads counting tools as an intermediary step. Notably, feature count tools, like HTSeq-count and featureCounts, tend to be conservative with regards to multi-mapped reads. For example, HTSeq-count discards these reads by default, which generally leads to lower counts for features. In contrast, Cuffdiff accounts for the multi-mapped reads, which are distributed either evenly or unevenly by the “multi-mapped read correction” mode. Some DE detection packages, including DESeq and edgeR, have been compared using defined datasets generated from mice and humans (Seyednasrollah et al. 2015). DESeq appeared to be a safer choice than edgeR when facing a small number of dataset replicates (below 5) (Seyednasrollah et al. 2015). A recent review (Costa-Silva et al. 2017) evaluated six mapping programs and five DEGs-identifying tools based on select human brain datasets (genome annotation file implemented), using RT-qPCR results as the reference. The results indicated that the use of different aligners had a minimal impact on final gene expression analysis (Costa-Silva et al. 2017). DESeq2 again presented congruent results. Remarkably, even though various DE detection tools were applied, a consensus was observed for the resulting DEGs lists. This suggests that implementing different programs during the same step of RNA-Seq data analysis may result in comparable DE analysis, verifying the results for each other and offering a more accurate identification of DEGs (Costa-Silva et al. 2017).

Following DE analysis, DEGs of interest can be further classified based on Gene Ontology (GO) enrichment (Ashburner et al. 2000) and the Kyoto Encyclopedia of Genes and Genomes (KEGG) database (Kanehisa and Goto 2000). Gene classification is performed based on biological processes (GO), molecular functions (GO), cellular components (GO), and related pathways (KEGG). Observing up-regulation or down-regulation for a GO term or a KEGG pathway usually infers an activation or an attenuation in this biological process, molecular function, cellular component, or pathway in a given condition/process. Hence, classification of genes of interest leads to an enhanced understanding of the DE results.

Due to the large sizes and complexity of RNA-Seq datasets, RNA-Seq analysis is often performed by bioinformaticians using Python and R programming languages and associated packages. However, some platforms have wrapped these RNA-Seq programs into user-friendly interfaces. These cloud-based or local softwares significantly reduce the learning barriers for ordinary practitioners who may not have prior sophisticated programming knowledge. For example, Galaxy (Goecks et al. 2010; Afgan et al. 2018) is one of the standard platforms. It is an open access, cloud-based resource, maintained and sponsored by top research institutions in the field. The Galaxy platform provides a large variety of bioinformatic tools targeting big datasets generated by next-generation sequencing, which include RNA-Seq programs. A local version of the Galaxy platform shared with small communities is also available. It should also be noted that the options to adjust every analytical parameter of a program are integrated into Galaxy's easy-to-use interface (Blankenberg and Hillman-Jackson 2014). Moreover, GENECODIS (Carmona-Saez et al. 2007) is a web-based platform to help perform gene classification (GO and KEGG) for a list of DEGs. Furthermore, ClustVis (Metsalu and Vilo 2015) provides an open access, user-friendly platform for creating Principal Component Analysis (PCA) plots and heatmaps.

2.2.2 qPCR

Quantitative polymerase chain reaction (qPCR), or real-time polymerase chain reaction, is used to perform absolute or relative quantification of targeted DNA sequences based on PCR technology (Heid et al. 1996). For gene expression analysis, qPCR is used to quantify reverse-transcribed transcripts (cDNA). While qPCR experiments cannot be used to analyze a complete set of transcript profiles, it is a well-developed and reliable method to measure DE for a given

number of target genes. In transcriptomic studies, qPCR is usually performed as a gold standard to confirm RNA-Seq results.

qPCR is essentially a polymerase chain reaction (PCR). During qPCR or PCR, DNA templates are amplified exponentially with reaction cycles. Sequence-specific oligonucleotides (primers), heat-stable polymerases, deoxynucleotide triphosphates (dNTPs), and temperature cycles are essential for successful amplification. In traditional PCR experiments, amplified DNA products can only be quantified at the end of the whole process. During qPCR, however, amplified DNA products are combined with fluorescent dyes or hydrolysis probes are cleaved during DNA amplification. These fluorescent signals are monitored in real time by qPCR machines and are eventually used to determine the initial amounts (inputs) of the target sequences (Heid et al. 1996).

To quantify transcript levels by qPCR, the first step is total RNA extraction and purification. Samples are collected from cultures grown or treated in specific conditions. RNA extraction is supposed to be performed directly after sample collection to avoid potential changes in transcriptome profiles. There are several popular methods to extract total RNA. A popular approach consists in using phenol and guanidine isothiocyanate (a chaotropic salt), which protect RNA from RNases during RNA extraction. Chloroform is then used to separate aqueous (containing most of the RNA), interphase, and organic phases, followed by isopropanol precipitation to recover the RNA (Chomczynski and Sacchi 1987). Another approach is based on silica column/filter or beads (Boom et al. 1990). After cell lysis and homogenization using guanidine isothiocyanate, RNA is bound to the affinity column or beads, followed by wash and elution. A third method relies on using detergents and protease K to lyse the cells. Protein precipitation, isopropanol recovery of the nucleic acids, and DNase treatment follow the step of cell lysis (Miller et al. 1988). Commercial kits are available for these methods, showing their advantages and disadvantages. Other RNA extraction methods also exist, and some of them are hybrid methods of the aforementioned ones. After RNA extraction, the quantity, quality, and integrity of total RNA need to be evaluated. Quantification can be made using methods relying on UV-absorbance (e.g., NanoDrop (Thermo Fisher)) or fluorescence affinity (e.g., Qubit Fluorometer (Thermo Fisher)). While NanoDrop can provide 260/230 and 260/280 values to indicate purities of extracted RNA, RNA degradation is not assessed (Bustin et al. 2009). In circumstances where RNA samples are of high purities with very little DNA, protein, salt, or

ethanol present but have been degraded significantly, spectrometry and fluorometry results will be as good as those from undegraded RNA samples. Thus, RNA electrophoresis or a measurement via a Bioanalyzer (Agilent) is necessary to assess the integrity of RNA. RNA quantity, purity, and integrity are all important metrics.

After RNA isolation, one-step or two-step RT-qPCR kits (reverse transcription (RT) and quantitative PCR in one or two reactions) (ThermoFisher Scientific 2019) are used (Figure 2.5). In many cases, two separated steps of reverse transcription and qPCR are recommended since the synthesized cDNA libraries can be preserved, for future needs or used to quantify multiple target genes. During reverse transcription, primer choices are important (Bustin et al. 2005). Random primers (hexamers) offer high sensitivity and generate large pools of cDNA. On the other hand, oligo(dT) primers can only work for eukaryotic organisms and may cause some biases due to 3' degradation of some transcripts. Notably, random and oligo(dT) primers can be employed in the same RT-reaction to combine the benefits from both. Sequence-specific primers are usually used only in one-step RT-qPCR. In that case, only a limited number of specific transcripts undergo reverse transcription, and real-time PCR takes place in the same tube directly after the RT reaction.

Double-stranded DNA (dsDNA) binding dyes, such as SYBR green (Ponchel et al. 2003), can be used as fluorescent reporters for cDNA libraries undergoing qPCR. SYBR green produces much stronger fluorescent signals after binding to the minor grooves of dsDNA. Another type of commonly used fluorescent reporter is hydrolysis probes – e.g., TaqMan probe, which comprises 5' reporter dye, 3' quencher, and a gene-specific sequence connecting the two ends. Hydrolysis probe assays rely on a mechanism named fluorescence resonance energy transfer (FRET) (Didenko 2001). During qPCR, the probe anneals to the target sequence located between the two primers. As amplicon elongation comes to the probe's position, the probe is cleaved by DNA polymerase and hence released from the template. As a result, quenchers no longer repress the fluorescent signal of the reporters. The two types of fluorescent reporters (SYBR green and hydrolysis probes) are expected to bring identical results in qPCR experiments. As SYBR green chemistry does not require specific probes, it tends to be more cost-effective, especially when there are many target genes to be studied. However, SYBR green chemistry may have a relatively low specificity compared to hydrolysis probes. For example, it can bind to any dsDNA, including primer dimers. Therefore, melting curve experiments following qPCR amplification are

recommended to detect potential false positive (Bustin et al. 2009). The specificity of SYBR green chemistry can also be verified via electrophoresis and further sequencing. On the other hand, hydrolysis probe chemistry provides excellent specificity and possibilities for multiplexing (detecting more than one gene within a single well). However, it requires an extra design step for probes and potentially costs more.

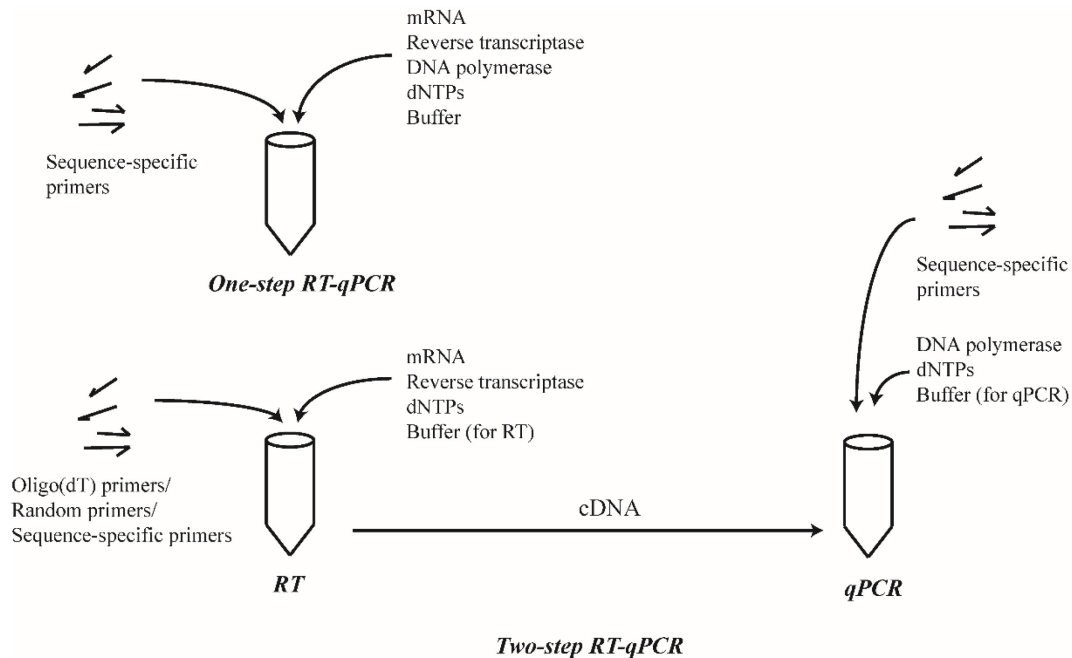


Figure 2.5 Schematic of one-step and two-step RT-qPCR experiments. Adapted based on an original figure in (ThermoFisher Scientific 2019).

The Minimum Information for Publication of Quantitative Real-Time PCR Experiments (MIQE) (Bustin et al. 2009) was proposed to describe general standards and requirements for qPCR experiments. Some critical points that are specific to the comparative quantification purpose can be found in the MIQE and qPCR handbooks (e.g., Thermo Fisher, 2016); they are described below.

Firstly, potential primer dimerization needs to be eliminated, particularly when SYBR green reagents are used. The best way to avoid primer dimerization is to have solid primer design procedures. A prediction of primer structure and self-complementarity should be incorporated.

Secondly, controls and normalization are essential. Regarding controls, both no-template and no-reverse transcriptase controls are required. These are mainly focusing on the detection of primer dimerization and genomic DNA contamination, respectively. As for normalization, the use of reference genes addresses virtually every source of variabilities for an RT-qPCR experiment, in comparison with normalization performed with cell numbers prior to RNA purification, RNA quantities prior to reverse transcription, or cDNA quantities in advance of qPCR experiments. This is to say, other normalization steps are important, but the implementation of reference genes is more crucial to the final results of relative gene expression. Ideally, selected reference genes are expected to be expressed consistently in every condition examined in an investigation. Normalization performed with at least two reference genes during a single assay is strongly recommended, increasing the accuracy of relative expression results and providing more reliable qPCR data.

Thirdly, a standard or calibration curve, correlating cDNA amounts from a series of dilutions (usually, 5 orders of magnitude) to the number of quantification cycles (C_q for short), should be determined for each gene before performing relative quantification. This is used to assess efficiency, sensitivity, and reproducibility of qPCR reactions. The acceptable range of efficiency is 90 – 110 %, corresponding to slopes of linearized standard curves between -3.1 ng^{-1} and -3.6 ng^{-1} (Efficiency = $10^{[-1/\text{slope}]}$). The lowest concentration of cDNA input that allows 95% positive detection can also be determined via the standard curve experiment if appropriate dilution ranges are set. For each curve, the R^2 value of a linear regression should exceed 0.99, which indicates good reproducibility. The amounts of cDNA to be used in further comparative quantification experiments must be selected from the linear dynamic range inferred from the standard curve. Also, when differences in amplification efficiencies between genes of interest and the reference genes cannot be neglected, efficiency correction should be employed during comparative quantification. In that case, the $\Delta\Delta C_t$ method is corrected by the efficiencies, and the corresponding equations for comparative quantification are used (Livak and Schmittgen 2001).

Finally, melting curve experiments should be performed following qPCR amplification cycles for SYBR green chemistries. This is a critical step that examines the specificity of qPCR amplification and the fitness of the designed primers. Careful primer design, no-template control, standard curve experiment, and melting curve experiment ensure that the primers are appropriate

for comparative qPCR experiments and that the target sequences are amplified with great specificity.

2.3 *Saccharomyces cerevisiae*

Saccharomyces cerevisiae, commonly referred to as baker's yeast, is one of the most used eukaryotic model organisms in laboratories due to its well-studied genome (it was the first eukaryote to be sequenced) (Goffeau et al. 1996) and the ease of manipulation. As gene sequence similarities between *S. cerevisiae* and *Homo sapiens* were identified (Foury 1997), *S. cerevisiae* has been utilized in a wide range of biological and biomedical studies focusing on DNA repair (Girard and Boiteux 1997; Boiteux and Jinks-Robertson 2013), telomeres (Teng and Zakian 1999; Askree et al. 2004; Wellinger and Zakian 2012), autophagy (Huang and Klionsky 2002; Suzuki and Ohsumi 2007), mitophagy (Abeliovich 2011; Müller et al. 2015), etc. As a microbial factory, *S. cerevisiae* has also been used in the bioproduction of a large variety of valuable chemicals, such as bioethanol (Hossain et al. 2017; Mohd Azhar et al. 2017), specialty chemicals (Markham and Alper 2015), and recombinant proteins (Porro et al. 2011; Çelik and Çalik 2012).

2.3.1 Life Cycle of *S. cerevisiae*

The life cycle of *S. cerevisiae* is composed of two broad aspects, cell proliferation and ploidy changes (Figure 2.6) (Herskowitz 1988). During cell proliferation (the mitotic cell cycle), an ellipsoidal “daughter” cell grows out from the “mother” cell by way of budding. In contrast with fission, in which the pinching-off of the enlarged initial cell results in two daughter cells, in budding the daughter cell is made of entirely new surface material (Herskowitz 1988). When nutrients are depleted, or another yeast cell in the vicinity can mate, the yeast cell will abandon proliferation and be arrested in the G1 phase (see next section). All three types of *S. cerevisiae*, **a**, α , and **a**/ α , can undergo the mitotic cell cycle. Mating type **a** cells and mating type α cells are haploids, with one copy of their chromosomes; **a**/ α cells are diploids having two copies of their chromosomes. Mating type **a** cells have an allele of *MATa*, while mating type α possesses one allele of *MAT α* . **a**/ α cells have both alleles. With the assistance of **a**-factor and α -factor (the mating factors, produced by type **a** cells and type α cells, respectively, and affecting the opposing mating

types of cells), two different types of haploid cells can mate and produce diploid cells by fusion. Upon nutrient starvation, four haploid meiotic progenies, two *a* cells and two α cells, are produced by one *a*/ α cell through sporulation.

In this thesis, only mating type α cells are utilized, so only mitotic division (and no meiosis) occurs throughout fermentation.

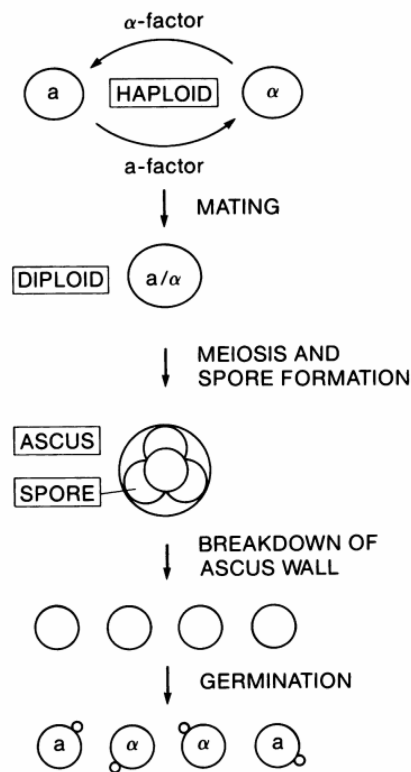


Figure 2.6 Schematic of the life cycle of *S. cerevisiae* (Herskowitz 1988). (Original figure reuse with permission from American Society for Microbiology)

2.3.2 Cell Cycle of *S. cerevisiae*

The mitotic cell cycle of *S. cerevisiae* is comprised of interphase and mitosis (Figure 2.7) (Feldmann 2012). The interphase is composed of the G1 phase (a pre-synthetic gap), S phase (DNA synthesis) and G2 phase (a post-synthetic gap). Mitosis (M phase) is constituted of prophase (chromosome condensation), metaphase (chromosome alignment), anaphase (chromosome separation), and telophase (chromosome decondensation) (Feldmann 2012). During the cell cycle,

three control points (Feldmann 2012) must successfully be passed to ensure serene progression of cell replication. START is the first control point situated in the late G1 phase. Before START, cells can choose to either enter the mitotic cycle (with adequate nutrients and a critical size reached) or initiate a sexual program (under starvation conditions, for instance). The second control point, which ensures complete DNA replication, lies in the late G2 phase. The third control point, which checks the correct alignment of chromosomes and proper formation of the spindle, is localized prior to anaphase. Cyclins (*Cln* and *Clb*) and cyclin-dependent kinases (CDKs) are gene products significantly involved in the regulation of cell replication, including the aforementioned control points. Cyclins, as the regulatory subunits of CDKs, are expressed periodically and activate CDKs at the appropriate time during the cell cycle (Feldmann 2012).

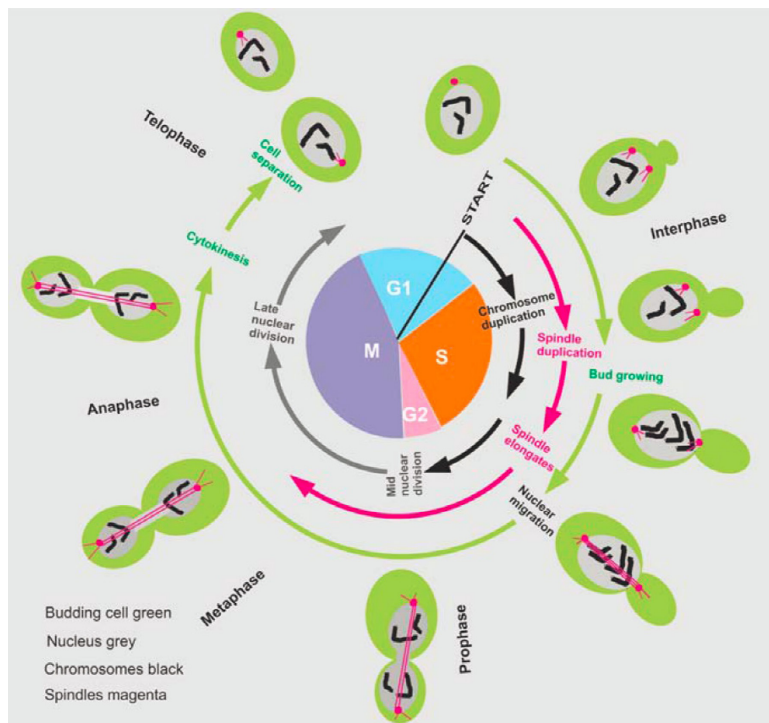


Figure 2.7 Schematic for the cell cycle of *S. cerevisiae* (Feldmann 2012). (Original figure reuse with permission from Wiley)

2.3.3 *S. cerevisiae* Growth in Batch Reactors

Generally, the growth of *S. cerevisiae* in BR is comprised of lag phase, log phase, diauxic shift, post-diauxic phase, stationary phase, and death phase (Radonjic et al. 2005). In this case, diauxic growth does not manifest itself from the presence of two types of main carbon sources in fresh medium. Rather, the main carbon source in the medium, typically glucose, based on which *S. cerevisiae*, as a facultative anaerobe (Lagunas 1981), can respire in aerobic conditions and ferment in the absence of oxygen. Most often than not, large amounts of ethanol are produced even in aerobic conditions since the respiratory bottleneck is reached when the specific growth rates pass 0.3 h^{-1} (Postma et al. 1989). From a metabolic perspective, once a high glycolytic rate leads to a rapid increase in the level of pyruvate, the pyruvate dehydrogenase complex is overwhelmed and excessive pyruvate cannot be converted to acetyl-CoA and shuttled to the citrate cycle (Otterstedt et al. 2004). Therefore, respiration is interrupted and the pyruvate overflow is diverted to the formation of ethanol via pyruvate decarboxylase (Otterstedt et al. 2004). Another proposed mechanism lies in the insufficiency of acetaldehyde dehydrogenase, which catalyzes acetate formation (Postma et al. 1989). Consequently, the second stage of diauxic growth primarily relies on ethanol previously produced, rather than initially added to the medium. This phenomenon is referred to as the Crabtree Effect (Crabtree 1929) and is recognized as a “make-accumulate-consume” life strategy used by *S. cerevisiae* to outcompete other microorganisms (Hagman et al. 2013). Log phase (or exponential phase) refers to the specific period when biomass increases in a logarithmic manner. A diauxic shift is a transition phase between log phase growth on glucose and post-diauxic growth on ethanol, which allows the yeast cells to adapt to the new carbon source. To some extent, the diauxic shift resembles a lag phase, as adaptation is the main theme for both phases and little or no biomass growth occurs in either stages (Chu and Barnes 2016).

A previous microarray study (Radonjic et al. 2005) revealed RNA polymerase II leading to the rapid response of *S. cerevisiae* upon the exit of stationary phase, wherein genome-wide expression were investigated during different stages of yeast growth. Total RNA for a fixed number of cells peaked exclusively during log phase (Radonjic et al. 2005). So did the expression ratios of ribosome-related genes (Radonjic et al. 2005). Similarly, another study (DeRisi et al. 1997) implemented DNA microarray hybridization and identified the up-regulation of genes related to the citrate cycle and down-regulation of genes associated with ribosomal proteins and

tRNA synthetase around the point of glucose exhaustion. Besides, a recent proteomics study from the same group (Murphy et al. 2015) uncovered some accordant trends in protein profiles and many more during the diauxic shift, including: induced protein profiles related to the citrate cycle, oxidative phosphorylation, fatty acid oxidation, proteolysis, stress response, etc.; and repressed protein profiles associated with ribosomal biogenesis, amino acid transport, RNA-mediated transposition, etc. A study (Pelechano and Pérez-Ortín 2010) assisted by genomic run-on (GEO) depicted the correctness of considering transcriptome steady-state during log-phase growth of *S. cerevisiae*. However, the investigation only involved mid-log phase samples with OD₆₀₀ from 0.36 to 0.47 in YPD medium (Pelechano and Pérez-Ortín 2010), which is a considerably short time window.

For *S. cerevisiae*, a feed-forward control strategy (Levy and Barkai 2009) infers that the cells can proactively regulate gene expression once sensing external changes, and a passive adjustment of the specific growth rate will follow accordingly with some time delay. In contrast, a feedback control strategy suggests external changes impact the specific growth rate in the first place, and changes in the transcriptome were induced due to growth rate variations (Levy and Barkai 2009). A deduction of the feed-forward control scheme has been given in a previous *S. cerevisiae* study (Ju and Warner 1994) investigating ribosome synthesis during growth phases through Northern analysis and pulse labeling. In this study, ribosomes per cell and transcriptions related to ribosome biosynthesis were found to unexpectedly decline while a log growth rate was still retained. It was concluded that the yeast cells could sense unfavorable changes proactively and modulate ribosome synthesis and degradation based on an estimation of the growth potential (Ju and Warner 1994). Actively reacting to the forthcoming nutrient deprivation has been written in the yeast genome, which benefits its survival during natural selections (Murphy et al. 2015).

2.4 Shikimic Acid

Shikimic acid, or shikimate (in its anionic form), is an intermediary metabolite in the aromatic amino acids (phenylalanine, tyrosine, and tryptophan) biosynthesis pathway found in microorganisms and plants (Ghosh et al. 2012; Estevez and Estevez 2012; Rawat et al. 2013a). This natural accruing compound can be used to produce many aromatic compounds, among others.

Perhaps its best-known application might be its use as a precursor for synthesizing an anti-flu medication known as Oseltamivir (also known under the brand name Tamiflu) (Ghosh et al. 2012; Rawat et al. 2013b; Martínez et al. 2015). Oseltamivir targets influenza neuraminidase, an enzyme necessary for viral replication. Hence, this medication can be used in the treatment and prophylaxis for both type A and type B influenza infections (McClellan and Perry 2001). The chemical structures of shikimic acid and Oseltamivir can be found in Figure 2.8.

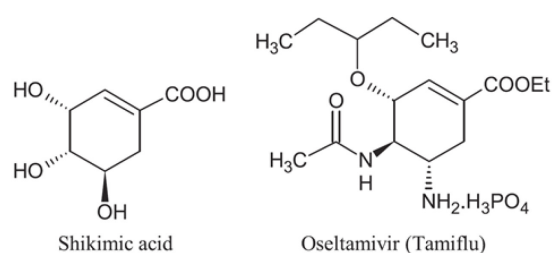


Figure 2.8 The chemical structures of shikimic acid and Oseltamivir (Ghosh et al. 2012). (Original figure reuse with permission from Elsevier)

Shikimic acid was first isolated from Japanese star anise (*Illicium anisatum*, inedible and highly toxic) in 1880s (Eijkman 1885). So far, shikimic acid has been found and extracted from sweetgum tree (*Liquidambar styraciflua*) (Enrich et al. 2008), Scots pine (*Pinus sylvestris*) (Sui 2008), and other plants. Shikimic acid is now commercially extracted from edible, nontoxic Chinese star anise (*Illicium verum*) (Rawat et al. 2013b). In fact, nearly 90% of the world Chinese star anise is consumed to extract shikimic acid, whereas the high demand for Oseltamivir during flu epidemics has once resulted in insufficient supplies of shikimic acid (Estevez and Estevez 2012; Martínez et al. 2015). In addition, planting and recovery are tedious and expensive and can result in mediocre yield (Rawat et al. 2013b). Chinese star anise plants need to grow for six years before allowing shikimic acid extraction from the seeds (Martínez et al. 2015). Usually, multi-step extraction starts from hot water extraction since shikimic acid has high solubility in water (Ghosh et al. 2012). Overall, nearly 30 kg of Chinese star anise seeds are required to extract one kg of shikimic acid; ~1.3 g shikimic acid is required to treat only one flu patient once converted to Oseltamivir (Martínez et al. 2015). Chemical synthesis of shikimic acid, a potential alternative

production route, is far from commercialization, though investigations are ongoing (Ghosh et al. 2012).

Consequently, many efforts have been made to engineer shikimic acid synthesis pathways in bacteria (Knop et al. 2001; Ghosh et al. 2012; Rawat et al. 2013b; Tripathi et al. 2013; Liu et al. 2014; Martínez et al. 2015; Zhang et al. 2016) and yeast (Mookerjee 2016; Suástegui and Shao 2016; Suástegui et al. 2016, 2017; Gao et al. 2017) to overproduce shikimic acid during fermentation. Assuming a sufficient yield can be achieved, the fermentation route can compete economically with the plant-based extraction route (Martínez et al. 2015). Models of these microorganisms that integrate omics data can assist rational metabolic engineering and thus improve shikimic acid production (Martínez et al. 2015). Interestingly, some inorganic catalysts can aid in shikimic acid bioproduction. For example, the presence of light-sensitive indium phosphide nanoparticles that catalyze NADPH reduction resulted in an overproduction of shikimic acid in engineered *S. cerevisiae* ($\Delta zwf1$) (Guo et al. 2018).

2.4.1 Yeast Producing Shikimic Acid

With regard to overproduction of shikimic acid in yeast, (Suástegui et al. 2016) should be the first publication that have described shikimic acid production in metabolically engineered *S. cerevisiae* strains. In this study, insertion of *ARO4* K229L, *ARO1* D920A, and *TKL1* via plasmids led to production of shikimic acid at a titer of 358 mg/L and a yield of 17.9 mg/g glucose (based on 20 g/L glucose) in shake flasks (productivity not mentioned), and it was the greatest production based on implementation of four *S. cerevisiae* strains. However, it should be noted that tryptophan, phenylalanine, and tyrosine were required to be supplemented (50 mg/L each) during fermentation to suppress shikimic acid further conversion to aromatic amino acids and to result in a successful accumulation of shikimic acid.

Furthermore, (Suástegui et al. 2017) has incorporated computational tools and established a multilevel engineering approach, leading to exceptional production of shikimic acid – as high as 2.0 g/L using 4 % glucose and 2.5 g/L using 4 % sucrose. Insightful suggestions provided by this article, e.g., deletion of *RIC1* and overexpression of *RKII*, should be followed in further strain engineering of *S. cerevisiae*. However, it should be noted that supplementation of aromatic amino

acids was required for all strains incorporating depletion of constitutive *ARO1* (including the best shikimic acid producing strain) to establish reasonable growth rates according to this article.

Remarkably, a nonconventional yeast platform, *Scheffersomyces stipites*, has also been engineered to produce shikimic acid at a titer of 3.11 g/L, representing the greatest production (so far) of shikimate in yeast (Gao et al. 2017). It would be of great interest to combine the advanced fermentation systems with this novel yeast platform.

A shikimic acid-producing *S. cerevisiae* strain based on the parental strain CEN.PK 113-1A *MAT α* has also been engineered (Mookerjee 2016). This strain has shown significant production of shikimic acid, while the parental strain has not; no supplementation of aromatic amino acids is needed. A schematic of the engineered pathway used in this work is presented in Figure 2.9. *E. coli* genes, *ARO B* and *ARO D* , were inserted; the constitutive *ARO 3* gene was deleted; and the constitutive *ARO 4* gene was substituted by the tyrosine feedback-resistant variant *ARO 4* K229L. These modifications were introduced in a pYES plasmid which allows auxotrophic selection. As the constitutive *URA 3* gene has been deleted, only cells containing the plasmid *URA 3* gene can synthesize uracil for cell growth.

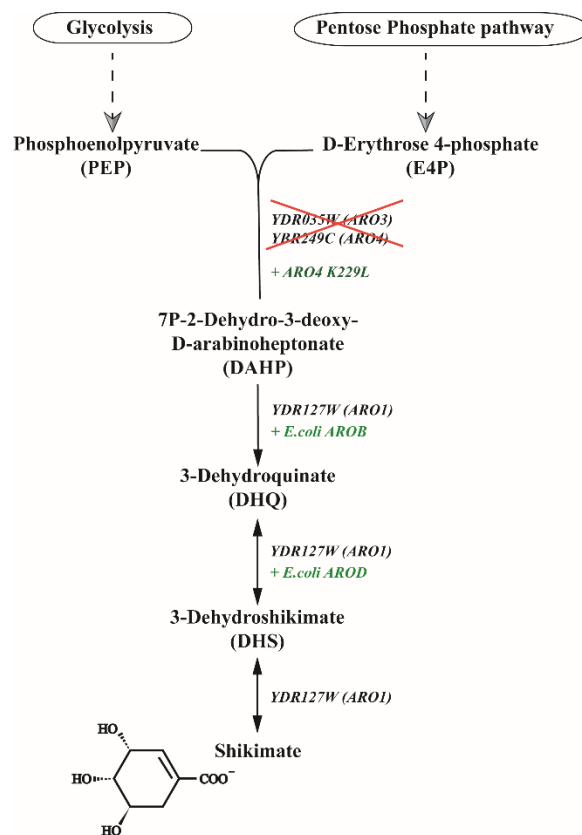


Figure 2.9 Schematic of metabolic engineering of a *S. cerevisiae* strain to overproduce shikimic acid (Mookerjee 2016).

2.5 *Escherichia coli*

Escherichia coli is a rod-shaped Gram-negative bacterium and a facultative anaerobe (Poolman 2016). It was first isolated from human fecal matter in 1885 (Escherich and Bettelheim 1888) and is commonly found in the gut of vertebrates (Tenaillon et al. 2010). Some *E. coli* strains are harmless, commensally constituting a part of the normal microbiota of the gut, even preventing infections from pathogenic bacteria (Hudault et al. 2001). However, extraintestinal pathogenic *E. coli* can cause bacteremia, urinary tract infections, neonatal meningitis, etc. (Poolman and Wacker 2016; Bonten et al. 2020), and intestinal pathogenic *E. coli* can cause intestinal diseases (Lindstedt et al. 2018). Food poisoning issues related to pathogenic *E. coli* are amongst the causes of increasing public concerns (Vogt and Dippold 2005; Currie et al. 2019).

E. coli is the most commonly used prokaryotic model organism. Given its well-understood genomic sequences (Blattner et al. 1997) and the ease of laboratory handling, a large number of studies have been conducted on *E. coli*. For example, it has been used in investigations of biological processes (such as phage infection (Bertani 1951; Bruttin and Brüssow 2005; Brüssow 2005; Korf et al. 2019; Zalewska-Piątek and Piątek 2020) and conjugation (Trieu-Cuot et al. 1987; Mazodier et al. 1989; Stabb and Ruby 2002; Phornphisutthimas et al. 2007)), building foundations of biological engineering (such as restriction enzymes (Lautenberger and Linn 1972; Roberts 1990; Kasarjian et al. 2003), recombinant DNA (Hennecke et al. 1982; Gushima et al. 1983), plasmid development (Vidal et al. 2008; Bubnov et al. 2018), etc.), heterologous protein production (Baneyx 1999), valuable chemical production (Clomburg and Gonzalez 2010), etc. The development of strains and cassettes of *E. coli* aids in many other research fields, for instance, structural biology (Fairman et al. 2011; Yan 2015), vaccine development (Ihssen et al. 2010; Wacker et al. 2014), biofuel production (Clomburg and Gonzalez 2010; Liu and Khosla 2010; Huffer et al. 2012), environmental studies (Verma and Kuila 2019; Wang et al. 2019), etc.

Consequently, there is a continuous interest in producing *E. coli* cells at large scales, and the SCF technique has been used to efficiently cultivate *E. coli* (ATCC 11303) using CER as the control parameter (Sauvageau et al. 2010). SCF operation was stable and reproducible, and synchrony of the *E. coli* population was achieved (Sauvageau et al. 2010).

2.6 *Methylovimicrobium buryatense* 5GB1C

Methanotrophic bacteria utilize methane or methanol, single carbon substrates, as their sole carbon source (Trotsenko and Murrell 2008). Methane is converted to methanol by the enzyme methane monooxygenase (MMO). Methanol, from methane oxidation or as the initial substrate, is oxidized to formaldehyde through methanol dehydrogenase (MDH). Formaldehyde can be further oxidized to formate by formaldehyde dehydrogenase or through the tetrahydromethanopterin pathway (Khmelenina et al. 2018). In addition, formaldehyde can be assimilated via the serine cycle in alphaproteobacterial methanotrophs (type II), while it can be incorporated in the ribulose monophosphate (RuMP) cycle in gammaproteobacterial methanotrophs (type I) (Khmelenina et al. 2018). Formate can be further oxidized to carbon dioxide (CO₂) via formate dehydrogenase.

Many species and strains of methanotrophs can be used for the bioconversion of the potent greenhouse gas methane and the low-valued chemical methanol into biomass and other valuable bioproducts. The gammaproteobacterial methanotroph “*Methylotheobacterium buryatense*” 5GB1C, or “*Methylomicrobium buryatense*” 5GB1C before its recent reclassification (Orata et al. 2018), stands out as an industrially promising strain, thanks to its relatively short doubling time, great resilience to potential contamination as a haloalkaliphile, and multiple genetic manipulation tools readily available.

M. buryatense 5GB1C is a variant of *M. buryatense* 5GB1 with intentional curing of its native plasmid, allowing conjugation with small vectors (Puri et al. 2015). Hence, *M. buryatense* 5GB1C is more genetically tractable while maintains most of the properties of *M. buryatense* 5GB1. Their parental strain, *M. buryatense* 5G, was first isolated from a soda lake in the Transbaikal region of Russia (Kaluzhnaya et al. 2001). For this haloalkaliphile, high pH and salinity of the media (Kaluzhnaya et al. 2001) can significantly reduce the risks of contamination. It also shows great tolerance to heat, desiccation, and freeze-drying and could be grown in a wide range of conditions (Kaluzhnaya et al. 2001). The specific growth rates of *M. buryatense* 5GB1 are appreciably high, $\sim 0.23 \text{ h}^{-1}$ on methane and $\sim 0.17 \text{ h}^{-1}$ on methanol (Gilman et al. 2015), facilitating its laboratory manipulations and potential industrial applications.

In regards to genetic engineering potential, the genome of *M. buryatense* 5GB1C has been published (NCBI Genome, ID 13071); small vectors and a sucrose counterselection system have been developed for conjugation-based genetic manipulations (Puri et al. 2015); electroporation-based genetic manipulation approaches have also been established, requiring fewer steps in gene insertions and deletions on the chromosomes (Yan et al. 2016); and a stoichiometric flux balance model has been developed, with which a direct coupling of electron transfer between methane oxidation and methanol oxidation was confirmed (Torre et al. 2015). Lactate production was improved significantly through insertion of a *Lactobacillus helveticus* L-lactate dehydrogenase (Henard et al. 2016). *farE* deletion increased the C18-fatty acid methyl ester pool (Demidenko et al. 2017), and overexpression of PktB (a phosphoketolase) enriched acetyl-CoA by 2-fold and increased lipids abundance by 2.6-fold (Henard et al. 2017). By diversion of the carbon flux from acetyl-CoA, *M. buryatense* 5GB1C was engineered to produce C4 carboxylic acids (Garg et al. 2018).

As shown in Figure 2.10, when *M. buryatense* 5GB1 is grown on methanol, the central carbon metabolism starts from methanol oxidation to formaldehyde (Fu et al. 2019). Then, formaldehyde is shuttled to CO₂ through further oxidations or incorporated in the RuMP cycle. C6 sugar phosphates from the RuMP cycle can enter glycolysis through the EMP and ED pathways or be involved in glycogen synthesis. After glycolysis is the TCA cycle followed by the serine cycle.

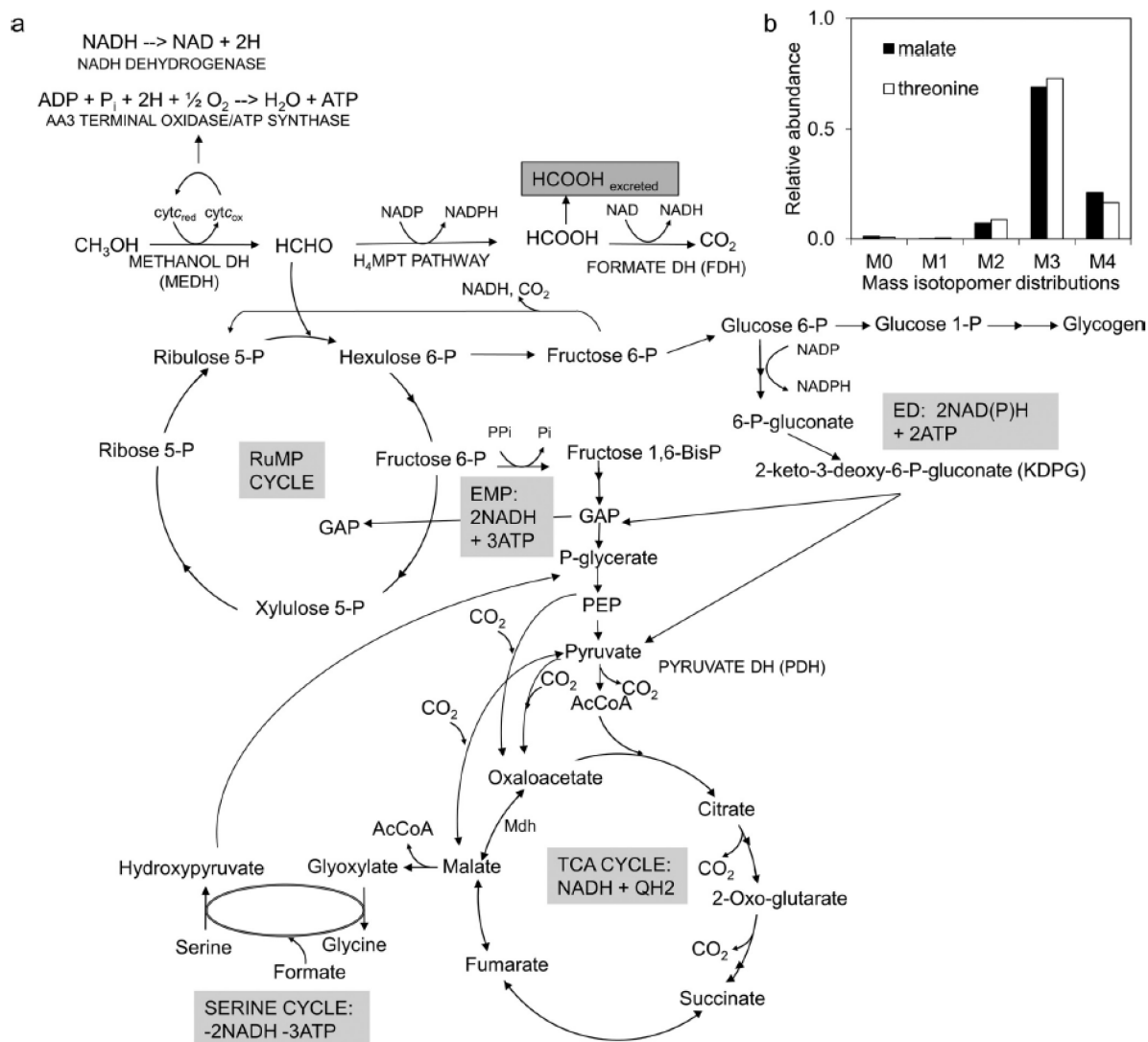


Figure 2.10 Central carbon metabolic pathways of *M. buryatense* 5GB1 grown on methanol (Fu et al. 2019). (Original figure reuse with permission from American Society for Microbiology)

It has been shown that formate and glycogen were intensively produced by *M. buryatense* 5GB1 when methanol was used as the carbon source, compared to methane (Gilman et al. 2015). Also, when growth was based on methanol (compared to methane), a ^{13}C tracer approach and a targeted metabolomics combined with a flux distribution model demonstrated significantly increased metabolic activity in the synthesis of formaldehyde, formate, and glycogen, the ED pathway, and the serine cycle, but decreased activity in methane oxidation, the EMP pathway, and the TCA cycle (Fu et al. 2019). ^{13}C nonstationary metabolic flux analysis identified that *M. buryatense* 5GB1C, grown either on methanol or methane, assimilated the single carbon molecules through a strong RuMP cycle and preferentially through the EMP pathway for glycolysis; the TCA cycle showed small but significant fluxes (He et al. 2019). The ED pathway, another glycolysis pathway, though, has shown to be essential for the healthy growth of the bacterium (He et al. 2020). Moreover, a complete, oxidative TCA cycle was identified for *M. buryatense* 5GB1 using ^{13}C tracer analysis (Fu et al. 2017).

Methanotroph-mediated methane conversion has been reviewed, with focus on mass transfer aspects, bioreactor configurations, methane operation safety, etc. (Stone et al. 2017) Notable applications include the use of packed-bed reactors as methane biofilters for gas streams with low methane concentration. The use of methanol in methanotroph cultivations, rather than methane, may largely mitigate mass transfer limitations, considering advantages in liquid-liquid transfer over the gas-liquid transfer.

2.7 References

- Abeliovich H (2011) Stationary-phase mitophagy in respiring *Saccharomyces cerevisiae*. Antioxid Redox Signal 14:2003–2011. <https://doi.org/10.1089/ars.2010.3807>
- Afgan E, Baker D, Batut B, et al (2018) The Galaxy platform for accessible, reproducible and collaborative biomedical analyses: 2018 update. Nucleic Acids Res 46:537–544. <https://doi.org/10.1093/nar/gky379>
- Agustin RVC (2015) The Impact of Self-Cycling Fermentation on the Production of Shikimic Acid in Populations of Engineered *Saccharomyces cerevisiae*. University of Alberta

- Anders S (2010) Babraham Bioinformatics - FastQC A Quality Control tool for High Throughput Sequence Data. <https://www.bioinformatics.babraham.ac.uk/projects/fastqc/>. Accessed 1 Nov 2021
- Anders S, Pyl PT, Huber W (2015) HTSeq--a Python framework to work with high-throughput sequencing data. *Bioinformatics* 31:166–169. <https://doi.org/10.1093/bioinformatics/btu638>
- Ashburner M, Ball CA, Blake JA, et al (2000) Gene ontology: Tool for the unification of biology. *Nat Genet* 25:25–29. <https://doi.org/10.1038/75556>
- Askree SH, Yehuda T, Smolikov S, et al (2004) A genome-wide screen for *Saccharomyces cerevisiae* deletion mutants that affect telomere length. *Proc Natl Acad Sci U S A* 101:8658–8663. <https://doi.org/10.1073/pnas.0401263101>
- Baneyx F (1999) Recombinant protein expression in *Escherichia coli*. *Curr Opin Biotechnol* 10:411–421. [https://doi.org/10.1016/S0958-1669\(99\)00003-8](https://doi.org/10.1016/S0958-1669(99)00003-8)
- Bates D, Epstein J, Boye E, et al (2005) The *Escherichia coli* baby cell column: a novel cell synchronization method provides new insight into the bacterial cell cycle. *Mol Microbiol* 57:380–391. <https://doi.org/10.1111/j.1365-2958.2005.04693.x>
- Bertani G (1951) Studies on lysogenesis. I. The mode of phage liberation by lysogenic *Escherichia coli*. *J Bacteriol* 62:293–300. <https://doi.org/10.1128/JB.62.3.293-300.1951>
- Blankenberg D, Hillman-Jackson J (2014) Analysis of next-generation sequencing data using galaxy. *Methods Mol Biol* 1150:21–43. https://doi.org/10.1007/978-1-4939-0512-6_2
- Blattner FR, Plunkett G, Bloch CA, et al (1997) The complete genome sequence of *Escherichia coli* K-12. *Science* (80-) 277:1453–1462. <https://doi.org/10.1126/science.277.5331.1453>
- Blumenthal LK, Zahler SA (1962) Index for measurement of synchronization of cell populations. *Science* (80-) 135:724. <https://doi.org/10.1126/science.135.3505.724.a>
- Boiteux S, Jinks-Robertson S (2013) DNA repair mechanisms and the bypass of DNA damage in *Saccharomyces cerevisiae*. *Genetics* 193:1025–1064. <https://doi.org/10.1534/genetics.112.145219>
- Bolger AM, Lohse M, Usadel B (2014) Trimmomatic: a flexible trimmer for Illumina sequence data. *Bioinformatics* 30:2114–2120. <https://doi.org/10.1093/bioinformatics/btu170>

- Bonten M, Johnson JR, van den Biggelaar AHJ, et al (2020) Epidemiology of *Escherichia coli* bacteremia: A systematic literature review. Clin Infect Dis. <https://doi.org/10.1093/cid/ciaa210>
- Boom R, Sol CJA, Salimans MMM, et al (1990) Rapid and simple method for purification of nucleic acids. J Clin Microbiol 28:495–503. <https://doi.org/10.1128/jcm.28.3.495-503.1990>
- Brown WA (2001) The self-cycling fermentor – development, applications, and future opportunities. In: Recent Research and Developments in Biotechnology and Bioengineering. pp 4: 61-90
- Brown WA, Cooper DG (1991) Self-cycling fermentation applied to *Acinetobacter calcoaceticus* RAG-1. Appl Environ Microbiol 57:2901–2906. <https://doi.org/10.1128/aem.57.10.2901-2906.1991>
- Brown WA, Cooper DG (1992) Hydrocarbon degradation by *Acinetobacter calcoaceticus* RAG-1 using the self-cycling fermentation technique. Biotechnol Bioeng 40:797–805. <https://doi.org/10.1002/bit.260400707>
- Brown WA, Cooper DG, Liss SN (2000) Toluene removal in an automated cyclical bioreactor. Biotechnol Prog 16:378–384. <https://doi.org/10.1021/bp0000149>
- Brown WA, Cooper DG, Liss SN (1999) Adapting the self-cycling fermentor to anoxic conditions. Environ Sci Technol 33:1458–1463. <https://doi.org/10.1021/ES980856S>
- Brüssow H (2005) Phage therapy: the *Escherichia coli* experience. Microbiology 151:2133–2140. <https://doi.org/10.1099/MIC.0.27849-0>
- Bruttin A, Brüssow H (2005) Human volunteers receiving *Escherichia coli* phage T4 orally: A safety test of phage therapy. Antimicrob Agents Chemother 49:2874–2878. <https://doi.org/10.1128/AAC.49.7.2874-2878.2005>
- Bubnov DM, Yuzbashev T V., Vybornaya T V., et al (2018) Development of new versatile plasmid-based systems for λ Red-mediated *Escherichia coli* genome engineering. J Microbiol Methods 151:48–56. <https://doi.org/10.1016/J.MIMET.2018.06.001>
- Bustin SA, Benes V, Garson JA, et al (2009) The MIQE guidelines: minimum information for publication of quantitative real-time PCR experiments. Clin Chem 55:611–22.

- <https://doi.org/10.1373/clinchem.2008.112797>
- Bustin SA, Benes V, Nolan T, Pfaffl MW (2005) Quantitative real-time RT-PCR--a perspective. *J Mol Endocrinol* 34:597–601. <https://doi.org/10.1677/jme.1.01755>
- Carmona-Saez P, Chagoyen M, Tirado F, et al (2007) GENECODIS: a web-based tool for finding significant concurrent annotations in gene lists. *Genome Biol* 8:R3. <https://doi.org/10.1186/gb-2007-8-1-r3>
- Çelik E, Çalik P (2012) Production of recombinant proteins by yeast cells. *Biotechnol Adv* 30:1108–1118. <https://doi.org/10.1016/j.biotechadv.2011.09.011>
- Chan K-Y, Cheng CY (1977) Synchronization of cell division in marine bacteria by amino acid starvation. *FEMS Microbiol Lett* 2:177–180. <https://doi.org/10.1111/j.1574-6968.1977.tb00934.x>
- Cho RJ, Campbell MJ, Winzler EA, et al (1998) A genome-wide transcriptional analysis of the mitotic cell cycle. *Mol Cell* 2:65–73. [https://doi.org/10.1016/S1097-2765\(00\)80114-8](https://doi.org/10.1016/S1097-2765(00)80114-8)
- Chomczynski P, Sacchi N (1987) Single-step method of RNA isolation by acid guanidinium thiocyanate-phenol-chloroform extraction. *Anal Biochem* 162:156–159. [https://doi.org/10.1016/0003-2697\(87\)90021-2](https://doi.org/10.1016/0003-2697(87)90021-2)
- Chu D, Barnes DJ (2016) The lag-phase during diauxic growth is a trade-off between fast adaptation and high growth rate. *Sci Rep* 6:1–15. <https://doi.org/10.1038/srep25191>
- Chu Y, Corey DR (2012) RNA sequencing: platform selection, experimental design, and data interpretation. *Nucleic Acid Ther* 22:271–4. <https://doi.org/10.1089/nat.2012.0367>
- Clomburg JM, Gonzalez R (2010) Biofuel production in *Escherichia coli*: The role of metabolic engineering and synthetic biology. *Appl Microbiol Biotechnol* 86:419–434. <https://doi.org/10.1007/s00253-010-2446-1>
- Conesa A, Madrigal P, Tarazona S, et al (2016) A survey of best practices for RNA-seq data analysis. *Genome Biol* 17:13. <https://doi.org/10.1186/s13059-016-0881-8>
- Costa-Silva J, Domingues D, Lopes FM (2017) RNA-Seq differential expression analysis: An extended review and a software tool. *PLoS One* 12:e0190152. <https://doi.org/10.1371/journal.pone.0190152>

- Crabtree HG (1929) Observations on the carbohydrate metabolism of tumours. *Biochem J* 23:536–545. <https://doi.org/10.1042/bj0230536>
- Crosman JT, Pinchuk RJ, Cooper DG (2002) Enhanced biosurfactant production by *Corynebacterium alkanolyticum* ATCC 21511 using self-cycling fermentation. *J Am Oil Chem Soc* 79:467–472. <https://doi.org/10.1007/s11746-002-0507-5>
- Currie A, Honish L, Cutler J, et al (2019) Outbreak of *Escherichia coli* O157:H7 Infections Linked to Mechanically Tenderized Beef and the Largest Beef Recall in Canada, 2012. *J Food Prot* 82:1532–1538. <https://doi.org/10.4315/0362-028X.JFP-19-005>
- Dawson PSS (1965) Continuous phased growth, with a modified chemostat. *Can J Microbiol* 11:893–903. <https://doi.org/10.1139/m65-119>
- Dawson PSS (1972) Continuously synchronised growth. *J Appl Chem Biotechnol* 22:79–103. <https://doi.org/10.1002/jctb.2720220112>
- Dawson PSS (1970) Cell cycle and post cycle changes during continuous phased growth of *Candida utilis*. *Can J Microbiol* 16:783–795. <https://doi.org/10.1139/m70-132>
- Demidenko A, Akberdin IR, Allemann M, et al (2017) Fatty Acid Biosynthesis Pathways in *Methylomicrobium buryatense* 5G(B1). *Front Microbiol* 0:2167. <https://doi.org/10.3389/FMICB.2016.02167>
- DeRisi JL, Iyer VR, Brown PO (1997) Exploring the metabolic and genetic control of gene expression on a genomic scale. *Science* (80-) 278:680–686. <https://doi.org/10.1126/science.278.5338.680>
- Didenko V V (2001) DNA probes using fluorescence resonance energy transfer (fret): Designs and applications. *Biotechniques* 31:1106–1121. <https://doi.org/10.2144/01315rv02>
- Dobin A, Davis CA, Schlesinger F, et al (2013) STAR: ultrafast universal RNA-seq aligner. *Bioinformatics* 29:15–21. <https://doi.org/10.1093/bioinformatics/bts635>
- Eijkman JF (1885) Sur les principes constituants de l’*Illicium religiosum* (Sieb.) (Shikimi-no-ki en japonais). *Recl des Trav Chim des Pays-Bas* 4:32–54. <https://doi.org/10.1002/recl.18850040202>
- Enrich LB, Scheuermann ML, Mohadjer A, et al (2008) *Liquidambar styraciflua*: a renewable

- source of shikimic acid. *Tetrahedron Lett* 49:2503–2505.
<https://doi.org/10.1016/j.tetlet.2008.02.140>
- Escherich T, Bettelheim KS (1888) The intestinal bacteria of the neonate and breast-fed infant. *Rev Infect Dis* 10:1220–1225. <https://doi.org/10.2307/4454681>
- Estevez AM, Estevez RJ (2012) A short overview on the medicinal chemistry of (—)-shikimic acid. *Mini-Reviews Med Chem* 12:1443–1454.
<https://doi.org/10.2174/138955712803832735>
- Fairman JW, Noinaj N, Buchanan SK (2011) The structural biology of β -barrel membrane proteins: a summary of recent reports. *Curr Opin Struct Biol* 21:523–531.
<https://doi.org/10.1016/J.SBI.2011.05.005>
- Feldmann H (2012) *Yeast: Molecular and Cell Biology*. Wiley-Blackwell
- Ferullo DJ, Cooper DL, Moore HR, Lovett ST (2009) Cell cycle synchronization of *Escherichia coli* using the stringent response, with fluorescence labeling assays for DNA content and replication. *Methods* 48:8–13. <https://doi.org/10.1016/j.ymeth.2009.02.010>
- Foury F (1997) Human genetic diseases: A cross-talk between man and yeast. *Gene* 195:1–10.
[https://doi.org/10.1016/S0378-1119\(97\)00140-6](https://doi.org/10.1016/S0378-1119(97)00140-6)
- Fu Y, He L, Reeve J, et al (2019) Core metabolism shifts during growth on methanol versus methane in the methanotroph *Methylomicrobium buryatense* 5GB1. *MBio* 10:.
<https://doi.org/10.1128/mBio.00406-19>
- Fu Y, Li Y, Lidstrom M (2017) The oxidative TCA cycle operates during methanotrophic growth of the Type I methanotroph *Methylomicrobium buryatense* 5GB1. *Metab Eng* 42:43–51. <https://doi.org/10.1016/j.ymben.2017.05.003>
- Gao M, Cao M, Suástegui M, et al (2017) Innovating a nonconventional yeast platform for producing shikimate as the building block of high-value aromatics. *ACS Synth Biol* 6:29–38. <https://doi.org/10.1021/acssynbio.6b00132>
- Garg S, Wu H, Clomburg JM, Bennett GN (2018) Bioconversion of methane to C-4 carboxylic acids using carbon flux through acetyl-CoA in engineered *Methylomicrobium buryatense* 5GB1C. *Metab Eng* 48:175–183. <https://doi.org/10.1016/j.ymben.2018.06.001>

- Ghosh S, Chisti Y, Banerjee UC (2012) Production of shikimic acid. *Biotechnol Adv* 30:1425–1431. <https://doi.org/10.1016/j.biotechadv.2012.03.001>
- Gilman A, Laurens LM, Puri AW, et al (2015) Bioreactor performance parameters for an industrially-promising methanotroph *Methylomicrobium buryatense* 5GB1. *Microb Cell Fact* 14:182. <https://doi.org/10.1186/s12934-015-0372-8>
- Girard PM, Boiteux S (1997) Repair of oxidized DNA bases in the yeast *Saccharomyces cerevisiae*. *Biochimie* 79:559–566. [https://doi.org/10.1016/S0300-9084\(97\)82004-4](https://doi.org/10.1016/S0300-9084(97)82004-4)
- Goecks J, Nekrutenko A, Taylor J, Galaxy Team T (2010) Galaxy: a comprehensive approach for supporting accessible, reproducible, and transparent computational research in the life sciences. *Genome Biol* 11:R86. <https://doi.org/10.1186/gb-2010-11-8-r86>
- Goffeau A, Barrell G, Bussey H, et al (1996) Life with 6000 genes. *Science* (80-) 274:546–567. <https://doi.org/10.1126/science.274.5287.546>
- Guo J, Suástegui M, Sakimoto KK, et al (2018) Light-driven fine chemical production in yeast biohybrids. *Science* (80-) 362:813–816. <https://doi.org/10.1126/science.aat9777>
- Gushima H, Miya T, Murata K, Kimura A (1983) Construction of glutathione-producing strains of *Escherichia coli* B by recombinant DNA techniques. *J Appl Biochem* 5:43–52
- Hagman A, Säll T, Compagno C, Piskur J (2013) Yeast “make-accumulate-consume” life strategy evolved as a multi-step process that predates the whole genome duplication. *PLoS One* 8:e68734. <https://doi.org/10.1371/journal.pone.0068734>
- He L, Fu Y, Lidstrom ME (2019) Quantifying Methane and Methanol Metabolism of “*Methylotuvimicrobium buryatense*” 5GB1C under Substrate Limitation. *mSystems* 4:. <https://doi.org/10.1128/msystems.00748-19>
- He L, Groom JD, Lidstrom ME (2020) The Entner-Doudoroff Pathway Is an Essential Metabolic Route for *Methylotuvimicrobium Buryatense* 5GB1C. *Appl Environ Microbiol* 87:1–11. <https://doi.org/10.1128/AEM.02481-20>
- Heid CA, Stevens J, Livak KJ, Williams PM (1996) Real time quantitative PCR. *Genome Res* 6:986–94. <https://doi.org/10.1101/GR.6.10.986>
- Henard CA, Smith H, Dowe N, et al (2016) Bioconversion of methane to lactate by an obligate

- methanotrophic bacterium. *Sci Rep* 6:1–9. <https://doi.org/10.1038/srep21585>
- Henard CA, Smith HK, Guarnieri MT (2017) Phosphoketolase overexpression increases biomass and lipid yield from methane in an obligate methanotrophic biocatalyst. *Metab Eng* 41:152–158. <https://doi.org/10.1016/J.YMBEN.2017.03.007>
- Hennecke H, Günther I, Binder F (1982) A novel cloning vector for the direct selection of recombinant DNA in *E. coli*. *Gene* 19:231–234. [https://doi.org/10.1016/0378-1119\(82\)90011-7](https://doi.org/10.1016/0378-1119(82)90011-7)
- Herskowitz I (1988) Life cycle of the budding yeast *Saccharomyces cerevisiae*. *Microbiol Rev* 52:536–553. <https://doi.org/10.1128/membr.52.4.536-553.1988>
- Hirsch I, Vondrejs V (1971) Division of *Escherichia coli* 15 TAU cells synchronized by arginine and uracil starvation. *Folia Microbiol (Praha)* 16:137–141. <https://doi.org/10.1007/BF02887484>
- Hossain N, Zaini JH, Mahlia TMI (2017) A review of bioethanol production from plant-based waste biomass by yeast fermentation. *Int J Technol* 8:5–18. <https://doi.org/10.14716/ijtech.v8i1.3948>
- Huang W-P, Klionsky DJ (2002) Autophagy in yeast: A review of the molecular machinery. *Cell Struct Funct* 27:409–420. <https://doi.org/10.1247/csf.27.409>
- Hudault S, Guignot J, Servin AL (2001) *Escherichia coli* strains colonising the gastrointestinal tract protect germfree mice against *Salmonella typhimurium* infection. *Gut* 49:47–55. <https://doi.org/10.1136/gut.49.1.47>
- Huffer S, Roche CM, Blanch HW, Clark DS (2012) *Escherichia coli* for biofuel production: bridging the gap from promise to practice. *Trends Biotechnol* 30:538–545. <https://doi.org/10.1016/J.TIBTECH.2012.07.002>
- Hughes SM, Cooper DG (1996) Biodegradation of phenol using the self-cycling fermentation (SCF) process. *Biotechnol Bioeng* 51:112–119. [https://doi.org/10.1002/\(SICI\)1097-0290\(19960705\)51:1<112::AID-BIT13>3.0.CO;2-S](https://doi.org/10.1002/(SICI)1097-0290(19960705)51:1<112::AID-BIT13>3.0.CO;2-S)
- Ihssen J, Kowarik M, Dilettoso S, et al (2010) Production of glycoprotein vaccines in *Escherichia coli*. *Microb Cell Factories* 2010 9:1–13. <https://doi.org/10.1186/1475-2859->

- Ishii T (2014) Transcriptome Analysis of Adrenocortical Cells in Health and Disease. In: Cellular Endocrinology in Health and Disease. Elsevier, pp 169–192
- Ju Q, Warner JR (1994) Ribosome synthesis during the growth cycle of *Saccharomyces cerevisiae*. *Yeast* 10:151–157. <https://doi.org/10.1002/yea.320100203>
- Kaluzhnaya M, Khmelenina V, Eshinimaev B, et al (2001) Taxonomic characterization of new alkaliphilic and alkalitolerant methanotrophs from soda lakes of the Southeastern Transbaikal region and description of *Methylomicrobium buryatense* sp.nov. *Syst Appl Microbiol* 24:166–176. <https://doi.org/10.1078/0723-2020-00028>
- Kanehisa M, Goto S (2000) KEGG: Kyoto Encyclopedia of Genes and Genomes. *Nucleic Acids Res* 28:27–30. <https://doi.org/10.1093/nar/28.1.27>
- Kasarjian JKA, Iida M, Ryu J (2003) New restriction enzymes discovered from *Escherichia coli* clinical strains using a plasmid transformation method. *Nucleic Acids Res* 31:e22–e22. <https://doi.org/10.1093/NAR/GNG022>
- Khmelenina VN, Colin Murrell J, Smith TJ, Trotsenko YA (2018) Physiology and Biochemistry of the Aerobic Methanotrophs. In: Aerobic Utilization of Hydrocarbons, Oils and Lipids. Springer International Publishing, pp 1–25
- Kim D, Langmead B, Salzberg SL (2015) HISAT: a fast spliced aligner with low memory requirements. *Nat Methods* 12:357–360. <https://doi.org/10.1038/nmeth.3317>
- Knop DR, Draths KM, Chandran SS, et al (2001) Hydroaromatic equilibration during biosynthesis of shikimic acid. *J Am Chem Soc* 123:10173–10182. <https://doi.org/10.1021/ja0109444>
- Korf IHE, Meier-Kolthoff JP, Adriaenssens EM, et al (2019) Still Something to Discover: Novel Insights into *Escherichia coli* Phage Diversity and Taxonomy. *Viruses* 2019, Vol 11, Page 454 11:454. <https://doi.org/10.3390/V11050454>
- Krueger F (2017) Babraham Bioinformatics - Trim Galore! In: Version 0.4.4. https://www.bioinformatics.babraham.ac.uk/projects/trim_galore/. Accessed 1 Nov 2021
- Lagunas R (1981) Is *Saccharomyces cerevisiae* a typical facultative anaerobe? *Trends Biochem*

- Sci 6:201–203. [https://doi.org/10.1016/0968-0004\(81\)90073-6](https://doi.org/10.1016/0968-0004(81)90073-6)
- Langmead B, Salzberg SL (2012) Fast gapped-read alignment with Bowtie 2. *Nat Methods* 9:357–359. <https://doi.org/10.1038/nmeth.1923>
- Lautenberger JA, Linn S (1972) The deoxyribonucleic acid modification and restriction enzymes of *Escherichia coli* B. I. Purification, subunit structure, and catalytic properties of the modification methylase. *J Biol Chem* 247:6176–6182. [https://doi.org/10.1016/S0021-9258\(19\)44779-0](https://doi.org/10.1016/S0021-9258(19)44779-0)
- Levy S, Barkai N (2009) Coordination of gene expression with growth rate: A feedback or a feed-forward strategy? *FEBS Lett* 583:3974–3978. <https://doi.org/10.1016/j.febslet.2009.10.071>
- Liao Y, Smyth GK, Shi W (2014) featureCounts: an efficient general purpose program for assigning sequence reads to genomic features. *Bioinformatics* 30:923–930. <https://doi.org/10.1093/bioinformatics/btt656>
- Lindstedt BA, Finton MD, Porcellato D, Brandal LT (2018) High frequency of hybrid *Escherichia coli* strains with combined Intestinal Pathogenic *Escherichia coli* (IPEC) and Extraintestinal Pathogenic *Escherichia coli* (ExPEC) virulence factors isolated from human faecal samples. *BMC Infect Dis* 18:. <https://doi.org/10.1186/s12879-018-3449-2>
- Liu DF, Ai GM, Zheng QX, et al (2014) Metabolic flux responses to genetic modification for shikimic acid production by *Bacillus subtilis* strains. *Microb Cell Fact* 13:1–11. <https://doi.org/10.1186/1475-2859-13-40>
- Liu T, Khosla C (2010) Genetic engineering of *Escherichia coli* for biofuel production. *Annu. Rev. Genet.* 44:53–69
- Livak KJ, Schmittgen TD (2001) Analysis of relative gene expression data using real-time quantitative PCR and the $2^{-\Delta\Delta CT}$ method. *Methods* 25:402–408. <https://doi.org/10.1006/METH.2001.1262>
- Love MI, Huber W, Anders S (2014) Moderated estimation of fold change and dispersion for RNA-seq data with DESeq2. *Genome Biol* 15:550. <https://doi.org/10.1186/s13059-014-0550-8>

- Marchessault P, Sheppard JD (1997) Application of self-cycling fermentation technique to the production of poly- β -hydroxybutyrate. *Biotechnol Bioeng* 55:815–820.
[https://doi.org/10.1002/\(SICI\)1097-0290\(19970905\)55:5<815::AID-BIT12>3.0.CO;2-A](https://doi.org/10.1002/(SICI)1097-0290(19970905)55:5<815::AID-BIT12>3.0.CO;2-A)
- Markham KA, Alper HS (2015) Synthetic Biology for Specialty Chemicals. *Annu Rev Chem Biomol Eng* 6:35–52. <https://doi.org/10.1146/annurev-chembioeng-061114-123303>
- Martínez JA, Bolívar F, Escalante A (2015) Shikimic acid production in *Escherichia coli*: From classical metabolic engineering strategies to omics applied to improve its production. *Front Bioeng Biotechnol* 3:145. <https://doi.org/10.3389/fbioe.2015.00145>
- Mazodier P, Petter R, Thompson C (1989) Intergeneric conjugation between *Escherichia coli* and *Streptomyces* species. *J Bacteriol* 171:3583–3585.
<https://doi.org/10.1128/JB.171.6.3583-3585.1989>
- McCaffrey WC, Cooper DG (1995) Sophorolipids production by *Candida bombicola* using self-cycling fermentation. *J Ferment Bioeng* 79:146–151. [https://doi.org/10.1016/0922-338X\(95\)94082-3](https://doi.org/10.1016/0922-338X(95)94082-3)
- McClellan K, Perry CM (2001) Oseltamivir: A review of its use in influenza. *Drugs* 61:263–283.
<https://doi.org/10.2165/00003495-200161020-00011>
- Metsalu T, Vilo J (2015) ClustVis: A web tool for visualizing clustering of multivariate data using Principal Component Analysis and heatmap. *Nucleic Acids Res* 43:W566–W570.
<https://doi.org/10.1093/nar/gkv468>
- Miller C, Schwalb B, Maier K, et al (2011) Dynamic transcriptome analysis measures rates of mRNA synthesis and decay in yeast. *Mol Syst Biol* 7:458.
<https://doi.org/10.1038/msb.2010.112>
- Miller SA, Dykes DD, Polesky HF (1988) A simple salting out procedure for extracting DNA from human nucleated cells. *Nucleic Acids Res* 16:1215.
<https://doi.org/10.1093/nar/16.3.1215>
- Mohd Azhar SH, Abdulla R, Jambo SA, et al (2017) Yeasts in sustainable bioethanol production: A review. *Biochem Biophys Reports* 10:52–61. <https://doi.org/10.1016/j.bbrep.2017.03.003>
- Mookerjee S (2016) Directing Precursor Flux to Optimize cis,cis-Muconic Acid Production in

Saccharomyces cerevisiae. Concordia University

Müller M, Lu K, Reichert AS (2015) Mitophagy and mitochondrial dynamics in *Saccharomyces cerevisiae*. *Biochim Biophys Acta - Mol Cell Res* 1853:2766–2774.

<https://doi.org/10.1016/j.bbamcr.2015.02.024>

Murphy JP, Stepanova E, Everley RA, et al (2015) Comprehensive temporal protein dynamics during the diauxic shift in *Saccharomyces cerevisiae*. *Mol Cell Proteomics* 14:2454–2465.

<https://doi.org/10.1074/mcp.M114.045849>

Orata FD, Meier-Kolthoff JP, Sauvageau D, Stein LY (2018) Phylogenomic analysis of the gammaproteobacterial methanotrophs (order methylococcales) calls for the reclassification of members at the genus and species levels. *Front Microbiol* 9:3162.

<https://doi.org/10.3389/fmicb.2018.03162>

Otterstedt K, Larsson C, Bill RM, et al (2004) Switching the mode of metabolism in the yeast *Saccharomyces cerevisiae*. *EMBO Rep* 5:532–537.

<https://doi.org/10.1038/sj.embor.7400132>

Pelechano V, Pérez-Ortín JE (2010) There is a steady-state transcriptome in exponentially growing yeast cells. *Yeast* 27:413–422. <https://doi.org/10.1002/yea.1768>

Pertea M, Kim D, Pertea GM, et al (2016) Transcript-level expression analysis of RNA-seq experiments with HISAT, StringTie and Ballgown. *Nat Protoc* 11:1650–1667.

<https://doi.org/10.1038/nprot.2016.095>

Phornphisutthimas S, Thamchaipenet A, Panijpan B (2007) Conjugation in *Escherichia coli*. *Biochem Mol Biol Educ* 35:440–445. <https://doi.org/10.1002/BMB.113>

Pinchuk RJ, Brown WA, Hughes SM, Cooper DG (2000) Modeling of biological processes using self-cycling fermentation and genetic algorithms. *Biotechnol Bioeng* 67:19–24.

[https://doi.org/10.1002/\(SICI\)1097-0290\(2000105\)67:1<19::AID-BIT3>3.0.CO;2-C](https://doi.org/10.1002/(SICI)1097-0290(2000105)67:1<19::AID-BIT3>3.0.CO;2-C)

Ponchel F, Toomes C, Bransfield K, et al (2003) Real-time PCR based on SYBR-Green I fluorescence: An alternative to the TaqMan assay for a relative quantification of gene rearrangements, gene amplifications and micro gene deletions. *BMC Biotechnol* 3:18.

<https://doi.org/10.1186/1472-6750-3-18>

- Poolman JT (2016) *Escherichia coli*. In: International Encyclopedia of Public Health. Elsevier Inc., pp 585–593
- Poolman JT, Wacker M (2016) Extraintestinal pathogenic *Escherichia coli*, a common human pathogen: challenges for vaccine development and progress in the field. *J Infect Dis* 213:6–13. <https://doi.org/10.1093/infdis/jiv429>
- Porro D, Gasser B, Fossati T, et al (2011) Production of recombinant proteins and metabolites in yeasts. *Appl Microbiol Biotechnol* 89:939–948. <https://doi.org/10.1007/s00253-010-3019-z>
- Postma E, Verduyn C, Scheffers WA, Van Dijken JP (1989) Enzymic analysis of the crabtree effect in glucose-limited chemostat cultures of *Saccharomyces cerevisiae*. *Appl Environ Microbiol* 55:468–477. <https://doi.org/10.1128/aem.55.2.468-477.1989>
- Puri AW, Owen S, Chu F, et al (2015) Genetic tools for the industrially promising methanotroph *Methylomicrobium buryatense*. *Appl Environ Microbiol* 81:1775–1781. <https://doi.org/10.1128/AEM.03795-14>
- Radonjic M, Andrau JC, Lijnzaad P, et al (2005) Genome-wide analyses reveal RNA polymerase II located upstream of genes poised for rapid response upon *S. cerevisiae* stationary phase exit. *Mol Cell* 18:171–183. <https://doi.org/10.1016/j.molcel.2005.03.010>
- Rawat G, Tripathi P, Jahan F, Saxena RK (2013a) A natural isolate producing shikimic acid: isolation, identification, and culture condition optimization. *Appl Microbiol Biotechnol* 169:2290–2302. <https://doi.org/10.1007/s12010-013-0150-1>
- Rawat G, Tripathi P, Saxena RK (2013b) Expanding horizons of shikimic acid: Recent progresses in production and its endless frontiers in application and market trends. *Appl Microbiol Biotechnol* 97:4277–4287. <https://doi.org/10.1007/s00253-013-4840-y>
- Roberts RJ (1990) Restriction enzymes and their isoschizomers. *Nucleic Acids Res* 18:2331. <https://doi.org/10.1093/NAR/18.SUPPL.2331>
- Robinson MD, McCarthy DJ, Smyth GK (2010) edgeR: a Bioconductor package for differential expression analysis of digital gene expression data. *Bioinformatics* 26:139–140. <https://doi.org/10.1093/bioinformatics/btp616>
- Sarkis BE, Cooper DG (1994) Biodegradation of aromatic compounds in a self-cycling

- fermenter (SCF). *Can J Chem Eng* 72:874–880. <https://doi.org/10.1002/cjce.5450720514>
- Sauvageau D, Cooper DG (2010) Two-stage, self-cycling process for the production of bacteriophages. *Microb Cell Fact* 9:1–10. <https://doi.org/10.1186/1475-2859-9-81>
- Sauvageau D, Storms Z, Cooper DG (2010) Synchronized populations of *Escherichia coli* using simplified self-cycling fermentation. *J Biotechnol* 149:67–73. <https://doi.org/10.1016/J.JBIOTECH.2010.06.018>
- Syednasrollah F, Laiho A, Elo LL (2015) Comparison of software packages for detecting differential expression in RNA-seq studies. *Brief Bioinform* 16:59–70. <https://doi.org/10.1093/bib/bbt086>
- Sheppard JD (1993) Improved volume control for self-cycling fermentations. *Can J Chem Eng* 71:426–430. <https://doi.org/10.1002/cjce.5450710312>
- Sheppard JD, Cooper DG (1990) Development of computerized feedback control for the continuous phasing of *Bacillus subtilis*. *Biotechnol Bioeng* 36:539–545. <https://doi.org/10.1002/bit.260360514>
- Sheppard JD, Cooper DG (1991) The response of *Bacillus subtilis* ATCC 21332 to manganese during continuous-phased growth. *Appl Microbiol Biotechnol* 35:72–76. <https://doi.org/10.1007/BF00180639>
- Sheppard JD, Dawson PSS (1999) Cell synchrony and periodic behaviour in yeast populations. *Can J Chem Eng* 77:893–902. <https://doi.org/10.1002/cjce.5450770515>
- Stabb E V., Ruby EG (2002) RP4-based plasmids for conjugation between *Escherichia coli* and members of the Vibrionaceae. *Methods Enzymol* 358:413–426. [https://doi.org/10.1016/S0076-6879\(02\)58106-4](https://doi.org/10.1016/S0076-6879(02)58106-4)
- Stone KA, Hilliard M V., He QP, Wang J (2017) A mini review on bioreactor configurations and gas transfer enhancements for biochemical methane conversion. *Biochem Eng J* 128:83–92. <https://doi.org/10.1016/j.bej.2017.09.003>
- Storms ZJ, Brown T, Sauvageau D, Cooper DG (2012) Self-cycling operation increases productivity of recombinant protein in *Escherichia coli*. *Biotechnol Bioeng* 109:2262–2270. <https://doi.org/10.1002/bit.24492>

- Suástegui M, Guo W, Feng X, Shao Z (2016) Investigating strain dependency in the production of aromatic compounds in *Saccharomyces cerevisiae*. *Biotechnol Bioeng* 113:2676–2685. <https://doi.org/10.1002/bit.26037>
- Suástegui M, Shao Z (2016) Yeast factories for the production of aromatic compounds: from building blocks to plant secondary metabolites. *J Ind Microbiol Biotechnol* 43:1611–1624. <https://doi.org/10.1007/s10295-016-1824-9>
- Suástegui M, Yu Ng C, Chowdhury A, et al (2017) Multilevel engineering of the upstream module of aromatic amino acid biosynthesis in *Saccharomyces cerevisiae* for high production of polymer and drug precursors. *Metab Eng* 42:134–144. <https://doi.org/10.1016/j.ymben.2017.06.008>
- Sui R (2008) Separation of shikimic acid from pine needles. *Chem Eng Technol* 31:469–473. <https://doi.org/10.1002/ceat.200700413>
- Suzuki K, Ohsumi Y (2007) Molecular machinery of autophagosome formation in yeast, *Saccharomyces cerevisiae*. *FEBS Lett* 581:2156–2161. [https://doi.org/10.1016/J.FEBSLET.2007.01.096@10.1002/\(ISSN\)1873-3468.NOBELPRIZEAUTOPHAGY](https://doi.org/10.1016/J.FEBSLET.2007.01.096@10.1002/(ISSN)1873-3468.NOBELPRIZEAUTOPHAGY)
- Tan Y, Agustin RVC, Stein LY, Sauvageau D (2021) Transcriptomic analysis of synchrony and productivity in self-cycling fermentation of engineered yeast producing shikimic acid. *Biotechnol Reports* 32:e00691. <https://doi.org/10.1016/j.btre.2021.e00691>
- Tenaillon O, Skurnik D, Picard B, Denamur E (2010) The population genetics of commensal *Escherichia coli*. *Nat Rev Microbiol* 8:207–217. <https://doi.org/10.1038/nrmicro2298>
- Teng S-C, Zakian VA (1999) Telomere-telomere recombination is an efficient bypass pathway for telomere maintenance in *Saccharomyces cerevisiae*. *Mol Cell Biol* 19:8083–8093. <https://doi.org/10.1128/mcb.19.12.8083>
- ThermoFisher Scientific (2019) Basic Principles of RT-qPCR | Thermo Fisher Scientific. <https://www.thermofisher.com/ca/en/home/brands/thermo-scientific/molecular-biology/molecular-biology-learning-center/molecular-biology-resource-library/spotlight-articles/basic-principles-rt-qpcr.html>. Accessed 22 Jul 2021

- Torre A, Metivier A, Chu F, et al (2015) Genome-scale metabolic reconstructions and theoretical investigation of methane conversion in *Methylobacterium buryatense* strain 5G(B1). *Microb Cell Fact* 14:188. <https://doi.org/10.1186/s12934-015-0377-3>
- Trapnell C, Pachter L, Salzberg SL (2009) TopHat: discovering splice junctions with RNA-Seq. *Bioinformatics* 25:1105–1111. <https://doi.org/10.1093/bioinformatics/btp120>
- Trapnell C, Roberts A, Goff L, et al (2012) Differential gene and transcript expression analysis of RNA-seq experiments with TopHat and Cufflinks. *Nat Protoc* 7:562–578. <https://doi.org/10.1038/nprot.2012.016>
- Trieu-Cuot P, Carlier C, Martin P, Courvalin P (1987) Plasmid transfer by conjugation from *Escherichia coli* to Gram-positive bacteria. *FEMS Microbiol Lett* 48:289–294. <https://doi.org/10.1111/J.1574-6968.1987.TB02558.X>
- Tripathi P, Rawat G, Yadav S, Saxena RK (2013) Fermentative production of shikimic acid: A paradigm shift of production concept from plant route to microbial route. *Bioprocess Biosyst Eng* 36:1665–1673. <https://doi.org/10.1007/s00449-013-0940-4>
- Trotsenko YA, Murrell JC (2008) Metabolic Aspects of Aerobic Obligate Methanotrophy {star, open}. *Adv Appl Microbiol* 63:183–229. [https://doi.org/10.1016/S0065-2164\(07\)00005-6](https://doi.org/10.1016/S0065-2164(07)00005-6)
- van Walsum GP, Cooper DG (1993) Self-cycling fermentation in a stirred tank reactor. *Biotechnol Bioeng* 42:1175–1180. <https://doi.org/10.1002/bit.260421007>
- Verma S, Kuila A (2019) Bioremediation of heavy metals by microbial process. *Environ Technol Innov* 14:100369. <https://doi.org/10.1016/J.ETI.2019.100369>
- Vidal L, Pinsach J, Striedner G, et al (2008) Development of an antibiotic-free plasmid selection system based on glycine auxotrophy for recombinant protein overproduction in *Escherichia coli*. *J Biotechnol* 134:127–136. <https://doi.org/10.1016/J.JBIOTECH.2008.01.011>
- Vogel C, Marcotte EM (2012) Insights into the regulation of protein abundance from proteomic and transcriptomic analyses. *Nat Rev Genet* 13:227–232. <https://doi.org/10.1038/nrg3185>
- Vogt RL, Dippold L (2005) *Escherichia coli* O157:H7 outbreak associated with consumption of ground beef, June–July 2002. *Public Health Rep* 120:174–178. <https://doi.org/10.1177/003335490512000211>

- Wacker M, Wang L, Kowarik M, et al (2014) Prevention of *Staphylococcus aureus* Infections by Glycoprotein Vaccines Synthesized in *Escherichia coli*. *J Infect Dis* 209:1551–1561. <https://doi.org/10.1093/INFDIS/JIT800>
- Wang J, Chae M, Beyene D, et al (2021) Co-production of ethanol and cellulose nanocrystals through self-cycling fermentation of wood pulp hydrolysate. *Bioresour Technol* 330:124969. <https://doi.org/https://doi.org/10.1016/j.biortech.2021.124969>
- Wang J, Chae M, Bressler DC, Sauvageau D (2020) Improved bioethanol productivity through gas flow rate-driven self-cycling fermentation. *Biotechnol Biofuels* 13:1–14. <https://doi.org/10.1186/s13068-020-1658-6>
- Wang J, Chae M, Sauvageau D, Bressler DC (2017) Improving ethanol productivity through self-cycling fermentation of yeast: a proof of concept. *Biotechnol Biofuels* 10:193. <https://doi.org/10.1186/s13068-017-0879-9>
- Wang W, Jiang F, Wu F, et al (2019) Biodetection and bioremediation of copper ions in environmental water samples using a temperature-controlled, dual-functional *Escherichia coli* cell. *Appl Microbiol Biotechnol* 2019 10316 103:6797–6807. <https://doi.org/10.1007/S00253-019-09984-9>
- Wang Z, Gerstein M, Snyder M (2009) RNA-Seq: a revolutionary tool for transcriptomics. *Nat Rev Genet* 10:57–63. <https://doi.org/10.1038/nrg2484>
- Wellinger RJ, Zakian VA (2012) Everything you ever wanted to know about *Saccharomyces cerevisiae* telomeres: Beginning to end. *Genetics* 191:1073–1105. <https://doi.org/10.1534/genetics.111.137851>
- Wentworth SD, Cooper DG (1996) Self-cycling fermentation of a citric acid producing strain of *Candida lipolytica*. *J Ferment Bioeng* 81:400–405. [https://doi.org/10.1016/0922-338X\(96\)85140-3](https://doi.org/10.1016/0922-338X(96)85140-3)
- Wincure BM, Cooper DG, Rey A (1995) Mathematical model of self-cycling fermentation. *Biotechnol Bioeng* 46:180–183. <https://doi.org/10.1002/bit.260460212>
- Yan N (2015) Structural Biology of the Major Facilitator Superfamily Transporters. *Annu Rev Biophys* 44:257–283. <https://doi.org/10.1146/annurev-biophys-060414-033901>

- Yan X, Chu F, Puri AW, et al (2016) Electroporation-based genetic manipulation in type I methanotrophs. *Appl Environ Microbiol* 82:2062–2069.
<https://doi.org/10.1128/AEM.03724-15>
- Yu L, Guo N, Yang Y, et al (2010) Microarray analysis of p-anisaldehyde-induced transcriptome of *Saccharomyces cerevisiae*. *J Ind Microbiol Biotechnol* 37:313–322.
<https://doi.org/10.1007/S10295-009-0676-Y>
- Zalewska-Piątek B, Piątek R (2020) Phage Therapy as a Novel Strategy in the Treatment of Urinary Tract Infections Caused by *E. Coli*. *Antibiot* 2020, Vol 9, Page 304 9:304.
<https://doi.org/10.3390/ANTIBIOTICS9060304>
- Zenaitis MG, Cooper DG (1994) Antibiotic production by *Streptomyces aureofaciens* using self-cycling fermentation. *Biotechnol Bioeng* 44:1331–1336.
<https://doi.org/10.1002/bit.260441109>
- Zhang B, Liu ZQ, Liu C, Zheng YG (2016) Application of CRISPRi in *Corynebacterium glutamicum* for shikimic acid production. *Biotechnol Lett* 38:2153–2161.
<https://doi.org/10.1007/s10529-016-2207-z>
- Zhu X, Zou S, Li Y, Liang Y (2017) Transcriptomic analysis of *Saccharomyces cerevisiae* upon honokiol treatment. *Res Microbiol* 168:626–635.
<https://doi.org/10.1016/J.RESMIC.2017.04.007>
- Methylovium buriatense* (ID 13071) - Genome - NCBI.
https://www.ncbi.nlm.nih.gov/genome/13071?genome_assembly_id=563816. Accessed 29 Jun 2021b

3. An Overview of Yeast Cell Synchronization

3.1 Abstract

Synchronization of microbial populations can serve many purposes, including facilitating biological studies that focus on cellular behaviors and mechanisms. In these cases, synchronization allows for the characterization of a population of synchronized cells instead of a single cell to infer cellular processes and properties. Although many different approaches can be undertaken, in general, synchronization primarily focuses on the achievement of cell cycle synchrony – the alignment of events and stages in the cell cycle.

Budding yeast *Saccharomyces cerevisiae* and fission yeast *Schizosaccharomyces pombe* have been used in numerous studies on molecular and structural events, and have helped gain insight into similar behaviors in higher eukaryotes. Unsurprisingly, a large number of findings in yeast cells relied on the implementation of synchronized populations. For instance, cell cycle-related genes, proteins, and events have been studied intensely in yeast often with the assistance of yeast cell synchronization techniques. This minireview highlights various methods that have been utilized to observe and obtain yeast cell synchrony, and a comparison of these methods and their implications is also briefly incorporated.

3.2 Introduction

Congregated Southeast Asian fireflies flashing in unison and sweat components inducing menstrual synchrony between individuals are perfect examples of synchrony in nature (Strogatz 1997). In addition to playing important roles in the behavior of many populations, the concept of synchrony can also aid in uncovering intricate biological events, responses and mechanisms in microorganisms and higher eukaryotic cells. In particular, the budding yeast *Saccharomyces cerevisiae* and the fission yeast *Schizosaccharomyces pombe* are important eukaryotic model organisms that share similar basic cellular mechanisms with human cells; hence they have been used in a wealth of biological studies on cellular processes (Forsburg 1999, 2005). Synchronized yeast populations, specifically, played significant roles in many of these studies (Forsburg and

Nurse 1991), as they provide the possibility of observing behaviors at the population level to effectively infer the behavior of individual cells. The ease of dealing with synchronized cell populations rather than single cells is manifest.

The yeast cell cycle is in many ways similar to that of higher eukaryotes: it is composed of the G1 phase (a presynthetic gap), S phase (DNA synthesis), G2 phase (a postsynthetic gap), and M phase (mitosis) (Forsburg and Nurse 1991; Feldmann 2012). Checkpoints along the cell cycle assure its successful and serene progression (Feldmann 2012). Growing to a critical size is a main criterion in *S. cerevisiae* cells deciding whether to pass the START checkpoint in the G1 phase (the restriction point for human cells) (Johnston et al. 1977; Schneider et al. 2004). As for *S. pombe*, a size control point is rather located in the G2 phase (Forsburg and Nurse 1991; Oliva et al. 2005). The buds of *S. cerevisiae* emerge during S phase and grow rapidly, concomitantly with the cell cycle progression and asymmetrically compared to the mother cells. *S. pombe*, in contrast, only grows in length during the cell cycle and symmetrically pinches off the enlarged mother cells via septation rather than budding. Consequently, the size of yeast cells is a reliable metric for the estimation of cell cycle progression (Smith et al. 2016; Tormos-Pérez et al. 2016; Rosebrock 2017a). Interestingly, cytokinesis occurs in S phase in *S. pombe* concomitantly with DNA replication, while it occurs within the M phase in *S. cerevisiae* (Oliva et al. 2005; Knutsen et al. 2011). Thereby, small cells, if isolated, would correspond to G1 phase for *S. cerevisiae*, but chiefly to G2 phase for *S. pombe* (Knutsen et al. 2011; Tormos-Pérez et al. 2016). The cell cycle phases in which yeast cells are arrested during the stationary phase are G1 for *S. cerevisiae* and G1/G2 for *S. pombe* (Hartwell et al. 1974; Costello et al. 1986). Cell division cycle (*CDC*) genes and cyclin genes are significantly involved in regulating the yeast cell cycle, and thereby, some are indispensable for its progression (Feldmann 2012). Of note, *cdc* mutants contributed to the early discovery of regulatory genes during the yeast cell cycle (Forsburg and Nurse 1991).

This being said, cell synchronization at the population level presents many challenges, perhaps the main one being that synchronization methods can directly affect cellular responses and behaviors. Hence the importance of differentiating between synchronous (cells being naturally merely in the same stage of their life cycle or selected accordingly) and synchronized (cells induced into synchrony through a forcing mechanism or intervention) populations.

This minireview focuses on different approaches used to achieve yeast cell synchronization. In most cases, yeast cells are selected/arrested at different positions during the cell cycle, depending on the methods being used; entrainment-induced synchrony is also seen in some other scenarios. Protocols (Foltman et al. 2016; Smith et al. 2016; Tormos-Pérez et al. 2016; Angeles Juanes 2017; Rosebrock 2017a) and reviews (Futcher 1999; Walker 1999; Sheppard and Dawson 1999) on this topic are available, but none provides a complete summary of approaches. This work summarizes synchronization methods and highlights recent approaches that are effective but often overlooked. The overview strives to provide a complete and quick introduction to yeast cell synchronization and to facilitate relevant advances.

3.3 Methods to Assess Cell Synchrony

A handy approach to determine the degree of synchrony of a microbial population lies in measuring the population cell number over time through microscopy or flow cytometry. In synchronous populations, the cell count doubles in a considerably short time window, practically stepwise, when the whole population completes cytokinesis. A pioneering work by Blumenthal and Zahler defined an equation for the synchrony index (see the equation below) in order to quantify the degree of synchrony based on cell count increases and the relative time needed for cell segregation compared to the entire growth time (Blumenthal and Zahler 1962). According to this measure, a completely synchronized population would have an index of 1 while a completely asynchronous population would have an index of 0. So, in general, a shorter time required for cell segregation leads to a synchrony index closer to 1. A cell population with a synchrony index of greater than 0.6 is considered to have a significant degree of synchronization (Brown 2001).

$F = N/N_0 - 2^{t/g}$, where F is the synchrony index; N represents cell number; t is the required time interval for an increase in cell number from N_0 to N . g represents the generation time (or doubling time) of an organism (Blumenthal and Zahler 1962).

Similarly, a budding index (the percentage of budded cells in the whole population) has been developed for *S. cerevisiae* (Richardson et al. 1989; Breeden 1997; Spellman et al. 1998;

Futcher 1999; Amon 2002; Manukyan et al. 2011; Foltman et al. 2016; Smith et al. 2016; Angeles Juanes 2017; Rosebrock 2017b); it can also be used to inversely infer the proportion of cells distributed in the G1 phase (G1 index) (Tian et al. 2012), hence suggesting a certain degree of synchrony. In *S. pombe* cells, synchrony can be reflected by a septation index (the percentage of cells with complete septa) (Kramhøft and Zeuthen 1975; Toda et al. 1983; Oliva et al. 2005; Luche and Forsburg 2009; Knutsen et al. 2011; Tormos-Pérez et al. 2016).

Another convenient metric for the characterization of populations is the DNA content. Propidium iodide/Sytox Green and 4',6-diamidino-2-phenylindole (DAPI), dyes commonly used for DNA staining, are implemented in flow cytometry and microscopy, respectively, to analyze cell cycle distribution (Gómez and Forsburg 2004; Knutsen et al. 2011; Foltman et al. 2016; Smith et al. 2016; Tormos-Pérez et al. 2016; Rosebrock 2017a). The 2C DNA peak in flow cytometry histogram plots becomes prominent once synchronized cell populations enter S phase (Foltman et al. 2016; Tormos-Pérez et al. 2016). On the other hand, counting binucleate cells and divided nuclei through microscopy specifies different stages in M phase (Futcher 1999; Gómez and Forsburg 2004; Foltman et al. 2016). Calcofluor can be applied together with DAPI to observe septation in *S. pombe* cells via microscopy (Gómez and Forsburg 2004; Luche and Forsburg 2009; Tormos-Pérez et al. 2016). Under the microscope, spindle staining using anti-tubulin antibodies aids in the identification of detailed cell cycle stages, although this method seems laborious (Pringle et al. 1991; Futcher 1999; Gómez and Forsburg 2004; Angeles Juanes 2017).

The size of yeast cells generally increases concomitantly with the progression of the cell cycle (Smith et al. 2016; Tormos-Pérez et al. 2016; Rosebrock 2017a). Thereby, cell size can be used to infer the stage of the cell cycle, and, in turn, most physical fractioning methods employ cell volume as a key parameter during separation. Coulter counting commonly contributes to the assessment of cell size distribution and, therefore, the assessment of synchrony (Smith et al. 2016; Angeles Juanes 2017; Rosebrock 2017a). Microscopy and flow cytometry can also serve for this purpose (Tormos-Pérez et al. 2016). For *S. cerevisiae*, the size of buds can also be measured via microscopy and used for the inference of the cell cycle stages (Foltman et al. 2016; Smith et al. 2016; Angeles Juanes 2017).

The regulation patterns of global and select genes during the yeast cell cycle have been investigated using DNA microarrays and Northern Blot; yeast cell synchrony was established

using elutriation, α -factor, and *cdc* mutants; cell cycle stage-specific genes were also identified (Fitch et al. 1992; Spellman et al. 1998; Cho et al. 1998; Oliva et al. 2005). In turn, identification of similar gene expression patterns should be able to evidence that cell replication under a condition or a process is in synchrony; relative expression levels of cell cycle phase-specific genes could also be used to assess the stages of the cell cycle which cells are corresponding to at different sampling points. Modern transcriptomic methods, such as RNA-Seq and real-time PCR, would also be used for these purposes.

3.4 Methods for Cell Synchrony

The techniques developed to obtain synchronous and synchronized yeast populations are generally comprised of physical and chemical approaches. The physical category includes methods of physical fractionation and physical synchrony induction (through, for example, temperature shifts). Chemical approaches include the utilization of essential-reaction inhibitors to growing cultures for chemical blockage and manipulation of the nutrient environment through nutrient deprivation or nutrient cycle.

These approaches to achieve synchronization can alternatively be grouped into two new categories: selection and induction. Physical selection is the only subset in the former category, while all other methods fall within induction. For most methods described here, log-phase cells are demanded as the starting materials, but for nutrient deprivation, cells in the stationary phase are needed.

3.4.1 Physical Selection

Compared to the induction methods (physical or chemical), physical selection brings the least perturbations to yeast cells, and as such can lead to synchronous, rather than synchronized, populations. They consist in selecting for cell subpopulations that are at the same stage in their cell cycle. The drawbacks rest on the requirement for specialized equipment and relatively small volumes of cells that can be handled.

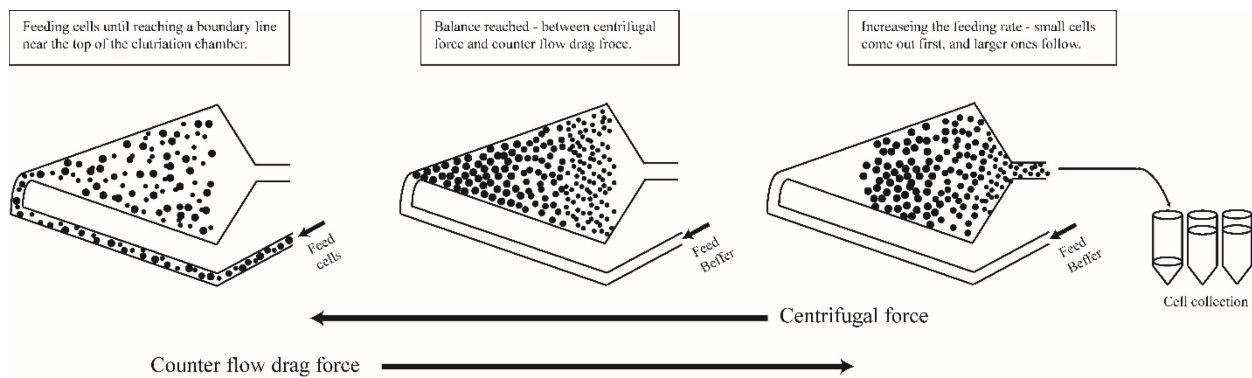


Figure 3.1 Schematic of experimental procedures of centrifugal elutriation. Adapted based on an original figure in (Johnston and Johnson 1997).

In centrifugal elutriations, two opposing forces – one from the feed pump and another from centrifugation – drive the fractionation of cells of different sizes in an elutriation rotor chamber (Creanor and Mitchison 1979; Johnston and Johnson 1997; Futcher 1999; Walker 1999; Amon 2002; Manukyan et al. 2011; Smith et al. 2016; Tormos-Pérez et al. 2016; Rosebrock 2017a). Figure 3.1 highlights the experimental procedures of centrifugal elutriation. Smaller cells, being in the early G1 phase for *S. cerevisiae* cells and in the late S/G2 phase for *S. pombe*, move further in the direction of counter flow drag force (i.e., the feeding force) and are collected at the onset of the separation process (Smith et al. 2016; Tormos-Pérez et al. 2016). Then, with increments in the fluid flow rate, larger cells come out (Smith et al. 2016). This method is based on the strong correlation between cell size and the stages in the cell cycle – the fact that cell volume increases with the progression of the cell cycle. The separation mechanism relies on the correlation between cell size and cell physical properties (flow and centrifugal laws). In order to reduce the influence of the centrifugal process on the intrinsic characteristics of the yeast cells, pre-chilled cells can be sent for elutriation (Smith et al. 2016), while other studies have suggested keeping cells at the growing temperature during elutriation and rendering cells to grow normally in the centrifugal chamber (Creanor and Mitchison 1979; Tormos-Pérez et al. 2016).

A lactose-gradient method has been reported for synchronization of *S. pombe* (Luche and Forsburg 2009; Tormos-Pérez et al. 2016). By implementing a lactose gradient for centrifugation, smaller cells in the early G2 phase could be collected in the upper sections of a centrifuged sample (Tormos-Pérez et al. 2016). There is no concern towards lactose-cell interactions as lactose cannot

be assimilated by *S. pombe* (Tormos-Pérez et al. 2016). Differential sedimentation of *S. cerevisiae* and *S. pombe* cells using sucrose gradients has also been used to select for small cells in top samples (Mitchison and Vincent 1965).

Baby machines have been used to collect newborn progeny cells within a short time window for various organisms, from prokaryotes to eukaryotes (Cooper 2002; Thornton et al. 2002). Although originally consisting of parent cells immobilized on a filter surface (adhesive-coated) and recently separated progeny cells being recovered in the flowthrough (Figure 3.2) (Thornton et al. 2002), in a recent study, the baby machine (or microfluidic synchronizer) comprised zigzagging polydimethylsiloxane channels with immobilized *S. pombe* cells in the slit array (Tian et al. 2013). Newly formed *S. pombe* cells were collected through pressure control via a syringe system (Tian et al. 2013). The collected cells presented a high degree of synchrony. Long-term cultivation was achieved in the microfluidic synchronizer, but *S. pombe* cells trapped in the slits are expected to have experienced some external forces and mass transfer limitations which could impact their behavior.

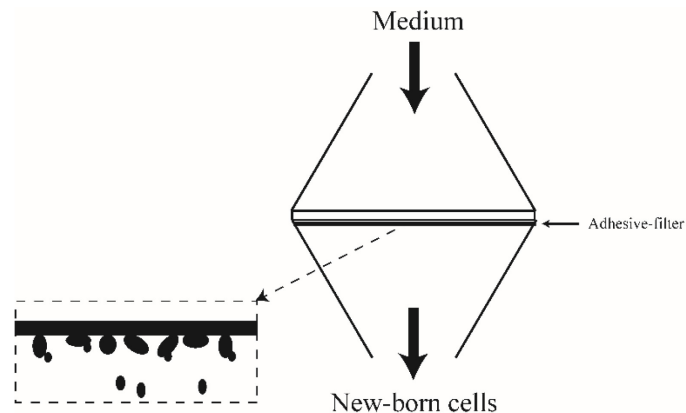


Figure 3.2 Schematic of a baby machine. Adapted based on an original figure in (Thornton et al. 2002).

A cell chip platform with micro-wall systems of specific dimensions was developed to capture small *S. cerevisiae* cells that are in the G1 phase (Hur et al. 2011). In contrast to baby machines, the micro-walls directly select for small cells from asynchronous populations, rather

than collecting newborn cells dividing from immobilized cells. The micro-wall systems presented similar synchronization effectiveness in *S. cerevisiae* compared to hydroxyurea blockage and were supposed to minimize unnecessary stresses to the cells (Hur et al. 2011).

Time-lapse microscopy can also be used to study individual *S. cerevisiae* cells in situ (Hartwell and Unger 1977; Lord and Wheals 1981; Bean et al. 2006; Di Talia et al. 2007; Yang et al. 2011; Smith et al. 2016); it is, to date, the only synchrony acquiring approach that has a single-cell resolution. In this technique, individual cells are imaged and tracked under the microscope while growing on a thin layer of agar. Combined with fluorescently labelled protein markers, time-lapse microscopy can become more powerful (Bean et al. 2006; Di Talia et al. 2007). Monitoring single-cell cellular behavior over time within an asynchronous population empowers the analysis of synchronous-equivalent populations with the aid of an algorithmic alignment based on parameters such as fluorescence peaks, fluorescence emergence and disappearance, and the time at which cell buds and at which cell divides (Hartwell and Unger 1977; Lord and Wheals 1981; Bean et al. 2006; Di Talia et al. 2007; Yang et al. 2011). Notably, this method is unobtrusive, hence barely causing any impact on the normal progression of the yeast cell cycle (Smith et al. 2016).

3.4.2 Physical Induction

Synchrony of yeast cell populations can be physically induced through, for example, temperature shifts. This synchronization strategy can handle larger culture volumes than physical selection methods, which, however, will be limited by heat transfer limitations to ensure the rapid shifts in temperature. Some variations in cellular regulation and response are expected, given the absence of indispensable proteins and the changes in temperature.

Elevated temperatures (e.g., 37 °C) lead to dysfunctions of essential Cdc proteins that have been mutated to present temperature-sensitive features (Manukyan et al. 2011). By inactivating different *cdc* mutants, the yeast cell cycle can be arrested at different stages. For instance, *cdc15-2* mutants block *S. cerevisiae* cells in the M phase at the restrictive temperature (Fitch et al. 1992; Futcher 1999; Rosebrock 2017a). *cdc10-129* and *cdc25-22* mutants are used to arrest *S. pombe* cell replication in G1 and late G2 phases, respectively (Tormos-Pérez et al. 2016). Many more *cdc*

temperature-sensitive mutants have been developed for *S. cerevisiae* and *S. pombe* (Walker 1999; Amon 2002; Gómez and Forsburg 2004; Smith et al. 2016; Angeles Juanes 2017). Returning cultures to a permissive temperature (e.g., 25 °C) allows the cell cycle to proceed. Inversely, cold-sensitive *nda3*-KM311 variants of *S. pombe* arrest the cells in M phase once a culture is placed in a cold environment (e.g., 20 °C) (Toda et al. 1983; Hiraoka et al. 1984; Tormos-Pérez et al. 2016).

Besides, heat-shock cycles can also align cell division without the involvement of *cdc* mutants. Simply by repetitively raising the temperature to 41 °C and returning to 32 °C, *S. pombe* cells were observed to divide in synchrony when released from heat shock for the 6th time (Kramhøft and Zeuthen 1975). Intervals between heat shocks were set to the doubling time of *S. pombe* at the non-restrictive temperature (Kramhøft and Zeuthen 1975). Synchrony should result from an entrainment effect as the lifted temperature is expected to impact differently on varying stages during the cell cycle.

3.4.3 Chemical Blockage

By leveraging specific inhibitory effects, chemical blockage can arrest cells at different stages of the yeast cell cycle; and releasing cells from the blockage, in turn, leads to a resumption of the progression of cell replication. An appreciable degree of synchrony can be achieved using this approach, but the disturbance of intrinsic cell metabolism is inevitable; the requirement of cell washes (in short timeframes) hinders scale-up of many of the methods. Examples of chemical blockage methods are found below.

The addition of hydroxyurea traps yeast cells in early S phase by inhibiting the synthesis of DNA (Futcher 1999; Foltman et al. 2016; Smith et al. 2016; Tormos-Pérez et al. 2016; Rosebrock 2017a). In detail, ribonucleotide reductase, which catalyzes deoxyribonucleotide formation using ribonucleotides as substrates, is blocked by hydroxyurea, and thus the DNA replication is inhibited (Koç et al. 2004). A thorough wash of the cells removes the inhibition and restarts cell proliferation.

For *S. cerevisiae*, adding α -factor induces the arrestment of haploid **a** cells in the G1 phase (Futcher 1999; Foltman et al. 2016; Rosebrock 2017a). As a mating pheromone (a small peptide) secreted by MAT α cells, α -factor naturally arrests **a** cells in G1 phase and facilitates the mating

process between the two mating types of haploid cells (Breedon 1997). In principle, **a**-factor could be used to evoke the synchronization of α cells, but synthesizing functional **a**-factor is complex, requiring the addition of farnesyl and methyl groups (Marcus et al. 1991; Breedon 1997). Here again, a solid washing procedure to rid the culture of α -factor can reinitiate the cell cycle.

Moreover, nocodazole can be used to block *S. cerevisiae* cells in G2/M phase (Foltman et al. 2016; Smith et al. 2016; Rosebrock 2017a). Nocodazole inhibits microtubule polymerization, and therefore, prevents the formation of mitotic spindles (Hoebeke et al. 1976; Jacobs et al. 1988). Without spindles, sister chromatids are not able to segregate, and the cell cycle is suspended in the G2/M phase.

Furthermore, *S. cerevisiae* cells lacking some key G1 cyclins can be arrested at the START during G1 phase (Breedon 1997; Smith et al. 2016), thanks to the indispensability of these proteins. Although *S. cerevisiae* cells can somehow keep increasing their sizes without these essential regulatory proteins, they are not able to pass the START checkpoint. For instance, arrestment occurred when *CLN1*, *CLN2*, *CLN3* were deleted from the genome of *S. cerevisiae*, and the cell cycle reinitiation was done via a plasmid expressing *CLN1* under the *GAL* promoter when galactose was added (Richardson et al. 1989; Schneider et al. 2004). Similarly, *CDC20* expression under the control of a *MET3* promoter can arrest *S. cerevisiae* cells in M phase when methionine is applied (Angeles Juanes 2017).

3.4.4 Nutrient Deprivation

In early stationary phase, *S. cerevisiae* and *S. pombe* cells are arrested in the G1 and G1/G2 phases, respectively (Hartwell et al. 1974; Costello et al. 1986; Gómez and Forsburg 2004). They are able to continue the cell cycle when the limiting nutrients are again available. Hence it is possible to induce synchrony by depriving a cell of one or more nutrients following by the addition of this or these nutrients. The methods of nutrient deprivation are categorized differently from the ones in chemical blockage since there is no chemical added to block the cell cycle progression. On the contrary, this type of arrestment happens naturally during normal batch growth once a limiting nutrient is depleted. For instance, nitrogen shortage (Luche and Forsburg 2009) and magnesium starvation (Walker and Duffus 1980) have been applied to induce synchrony. Notably, a lag phase

after nutrient replenishment usually occurs and, likely, synchrony induced by nutrient deprivation is less prominent than that obtained from chemical blockage methods (Smith et al. 2016).

3.4.5 Nutrient Cycle

The nutrient cycle methods for yeast cell synchronization usually produce synchrony in large cell populations while generally causing minor perturbations to the cells. No obstructive chemicals or temperature shifts are applied, but rather, an entrainment mechanism resulting from nutrient oscillation leads to synchrony. Some nutrient cycle methods involve nutrient starvation; however, the duration of the nutrient deprivation is always short, and the emphasis is on the periodic changes of nutrient availability rather than one-time starvation. Nutrient cycle approaches can be operated in either continuous or semi-continuous reactors.

In continuous cultures, both macro- and micro-fluidic systems have been used. In a chemostat bioreactor, periodic variations (e.g., periodic pulsing) of at least one essential nutritional component have induced yeast cell synchrony (Münch et al. 1992; Sheppard and Dawson 1999; Danø et al. 2001). Nutrient insufficiency aligns yeast cells towards their stationary phase-associated cell cycle stages, while nutrient sufficiency favors some other stages of the cell cycle (e.g., DNA and protein synthesis). Eventually, cell cycle oscillations become synchronized with the nutrient oscillation, and the continuous cultures are in synchrony. In a similar approach, a microfluidic platform was developed to cultivate *S. cerevisiae* continuously with programmed medium switching (a square-wave function) and the G1 index (G1 phase cell percentage) was monitored (Tian et al. 2012). The cell population was entrained to a decent degree of synchrony, and the G1 index oscillated with nutrient switches at the same frequency (Tian et al. 2012).

Continuous phased cultures (Dawson 1965, 1972; Sheppard and Cooper 1990, 1991) and self-cycling fermentation (SCF) (Brown and Cooper 1991; McCaffrey and Cooper 1995; Wentworth and Cooper 1996; Sauvageau et al. 2010; Sauvageau and Cooper 2010) are two typical synchrony-inducing semi-continuous systems. Continuous phasing, a predecessor to SCF, introduces a cyclical nutrient environment by draining one-half of the working volume and replenishing with the equivalent amount of fresh medium after a preset, fixed cycle time (Dawson 1972; Sheppard and Dawson 1999). One generation of synchronized cell replication occurs during

each cycle, based on which events associated with *Candida utilis* (a species of yeast) cell cycle were studied (Dawson 1970, 1985). However, as the cycle time was preset, washout or adverse starvation would result from cycle time set too short or too long, respectively (Sheppard and Dawson 1999; Brown 2001).

Consequently, an upgrade was proposed – SCF incorporates an automated feedback control loop based on the cellular mechanism of the population itself to dictate the cycling time and further couples the nutrient cycle and the cell cycle (Sheppard and Cooper 1990). By monitoring dissolved oxygen, carbon dioxide evolution rate, or oxidation-reduction potential, medium replacement (cycling) can be executed once the limiting nutrient is depleted (not with a predetermined cycling time) (Brown 2001). Nutrient deprivation is thus excluded from SCF, as are lag phases. Continued growth from cycle to cycle without readaptation depicts the nondisruptive feature of SCF (Brown and Cooper 1991; Sauvageau et al. 2010). This method can be implemented at scale and has been used in a wide-range of processing operations ranging from studies of the microbial physiology (Sheppard and Cooper 1991; Brown and Cooper 1991; Sarkis and Cooper 1994; Zenaitis and Cooper 1994), biodegradation (Brown and Cooper 1992; Sarkis and Cooper 1994; Hughes and Cooper 1996; Brown et al. 1999, 2000), and bioproduction (Sheppard and Cooper 1991; Brown and Cooper 1991, 1992; van Walsum and Cooper 1993; Zenaitis and Cooper 1994; McCaffrey and Cooper 1995; Wentworth and Cooper 1996; Marchessault and Sheppard 1997; Crosman et al. 2002; Sauvageau et al. 2010; Sauvageau and Cooper 2010; Storms et al. 2012; Wang et al. 2017, 2020).

3.5 Comparative Analysis

The aforementioned yeast cell synchronization methods can be compared in consideration of three factors: perturbations to cellular processes, scalability of method, and requirements for expertise and equipment.

Physical selection methods, in general, bring the slightest perturbances to the cells. Time-lapse microscopy is completely non-intrusive, and hence, perturbation is hardly a factor. Centrifugal elutriations, which avoids exposure to lactose/sucrose gradients, lead to fewer artifacts (Creanor and Mitchison 1979). As for microfluidic systems, micro-wall chips should be expected

to lead to fewer perturbations than baby machines since the latter constrains growing cells in slits, likely introducing greater external forces and mass transfer limitations. In addition, among all the methods involving induction of synchrony, SCF should cause the least disruptions to cell mechanisms; this is thanks to the mild entrainment effect utilized and the avoidance of nutrient deprivation. In contrast, methods relying on inhibition – relying on chemical inhibitors, gene and protein manipulations, temperature changes, or prolonged starvation – tend to introduce significant perturbations and deviations from the profiles observed during regular cell growth.

The size of a synchronized population is an important parameter, and thus the scalability of synchronization methods can dictate which ones can be used for a given application. Some downstream assays to assess synchrony or cellular mechanisms require large numbers of cells. In that case, induction methods are generally preferred. In particular, nutrient deprivation, continuous phasing and SCF can be performed at the bioreactor scale and provide large amounts of synchronized cells. Some chemical blockage methods tend to be limited by the difficulty in performing cell washes in short timeframes at large scales. Physical selection methods, though introducing minor perturbations to cells, are in turn limited by their equipment (e.g., centrifugal chambers, microfluidic platforms, and time-lapse microscopy systems) with regards to synchronized population sizes. Time-lapse microscopy and microfluidic systems usually deal with tiny populations. Centrifugation-based selection methods work for larger cell populations. Notably, collecting synchronous cells for further examinations is currently infeasible in time-lapse microscopy.

An operation with ease-of-use and low expenses is always desired. Physical and chemical induction methods precede the others as they barely require highly specialized facilities and complicated procedures. On the contrary, physical selection methods overall require skilled operators and relatively complex equipment. Besides, all the approaches summarized under *Nutrient Cycle* require at least laboratory-scale continuous/semi-continuous fermenters or microfluidic continuous reactors.

In essence, the best synchronization method will vary depending on the objectives of the studies or applications of interest. All three factors described above should be considered, as well as the biological entities to be investigated and the corresponding cell cycle stages. Markedly, in some instances it may be necessary to conduct experiments with at least two different approaches

in parallel such that the results can be compared and potential biases can be eliminated. Moreover, synchronized yeast cells obtained via different methods can be put in contrast at the transcriptomic and proteomic levels to better characterize and compare these methods.

3.6 Conclusions

In this work, methods for the synchronization of yeast cells are reviewed. These are part of various categories: physical selection, physical induction, chemical blockage, nutrient deprivation, and nutrient cycling. Based on a brief relative comparison, it is emphasized that each method has its own advantages and disadvantages. We encourage researchers to make choices based on the features of these methods in relation to their research objectives. Consensus findings from multiple synchronization methods may enhance the confidence of the studies and minimize biases.

3.7 Acknowledgments

This work was supported by Natural Sciences and Engineering Research Council of Canada (NSERC) Discovery Grant program, the Canada First Research Excellence Fund – Future Energy System, and the University of Alberta Faculty of Engineering.

3.8 References

- Amon A (2002) Synchronization procedures. In: *Methods in Enzymology*. Academic Press Inc., pp 457–467
- Angeles Juanes M (2017) Methods of synchronization of yeast cells for the analysis of cell cycle progression. In: *Methods in Molecular Biology*. Humana Press Inc., pp 19–34
- Bean JM, Siggia ED, Cross FR (2006) Coherence and timing of cell cycle start examined at single-cell resolution. *Mol Cell* 21:3–14. <https://doi.org/10.1016/j.molcel.2005.10.035>
- Blumenthal LK, Zahler SA (1962) Index for measurement of Synchronization of cell

- populations. *Science* (80-) 135:724. <https://doi.org/10.1126/science.135.3505.724.a>
- Breeden LL (1997) α -Factor synchronization of budding yeast. In: *Methods in Enzymology*. Academic Press Inc., pp 332–342
- Brown WA (2001) The self-cycling fermentor – development, applications, and future opportunities. In: *Recent Research and Developments in Biotechnology and Bioengineering*. pp 4: 61-90
- Brown WA, Cooper DG (1991) Self-cycling fermentation applied to *Acinetobacter calcoaceticus* RAG-1. *Appl Environ Microbiol* 57:2901–2906. <https://doi.org/10.1128/aem.57.10.2901-2906.1991>
- Brown WA, Cooper DG (1992) Hydrocarbon degradation by *Acinetobacter calcoaceticus* RAG-1 using the self-cycling fermentation technique. *Biotechnol Bioeng* 40:797–805. <https://doi.org/10.1002/bit.260400707>
- Brown WA, Cooper DG, Liss SN (2000) Toluene removal in an automated cyclical bioreactor. *Biotechnol Prog* 16:378–384. <https://doi.org/10.1021/bp0000149>
- Brown WA, Cooper DG, Liss SN (1999) Adapting the self-cycling fermentor to anoxic conditions. *Environ Sci Technol* 33:1458–1463. <https://doi.org/10.1021/es980856s>
- Cho RJ, Campbell MJ, Winzeler EA, et al (1998) A genome-wide transcriptional analysis of the mitotic cell cycle. *Mol Cell* 2:65–73. [https://doi.org/10.1016/S1097-2765\(00\)80114-8](https://doi.org/10.1016/S1097-2765(00)80114-8)
- Cooper S (2002) Minimally disturbed, multicycle, and reproducible synchrony using a eukaryotic “baby machine.” *BioEssays* 24:499–501. <https://doi.org/10.1002/bies.10108>
- Costello G, Rodgers L, Beach D (1986) Fission yeast enters the stationary phase G0 state from either mitotic G1 or G2. *Curr Genet* 11:119–125. <https://doi.org/10.1007/BF00378203>
- Creanor J, Mitchison JM (1979) Reduction of perturbations in leucine incorporation in synchronous cultures of *Schizosaccharomyces pombe* made by elutriation. *J Gen Microbiol* 112:385–388. <https://doi.org/10.1099/00221287-112-2-385>
- Crosman JT, Pinchuk RJ, Cooper DG (2002) Enhanced biosurfactant production by *Corynebacterium alkanolyticum* ATCC 21511 using self-cycling fermentation. *J Am Oil Chem Soc* 79:467–472. <https://doi.org/10.1007/s11746-002-0507-5>

- Danø S, Danø S, Hynne F, et al (2001) Synchronization of glycolytic oscillations in a yeast cell population. *Faraday Discuss* 120:261–276. <https://doi.org/10.1039/b103238k>
- Dawson PSS (1985) Growth, cell cultivation, cell metabolism, and the cell cycle of *Candida utilis* as explored by continuous phased culture. *Can J Microbiol* 31:183–189. <https://doi.org/10.1139/m85-036>
- Dawson PSS (1965) Continuous phased growth, with a modified chemostat. *Can J Microbiol* 11:893–903. <https://doi.org/10.1139/m65-119>
- Dawson PSS (1972) Continuously synchronised growth. *J Appl Chem Biotechnol* 22:79–103. <https://doi.org/10.1002/jctb.2720220112>
- Dawson PSS (1970) Cell cycle and post cycle changes during continuous phased growth of *Candida utilis*. *Can J Microbiol* 16:783–795. <https://doi.org/10.1139/m70-132>
- Di Talia S, Skotheim JM, Bean JM, et al (2007) The effects of molecular noise and size control on variability in the budding yeast cell cycle. *Nature* 448:947–951. <https://doi.org/10.1038/nature06072>
- Feldmann H (2012) *Yeast: Molecular and Cell Biology*. Wiley-Blackwell
- Fitch I, Dahmann C, Surana U, et al (1992) Characterization of four B-type cyclin genes of the budding yeast *Saccharomyces cerevisiae*. *Mol Biol Cell* 3:805–818. <https://doi.org/10.1091/mbc.3.7.805>
- Foltman M, Molist I, Sanchez-Diaz A (2016) Synchronization of the budding yeast: *Saccharomyces cerevisiae*. In: *Methods in Molecular Biology*. Humana Press Inc., pp 279–291
- Forsburg SL (1999) The best yeast? *Trends Genet* 15:340–344. [https://doi.org/10.1016/S0168-9525\(99\)01798-9](https://doi.org/10.1016/S0168-9525(99)01798-9)
- Forsburg SL (2005) The yeasts *Saccharomyces cerevisiae* and *Schizosaccharomyces pombe*: models for cell biology research. *Gravitational Sp Biol* 18(2):3–10
- Forsburg SL, Nurse P (1991) Cell cycle regulation in the yeasts *Saccharomyces cerevisiae* and *Schizosaccharomyces pombe*. *Annu Rev Cell Biol* 7:227–256. <https://doi.org/10.1146/annurev.cb.07.110191.001303>

- Futcher B (1999) Cell cycle synchronization. *Methods Cell Sci* 21:79–86.
<https://doi.org/10.1023/A:1009872403440>
- Gómez EB, Forsburg SL (2004) Analysis of the fission yeast *Schizosaccharomyces pombe* cell cycle. In: *Methods in Molecular Biology*. Humana Press, New Jersey, pp 93–111
- Hartwell LH, Culotti J, Pringle JR, Reid BJ (1974) Genetic control of the cell division cycle in yeast. *Science* (80-.). 183:46–51
- Hartwell LH, Unger MW (1977) Unequal division in *Saccharomyces cerevisiae* and its implications for the control of cell division. *J Cell Biol* 75:422–435.
<https://doi.org/10.1083/JCB.75.2.422>
- Hiraoka Y, Toda T, Yanagida M (1984) The NDA3 gene of fission yeast encodes β -tubulin: A cold-sensitive *nda3* mutation reversibly blocks spindle formation and chromosome movement in mitosis. *Cell* 39:349–358. [https://doi.org/10.1016/0092-8674\(84\)90013-8](https://doi.org/10.1016/0092-8674(84)90013-8)
- Hoebeke J, Van Nijen G, De Brabander M (1976) Interaction of oncodazole (R 17934), a new anti-tumoral drug, with rat brain tubulin. *Biochem Biophys Res Commun* 69:319–324.
[https://doi.org/10.1016/0006-291X\(76\)90524-6](https://doi.org/10.1016/0006-291X(76)90524-6)
- Hughes SM, Cooper DG (1996) Biodegradation of phenol using the self-cycling fermentation (SCF) process. *Biotechnol Bioeng* 51:112–119. [https://doi.org/10.1002/\(SICI\)1097-0290\(19960705\)51:1<112::AID-BIT13>3.0.CO;2-S](https://doi.org/10.1002/(SICI)1097-0290(19960705)51:1<112::AID-BIT13>3.0.CO;2-S)
- Hur JY, Park MC, Suh KY, Park SH (2011) Synchronization of cell cycle of *Saccharomyces cerevisiae* by using a cell chip platform. *Mol Cells* 32:483–488.
<https://doi.org/10.1007/s10059-011-0174-8>
- Jacobs CW, Adams AE, Szaniszlo PJ, Pringle JR (1988) Functions of microtubules in the *Saccharomyces cerevisiae* cell cycle. *J Cell Biol* 107:1409–1426.
<https://doi.org/10.1083/jcb.107.4.1409>
- Johnston GC, Pringle JR, Hartwell LH (1977) Coordination of growth with cell division in the yeast *Saccharomyces cerevisiae*. *Exp Cell Res* 105:79–98. [https://doi.org/10.1016/0014-4827\(77\)90154-9](https://doi.org/10.1016/0014-4827(77)90154-9)
- Johnston LH, Johnson AL (1997) Elutriation of budding yeast. In: *Methods in Enzymology*.

Academic Press Inc., pp 342–350

Knutsen J, Rein ID, Rothe C, et al (2011) Cell-cycle analysis of fission yeast cells by flow cytometry. *PLoS One* 6:17175. <https://doi.org/10.1371/journal.pone.0017175>

Koç A, Wheeler LJ, Mathews CK, Merrill GF (2004) Hydroxyurea Arrests DNA Replication by a Mechanism that Preserves Basal dNTP Pools. *J Biol Chem* 279:223–230. <https://doi.org/10.1074/jbc.M303952200>

Kramhøft B, Zeuthen E (1975) Chapter 18 synchronization of the fission yeast *Schizosaccharomyces pombe* using heat shocks. In: *Methods in Cell Biology*. Academic Press, pp 373–380

Lord PG, Wheals AE (1981) Variability in individual cell cycles of *Saccharomyces cerevisiae*. *J Cell Sci* 50:361–376. <https://doi.org/10.1242/JCS.50.1.361>

Luche DD, Forsburg SL (2009) Cell-cycle synchrony for analysis of *S. pombe* DNA replication. *Methods Mol Biol* 521:437–448. https://doi.org/10.1007/978-1-60327-815-7_24

Manukyan A, Abraham L, Dungrawala H, Schneider BL (2011) Synchronization of yeast. In: *Methods in Molecular Biology*. Humana Press, pp 173–200

Marchessault P, Sheppard JD (1997) Application of self-cycling fermentation technique to the production of poly- β -hydroxybutyrate. *Biotechnol Bioeng* 55:815–820. [https://doi.org/10.1002/\(SICI\)1097-0290\(19970905\)55:5<815::AID-BIT12>3.0.CO;2-A](https://doi.org/10.1002/(SICI)1097-0290(19970905)55:5<815::AID-BIT12>3.0.CO;2-A)

Marcus S, Caldwell GA, Miller D, et al (1991) Significance of C-terminal cysteine modifications to the biological activity of the *Saccharomyces cerevisiae* a-factor mating pheromone. *Mol Cell Biol* 11:3603–3612. <https://doi.org/10.1128/mcb.11.7.3603>

McCaffrey WC, Cooper DG (1995) Sophorolipids production by *Candida bombicola* using self-cycling fermentation. *J Ferment Bioeng* 79:146–151. [https://doi.org/10.1016/0922-338X\(95\)94082-3](https://doi.org/10.1016/0922-338X(95)94082-3)

Mitchison JM, Vincent WS (1965) Preparation of synchronous cell cultures by sedimentation. *Nature* 205:987–989. <https://doi.org/10.1038/205987a0>

Münch T, Sonnleitner B, Fiechter A (1992) New insights into the synchronization mechanism with forced synchronous cultures of *Saccharomyces cerevisiae*. *J Biotechnol* 24:299–314.

[https://doi.org/10.1016/0168-1656\(92\)90039-C](https://doi.org/10.1016/0168-1656(92)90039-C)

Oliva A, Rosebrock A, Ferrezuelo F, et al (2005) The cell cycle-regulated genes of *Schizosaccharomyces pombe*. PLOS Biol 3:1239–1260.

<https://doi.org/10.1371/journal.pbio.0030225>

Pringle JR, Adams AEM, Drubin DG, Haarer BK (1991) Immunofluorescence methods for yeast. In: Methods in Enzymology. pp 565–602

Richardson HE, Wittenberg C, Cross F, Reed SI (1989) An essential G1 function for cyclin-like proteins in yeast. Cell 59:1127–1133. [https://doi.org/10.1016/0092-8674\(89\)90768-X](https://doi.org/10.1016/0092-8674(89)90768-X)

Rosebrock AP (2017a) Methods for synchronization and analysis of the budding yeast cell cycle. Cold Spring Harb Protoc 2017:5–7. <https://doi.org/10.1101/pdb.top080630>

Rosebrock AP (2017b) Synchronization of budding yeast by centrifugal elutriation. Cold Spring Harb Protoc 2017:53–62. <https://doi.org/10.1101/pdb.prot088732>

Sarkis BE, Cooper DG (1994) Biodegradation of aromatic compounds in a self-cycling fermenter (SCF). Can J Chem Eng 72:874–880. <https://doi.org/10.1002/cjce.5450720514>

Sauvageau D, Cooper DG (2010) Two-stage, self-cycling process for the production of bacteriophages. Microb Cell Fact 9:1–10. <https://doi.org/10.1186/1475-2859-9-81>

Sauvageau D, Storms Z, Cooper DG (2010) Synchronized populations of *Escherichia coli* using simplified self-cycling fermentation. J Biotechnol 149:67–73. <https://doi.org/10.1016/j.jbiotec.2010.06.018>

Schneider BL, Zhang J, Markwardt J, et al (2004) Growth rate and cell size modulate the synthesis of, and requirement for, G1-phase cyclins at Start. Mol Cell Biol 24:10802–10813. <https://doi.org/10.1128/MCB.24.24.10802-10813.2004>

Sheppard JD, Cooper DG (1991) The response of *Bacillus subtilis* ATCC 21332 to manganese during continuous-phased growth. Appl Microbiol Biotechnol 35:72–76. <https://doi.org/10.1007/BF00180639>

Sheppard JD, Cooper DG (1990) Development of computerized feedback control for the continuous phasing of *Bacillus subtilis*. Biotechnol Bioeng 36:539–545. <https://doi.org/10.1002/bit.260360514>

- Sheppard JD, Dawson PSS (1999) Cell synchrony and periodic behaviour in yeast populations. *Can J Chem Eng* 77:893–902. <https://doi.org/10.1002/cjce.5450770515>
- Smith J, Manukyan A, Hua H, et al (2016) Synchronization of yeast. In: *Methods in Molecular Biology*. Humana Press Inc., pp 215–242
- Spellman PT, Sherlock G, Zhang MQ, et al (1998) Comprehensive identification of cell cycle-regulated genes of the yeast *Saccharomyces cerevisiae* by microarray hybridization. *Mol Biol Cell* 9:3273–3297. <https://doi.org/10.1091/mbc.9.12.3273>
- Storms ZJ, Brown T, Sauvageau D, Cooper DG (2012) Self-cycling operation increases productivity of recombinant protein in *Escherichia coli*. *Biotechnol Bioeng* 109:2262–2270. <https://doi.org/10.1002/bit.24492>
- Strogatz SH (1997) Spontaneous synchronization in nature. In: *IEEE International Frequency Control Symposium*. pp 2–4
- Thornton M, Eward KL, Helmstetter CE (2002) Production of minimally disturbed synchronous cultures of hematopoietic cells. *Biotechniques* 32:1098–1105. <https://doi.org/10.2144/02325rr05>
- Tian Y, Luo C, Lu Y, et al (2012) Cell cycle synchronization by nutrient modulation. *Integr Biol (Camb)* 4:328–334. <https://doi.org/10.1039/c2ib00083k>
- Tian Y, Luo C, Ouyang Q (2013) A microfluidic synchronizer for fission yeast cells. *Lab Chip* 13:4071–4077. <https://doi.org/10.1039/c3lc50639h>
- Toda T, Umesono K, Hirata A, Yanagida M (1983) Cold-sensitive nuclear division arrest mutants of the fission yeast *Schizosaccharomyces pombe*. *J Mol Biol* 168:251–270. [https://doi.org/10.1016/S0022-2836\(83\)80017-5](https://doi.org/10.1016/S0022-2836(83)80017-5)
- Tormos-Pérez M, Pérez-Hidalgo L, Moreno S (2016) Fission yeast cell cycle synchronization methods. In: *Methods in Molecular Biology*. Humana Press Inc., pp 293–308
- van Walsum GP, Cooper DG (1993) Self-cycling fermentation in a stirred tank reactor. *Biotechnol Bioeng* 42:1175–1180. <https://doi.org/10.1002/bit.260421007>
- Walker GM (1999) Synchronization of yeast cell populations. *Methods Cell Sci* 21:87–93. <https://doi.org/10.1023/A:1009824520278>

- Walker GM, Duffus JH (1980) Magnesium ions and the control of the cell cycle in yeast. *J Cell Sci* VOL.42:329–356. <https://doi.org/10.1242/jcs.42.1.329>
- Wang J, Chae M, Bressler DC, Sauvageau D (2020) Improved bioethanol productivity through gas flow rate-driven self-cycling fermentation. *Biotechnol Biofuels* 13:1–14. <https://doi.org/10.1186/s13068-020-1658-6>
- Wang J, Chae M, Sauvageau D, Bressler DC (2017) Improving ethanol productivity through self-cycling fermentation of yeast: A proof of concept. *Biotechnol Biofuels* 10:193. <https://doi.org/10.1186/s13068-017-0879-9>
- Wentworth SD, Cooper DG (1996) Self-cycling fermentation of a citric acid producing strain of *Candida lipolytica*. *J Ferment Bioeng* 81:400–405. [https://doi.org/10.1016/0922-338X\(96\)85140-3](https://doi.org/10.1016/0922-338X(96)85140-3)
- Yang J, Dungrawala H, Hua H, et al (2011) Cell size and growth rate are major determinants of replicative lifespan. *Cell Cycle* 10:144–155. <https://doi.org/10.4161/cc.10.1.14455>
- Zenaitis MG, Cooper DG (1994) Antibiotic production by *Streptomyces aureofaciens* using self-cycling fermentation. *Biotechnol Bioeng* 44:1331–1336. <https://doi.org/10.1002/bit.260441109>

4. Transcriptomic Analysis of Synchrony and Productivity in Self-cycling Fermentation of Engineered Yeast Producing Shikimic Acid

(The contents have been published on Biotechnology Reports. Shikimic acid analysis in SCF was performed by Agustin, R. V. C and included in his M.Sc. thesis (2015, University of Alberta).)

4.1 Abstract

Industrial fermentation provides a wide variety of bioproducts, such as food, biofuels and pharmaceuticals. Self-cycling fermentation (SCF), an advanced automated semi-continuous fermentation approach, has shown significant advantages over batch reactors (BR); including cell synchrony and improved production. Here, *Saccharomyces cerevisiae* engineered to overproduce shikimic acid was grown under SCF operation. This led to four-fold increases in product yield and volumetric productivity compared to BR. Transcriptomic analyses were performed to understand the cellular mechanisms leading to these increases. Results indicate an up-regulation of a large number of genes related to the cell cycle and DNA replication in the early stages of SCF cycles, inferring substantial synchronization. Moreover, numerous genes related to gluconeogenesis, the citrate cycle and oxidative phosphorylation were significantly up-regulated in the late stages of SCF cycles, consistent with significant increases in shikimic acid yield and productivity.

4.2 Introduction

Self-cycling fermentation (SCF), a semi-continuous fermentation process adapted from continuous phasing (Dawson 1965, 1972; Sheppard and Cooper 1990, 1991), has been introduced, studied, and applied to a large variety of microbial systems (Brown and Cooper 1991, 1992; Sheppard 1993; van Walsum and Cooper 1993; Sarkis and Cooper 1994; Zenaitis and Cooper 1994;

McCaffrey and Cooper 1995; Wincure et al. 1995; Wentworth and Cooper 1996; Hughes and Cooper 1996; Marchessault and Sheppard 1997; Brown et al. 1999, 2000; Pinchuk et al. 2000; Crosman et al. 2002; Sauvageau et al. 2010; Sauvageau and Cooper 2010; Storms et al. 2012; Wang et al. 2017, 2020). SCF has been implemented in the discovery of physiological properties (Sheppard and Cooper 1991; Brown and Cooper 1991; Sarkis and Cooper 1994; Zenaitis and Cooper 1994), the removal of pollutants (Brown and Cooper 1992; Sarkis and Cooper 1994; Hughes and Cooper 1996; Brown et al. 1999, 2000), and the efficient production of valued bioproducts (Sheppard and Cooper 1991; Brown and Cooper 1991, 1992; van Walsum and Cooper 1993; Zenaitis and Cooper 1994; McCaffrey and Cooper 1995; Wentworth and Cooper 1996; Marchessault and Sheppard 1997; Crosman et al. 2002; Sauvageau et al. 2010; Sauvageau and Cooper 2010; Storms et al. 2012; Wang et al. 2017, 2020). Three important cell culture properties result from the feedback control-based cycling procedure of SCF – which consists of draining and refilling half the working volume once the limiting nutrient is depleted. Firstly, the timing of the SCF cycling is dictated by the metabolic activity of the population, not by a fixed cycle time. Consequentially, the cycle time reflects the nutritional quality of the growth medium and the metabolic activity of the cell population (Brown 2001). Incorporating feedback control systems brings stability and reproducibility to the SCF process encountering perturbation (van Walsum and Cooper 1993; Sauvageau et al. 2010) or feedstock heterogeneity (Brown and Cooper 1991, 1992; van Walsum and Cooper 1993) during the process. Secondly, the population growing under SCF operation often display high levels of synchrony (with synchrony indices (Blumenthal and Zahler 1962) greater than 0.66 in most studies (Brown and Cooper 1991; McCaffrey and Cooper 1995; Wentworth and Cooper 1996; Sauvageau et al. 2010; Sauvageau and Cooper 2010)). Hence, it provides an undisrupted and efficient approach to the production of large volumes of synchronized microbial populations, avoiding the need for disruptive measures such as starvation (Hirsch and Vondrejs 1971; Chan and Cheng 1977; Walker and Duffus 1980), elevated temperature (Kramhøft and Zeuthen 1975), and growth inhibition (Jacobs et al. 1988; Koç et al. 2004; Ferullo et al. 2009).

Thirdly, SCF has been shown to boost volumetric productivity of many microbial systems in comparison with batch reactor (BR) operation (Brown and Cooper 1991; Zenaitis and Cooper 1994; Wentworth and Cooper 1996; Sauvageau and Cooper 2010; Storms et al. 2012; Wang et al. 2017, 2020). This is attributed in part to the elimination of the non-productive growth phases (including lag phase and stationary phase) and the achievement of a greater productivity per cell (Sauvageau and Cooper 2010; Storms et al. 2012).

Improving the performance of bioproduction is an important challenge of the bioeconomy, and SCF operation has shown its potential in recent studies for the production of ethanol (Wang et al. 2017, 2020), recombinant protein (Storms et al. 2012) and bacteriophage (Sauvageau and Cooper 2010), among others. Due to elevated productivities associated with SCF, there is a clear incentive to produce valuable bioproducts using this mode of operation, and it is important to understand the effects of the process on cells towards further improvements.

Shikimic acid is a metabolite in the aromatic amino acid biosynthesis pathway that can be used directly as a product or as a precursor to aromatic compounds. It is, for example, used for the production of the anti-flu medication Oseltamivir (Ghosh et al. 2012; Rawat et al. 2013; Martínez et al. 2015), which targets viral neuraminidase for the prevention and treatment of influenza infections (McClellan and Perry 2001). Shikimic acid is commercially extracted from Chinese star anise (*Illicium verum*); in fact, nearly 90% of the world's Chinese star anise is consumed for this purpose (Martínez et al. 2015). However, planting and product extraction and recovery are tedious and expensive, accompanying a mediocre yield (Rawat et al. 2013). Many efforts have been made to engineer bacteria (Knop et al. 2001; Ghosh et al. 2012; Rawat et al. 2013; Tripathi et al. 2013; Liu et al. 2014; Martínez et al. 2015; Zhang et al. 2016) and yeast (Mookerjee 2016; Suástegui and Shao 2016; Suástegui et al. 2016, 2017; Gao et al. 2017) to overproduce shikimic acid during fermentation. Microbial production of shikimic acid in bioreactors has many potential benefits: circumventing low crop yields and their vulnerability to severe weather events (droughts, floods, storms, etc.), reducing the variability in product concentrations and purities, facilitating process

optimization, etc. The combination of synthetic biology and SCF operation can represent important tools towards the implementation of economically viable shikimic acid production in microbial systems.

Despite the multiple observations of improved productivity in SCF studies, the underlying cellular mechanisms leading to these benefits have yet to be elucidated. The present work focuses on the implementation of SCF operation for a strain of *Saccharomyces cerevisiae* (Mookerjee 2016) engineered to overproduce shikimic acid and the determination of metabolic regulation patterns involved in the process. The yield, volumetric productivity, and specific productivity are highlighted along with a demonstration of the stability of the SCF operation. These parameters are compared for BR and SCF operations. Then, the effects of SCF operation on the cell population at the transcriptomic level are elucidated to establish the regulatory patterns involved in synchrony and increased shikimic acid production.

4.3 Materials and Methods

4.3.1 Yeast Strain and Medium

Saccharomyces cerevisiae, genetically modified from the parental strain CEN.PK 113-1A Mata α to overproduce shikimic acid, was kindly provided by Prof. Vincent Martin at Concordia University (Mookerjee 2016). Briefly, 3-dehydroquinate synthase gene *ARO3* and 3-dehydroquinate dehydratase gene *ARO4* from *Escherichia coli* (Dell and Frost 1993) and the tyrosine feedback resistant variant of constitutive 3-deoxy-D-arabino-heptulosonate-7-phosphate synthase gene *ARO4* (*ARO4* K229L) from *S. cerevisiae* (Hartmann et al. 2003) were introduced using a pYES plasmid with *URA3* for auxotrophic selection on uracil-deficient media (plasmid information in Supplementary Table A3 according to (Mookerjee 2016)). Constitutive *URA3*, *ARO3*, and *ARO4* genes were deleted from the yeast genome. Yeast nitrogen base (YNB) without

amino acids (Sigma Aldrich) and dextrose (Fisher Scientific) were added to deionized water (MilliQ, Millipore) to concentrations of 6.7 g/L and 20 g/L, respectively, for medium formulation.

Pre-cultures were grown overnight in 20 mL medium at 30 °C and 150 rpm in an incubator-shaker (Ecotron, Infors, Montreal, Canada). Approximately 8×10^8 cells from pre-cultures were used to inoculate batch or SCF fermenters.

4.3.2 Reactor Operation

The same reactor configuration (Figure 4.1), built based on a set-up described previously (Sauvageau et al. 2010) and incorporating a new 2-L stainless steel fermenter body (10.5 cm I.D.), was used for BR and SCF operation. During fermentation, the working volume was 1 L, temperature was maintained at 30 °C, agitation with a Rushton impeller (4 cm diameter) was 250 rpm, and aeration was 845 mL (STP)/min. The carbon dioxide (CO₂) evolution rate (CER) was measured using an IR-spectrometry CO₂ gas sensor (Vernier Scientific) based on CO₂ concentration in the exit gas (Sauvageau et al. 2010). Real-time data was monitored and recorded by LabView via an OPTO 22 data acquisition board. The first cycle of SCF operation was performed as BR. For SCF, the automated cycling sequence – consisting of draining and replenishing half the working volume – was controlled using a program built in LabView. Cycling was triggered when all the following conditions were met: (1) cycle time was greater than 300 min; (2) CER was less than 5.08 mmol/L/h (CO₂ concentration less than 3000 ppm); (3) the absolute value of the first derivative of CER over the last 7 min was less than 1.94×10^{-5} mmol/L/h/min (0.01 ppm/min for the derivative of CO₂ concentration); (4) the first derivative of CER over the last 15 min was less than 0.

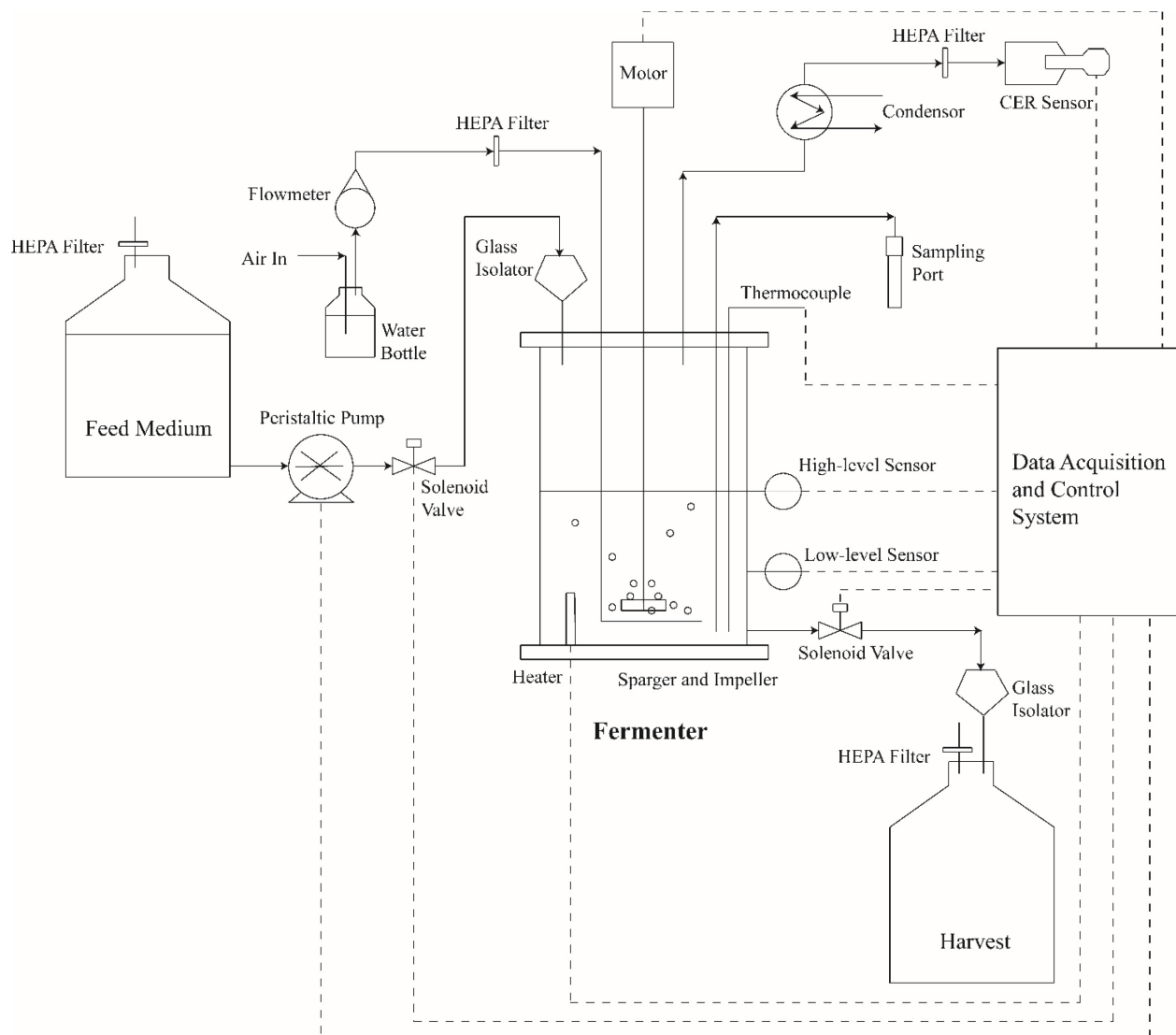


Figure 4.1 Schematic of the SCF configuration. Automated cycling was triggered based on conditions related to cycle time, CER, and the derivative of CER.

4.3.3 Optical Density and Cell Count

A spectrophotometer (Ultrospec 50, Biochrom) was used to measure the optical density of the cell cultures at a wavelength of 600 nm. A Petroff-Hausser counting chamber (Hausser Scientific) and a light microscope (Leica Microsystems DMRXA2, Heerbrugg, Switzerland)

equipped with a digital camera (QImaging, Retiga EX, Surrey, BC) were utilized for cell count measurements.

4.3.4 Measurement of Shikimic Acid, Glucose, and Ethanol

1-mL samples of culture were collected from the reactor and centrifuged (5424R, Eppendorf) at 19,000 rcf for 2 min. The supernatant was then removed and filtered through a 0.2- μm syringe filter (Fisher Scientific). 10 μL of samples were loaded onto a high-performance liquid chromatography (HPLC) system (Agilent Technologies 1200 series) to measure the concentrations of shikimic acid and glucose. Shikimic acid was detected using a diode array detector at 216 nm after passing through an Aminex HPX-87H organic acids analysis column (Bio-Rad Labs). Glucose and ethanol were monitored by a refractive index detector after elution from a SupelcoGel PB carbohydrate column (Sigma Aldrich). 5 mM sulfuric acid (Fisher Scientific) and deionized water were used as the mobile phase for each column, respectively, at a flow rate of 0.5 mL/min.

4.3.5 Production Parameters

The following equations were used to calculate yield of shikimic acid to glucose ($Y_{P/S}$; mol/mol of glucose) (Eq. 1), (intra-cycle) productivity of shikimic acid (r_P ; mol/L/h) (Eq. 2), (intra-cycle) integrated specific productivity of shikimic acid (\bar{r}_P ; mol/cell/h) (Eq. 3), and normalized cycle time (t_{norm} ; dimensionless) (Eq. 4).

N_P represents the amount of the product (mol of shikimic acid). N_S is the amount of the substrate (mol of glucose). V represents the working volume (L). t represents operation time or in-cycle time (h). c_X is the cell density (cell/L). t_{cycle} represents the cycle time (h).

$$Y_{P/S} = \frac{\Delta N_P}{-\Delta N_S} \quad \text{- Eq. (1)}$$

$$r_P = \frac{\Delta N_P}{V \cdot \Delta t} \quad \text{- Eq. (2)}$$

$$\bar{r}_P = \frac{\Delta N_P/V}{\int c_X dt} \quad - \text{Eq. (3)}$$

$$t_{norm} = \frac{\Delta t}{t_{cycle}} \quad - \text{Eq. (4)}$$

4.3.6 RNA-Seq Analysis

For RNA-Seq analyses, four sampling points (BR₁₋₄, corresponding to late-log phase and diauxic shift) were selected for BR operation, while six sampling points (SCF₁₋₆) were selected for SCF cycle 23. Technical triplicate samples were collected for each sampling point. The details of sampling times are given in Supplementary Table A1. The sampling points for SCF cycle 23 were inferred based on preliminary qPCR results showing up-regulation of cyclin genes in the first half of SCF cycles.

0.35 mL to 1 mL of *S. cerevisiae* cultures were collected and centrifuged (5424R, Eppendorf) at 20,000 ref for 2 min. Cell pellets were quickly frozen in liquid nitrogen and cryopreserved at -80 °C until the next step. Total RNA purification was performed using a Masterpure Complete DNA and RNA Purification kit (Lucigen). The main steps involved cell lysis, protein precipitation, nucleic acid recovery, and genomic DNA removal. Purification was performed as per the manufacturer's instructions with the following modifications: 1 mM of dithiothreitol (DTT) was added before cell lysis, and ethylenediaminetetraacetic acid (EDTA) was added to 2.5 mM to cease the reaction of DNase I digestion at the final step. After extraction, the concentration, quality, and integrity of the total RNA was measured using a NanoDrop 1000 (Thermo Fisher) and a Bioanalyzer 2100 (Agilent). Library preparation (reverse strand) and second-generation sequencing were performed using an mRNA stranded library preparation kit (NEB) and HiSeq4000 sequencing platform (Illumina) at Génome Québec. Approximately 10 million reads (PE100) were generated for each RNA sample. RNA-Seq data analyses were performed using the Galaxy platform (Afgan et al. 2018). In detail, adapter sequences (AGATCGGAAGAGCACACGTCTGAACTCCAGTCAC for R1 and

AGATCGGAAGAGCGTCGTGTAGGGAAAGAGTGT for R2) were removed and the raw data was trimmed using default setting via Trimmomatic (Bolger et al. 2014). Read alignment was carried out using HISAT2 (Kim et al. 2015) based on genome sequence and annotation files (genome assembly R64-1-1 of *S. cerevisiae* retrieved from Ensembl (Cunningham et al. 2019) with modifications for strain engineering). Feature counting was fulfilled by HTSeq-count (Anders et al. 2015) with the mode of “Union” based on the genome annotation file. Differential expression analysis was carried out by DESeq2 (Love et al. 2014) using BR₃ as the reference sampling point (except for Supplementary Figures A12-A18 for which SCF₆ was used as an external reference) with the fit type of “parametric”. Another workflow, TopHat2 (Kim et al. 2013)-Cuffdiff (Trapnell et al. 2010), was performed for confirmation, resulting in an identical outcome. To analyze gene regulation patterns, pathway information was retrieved from KEGG (Kanehisa and Goto 2000). Heatmaps were made using ClustVis platform (Metsalu and Vilo 2015) focusing on a number of characteristic KEGG pathways, to illustrate the comparison of relative expression levels ($\log_2(\text{FC})$, with statistical significance) amongst different sampling points. The threshold for calling statistical significance was set to $p\text{-adj} < 0.05$ based on DESeq2 performing the Benjamini-Hochberg procedure.

4.3.7 qPCR Analysis

For qPCR experiments, samples were collected at various time points in late-log phase and diauxic shift of BR, as well as during SCF cycles 2 and 21. Supplementary Table A2 lists the sampling time points for cycle 21. Notably, qPCR samples were collected in replicated SCF operations different from the ones for RNA-Seq sampling; qPCR results agreed with RNA-Seq findings and served as validation for RNA-Seq experiments.

Total RNA samples were prepared as mentioned for RNA-Seq above. Reverse transcription was accomplished utilizing the High-Capacity cDNA Reverse Transcription kit with RNase

Inhibitor (Thermo Fisher) with random primers and the standard temperature program. PowerUp SYBR Green Master Mix (Thermo Fisher) was used as directed to carry out qPCR using a real-time PCR system (QuantStudio 3, Thermo Fisher). BR₃ samples, collected at the transition point from late-log phase to diauxic shift, were utilized as reference for all alignments. Technical triplicates were tested for each condition. *ACT1* and *ALG9* were chosen as reference genes (Teste et al. 2009; Cankorur-Cetinkaya et al. 2012; Davison et al. 2016). The following genes, known to be regulated according to the yeast cell cycle (Futcher 1996; Feldmann 2012), were investigated: *CLN1* and *CLN2* (up-regulated from G₁ phase to early S phase), *CLB3* (expressed in late S phase and G₂ phase), *CLB1* and *CLB2* (accumulating transcripts in the mitotic phase). Primers were designed using Primer3 (Untergasser et al. 2012) – sequences (from 5' to 3') and amplicon sizes are shown in Table 4.1 along with efficiencies obtained from standard curve experiments. The relative gene expression levels (fold change) were calculated using the double delta C_t method (Livak and Schmittgen 2001).

Table 4.1 Primer sequences, amplicon sizes, and efficiencies for qPCR experiments.

Gene	Forward and reverse primers	Amplicon size (bp)	Efficiency (%)
<i>ACT1</i>	CTCGTGCTGTCTTCCCATCT TTTGACCCATAACCGACCAT	69	101.15
<i>ALG9</i>	ACATCGTCGCCCAATAAA CGTAAAATGCTCTACCCAAAATCCT	132	92.69
<i>CLN1</i>	CTCGTATTCCACGCCTTCT CGTCCCAGTTCAGAGTATCCA	114	93.52
<i>CLB3</i>	AGGATGAAGAAGAAGACCAGGA GCTCCCAGACCAATGTATCA	69	105.86
<i>CLB1</i>	CTCAGCGGCAATGTTCT GCCTTTGTGTAACCACCACT	90	102.68
<i>CLN2</i>	TTCCTCATCTCAAAGCCACA TGACTGCTGCTGACCAAATT	130	93.93
<i>CLB2</i>	TGCCTTTTCATTGCCTCTAA GCACCGTCTGTCTCTGATG	77	89.35

4.4 Results

4.4.1 BR and SCF Operation

SCF was implemented for cultures of the engineered yeast strain using CER to monitor cellular activity. Figure 4.2 shows six different operating parameters (CER, intra-cycle integral of CER, cycle time, OD₆₀₀, and glucose and shikimic acid concentrations) over 25 cycles of SCF operation. Figure 4.2A shows the pattern of CER, where each individual peak corresponds to one SCF cycle. Cycle 1 can be considered as a BR with 1% inoculum, while all subsequent cycles were operated based on the harvest and replenishment of 50% of the working volume during cycling. The CER trends demonstrated a consistent pattern after 5 cycles, with an average maximum CER of 0.013 ± 0.0014 mol/h. Maximum CERs of approximately 0.018 mol/h were obtained for cycles 2, 3, and 5. Cycle 4 had a low CER due to an equipment malfunction unrelated to the growth of the yeast population. Aside from that outlier, the maximum CER achieved was lowest between cycles 11 and 22.

Figure 4.2B presents the cycle time throughout SCF operation. After cycle 1 (24.5 h), the cycle time remained relatively constant, with an average value of 8.87 ± 0.77 h. From cycles 2 to 11, the cycle time was near the lower end of the 68% confidence interval at approximately 8.10 h. For subsequent cycles, the cycle time increased to the higher end of the 68% confidence interval at 9.64 h. Figure 4.2C displays the total moles of carbon dioxide evolved per cycle, which was calculated as the integral CER area for each cycle. After cycle 1 (BR; 0.186 mol CO₂), a constant amount of carbon dioxide was evolved (0.090 ± 0.006 mol CO₂) in each subsequent SCF cycle. For cycles 2-25, the average start-of-cycle OD₆₀₀ was 2.46 ± 0.12 and the average end-of-cycle value was 4.65 ± 0.13 (Figure 4.2D). In Figure 4.2E, the initial glucose concentration for the first cycle was 20 g/L, whereas it was 9.28 ± 0.42 g/L for the subsequent cycles – which is approximately half the initial value, consistent with the replenishment of half the reactor content

following complete glucose consumption within each cycle. At the end of all cycles, the concentration of glucose – the limiting nutrient – was below or near the detection limit.

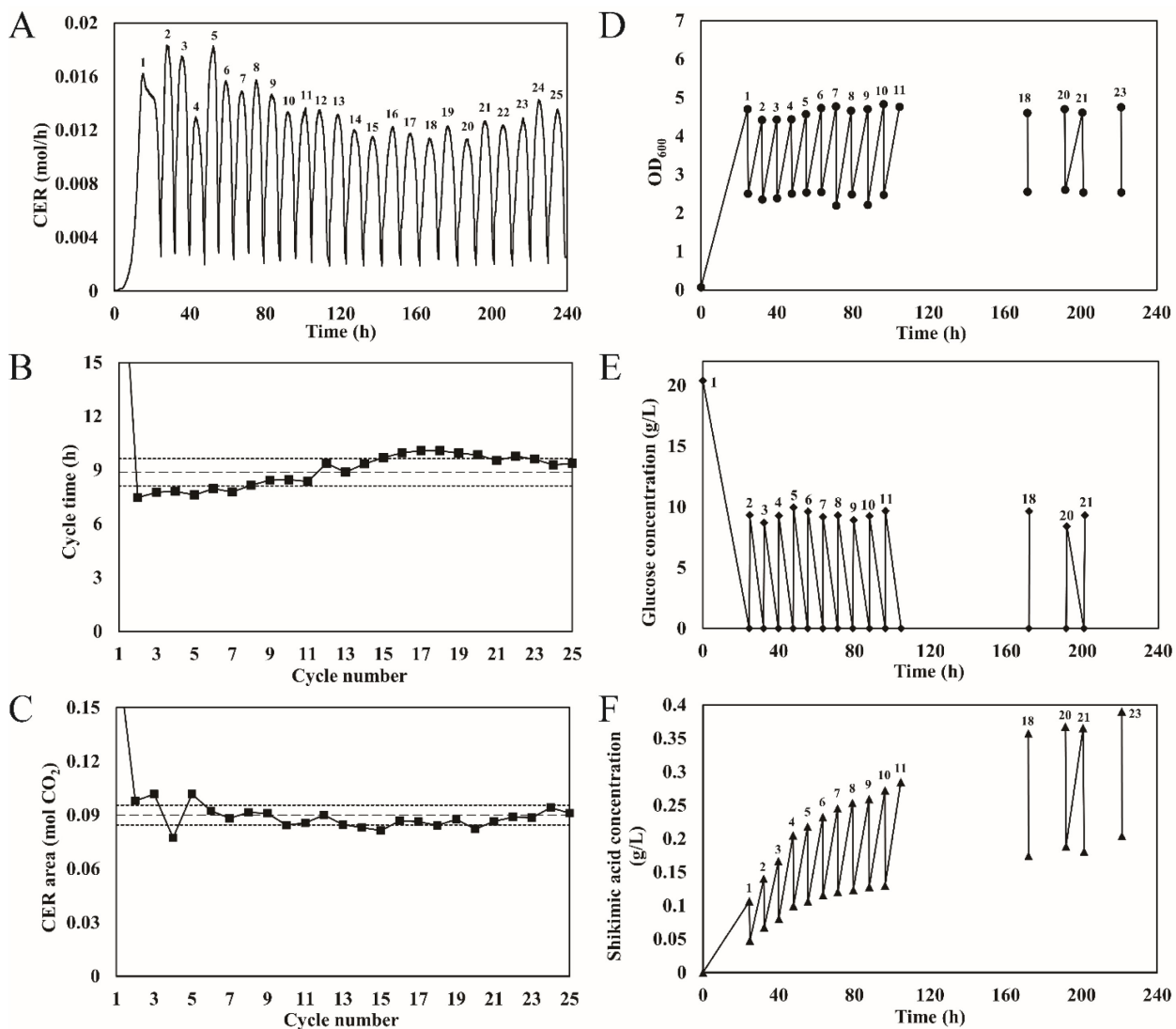


Figure 4.2 SCF operation of engineered *S. cerevisiae* for 25 cycles. A) CER profile during SCF operation. B) Total moles of carbon dioxide evolved per cycle, calculated as the integral under each peak in Figure A). C) Cycle time over the 25 cycles. D) Optical density of the culture taken at the start and the end of each cycle. E) Glucose concentration at the start and end of each cycle. F) Shikimic acid concentration at the start and end of each cycle. Cycle numbers are labeled above each CER peak in A), at the end-of-cycle in D) and F), and at the start-of-cycle in E). The dashed lines in B) and C) indicate average values \pm one standard deviation for cycles 2 to 25.

Figure 4.2F shows the pattern of shikimic acid production over the 25 cycles of SCF operation. At the end of BR (cycle 1), the shikimic acid concentration was 0.11 g/L. The end-of-cycle shikimic acid concentration increased continuously for each subsequent cycle monitored. This increase eventually subsided and seemed to plateau from cycle 18 onward. By the end of cycle 23, the shikimic acid concentration reached 0.39 g/L, a more than three-fold increase on the value obtained at the end of the BR (Figure 4.2F).

The yield, productivity, and specific productivity of shikimic acid during SCF operation were determined from the data in Figure 4.2, using Eq. 1-4, and reported in Figure 4.3. The integral of cell density used for Eq. 3 was inferred by the start-and-end-of-cycle cell counts. Figures 4.3A and 4.3B report the yield and productivities for each SCF cycle. An increasing trend of yield was observed over the whole SCF operation (Figure 4.3A). In contrast to the BR (yield of 0.541×10^{-2} mol/mol glucose), a four-fold increase in yield of shikimic acid was obtained after 21 cycles (2.17×10^{-2} mol/mol glucose; Figure 4.3A). Sharp increases in productivity and integrated specific productivity were observed from cycles 1 to 4 (Figure 4.3B). In particular, productivities more than doubled between cycles 1 and 2. By the end of SCF operation, four-fold and three-fold increases in productivity and integrated specific productivity were achieved, reaching 10.6×10^{-5} mol/L/h and 2.55×10^{-15} mol/cell/h, respectively (Figure 4.3B). Figures 4.3C and 4.3D present the intra-cycle productivities for two SCF cycles, one in mid-campaign (cycle 11) and another in late-campaign (cycle 21). These results are reported as a function of normalized cycle time (time in cycle over total cycle time). The intra-cycle productivity of cycle 11 and cycle 21 (Figure 4.3C) showed comparable increasing trends, with greater productivities observed in the later stages of both cycles. Parabolic trends in intra-cycle integrated specific productivity were observed for both cycles 11 and 21 (Figure 4.3D). Strikingly, the maximal intra-cycle integrated specific productivity of cycle 21 occurred in the first half of the cycle (between normalized cycle times of 0.2 and 0.4) and was significantly greater than that of cycle 11 (Figure 4.3D).

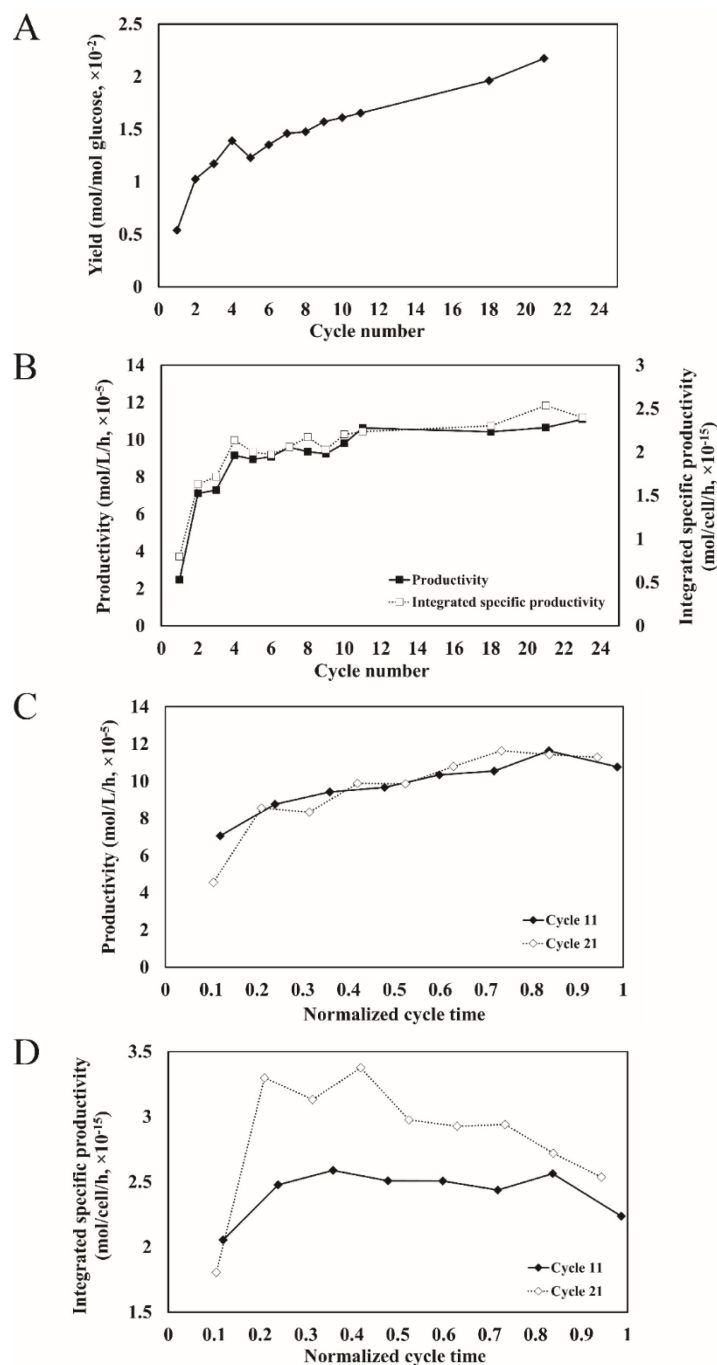


Figure 4.3 Yield, productivity, and integrated specific productivity of shikimic acid during SCF operation. A) The yield of shikimic acid per glucose over the SCF campaign. B) Productivity and integrated specific productivity of shikimic acid over the SCF campaign. Integrated specific productivity were calculated based on start-and-end-of-cycle cell counts. C) Intra-cycle productivity of shikimic acid for cycles 11 and 21. D) Intra-cycle integrated specific productivity of shikimic acid for cycles 11 and 21. Intra-cycle assessments in C) and D) are cumulative and reported as a function of normalized cycle time (in-cycle time over total cycle time) so that a complete cycle has a normalized time of 1.

4.4.2 Cellular Regulation

Relative expression levels ($\log_2(\text{FC})$) of genes were assessed at each of the four time points in BR and six time points in SCF cycle 23 (see Supplementary Table A1 and Figures 4.4A and 4.4B) through RNA-Seq analyses using the time point BR₃ as reference. Then, gene regulations related to select KEGG pathways were investigated. The results are shown as heatmaps for genes related to DNA replication (Figure 4.4C), cell cycle (Figure 4.5), the proteasome (Figure 4.6), the citric acid cycle (Figure 4.7), and oxidative phosphorylation (Figure 4.8) (heatmaps for other pathways and for comparisons amongst only BR sampling points can be found in Supplementary Materials). The first observation from a global perspective was that regulation was more pronounced in the SCF cycle compared to the BR; the fold-changes were greater, as indicated by the intensity of the red and blue colours in the heatmap figures.

As can be seen in Figure 4.4C, in BR, most genes associated with DNA replication were slightly up-regulated at BR₁ and down-regulated by BR₃. In SCF operation, almost all genes related to DNA replication were highly expressed at the SCF₂ sampling point – corresponding to a normalized cycle time of 0.077. It should also be noted that strong down-regulation was observed for approximately one third of the genes assessed at SCF₆.

Similarly, when assessing the regulation of genes related to the yeast cell cycle (Figure 4.5), slight up-regulation of different subsets of genes was observed at BR₁ and BR₃ (combined with significant down-regulation of other subsets of genes at the latter sampling point), but nearly half the total genes investigated were up-regulated at SCF₂. It should also be noted that a strong regulatory response, with both significant up-regulation (for approximately one quarter of the genes) and down-regulation (for approximately one third of the genes), was observed at SCF₆.

In addition, substantial down-regulation was found for proteasome-related genes in the earlier sampling points for both batch (BR₁) and SCF (SCF₂ and SCF₃; at normalized cycle times

of 0.077 and 0.195, respectively) operation (Figure 4.6). In fact, up-regulation was notable in the later stages of the cultures, reaching maxima at BR₃, and SCF₅ and SCF₆.

The majority of genes related to the citrate cycle (Figure 4.7) were down-regulated in the early sampling points of BR and slightly up-regulated in BR₃ and BR₄. In contrast, these genes were highly up-regulated at the onset and the end of the SCF cycle, SCF₁ and SCF₆ (at normalized cycle times of 0.001 and 1, respectively).

When looking at the genes involved in oxidative phosphorylation (Figure 4.8), two different trends occurred for two gene clusters: ATPase in cluster 1 and ATP synthases, cytochromes, etc. in cluster 2. During BR, genes from cluster 1 were strongly up-regulated at the earlier sampling times (BR₁ and BR₂) and less so at the later sampling times; in contrast, genes in cluster 2 that were initially down-regulated were slightly up-regulated by BR₃ and BR₄. During SCF cycle 23, genes from cluster 1 were down-regulated at the start and end of the cycle, and slightly up-regulated in between. Genes from cluster 2 showed the inverse trend, with strong up-regulation at the start and end of the cycle and down-regulation in between.

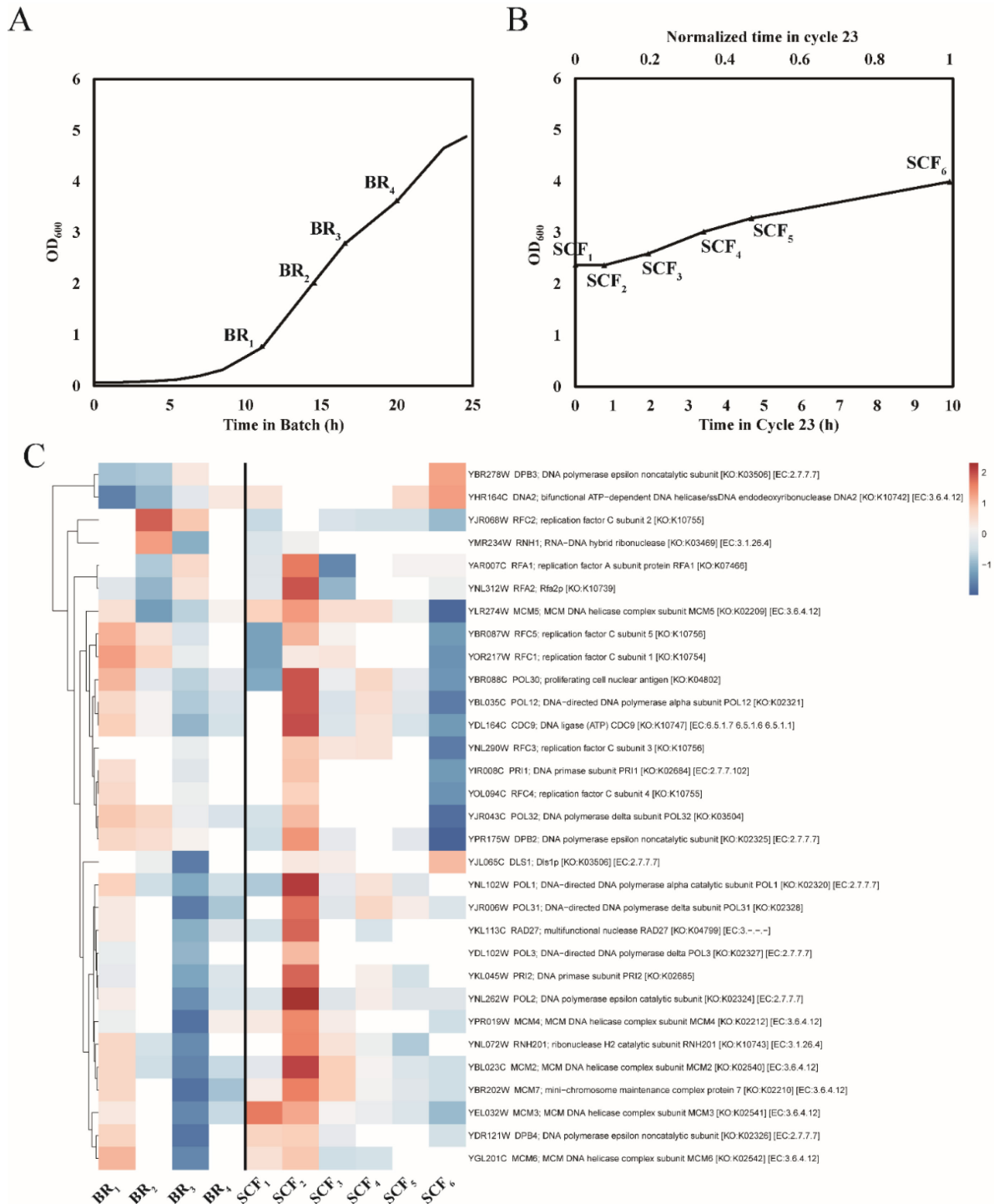


Figure 4.4 Relative expression levels ($\log_2(\text{FC})$) of genes related to DNA replication at different time points during BR and SCF cycle 23, with growth curves to show these time points. A) A growth curve shows when sampling points occurred during BR. B) A growth curve shows when sampling points occurred during SCF cycle 23. C) Heatmap of the relative differential expression at different sampling times in BR (left) and SCF cycle 23 (right). The names, descriptions, and

affiliations of genes related to DNA replication were retrieved from KEGG. Each column illustrates $\log_2(\text{FC})$ (with statistical significance) from DESeq2 comparisons using BR₃ as reference. Normalization within each row and clustering for rows were employed. Red to white to blue represents a decreasing trend of relative expression level. Data points without statistically significant differences are colored in pure white.

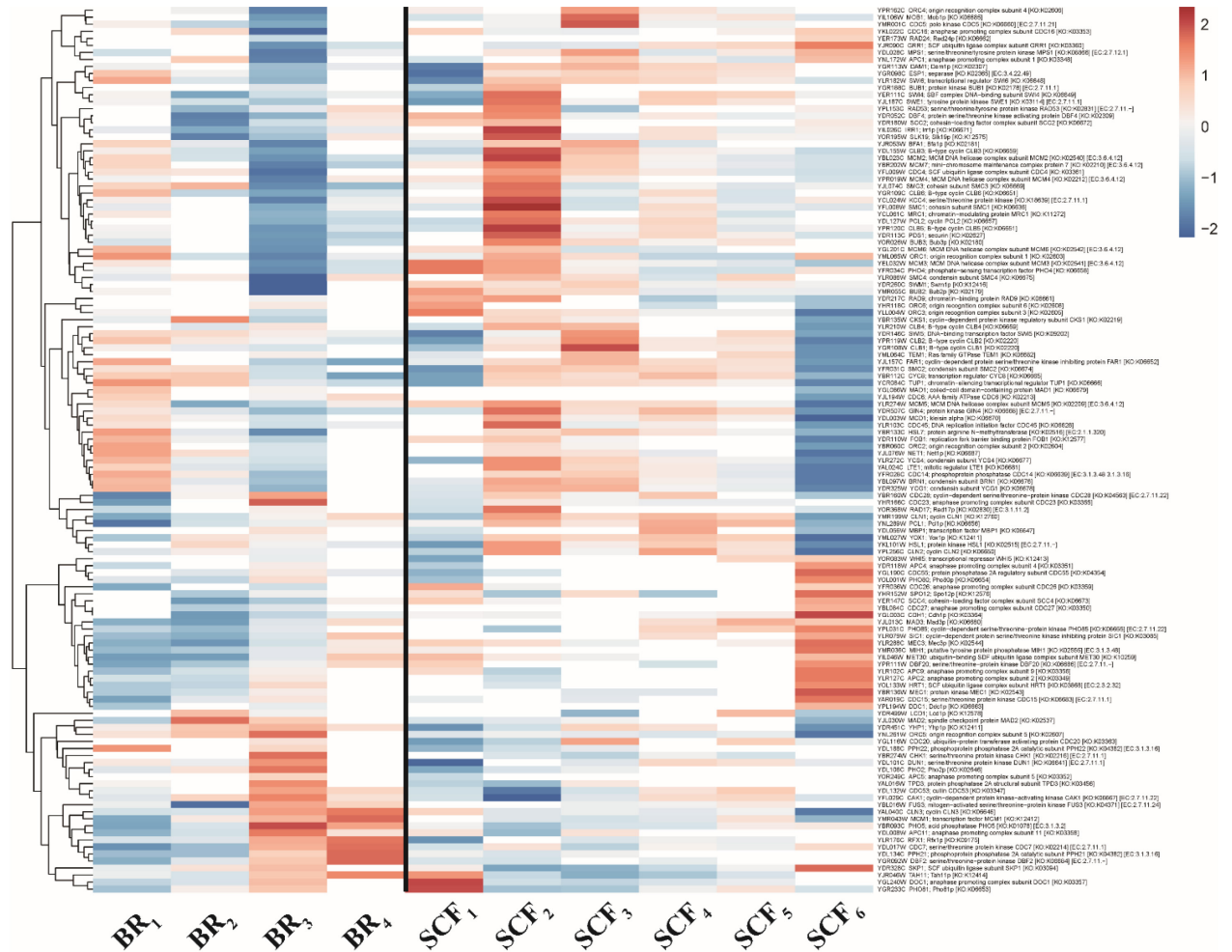


Figure 4.5 Relative expression levels ($\log_2(\text{FC})$) of genes related to the cell cycle at different time points during BR and SCF cycle 23. The names, descriptions, and affiliations of genes related to the cell cycle were retrieved from KEGG. Each column illustrates $\log_2(\text{FC})$ (with statistical significance) from DESeq2 comparison using BR₃ as reference. Normalization within each row and clustering for rows were employed. Red to white to blue represents a decreasing trend of relative expression level. Data points without statistically significant differences are colored in pure white.

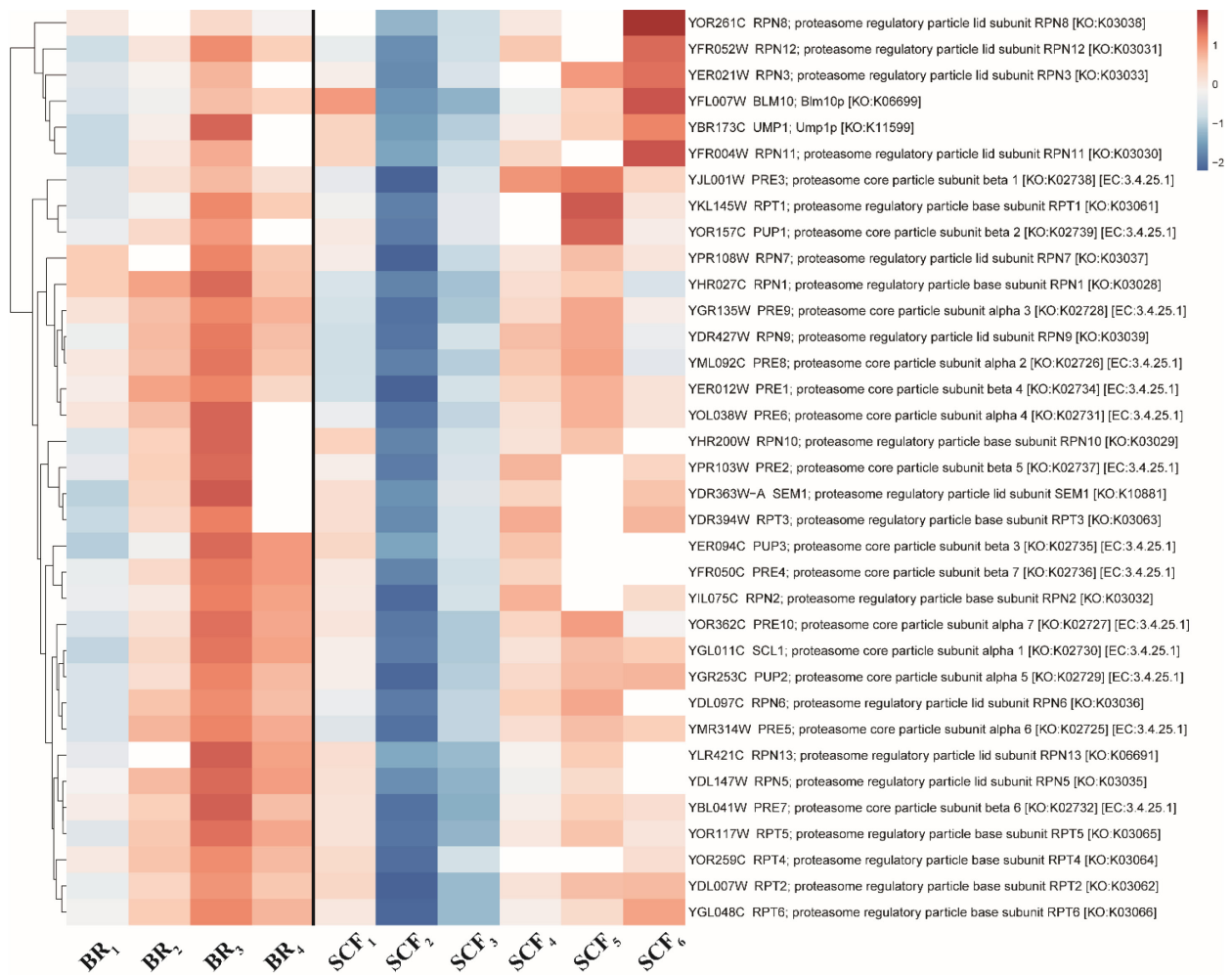


Figure 4.6 Relative expression levels ($\log_2(\text{FC})$) of genes related to proteasome at different time points during BR and SCF cycle 23. The names, descriptions, and affiliations of genes related to proteasome were retrieved from KEGG. Each column illustrates $\log_2(\text{FC})$ (with statistical significance) from DESeq2 comparison using BR₃ as reference. Normalization within each row and clustering for rows were employed. Red to white to blue represents a decreasing trend of relative expression level. Data points without statistically significant differences are colored in pure white.

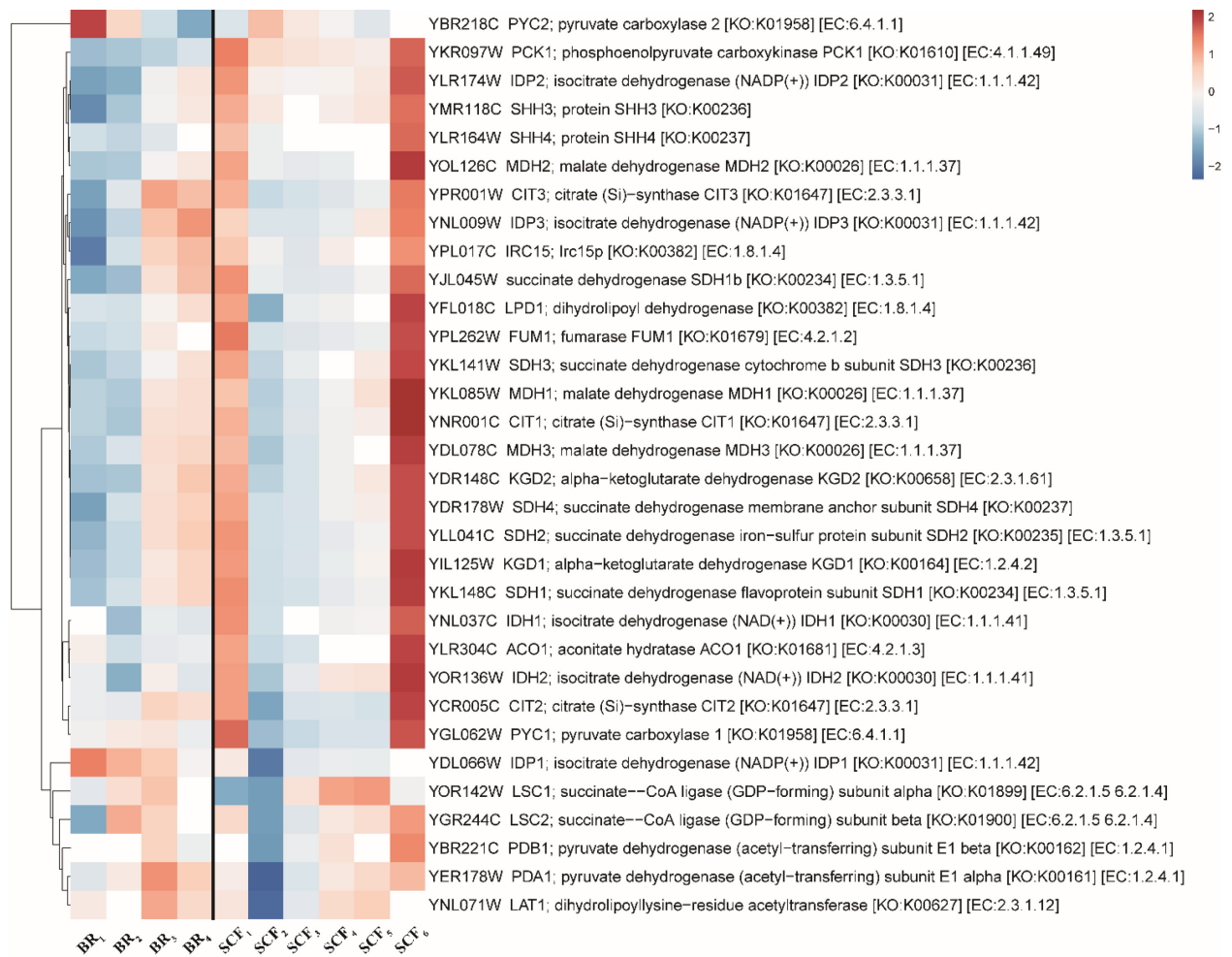


Figure 4.7 Relative expression levels ($\log_2(\text{FC})$) of genes related to the citrate cycle at different time points during BR and SCF cycle 23. The names, descriptions, and affiliations of genes related to the citrate cycle were retrieved from KEGG. Each column illustrates $\log_2(\text{FC})$ (with statistical significance) from DESeq2 comparison using BR₃ as reference. Normalization within each row and clustering for rows were employed. Red to white to blue represents a decreasing trend of relative expression level. Data points without statistically significant differences are colored in pure white.

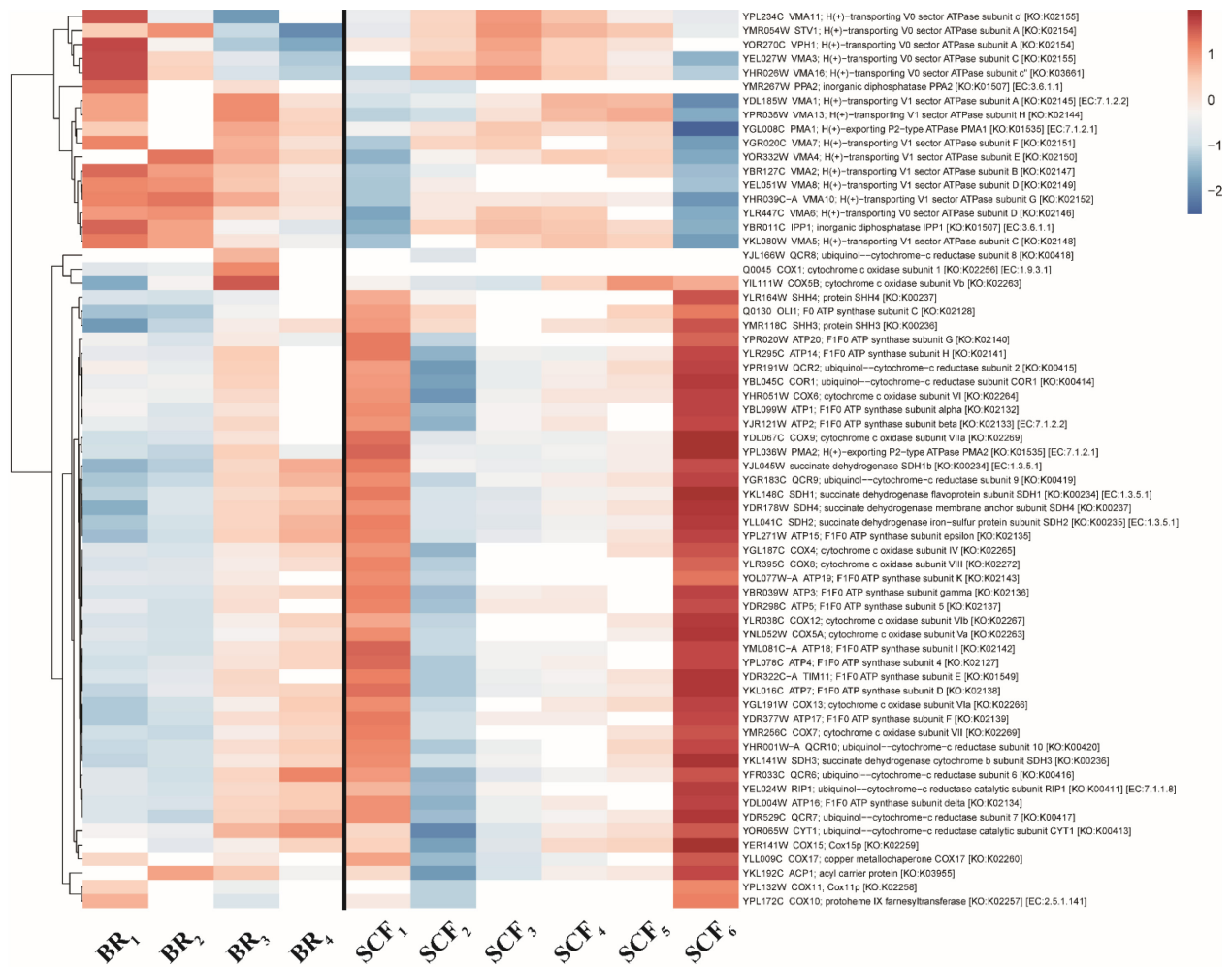


Figure 4.8 Relative expression levels ($\log_2(\text{FC})$) of genes related to oxidative phosphorylation at different time points during BR and SCF cycle 23. The names, descriptions, and affiliations of genes related to oxidative phosphorylation were retrieved from KEGG. Each column illustrates $\log_2(\text{FC})$ (with statistical significance) from DESeq2 comparison using BR₃ as reference. Normalization within each row and clustering for rows were employed. Red to white to blue represents a decreasing trend of relative expression level. Data points without statistically significant differences are colored in pure white.

More in-depth analysis of the relative expression levels (fold changes) of selected cyclin genes during SCF cycles was performed. Results from samples taken at different times in SCF cycles 21 and 23 are shown in Supplementary Figure A1. Since SCF cycles are stable and reproducible after a number of cycles from the onset of operation (Brown 2001), cycles 21 and 23

can be considered as equivalent in terms of transcription patterns. RNA-Seq was used to determine the fold change in regulation of selected cyclin genes, *CLN1*, *CLN2*, *CLB3*, *CLB1*, and *CLB2*, during SCF cycle 23, using BR₃ as the reference (Supplementary Figure A1A). *CLN1*, *CLN2* and *CLB3* were significantly up-regulated at a normalized time of 0.077, which was the second time point measured during the SCF cycle. Maximum transcription of *CLB1* and *CLB2* occurred at the subsequent sampling time point – at a normalized time of 0.195. It was also noticed that *CLN1* and *CLN2* were slightly up-regulated a second time at a normalized time of 0.343. For every investigated cyclin gene, the lowest relative expression level was found at the onset and the end of the SCF cycle, and the expression levels were similar between these two time points.

qPCR experiments were performed to determine the relative expression levels of *CLN1*, *CLB3*, and *CLB1* (using *ACT1* as the reference gene), and *CLN2*, *CLB3*, and *CLB2* (using *ACT1* and *ALG9* as the reference genes), respectively, in SCF cycle 21, using a BR₃ sample as the reference sample (Supplementary Figures A1B and A1C). The reference genes *ACT1* and *ALG9* showed equivalently stable expression throughout BR late-log phase and diauxic shift, SCF cycle 2, and SCF cycle 21 (data not shown). Consequently, either one or two reference genes were used for alignments, the expression trends shown for *CLB3* and the homologous genes, *CLN1* and *CLN2* or *CLB1* and *CLB2*, were similar between all qPCR experiments (Supplementary Figures A1B and A1C). The cyclin genes were mostly highly expressed in the first half of the cycle and their expression levels remained low in the second half of the cycle. Specifically, *CLN1*, *CLN2*, and *CLB3* were up-regulated (at a normalized cycle time of approximately 0.1) earlier than *CLB1* and *CLB2* (attaining maximum expression at a normalized cycle time of around 0.2), which is in accordance with the expression sequence of cyclin genes during a standard progression of the yeast cell cycle (Fitch et al. 1992; Cho et al. 1998). Identical trends in up-regulation of the cyclin genes were identified via RNA-Seq analyses (Supplementary Figure A1A), only with lower relative expression levels and fewer sampling points as compared to the qPCR results (Supplementary Figures A1B and A1C). In comparison, these trends in up-regulation of cyclin genes were not

observed during BR late-log phase and diauxic shift, even if there was still agreement between RNA-Seq and qPCR results (Supplementary Figure A2).

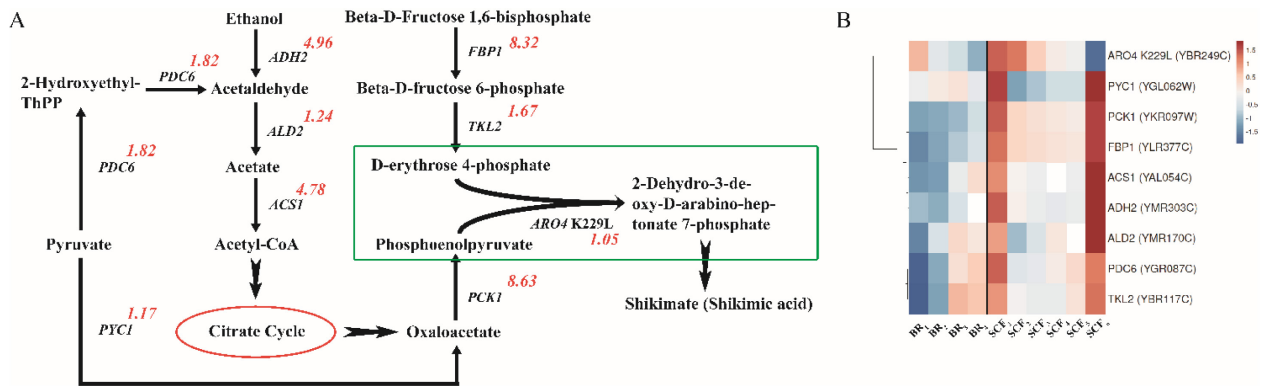


Figure 4.9 Reactions and up-regulation of genes related to shikimic acid production in SCF operation. A) Pathways and up-regulation of genes involved in shikimic acid synthesis. $\log_2(\text{FC})$ values are labeled in orange beside the standard gene names for time-point SCF₆, except for *ARO4* K229L (inside the green frame) which is reported for SCF₁. Arrows with a fletching shape indicate metabolites that are shuttled between pathways or undergoing multiple reactions. Straight arrows represent single reactions. B) A heatmap comparing the relative expression levels ($\log_2(\text{FC})$) for the genes described in A) at different time points during BR (left) and SCF cycle 23 (right). Each column illustrates $\log_2(\text{FC})$ (with statistical significance) from DESeq2 comparison using BR₃ as reference. Normalization within each row and clustering for rows were employed. Red to white to blue represents a decreasing trend of relative expression level. Data points without statistical significance are colored in pure white.

Figure 4.9 focuses on the segment of pathways and regulation of gene expression involved in shikimic acid synthesis. The up-regulated genes and associated reactions are summarized in Figure 4.9A, where relative expression levels ($\log_2(\text{FC})$) are labeled in orange next to the respective standard gene names for the time-point SCF₆ during SCF cycle 23, except for *ARO4* K229L (inside the green frame) for which the value corresponds to up-regulation at SCF₁. Figure 4.9B depicts the transient relative expression levels ($\log_2(\text{FC})$) of the same genes at different time-points in BR and SCF cycle 23 (sampling points shown in Figures 4.4A and 4.4B). Genes involved in reactions forming the precursors phosphoenolpyruvate and D-erythrose 4-phosphate, including the ones in

the citrate cycle (Figure 4.7), were highly up-regulated at the end and the onset of the SCF cycle (SCF₆ and SCF₁; at normalized cycle times of 1 and 0.001, respectively), whereas the condensation of phosphoenolpyruvate and D-erythrose 4-phosphate (shown in the green frame) was activated during the early stages of the SCF cycle (SCF₁₋₄; normalized cycle times of 0.001, 0.077, 0.195, and 0.343, respectively) (Figures 4.9A and 4.9B). Notably, *FBPI* and *PCK1* were consistently up-regulated throughout the SCF cycle, suggesting a consistent significant expression of Fbp1 and Pck1 during SCF operation – a sharp contrast to BR (Figure 4.9B).

4.5 Discussion

4.5.1 Impact of SCF Operation

SCF operation has been shown to have many advantages, most prominently related to stability and reproducibility of cycles, synchronization and improved productivity.

In this study, CER and its first derivative were used as control parameters to establish SCF cycling; a strategy that had previously been demonstrated in bacteria (Sauvageau et al. 2010; Sauvageau and Cooper 2010; Storms et al. 2012) but not yeast. After 5 cycles, CER followed stable and repeatable patterns (Figure 4.2). Even though the CER maximum and cycle time for each cycle varied slightly (Figure 4.2A), the total CO₂ evolved per cycle was consistent (Figure 4.2C). Remarkably, the patterns of OD₆₀₀ and glucose concentration became reproducible directly after the first cycle (Figures 4.2D and 4.2E). Glucose was consumed at a relatively constant rate throughout a given cycle (Supplementary Figure A3) and was depleted by the end of each cycle. As per the control strategy implemented, cycling was triggered once glucose was fully consumed. In detail, a decreased, flattened CER signal indicated the depletion of the main carbon source and initiated the cycling procedure. Complete substrate utilization, one of the advantages of implementing SCF operation, leads to better substrate use efficiency and can benefit downstream processing without the need for substrate recycling. The equivalent glucose concentrations used

for the BR culture and refilling media in the present study contrasted with different concentrations used in a previous *E. coli* SCF study (Sauvageau et al. 2010) and led to a greater stability during the initial SCF cycles.

Multiple SCF studies have reported cell synchrony during operation as assessed by a stepwise increase in cell density within SCF cycles once stable operation has been established (McCaffrey and Cooper 1995; Wentworth and Cooper 1996; Sauvageau et al. 2010). In addition to the determination of synchrony by cell density (results for cycles 11 and 21 are shown in Supplementary Figure A4), the present study is the first to characterize SCF synchronization at the transcriptomic level. Firstly, the patterns of gene regulation uncovered evidence of the synchronization effect. For instance, the majority of genes related to DNA replication and approximately half the genes related to the yeast cell cycle were highly expressed concurrently early in the SCF cycle (SCF₂, a normalized cycle time of 0.077) (Figures 4.4C and 4.5). The absence of proteasome-related transcripts at this and subsequent sampling points (SCF₂ and SCF₃; normalized cycle times of 0.077 and 0.195, respectively) provides further evidence of synchronization (Figure 4.6). In fact, the proteasome pathway was virtually shut down when culture-wide cell replication started synchronously, even though the pathway is required for cell cycle control (Feldmann 2012). Secondly, the significant trends and the sequence of up-regulation of the cyclin genes investigated, as determined by both RNA-Seq and qPCR (Supplementary Figure A1), agreed with the standard progression of the yeast cell cycle (Fitch et al. 1992; Cho et al. 1998) and further confirmed the synchronized cell replication during SCF cycles.

Considering the evolution of cell number within a cycle for which synchrony is well established (e.g., cycle 21; Supplementary Figure A4B), cell replication occurred only once per cycle. Looking at the results of cyclin genes expression during SCF cycles (Supplementary Figure A1), it can be deduced that cell replication occurred within the first half of the cycles and segregation of mother and daughter cells happened around the cycle midpoints. The normalized cycle time of 0.08 corresponded to the interphase of the cell cycle, as demonstrated by the high

expression levels of *CLN1*, *CLN2*, and *CLB3*. The mitosis phase, indicated by the significant up-regulation of *CLB1* and *CLB2*, occurred at a normalized cycle time of 0.2. The expression levels of the investigated cyclin genes were relatively low during the second half of the SCF cycle, indicating a completion of synchronized cell replication prior to the late stages of the cycle. A sharp, stepwise increase in cell density occurred within a narrow time frame close to the normalized cycle time of 0.45 in cycle 21 (Supplementary Figure A4B), which is further evidence of the aligned completion of cell division around the midpoint of the cycle. In addition, the total RNA concentration increased only before the midpoint of the cycle and then plateaued (Supplementary Figure A5), which is congruent with a decrease in expression of genes related to the ribosome and ribosome biogenesis during the cycle (Supplementary Figures A6 and A7). This is reasonable if cell doubling occurred only once prior to the midpoint of the cycle. Moreover, comparing the trends of intra-cycle productivities during SCF cycle 21 (Figures 4.3C and 4.3D), a sudden decrease in specific productivity and a slight increase in productivity in the middle of the cycle align with the sharp increase in cell density (Supplementary Figure A4). Based on the profile of cell density within cycles 11 and 21 (Supplementary Figure A4), we can also establish that cycle 21 presented a greater degree of synchronization.

Most likely, the characteristic change in glucose levels during SCF cycling (Figure 4.2E) constituted the forcing function that drove the cell population into synchrony (Wincure et al. 1995; Pinchuk et al. 2000) (i.e. entrainment mechanism (Sheppard and Dawson 1999)), since a high glucose concentration at the early stages of SCF cycles would substantially favor certain stages of the cell cycle progression (e.g., DNA replication and protein synthesis).

4.5.2 Production of Shikimic Acid

The most notable effect of SCF operation on the production of shikimic acid was its significant accumulation as the cycle number increased (Figure 4.2F). In fact, SCF cycle 23

produced over three-fold more shikimic acid than BR (SCF cycle 1) (Figure 4.2F); this even though twice the amount of glucose was consumed in BR than in the SCF cycle (Figure 4.2E). Yield on glucose and productivity rose drastically between cycle 1 (BR) and cycle 2, showing two-fold and three-fold increases, respectively (Figures 4.3A and 4.3B). After cycle 4, the productivity plateaued, with a small increase observed from cycles 9 to 11 (Figure 4.3B). In contrast, the shikimic acid yield increased consistently up to the end of SCF operation, suggesting a continuous improvement in selectivity of shikimic acid over biomass (Figures 4.3A and 4.2D). Moreover, by the end of SCF operation, four-fold increases were achieved in yield and productivity, and a three-fold improvement in integrated specific productivity was observed (Figures 4.3A and 4.3B). In addition, the pattern of integrated specific productivity was identical to that of productivity (Figure 4.3B), due to the stability of cell density throughout the SCF operation. Meanwhile, ethanol accumulation was found to decrease throughout SCF operation (Supplementary Figure A8). The fact that shikimic acid yield and selectivity increased throughout SCF operation while ethanol levels and inferred selectivity decreased suggests that the cells became more efficient at channeling carbon towards shikimic acid synthesis during the SCF operation. It should be considered that, for the same amount of substrate processed, the same amount of biomass was produced (Figure 4.2D) but an increasing amount of bioproduct was accumulated and at a faster rate.

Here, these substantial improvements in yield, productivity, and specific productivity during SCF cycles are interpreted using growth-related parameters and transcriptomics. On the basis of growth-related parameters, the early stages of BR – including lag phase, early and mid-log phase – require a considerable portion of the operation time but generally yield mediocre cell density. In comparison, SCF cycles did not display significant lag phases as indicated by near-linear trends in OD₆₀₀ (growth curve for cycle 23 in Figure 4.4B) and glucose concentration (Supplementary Figure A3, for cycle 21), as starvation or readaptation seemed to be excluded from SCF operation. As a result, the productivity of biomass during SCF cycles 2-25 was approximately 1.4-fold that obtained in BR (based on Figures 4.2A and 4.2D). While more efficient biomass

synthesis could benefit production of shikimic acid as a primary metabolite, this did not fully account for the observed increase in productivity. Regulation of genes related to shikimic acid production is expected to have played a greater role in the four-fold improvements in yield and volumetric productivity of shikimic acid.

Transcriptomic analyses highlight the significant changes in gene expression in the citrate cycle (Figure 4.7) and oxidative phosphorylation (Figure 4.8) during SCF cycle 23. The two pathways were attenuated (except for ATPase-related genes) while the population underwent synchronized cell replication (at SCF₂ and SCF₃; normalized cycle times of 0.077 and 0.195). Once the synchronous cell doubling was almost complete (at SCF₅; normalized cycle time of 0.471), the abundance of transcripts related to these pathways increased. Eventually, at the end of the cycle (SCF₆; normalized cycle time of 1), high expression was observed for the majority of genes associated with the citrate cycle and oxidative phosphorylation; abundance of transcripts left-over from the end of the cycle likely explain the high levels also observed at the onset of the next cycle (SCF₁; normalized time of 0.001). The highly activated citrate cycle and oxidative phosphorylation, both taking place in mitochondria, would lead to the generation of precursors and energy for shikimic acid production and other cellular reactions. This is consistent with the high expression of mitochondrial ribosomal proteins (upper cluster in Supplementary Figure A6) and, more importantly, up-regulated gluconeogenesis (upper cluster in Supplementary Figure A8) approaching to the end of the cycle. In extended BR, shikimic acid was also found to be produced based on ethanol during diauxic shift and post-diauxic shift, not only based on glucose during the previous stages (Supplementary Figure A9). In SCF cycles, a diauxic shift would be expected to impact the later stages of the cycles, as can be inferred by the significant up-regulation of genes related to gluconeogenesis at SCF₅ and SCF₆ (normalized cycle times of 0.471 and 1, respectively; upper cluster in Supplementary Figure A8); yeast cells prepared or initiated ethanol consumption in advance of glucose depletion by the end of each cycle (glucose concentration for cycle 21 in Supplementary Figure A3). It is likely that the up-regulation of the citrate cycle, oxidative

phosphorylation, and gluconeogenesis drove an increased gluconeogenesis activity in SCF cycles compared to BR (Figures 4.7, 4.8 and Supplementary Figure A8). The decrease in produced ethanol over SCF operation (Supplementary Figure A10) agrees with this speculation and further suggests a continuous increase in gluconeogenesis activity across SCF cycles, which should contribute to the continuous increase in shikimic acid yield and inferred selectivity (Figure 4.3A).

Figure 4.9A highlights the segmental pathways that are more directly related to the synthesis of shikimic acid. Phosphoenolpyruvate from glycolysis and gluconeogenesis and D-erythrose 4-phosphate from the pentose phosphate pathway are the two main precursors for shikimic acid synthesis. The regulation of gene expressions associated with these compounds suggests they accumulated near the end of the cycle (SCF₆; a normalized cycle time of 1) and at the start of the subsequent cycle (equivalent to SCF₁; a normalized cycle time of 0.001) (Figure 4.9B). In detail, ethanol and pyruvate conversion to acetyl-CoA was activated due to glucose exhaustion. Additionally, oxaloacetate was generated not only from acetyl-CoA through the up-regulated citrate cycle but also from activated pyruvate carboxylation via Pyc1. Then, oxaloacetate was shuttled to phosphoenolpyruvate by Pck1 (consistently expressed over the cycle, Figure 4.9B). As a precursor for D-erythrose 4-phosphate, beta-D-fructose 6-phosphate accumulated from beta-D-fructose 1,6-bisphosphate by Fbp1 (also consistently expressed over the cycle, Figure 4.9B). D-erythrose 4-phosphate was then generated (along with D-xylulose 5-phosphate) from beta-D-fructose 6-phosphate and D-glyceraldehyde 3-phosphate via expressed Tk12.

In the early stages of the SCF cycle (SCF₁₋₄; normalized cycle times of 0.001 to 0.343), the high expression of Aro4_{fbr}, inferred by the up-regulation of *ARO4* K229L, catalysed the condensation of phosphoenolpyruvate and D-erythrose 4-phosphate and shuttled them to shikimic acid (or shikimate) through the segmental pathway of aromatic amino acids biosynthesis (highlighted by the green frame in Figure 4.9A). Overall, from a transcriptomics perspective, the greater generation of precursors and energy close to the end of the cycle and the start of the subsequent cycle, as well as the significant expression of Aro4_{fbr} in the early stages of the cycle,

are likely the mechanisms leading to the highly improved yield, productivity, and specific productivity of shikimic acid during SCF operation. Strikingly, again based on the transcriptomic profiles, the drive for the synthesis of phosphoenolpyruvate and beta-D-fructose 6-phosphate remained relatively constant throughout the entire SCF cycle, owing to the continuous up-regulation of *PCK1* and *FBP1* (Figure 4.9B). In comparison, the expression of *PCK1* and *FBP1* remained at a much lower level during all four BR sampling points.

The intra-cycle profiles of shikimic acid productivity and integrated specific productivity in cycle 21 showed significant increases in the early stages of the cycle (Figures 4.3C, 3D). While productivity continued to increase through the cycle, the integrated productivity, which is a direct indicator of cell performance, increased rapidly before eventually decreasing once cell doubling was completed. As discussed above, in the beginning of the SCF cycle, the synchronized cell population is expected to be in interphase. The allocation of cellular resources towards protein and DNA synthesis during this phase of the cell cycle likely caused the lower shikimic acid specific productivity observed. Following this, two maxima were observed at normalized cycle times of 0.21 and 0.42 – corresponding to the mitosis phase of the cell cycle – with a local minimum observed at 0.32 (Figure 4.3D). These maxima in specific productivity of shikimic acid are consistent with the accumulation of the precursors at the end of the preceding cycle and onset of the current cycle, and increased synthesis of relevant enzymes (e.g., *Aro4_{br}*) in the early stages of the cycle (Figure 4.9). A similar trend for specific productivity was presented in a previous study of *E. coli* producing recombinant protein in a SCF process (Storms et al. 2012), where two distinct maxima of specific productivity were observed at the onset and completion of the synchronized cell segregation within a cycle.

In addition, the improvement in shikimic acid yield, selectivity, and specific productivity observed in cycle 21 as compared to both BR and cycle 11, highlights the beneficial effect of SCF operation in general and, potentially, synchronization in specific on the production of bioproducts such as shikimic acid.

In the engineered yeast used in this study, shikimic acid is considered a growth-associated primary metabolite. The selected cycling point for cycle 1 (at 24.5 h) corresponds to glucose depletion and the maximal productivity observed during extended BR (160 h) in the fermenter (Supplementary Figure A11). However, shikimic acid concentration and the suggested yield of shikimic acid from glucose can be further improved beyond this point in compensation for a lower productivity (Supplementary Figure A9). In later stages of extended BR, ethanol and other organic acids become substrates for production of shikimic acid as glucose becomes depleted (a process based on the well-demonstrated “make-accumulate-consume” life strategy of budding yeast (Hagman et al. 2013)). While a two-stage SCF scheme (van Walsum and Cooper 1993; McCaffrey and Cooper 1995; Wentworth and Cooper 1996; Sauvageau and Cooper 2010; Storms et al. 2012) or an extended cycle strategy (McCaffrey and Cooper 1995; Wentworth and Cooper 1996; Crosman et al. 2002) (two approaches used mostly for production of non-growth associated products) could have been considered to maximize yield, this would have come at the expense of productivity. In this study we pursued a balance between these two parameters; hence the focus on a single stage SCF operation.

The first study that described engineered *S. cerevisiae* strains producing shikimic acid incorporated overexpression of Aro4 K229L, Aro1 D920A, and Tk11. It led to a titer of 358 mg/L shikimic acid with a yield of 17.9 mg/g glucose (based on 20 g/L glucose) (Suástegui et al. 2016). In the present study, using a *S. cerevisiae* strain that had previously been engineered using a different approach based on a different parental strain, SCF cycle 21 resulted in a comparable, if slightly higher, shikimic acid concentration and yield – 365 mg/L and 21.0 mg/g glucose, respectively – in a bioreactor (Figures 4.2F and 4.3A). BR (including elongated BR) resulted in less significant production of shikimic compared to that observed previously (Suástegui et al. 2016) (Fig 2F, 3A, and S9). The impact of combining metabolic engineering with advanced fermentation strategies was, hence, highlighted by the current study.

Other studies investigating the production of shikimic acid in yeast lead to significant titers. Suástegui et al. (Suástegui et al. 2017) incorporated computational tools and a multilevel engineering approach to *S. cerevisiae* cells to reach shikimic acid concentrations of 2.0 g/L and 2.5 g/L using 4 % glucose and 4 % sucrose, respectively. Interestingly, a nonconventional yeast platform, *Scheffersomyces stipitis*, has also been engineered to overproduce shikimic acid to a concentration of 3.11 g/L, representing the highest production to date in yeast (Gao et al. 2017).

It should also be noted that additional tryptophan, phenylalanine, and tyrosine were required as supplements in the prior study (Suástegui et al. 2016) to suppress further shikimic acid conversion and in (Suástegui et al. 2017) to ensure the availability of aromatic amino acids for growth – a strategy which was not necessary in the present study.

In terms of further modifications and selections of yeast platforms, it seems that overexpression of gluconeogenesis proteins, e.g., Acs1, Fbp1, and Pck1, can lead to further enhancement in shikimic acid biosynthesis (Figure 4.9); incorporation of overexpression of Tkl1 and Aro1 D920A suggested previously (Suástegui et al. 2016) and multilevel metabolic engineering strategies (Suástegui et al. 2017) (e.g., deletion of *RIC1* and overexpression of *RKII* gene) could help develop highly efficient *S. cerevisiae* platforms for shikimic acid production; also, nonconventional yeast platforms, e.g., *S. stipitis* described before (Gao et al. 2017), could offer attractive opportunities. Indicated by the present study, the combinations of novel yeast platforms and the SCF technique would attract further exploratory interests.

4.6 Conclusions

Shikimic acid production was performed by growing an engineered *S. cerevisiae* strain under SCF operation. The SCF process was stable and cycles were reproducible. Notably, four-fold increases in yield and productivity, and a three-fold increase in integrated specific productivity

were obtained in SCF cycle 21 compared to SCF cycle 1 (a BR). For the first time, transcriptomic analyses (through RNA-Seq and qPCR) were carried out to characterize the SCF process. Synchronization of the cell population – a defining feature of SCF – was thus verified and interpreted at the transcriptomic level; most genes related to DNA replication and half the genes related to the yeast cell cycle were significantly up-regulated in the early stages of SCF cycles. The cellular mechanisms leading to the highly improved shikimic acid yield, volumetric productivity, and specific productivity were also elucidated on the basis of transcriptomic data: substantial up-regulation of genes related to gluconeogenesis, the citrate cycle, and oxidative phosphorylation near the start and end of SCF cycles enhanced the production of precursors and energy; *ARO4_{fbr}* was significantly up-regulated during the early stages of the SCF cycle to facilitate the synthesis of shikimic acid. Overall, the present study leads to a greater understanding of the impact of SCF operation on cellular mechanisms and demonstrates how its application to an engineered yeast system leads to a more effective production of shikimic acid towards industrial fermentation.

4.7 Supplementary Materials

In this thesis, the supplementary documents for Chapter 4 is incorporated as Appendix A, including: Continued Discussion; sampling time points for RNA-Seq (Supplementary Table A1) and qPCR experiments (for SCF cycle 21, Supplementary Table A2); information about the plasmid used by the engineered yeast strain (Supplementary Table A3); relative expression levels (fold changes) of selected cyclin genes during SCF cycles 21 and 23 (Supplementary Figure A1); the agreement between RNA-Seq and qPCR results during BR late-log phase and diauxic shift (Supplementary Figure A2); glucose concentration during SCF cycle 21 (Supplementary Figure A3); intra-cycle normalized cell density during SCF cycles 11 and 21 (Supplementary Figure A4); total RNA concentration (after extraction) during SCF cycle 21 (Supplementary Figure A5); heatmaps presenting relative expression levels ($\log_2(\text{FC})$) of genes related to the ribosome

(Supplementary Figure A6), ribosome biogenesis (Supplementary Figure A7), glycolysis and gluconeogenesis (Supplementary Figure A8), RNA polymerase (Supplementary Figure A19), pentose phosphate pathway (Supplementary Figure A20), and phenylalanine, tyrosine, and tryptophan biosynthesis (Supplementary Figure A21), at different time points during BR and SCF cycle 23; shikimic acid, glucose, and ethanol concentration during extended BR operation (Supplementary Figure A9); ethanol concentration during SCF operation (Supplementary Figure A10); productivity and integrated specific productivity of shikimic acid during extended BR operation (Supplementary Figure A11); heatmaps presenting relative expression levels ($\log_2(\text{FC})$) for genes related to the ribosome (Supplementary Figure A12), ribosome biogenesis (Supplementary Figure A13), RNA polymerase (Supplementary Figure A14), ubiquitin-mediated proteolysis (Supplementary Figure A15), glycolysis and gluconeogenesis (Supplementary Figure A16), the citrate cycle (Supplementary Figure A17), and oxidative phosphorylation (Supplementary Figure A18), at different time points during late-log phase and diauxic shift in BR, using an external sampling point SCF₆ as reference.

4.8 Acknowledgments

We would like to thank Prof. Vincent Martin from Concordia University for providing the engineered *S. cerevisiae* strain, Les Dean for the help in building the acquisition and control system, Prof. David C. Bressler for the help with HPLC systems, Troy Locke at MBSU from the University of Alberta for the help in operating the Bioanalyzer, Génome Québec for conducting library construction and RNA-Sequencing, and Melissa Harrison for the help during manuscript edition.

This work was supported by Natural Sciences and Engineering Research Council of Canada (NSERC) Discovery Grant and CGS-M programs, the Canada First Research Excellence Fund – Future Energy Systems, the Canada Foundation for Innovation – John R. Evans Leaders Fund, the

Government of Alberta – Ministry of Economic Development and Trade Small Equipment Grant, and the University of Alberta Faculty of Engineering.

4.9 References

- Afgan E, Baker D, Batut B, et al (2018) The Galaxy platform for accessible, reproducible and collaborative biomedical analyses: 2018 update. *Nucleic Acids Res* 46:537–544.
<https://doi.org/10.1093/nar/gky379>
- Anders S, Pyl PT, Huber W (2015) HTSeq-A Python framework to work with high-throughput sequencing data. *Bioinformatics* 31:166–169. <https://doi.org/10.1093/bioinformatics/btu638>
- Blumenthal LK, Zahler SA (1962) Index for measurement of Synchronization of cell populations. *Science* (80-) 135:724. <https://doi.org/10.1126/science.135.3505.724.a>
- Bolger AM, Lohse M, Usadel B (2014) Trimmomatic: A flexible trimmer for Illumina sequence data. *Bioinformatics* 30:2114–2120. <https://doi.org/10.1093/bioinformatics/btu170>
- Brown WA (2001) The self-cycling fermentor: development, applications, and future opportunities. In: *Recent research developments in biotechnology and bioengineering*. Research Signpost, pp 61–90
- Brown WA, Cooper DG (1991) Self-cycling fermentation applied to *Acinetobacter calcoaceticus* RAG-1. *Appl Environ Microbiol* 57:2901–2906. <https://doi.org/10.1128/aem.57.10.2901-2906.1991>
- Brown WA, Cooper DG (1992) Hydrocarbon degradation by *Acinetobacter calcoaceticus* RAG-1 using the self-cycling fermentation technique. *Biotechnol Bioeng* 40:797–805.
<https://doi.org/10.1002/bit.260400707>
- Brown WA, Cooper DG, Liss SN (2000) Toluene removal in an automated cyclical bioreactor. *Biotechnol Prog* 16:378–384. <https://doi.org/10.1021/bp0000149>
- Brown WA, Cooper DG, Liss SN (1999) Adapting the self-cycling fermentor to anoxic conditions. *Environ Sci Technol* 33:1458–1463. <https://doi.org/10.1021/es980856s>

- Cankorur-Cetinkaya A, Dereli E, Eraslan S, et al (2012) A novel strategy for selection and validation of reference genes in dynamic multidimensional experimental design in yeast. PLoS One 7:e38351. <https://doi.org/10.1371/journal.pone.0038351>
- Chan K-Y, Cheng CY (1977) Synchronization of cell division in marine bacteria by amino acid starvation. FEMS Microbiol Lett 2:177–180. <https://doi.org/10.1111/j.1574-6968.1977.tb00934.x>
- Cho RJ, Campbell MJ, Winzeler EA, et al (1998) A genome-wide transcriptional analysis of the mitotic cell cycle. Mol Cell 2:65–73. [https://doi.org/10.1016/S1097-2765\(00\)80114-8](https://doi.org/10.1016/S1097-2765(00)80114-8)
- Crosman JT, Pinchuk RJ, Cooper DG (2002) Enhanced biosurfactant production by *Corynebacterium alkanolyticum* ATCC 21511 using self-cycling fermentation. J Am Oil Chem Soc 79:467–472. <https://doi.org/10.1007/s11746-002-0507-5>
- Cunningham F, Achuthan P, Akanni W, et al (2019) Ensembl 2019. Nucleic Acids Res 47:D745–D751. <https://doi.org/10.1093/nar/gky1113>
- Davison SA, den Haan R, van Zyl WH (2016) Heterologous expression of cellulase genes in natural *Saccharomyces cerevisiae* strains. Appl Microbiol Biotechnol 100:8241–8254. <https://doi.org/10.1007/s00253-016-7735-x>
- Dawson PSS (1965) Continuous phased growth, with a modified chemostat. Can J Microbiol 11:893–903. <https://doi.org/10.1139/m65-119>
- Dawson PSS (1972) Continuously synchronised growth. J Appl Chem Biotechnol 22:79–103. <https://doi.org/10.1002/jctb.2720220112>
- Dell KA, Frost JW (1993) Identification and Removal of Impediments to Biocatalytic Synthesis of Aromatics from D-Glucose: Rate-Limiting Enzymes in the Common Pathway of Aromatic Amino Acid Biosynthesis. J Am Chem Soc 115:11581–11589. <https://doi.org/10.1021/ja00077a065>
- Feldmann H (2012) Yeast: Molecular and Cell Biology. Wiley-Blackwell
- Ferullo DJ, Cooper DL, Moore HR, Lovett ST (2009) Cell cycle synchronization of *Escherichia coli* using the stringent response, with fluorescence labeling assays for DNA content and replication. Methods 48:8–13. <https://doi.org/10.1016/j.ymeth.2009.02.010>

- Fitch I, Dahmann C, Surana U, et al (1992) Characterization of four B-type cyclin genes of the budding yeast *Saccharomyces cerevisiae*. *Mol Biol Cell* 3:805–818.
<https://doi.org/10.1091/mbc.3.7.805>
- Futcher B (1996) Cyclins and the wiring of the yeast cell cycle. *Yeast* 12:1635–1646.
[https://doi.org/10.1002/\(SICI\)1097-0061\(199612\)12:16<1635::AID-YEA83>3.0.CO;2-O](https://doi.org/10.1002/(SICI)1097-0061(199612)12:16<1635::AID-YEA83>3.0.CO;2-O)
- Gao M, Cao M, Suástegui M, et al (2017) Innovating a nonconventional yeast platform for producing shikimate as the building block of high-value aromatics. *ACS Synth Biol* 6:29–38. <https://doi.org/10.1021/acssynbio.6b00132>
- Ghosh S, Chisti Y, Banerjee UC (2012) Production of shikimic acid. *Biotechnol Adv* 30:1425–1431. <https://doi.org/10.1016/j.biotechadv.2012.03.001>
- Hagman A, Säll T, Compagno C, Piskur J (2013) Yeast “make-accumulate-consume” life strategy evolved as a multi-step process that predates the whole genome duplication. *PLoS One* 8:e68734. <https://doi.org/10.1371/journal.pone.0068734>
- Hartmann M, Schneider TR, Pfeil A, et al (2003) Evolution of feedback-inhibited β/α barrel isoenzymes by gene duplication and a single mutation. *Proc Natl Acad Sci U S A* 100:862–867. <https://doi.org/10.1073/pnas.0337566100>
- Hirsch I, Vondrejs V (1971) Division of *Escherichia coli* 15 TAU cells synchronized by arginine and uracil starvation. *Folia Microbiol (Praha)* 16:137–141.
<https://doi.org/10.1007/BF02887484>
- Hughes SM, Cooper DG (1996) Biodegradation of phenol using the self-cycling fermentation (SCF) process. *Biotechnol Bioeng* 51:112–119. [https://doi.org/10.1002/\(SICI\)1097-0290\(19960705\)51:1<112::AID-BIT13>3.0.CO;2-S](https://doi.org/10.1002/(SICI)1097-0290(19960705)51:1<112::AID-BIT13>3.0.CO;2-S)
- Jacobs CW, Adams AE, Szaniszló PJ, Pringle JR (1988) Functions of microtubules in the *Saccharomyces cerevisiae* cell cycle. *J Cell Biol* 107:1409–1426.
<https://doi.org/10.1083/jcb.107.4.1409>
- Kanehisa M, Goto S (2000) KEGG: Kyoto Encyclopedia of Genes and Genomes. *Nucleic Acids Res* 28:27–30. <https://doi.org/10.1093/nar/28.1.27>
- Kim D, Langmead B, Salzberg SL (2015) HISAT: A fast spliced aligner with low memory

- requirements. *Nat Methods* 12:357–360. <https://doi.org/10.1038/nmeth.3317>
- Kim D, Pertea G, Trapnell C, et al (2013) TopHat2: Accurate alignment of transcriptomes in the presence of insertions, deletions and gene fusions. *Genome Biol* 14:R36. <https://doi.org/10.1186/gb-2013-14-4-r36>
- Knop DR, Draths KM, Chandran SS, et al (2001) Hydroaromatic equilibration during biosynthesis of shikimic acid. *J Am Chem Soc* 123:10173–10182. <https://doi.org/10.1021/ja0109444>
- Koç A, Wheeler LJ, Mathews CK, Merrill GF (2004) Hydroxyurea Arrests DNA Replication by a Mechanism that Preserves Basal dNTP Pools. *J Biol Chem* 279:223–230. <https://doi.org/10.1074/jbc.M303952200>
- Kramhøft B, Zeuthen E (1975) Chapter 18 synchronization of the fission yeast *Schizosaccharomyces pombe* using heat shocks. In: *Methods in Cell Biology*. Academic Press, pp 373–380
- Liu DF, Ai GM, Zheng QX, et al (2014) Metabolic flux responses to genetic modification for shikimic acid production by *Bacillus subtilis* strains. *Microb Cell Fact* 13:1–11. <https://doi.org/10.1186/1475-2859-13-40>
- Livak KJ, Schmittgen TD (2001) Analysis of relative gene expression data using real-time quantitative PCR and the 2- $\Delta\Delta$ CT method. *Methods* 25:402–408. <https://doi.org/10.1006/meth.2001.1262>
- Love MI, Huber W, Anders S (2014) Moderated estimation of fold change and dispersion for RNA-seq data with DESeq2. *Genome Biol* 15:550. <https://doi.org/10.1186/s13059-014-0550-8>
- Marchessault P, Sheppard JD (1997) Application of self-cycling fermentation technique to the production of poly- β -hydroxybutyrate. *Biotechnol Bioeng* 55:815–820. [https://doi.org/10.1002/\(SICI\)1097-0290\(19970905\)55:5<815::AID-BIT12>3.0.CO;2-A](https://doi.org/10.1002/(SICI)1097-0290(19970905)55:5<815::AID-BIT12>3.0.CO;2-A)
- Martínez JA, Bolívar F, Escalante A (2015) Shikimic acid production in *Escherichia coli*: From classical metabolic engineering strategies to omics applied to improve its production. *Front Bioeng Biotechnol* 3:145. <https://doi.org/10.3389/fbioe.2015.00145>

- McCaffrey WC, Cooper DG (1995) Sophorolipids production by *Candida bombicola* using self-cycling fermentation. *J Ferment Bioeng* 79:146–151. [https://doi.org/10.1016/0922-338X\(95\)94082-3](https://doi.org/10.1016/0922-338X(95)94082-3)
- McClellan K, Perry CM (2001) Oseltamivir: A review of its use in influenza. *Drugs* 61:263–283. <https://doi.org/10.2165/00003495-200161020-00011>
- Metsalu T, Vilo J (2015) ClustVis: A web tool for visualizing clustering of multivariate data using Principal Component Analysis and heatmap. *Nucleic Acids Res* 43:W566–W570. <https://doi.org/10.1093/nar/gkv468>
- Mookerjee S (2016) Directing Precursor Flux to Optimize cis,cis-Muconic Acid Production in *Saccharomyces cerevisiae*. Concordia University
- Pinchuk RJ, Brown WA, Hughes SM, Cooper DG (2000) Modeling of biological processes using self-cycling fermentation and genetic algorithms. *Biotechnol Bioeng* 67:19–24. [https://doi.org/10.1002/\(SICI\)1097-0290\(20000105\)67:1<19::AID-BIT3>3.0.CO;2-C](https://doi.org/10.1002/(SICI)1097-0290(20000105)67:1<19::AID-BIT3>3.0.CO;2-C)
- Rawat G, Tripathi P, Saxena RK (2013) Expanding horizons of shikimic acid: Recent progresses in production and its endless frontiers in application and market trends. *Appl Microbiol Biotechnol* 97:4277–4287. <https://doi.org/10.1007/s00253-013-4840-y>
- Sarkis BE, Cooper DG (1994) Biodegradation of aromatic compounds in a self-cycling fermenter (SCF). *Can J Chem Eng* 72:874–880. <https://doi.org/10.1002/cjce.5450720514>
- Sauvageau D, Cooper DG (2010) Two-stage, self-cycling process for the production of bacteriophages. *Microb Cell Fact* 9:1–10. <https://doi.org/10.1186/1475-2859-9-81>
- Sauvageau D, Storms Z, Cooper DG (2010) Synchronized populations of *Escherichia coli* using simplified self-cycling fermentation. *J Biotechnol* 149:67–73. <https://doi.org/10.1016/j.jbiotec.2010.06.018>
- Sheppard JD (1993) Improved volume control for self-cycling fermentations. *Can J Chem Eng* 71:426–430. <https://doi.org/10.1002/cjce.5450710312>
- Sheppard JD, Cooper DG (1991) The response of *Bacillus subtilis* ATCC 21332 to manganese during continuous-phased growth. *Appl Microbiol Biotechnol* 35:72–76. <https://doi.org/10.1007/BF00180639>

- Sheppard JD, Cooper DG (1990) Development of computerized feedback control for the continuous phasing of *Bacillus subtilis*. *Biotechnol Bioeng* 36:539–545.
<https://doi.org/10.1002/bit.260360514>
- Sheppard JD, Dawson PSS (1999) Cell synchrony and periodic behaviour in yeast populations. *Can J Chem Eng* 77:893–902. <https://doi.org/10.1002/cjce.5450770515>
- Storms ZJ, Brown T, Sauvageau D, Cooper DG (2012) Self-cycling operation increases productivity of recombinant protein in *Escherichia coli*. *Biotechnol Bioeng* 109:2262–2270.
<https://doi.org/10.1002/bit.24492>
- Suástegui M, Guo W, Feng X, Shao Z (2016) Investigating strain dependency in the production of aromatic compounds in *Saccharomyces cerevisiae*. *Biotechnol Bioeng* 113:2676–2685.
<https://doi.org/10.1002/bit.26037>
- Suástegui M, Shao Z (2016) Yeast factories for the production of aromatic compounds: from building blocks to plant secondary metabolites. *J Ind Microbiol Biotechnol* 43:1611–1624.
<https://doi.org/10.1007/s10295-016-1824-9>
- Suástegui M, Yu Ng C, Chowdhury A, et al (2017) Multilevel engineering of the upstream module of aromatic amino acid biosynthesis in *Saccharomyces cerevisiae* for high production of polymer and drug precursors. *Metab Eng* 42:134–144.
<https://doi.org/10.1016/j.ymben.2017.06.008>
- Teste MA, Duquenne M, François JM, Parrou JL (2009) Validation of reference genes for quantitative expression analysis by real-time RT-PCR in *Saccharomyces cerevisiae*. *BMC Mol Biol* 10:1–15. <https://doi.org/10.1186/1471-2199-10-99>
- Trapnell C, Williams BA, Pertea G, et al (2010) Transcript assembly and quantification by RNA-Seq reveals unannotated transcripts and isoform switching during cell differentiation. *Nat Biotechnol* 28:511–515. <https://doi.org/10.1038/nbt.1621>
- Tripathi P, Rawat G, Yadav S, Saxena RK (2013) Fermentative production of shikimic acid: A paradigm shift of production concept from plant route to microbial route. *Bioprocess Biosyst Eng* 36:1665–1673. <https://doi.org/10.1007/s00449-013-0940-4>
- Untergasser A, Cutcutache I, Koressaar T, et al (2012) Primer3-new capabilities and interfaces.

- Nucleic Acids Res 40:1–12. <https://doi.org/10.1093/nar/gks596>
- van Walsum GP, Cooper DG (1993) Self-cycling fermentation in a stirred tank reactor. *Biotechnol Bioeng* 42:1175–1180. <https://doi.org/10.1002/bit.260421007>
- Walker GM, Duffus JH (1980) Magnesium ions and the control of the cell cycle in yeast. *J Cell Sci* VOL.42:329–356. <https://doi.org/10.1242/jcs.42.1.329>
- Wang J, Chae M, Bressler DC, Sauvageau D (2020) Improved bioethanol productivity through gas flow rate-driven self-cycling fermentation. *Biotechnol Biofuels* 13:1–14. <https://doi.org/10.1186/s13068-020-1658-6>
- Wang J, Chae M, Sauvageau D, Bressler DC (2017) Improving ethanol productivity through self-cycling fermentation of yeast: A proof of concept. *Biotechnol Biofuels* 10:193. <https://doi.org/10.1186/s13068-017-0879-9>
- Wentworth SD, Cooper DG (1996) Self-cycling fermentation of a citric acid producing strain of *Candida lipolytica*. *J Ferment Bioeng* 81:400–405. [https://doi.org/10.1016/0922-338X\(96\)85140-3](https://doi.org/10.1016/0922-338X(96)85140-3)
- Wincure BM, Cooper DG, Rey A (1995) Mathematical model of self-cycling fermentation. *Biotechnol. Bioeng.* 46:180–183
- Zenaitis MG, Cooper DG (1994) Antibiotic production by *Streptomyces aureofaciens* using self-cycling fermentation. *Biotechnol Bioeng* 44:1331–1336. <https://doi.org/10.1002/bit.260441109>
- Zhang B, Liu ZQ, Liu C, Zheng YG (2016) Application of CRISPRi in *Corynebacterium glutamicum* for shikimic acid production. *Biotechnol Lett* 38:2153–2161. <https://doi.org/10.1007/s10529-016-2207-z>

5. The Influence of Long and Short Cycle Schemes of Self-cycling Fermentation on the Growth of *E. coli* and *S. cerevisiae*

5.1 Abstract

Self-cycling fermentation (SCF), a cyclic process in which cells divide once per cycle, has been shown to lead to improvements in productivity during bioconversion and, often, whole-culture synchronization. Previous studies have found that in some cases, the completion of synchronized cell replication occurred simultaneously with depletion of a limiting nutrient. However, exceptions were also observed when the end of cell doubling occurred before the exhaustion of the limiting nutrient. In order to better understand the underlying mechanisms and impacts of these growth patterns on bioprocessing, we investigated the growth of *Escherichia coli* and *Saccharomyces cerevisiae* in long- and short-cycle SCF strategies. Three characteristic events linked to SCF cycles were identified: (1) the completion of synchronized cell replication, (2) the depletion or a plateau of the limiting nutrient, and (3) characteristic points of control parameters (e.g., the minimum of dissolved oxygen and the maximum of carbon dioxide evolution rate). Three major trends stemming from this study and SCF literature were observed: (A) co-occurrence of the three key events in SCF cycles, (B) cycles for which cell replication ended prior to the co-occurrence of the other two events, and (C) cycles for which the time of depletion or a plateau of the limiting nutrient occurred later than the concurrence of the other two events. Based on these observations, a novel definition for SCF is proposed.

5.2 Introduction

Self-cycling fermentation (SCF) is an advanced fermentation technique that improves productivity in many bioconversion processes (Sauvageau and Cooper 2010; Storms et al. 2012; Agustin 2015; Wang et al. 2017). It is a semi-continuous, unsteady-state, cyclical mode of operation, in which, following an initial batch growth, cycles are triggered when the depletion of a limiting nutrient occurs (Brown and Cooper 1991; Sauvageau et al. 2010). Many metabolism- and growth-related parameters, including dissolved oxygen (DO), carbon dioxide evolution rate

(CER), oxidation-reduction potential (ORP), and exit gas mass flow rate, have served as control parameters to fulfill the automated feedback-control necessary for SCF cycling (Brown 2001; Wang et al. 2020, 2021). When a pre-established condition of the control parameter is met, SCF cycling is triggered and exactly one half of the working volume is harvested before being replenished with the same amount of fresh medium (Brown and Cooper 1991; Sauvageau et al. 2010).

The increased productivity demonstrated in many SCF studies (Brown and Cooper 1991; Zenaitis and Cooper 1994; Wentworth and Cooper 1996; Sauvageau and Cooper 2010; Storms et al. 2012; Wang et al. 2017, 2020) is strongly related to the operational characteristics of this semi-continuous process. Compared to a conventional batch reactor (BR), SCF cycles have negligible lag or stationary phases. Also, in contrast to chemostats, SCF greatly minimizes nutrient waste, especially the limiting one, and the products can be harvested at higher concentrations, facilitating downstream processing. Moreover, since the limiting nutrient is completely depleted every cycle, SCF operation has shown strong potential for pollutant degradation when pollutants were used as limiting carbon or nitrogen sources (Brown and Cooper 1992; Sarkis and Cooper 1994; Hughes and Cooper 1996; Brown et al. 1999, 2000).

SCF and continuous phasing (Dawson 1965, 1972; Sheppard and Cooper 1990, 1991), its forebearer, share many similarities. One is the entrainment mechanism that describes the periodic availability of essential nutrients inducing synchronization (Sheppard and Dawson 1999). A sharp increase in cell count within a narrow time window during a given cycle was observed for both continuous phasing and SCF (Sheppard and Dawson 1999). Flow cytometry validated that synchrony had been achieved during continuous phasing of bacteria by the determination of DNA content and cell sizes (Fritsch et al. 2005). Transcriptomic patterns were used to confirm that synchrony was obtained during SCF of yeast (Chapter 4). Many relevant trends could be observed in the prior study, including that most genes related to DNA replication and half of the genes associated with the yeast cell cycle were significantly up-regulated at the same point during the early SCF cycles (Chapter 4).

The incorporation of a feedback control system in SCF is a major difference and improvement compared to continuous phasing. It prevents either starvation or washout, and triggers medium replacement precisely at the exhaustion of the limiting nutrient (Brown 2001).

The decisive influence of cell growth on cycle time is paramount to SCF operation. In a large number of studies implementing the SCF technique, the cycle time was found to be equal to the doubling time of the same microorganism growing under the same nutrient conditions (Sheppard and Cooper 1990; Brown and Cooper 1991; Sarkis and Cooper 1994; McCaffrey and Cooper 1995; Wentworth and Cooper 1996; Brown et al. 1999). Subsequently, SCF cycle time was used to reflect the nutrient quality of the environment in a number of physiological studies; wherein a shorter cycle time suggested more efficient cell replication and thus a more beneficial nutrient condition (Brown 2001).

Although many SCF studies have depicted the concurrence of the completion of the cell cycle with the depletion of the limiting nutrient and a minimum in DO (corresponding to a maximum in CER) (Sheppard and Cooper 1990; Brown and Cooper 1991; Sarkis and Cooper 1994; McCaffrey and Cooper 1995; Wentworth and Cooper 1996; Brown et al. 1999), recent studies conducted with *Escherichia coli* and *Saccharomyces cerevisiae* (Sauvageau et al. 2010; Storms et al. 2012; Agustin 2015) (as well as Chapter 4) showed the completion of synchronized cell division (corresponding to the maximum in CER) occurring before depletion of the limiting nutrient. The end of synchronized cell doubling was identified by a sudden step-wise increase in cell density (Sauvageau et al. 2010; Storms et al. 2012; Agustin 2015) and flattened expression of selected cyclin genes (Chapter 4). Revisiting earlier SCF results, a similar misalignment between the end of synchronized cell division and the exhaustion of the limiting nutrient was also found for other microorganisms (Sheppard 1993; Marchessault and Sheppard 1997; Crosman et al. 2002). However, the trends in the control parameters could be different (Sheppard 1993; Marchessault and Sheppard 1997). With these discrepancies in mind, we show that an SCF short cycle strategy, cycling when the maximum in CER occurred, could lead to stable cyclic operation of *E. coli* and *S. cerevisiae* with enhanced volumetric biomass productivity. Also, transcriptional shifts of selected cyclin genes were explored during *S. cerevisiae* short cycles. These results confirmed the time at which cell replication of these microbes was completed and led to the identification of three typical trends during all SCF scenarios. In trend A, the end of synchronized cell replication, the exhaustion of the limiting nutrient, and the characteristic points of control parameters (three characteristic events) occur concomitantly. In Trend B, cell doubling completes before the co-occurrence of the other two events. Finally, in Trend C, the limiting nutrient is depleted or reaches a plateau after the joint occurrence of the other two events. The results from this study enable a

better understanding of the cellular processes during SCF and can guide the development of more efficient bioconversion processes.

5.3 Materials and Methods

5.3.1 Strains, Media, and Pre-cultures

Escherichia coli MG1655 (CGSC 6300) was used in *E. coli* studies. Luria-Bertani (LB) broth (all chemicals used in this study were purchased from Fisher Scientific and Sigma Aldrich, Canada) was used for agar plates (1.5% w/v of agar). Semi-defined liquid medium was used in Erlenmeyer flasks or fermenters, containing 6 g/L sodium phosphate dibasic, 4 g/L ammonium nitrate, 4 g/L potassium phosphate monobasic, 0.014 g/L disodium EDTA, 0.05 g/L yeast extract, 0.01 g/L calcium chloride dihydrate, 0.01 g/L iron sulfate heptahydrate, 6 g/L glucose, and 0.2 g/L magnesium sulfate heptahydrate. Pre-cultures were grown in 250-mL Erlenmeyer flasks at 37 °C, 250 rpm for 12 h. Approximately 4×10^{10} cells (10 mL) were withdrawn from pre-cultures and used to inoculate the 1-L fermenter working volume to achieve 1 % v/v inoculation.

An engineered *Saccharomyces cerevisiae* (Mookerjee 2016), genetically modified to overproduce shikimic acid based on parental strain CEN.PK 113-1A *MAT α* , was kindly provided by Prof. Vincent Martin at Concordia University. *E. coli* *ARO B* , *ARO D* , and the feedback-resistant variant of constitutive *ARO 4* (*ARO 4* K229L) were introduced using a pYES plasmid with *URA 3* for auxotrophic selection (Mookerjee 2016). 1.92 g/L yeast synthetic drop-out medium excluding uracil was used for auxotrophic selection on agar plates (1.5 % w/v of agar). 6.7 g/L yeast nitrogen base (YNB) without amino acids and 20 g/L dextrose comprised liquid medium. Pre-cultures were grown in Erlenmeyer flasks at 30 °C and 150 rpm for 48 h. Approximately 8×10^8 cells (10 mL) from pre-cultures were added to the 1-L working volume in the fermenter to achieve 1 % v/v inoculation.

5.3.2 SCF Configuration and Operation

The SCF configuration was previously described in (Sauvageau et al. 2010) (also in Chapter 4), with a 2-L stainless steel fermenter (10.5 cm I.D.). The feed system included a 10-L

carboy (Nalgene, Fisher Scientific) containing fresh medium, a peristaltic pump (77201-60, Cole Parmer), a solenoid valve (SV125, Omega), and a glass isolator. The harvesting system consisted of a solenoid valve (SV125, Omega) and a 10-L harvest carboy (Nalgene, Fisher Scientific). Air was supplied by passing through an air regulator (R07-200-RGKA, Norgren), a sterilized water bottle (for stabilization and humidification), a rotameter (03294-20, Cole Parmer), and a HEPA filter (Whatman). Exit gas flew through a glass condenser and a HEPA filter (Whatman). Carbon dioxide (CO₂) in the exit gas was measured with an in-line CO₂ gas sensor (CO₂-BTA, Vernier) located after the filter. Precise volume control during cycling was realized using high-level and low-level optical sensors (ELS-900 series, Gems Sensors) at 1 L and 0.5 L, respectively. The temperature was monitored and controlled using a K-type thermocouple (GKQSS-18G-10, Omega) and a cartridge heater (CIR-1032/120V, Omega). Real-time data of cycle time, temperature, carbon dioxide evolution rate (CER, based on CO₂ concentration in the exit gas), and the first derivatives of CER over 20 min and 60 min (referred to as short dCER and long dCER) were monitored and recorded by LabView (National Instruments) via an OPTO 22 data acquisition board. A LabView program was used to control conditions and automate cycling.

The fermenter temperature was maintained at 37 °C during bacterial growth and 30 °C during yeast growth. Agitation at 250 rpm with a Rushton impeller (4-cm diameter) and aeration at 400 mL/min for *E. coli* and 845 mL/min for *S. cerevisiae* provided sufficient mixing and aerobic conditions. During the SCF cycling procedure, agitation was ceased to maintain liquid level stability. Cell culture drainage driven by gravity stopped when the liquid level reached the low-level sensor. Fresh medium was then pumped into the bioreactor until the 1-L working volume was reached.

The following conditions were used to trigger automated cycling (see above definitions of short and long dCER). For the *E. coli* SCF long cycle operation: (1) cycle time was greater than 90 min; (2) the absolute value of short dCER was less than 2.00×10^{-5} mmol/L/h/min (0.02 ppm/min for the derivative of CO₂ concentration); (3) long dCER was less than 0. For the *E. coli* SCF short cycle scheme: (1) cycle time was greater than 60 min; (2) short dCER was less than -2.00×10^{-5} mmol/L/h/min (-0.02 ppm/min for the derivative of CO₂ concentration). For the *S. cerevisiae* SCF long cycle scheme: (1) cycle time was greater than 300 min; (2) CER was less than 5.08 mmol/L/h (3000 ppm for CO₂ concentration); (3) the absolute value of short dCER was less

than 9.69×10^{-5} mmol/L/h/min (0.05 ppm/min for the derivative of CO₂ concentration); (4) long dCER was less than 0. For the *S. cerevisiae* SCF short cycle strategy: (1) cycle time was greater than 110 min; (2) short dCER was less than -3.88×10^{-5} mmol/L/h/min (-0.02 ppm/min for the derivative of CO₂ concentration); (3) CER was more than 5.08 mmol/L/h (3000 ppm for CO₂ concentration).

5.3.3 Batch Reactor Configuration and Operation

Supplementary Figure B1 depicts the BR set-up, which was adapted from the SCF set-up and used when BR operation was decoupled from SCF operation in cultivating *E. coli*. Cultivation conditions during BR were congruent with those used for SCF operation. Additionally, the first cycles of SCF operation are analogues of BR.

5.3.4 Measurement of Optical Density, Glucose, Ammonium, and Nitrate & Nitrite

A spectrophotometer (Ultrospec 50, Biochrom) was used to measure optical density of culture samples at a wavelength of 600 nm (OD₆₀₀).

Glucose concentration was determined using the reducing sugar method (Miller 1959). Dinitrosalicylic acid (DNS) reagent was used, containing 10 g dinitrosalicylic acid, 2 g phenol, 0.5 g sodium sulfite, and 10 g sodium hydroxide in 1 L deionized water. 20 µL of the filtered samples were mixed with 140 µL of DNS reagent, followed by a 5-min incubation at 95 °C. Samples were then cooled on ice for 5 min to stop the reactions. After that, 840 µL of deionized water was added. Samples were finally measured through a spectrophotometer (Ultrospec 50, Biochrom) set to a wavelength of 540 nm. A standard curve was established based on standards and used for quantification.

Nitrogen measurement followed methods detailed in (Bollmann et al. 2011). To measure ammonium, a solution of 12 g/L of sodium hydroxide was mixed with another containing 85 g/L sodium salicylate and 0.6 g/L sodium nitroprusside at a 2:1 volume ratio. 375 µL of this freshly prepared mixture was added to 750 µL of every sample. 150 µL of 0.2 g/L sodium dichloroisocyanurate was then added, followed by 30 min of incubation in a dark environment.

After incubation, absorbance of samples was measured at 660 nm using a spectrophotometer (Ultrospec 50, Biochrom). A standard curve was established based on standards. The concentration of ammonium in samples was determined based on the standard curve. To measure nitrate and nitrite, 75 μL of a catalyst solution containing 35.4 mg/L copper sulfate pentahydrate and 0.9 g/L zinc sulfate monohydrate was added to 500 μL of every sample. Then, 75 μL of 40 g/L sodium hydroxide and 75 μL of 1.71 g/L hydrazine sulfate were added sequentially, and samples were incubated in the dark for 15 min. After incubation, 250 μL of 10 g/L sulfanilamide dissolved in 3.5 M hydrochloric acid and 75 μL of 1 g/L naphthylethylene diamine dichloride were added sequentially, and samples were incubated in the dark for an additional 10 min. Samples were finally assessed by measuring absorbance at 540 nm using a spectrophotometer (Ultrospec 50, Biochrom). A standard curve was established based on standard solutions and used for quantification.

5.3.5 Calculation of Yield and Productivity for Biomass Production

Eq. 1 and 2 were used to calculate the yield and productivity in the production of *E. coli* or *S. cerevisiae* cells.

$$Y_{X/S} = \frac{\Delta OD_{600}}{-\Delta c_S} \quad - \text{Eq. 1}$$

$$r_p = \frac{\Delta OD_{600}}{\Delta t} \quad - \text{Eq. 2}$$

$Y_{X/S}$ is the yield of *E. coli* and *S. cerevisiae* biomass (assessed by OD_{600}) on glucose in L/g glucose. r_p represents the volumetric productivity of *E. coli* and *S. cerevisiae* biomass (assessed by OD_{600}) in 1/h. c_S is the substrate concentration in g glucose/L. t represents operation time in h.

5.3.6 qPCR Experiments for *S. cerevisiae*

Samples (0.5 mL) were collected at multiple sampling points during *S. cerevisiae* BR and SCF operation. Cells were centrifuged (13,000 g, 2 min), and the supernatant was discarded. Total RNA purification was performed using a Masterpure Complete DNA and RNA Purification Kit (Lucigen). The main steps consisted of cell lysis, protein precipitation, nucleic acid recovery, and

genomic DNA removal. The manufacturer's instructions were followed with the following modifications: dithiothreitol (DTT) was added to 1 mM before cell lysis, and disodium EDTA (pH = 8.5) was added to 2.5 mM at the end of the DNA removal step to cease the digestion by DNase I. After RNA extraction, a NanoDrop 1000 (Thermo Fisher) and a Bioanalyzer 2100 (Agilent) were used to measure the concentration, quality, and integrity of the total RNA samples. A High-Capacity cDNA Reverse Transcription Kit with RNase Inhibitor (Thermo Fisher) was used for reverse transcription, implementing random primers and a standard temperature program. qPCR experiments were carried out using PowerUp SYBR Green Master Mix (Thermo Fisher) in a QuantStudio 3 real-time PCR instrument (Thermo Fisher). Each condition was tested in triplicate. A BR sample collected at the transition point from late-log phase to diauxic shift (at 16.2 h) was utilized as the reference sample for all alignments. *ACT1* and *ALG9* were used as reference genes based on literature (Teste et al. 2009; Cankorur-Cetinkaya et al. 2012; Davison et al. 2016). The following genes were selected to assess the yeast cell cycle (Fitch et al. 1992; Futcher 1996; Cho et al. 1998; Feldmann 2012): *CLN1* and *CLN2* (up-regulated from G1 phase to early S phase), *CLB3* (expressed in late S phase and G2 phase), *CLB1* and *CLB2* (accumulating transcripts in mitotic phase). Primers were designed using Primer3 (Untergasser et al. 2012). Their sequences, amplicon sizes, and efficiencies determined via standard curve experiments are shown in Table 5.1. Relative gene expression levels were calculated using the double delta C_t method (Livak and Schmittgen 2001).

Table 5.1 Primer sequences, amplicon sizes, and efficiencies for qPCR experiments

Gene	Forward and reverse primers	Amplicon size (bp)	Efficiency (%)
<i>ACT1</i>	5'-CTCGTGCTGTCTTCCCATCT-3' 5'-TTTGACCCATACCGACCAT-3'	69	101.15
<i>ALG9</i>	5'-ACATCGTCGCCCAATAAA-3' 5'-CGTAAAATGCTCTACCCAAAATCTT-3'	132	92.69
<i>CLN1</i>	5'-CTCGTATTCCACGCCTTTCT-3' 5'-CGTCCCAGTTCAGAGTATCCA-3'	114	93.52
<i>CLB3</i>	5'-AGGATGAAGAAGAAGACCAGGA-3' 5'-GCTCCCAGACCAATGTATCA-3'	69	105.86
<i>CLB1</i>	5'-CTCAGCGGCAATGTTTCCT-3' 5'-GCCTTTGTGTAACCACCACT-3'	90	102.68
<i>CLN2</i>	5'-TTCCTCATCTCAAAGCCACA-3' 5'-TGACTGCTGCTGACCAAATT-3'	130	93.93
<i>CLB2</i>	5'-TGCCTTTTCATTGCCTCTAA-3' 5'-GCACCGTCTGTCTCTGATG-3'	77	89.35

5.4 Results

5.4.1 *E. coli* grown in BR and SCF operation

E. coli MG1655 was grown in a batch set-up for over 24 h. Two CER local minima were observed, one at 2 h and another at 7.5 h (Figure 5.1A). These were likely due to either metabolic stalling or transitions between metabolic regimes. OD₆₀₀ reached its maximum at 7.5 h, as CER reached a local minimum, and remained at approximately 2.5 for the remainder of the experiment (Figure 5.1B). Glucose was consumed rapidly until ~9 h, corresponding to the second CER maximum, after which point it remained relatively constant. Glucose, which was expected to be the limiting nutrient, was not exhausted even after an extension of the experiment well into stationary phase. Therefore, the abundance of nitrogen, in the form of ammonium, nitrate and nitrite, was examined; nitrogen compounds were found to remain abundant during the entire batch operation (Figure 5.1C). Additional calcium and iron, and yeast extract were added to fresh media in independent experiments; these approaches did not result in glucose exhaustion after batch operation (data not shown). Hence, the cessation of glucose consumption was likely not due to a deprivation of a limiting nutrient but more likely due to an inhibitory effect of excessive

intermediate metabolites. For example, organic acid overproduction could impact growth. However, pH only decreased from 6.76 to below 6 during operation, which is unlikely to cause cessation of growth by itself.

E. coli MG1655 was then grown under SCF operation. The first 26 cycles were run in an SCF long cycle scheme, while the succeeding 10 cycles were operated under a short cycle scheme. The transition from long to short cycles occurred within cycle 27, which could be regarded as a disrupted long cycle and was not considered a cycle in either mode of operation. In the long cycle scheme, cycles were triggered when the decreasing trend in CER flattened, while in the short cycle operation, cycling was triggered when CER reached its maximum. For SCF long cycles, a repeatable pattern of CER was established directly after the second cycle – an increase in the early stages of a cycle, a decrease during the late campaign, and a plunge upon cycling (Figure 5.2A). The cycle time during long cycle operation averaged 4.54 ± 0.32 h for cycles 3 to 26 (Figure 5.2A). When the operation was tuned to the short cycle scheme, readaptation occurred within the first two cycles after the transition cycle, and a new stable pattern of CER was obtained after it (Figure 5.2C). The new CER pattern only displayed a decrease in CER upon cycling, and the cycle time was reduced to 1.43 ± 0.06 h for short cycles 3 to 10 (Figure 5.2C). Meanwhile, the CER maximum increased from 0.0026 mol/L/h to 0.0036 mol/L/h and the average CER (integrated CER per cycle time) significantly increased once long cycles were switched to short cycles. Moreover, the stability of SCF long cycle and short cycle operation demonstrated that cells completed one round of cell replication per cycle, regardless of the cycling regime.

The increase in OD₆₀₀ and the decrease in glucose concentration were essentially linear towards the end of the cycling regimes represented by long cycle 24 and short cycle 10 (Figures 5.2B and 5.2D). Long cycle 24 accumulated more biomass, consistent with a greater amount of glucose consumed, over its significantly greater cycle time, as compared to short cycle 10 (Figures 5.2B and 5.2D). The yield of *E. coli* biomass from glucose was 0.34 L/g glucose during long cycle 24 and was 0.63 L/g glucose for short cycle 10. The productivity of *E. coli* biomass was 0.15 1/h and 0.42 1/h for the long and short cycles, respectively. The glucose consumption rate was also improved in short cycle 10 (Figures 5.2B and 5.2D). By adjusting to a short cycle scheme, the yield of *E. coli* cells from glucose increased 1.8-fold, and volumetric biomass productivity was improved 2.7-fold (both relative to the long cycle scheme).

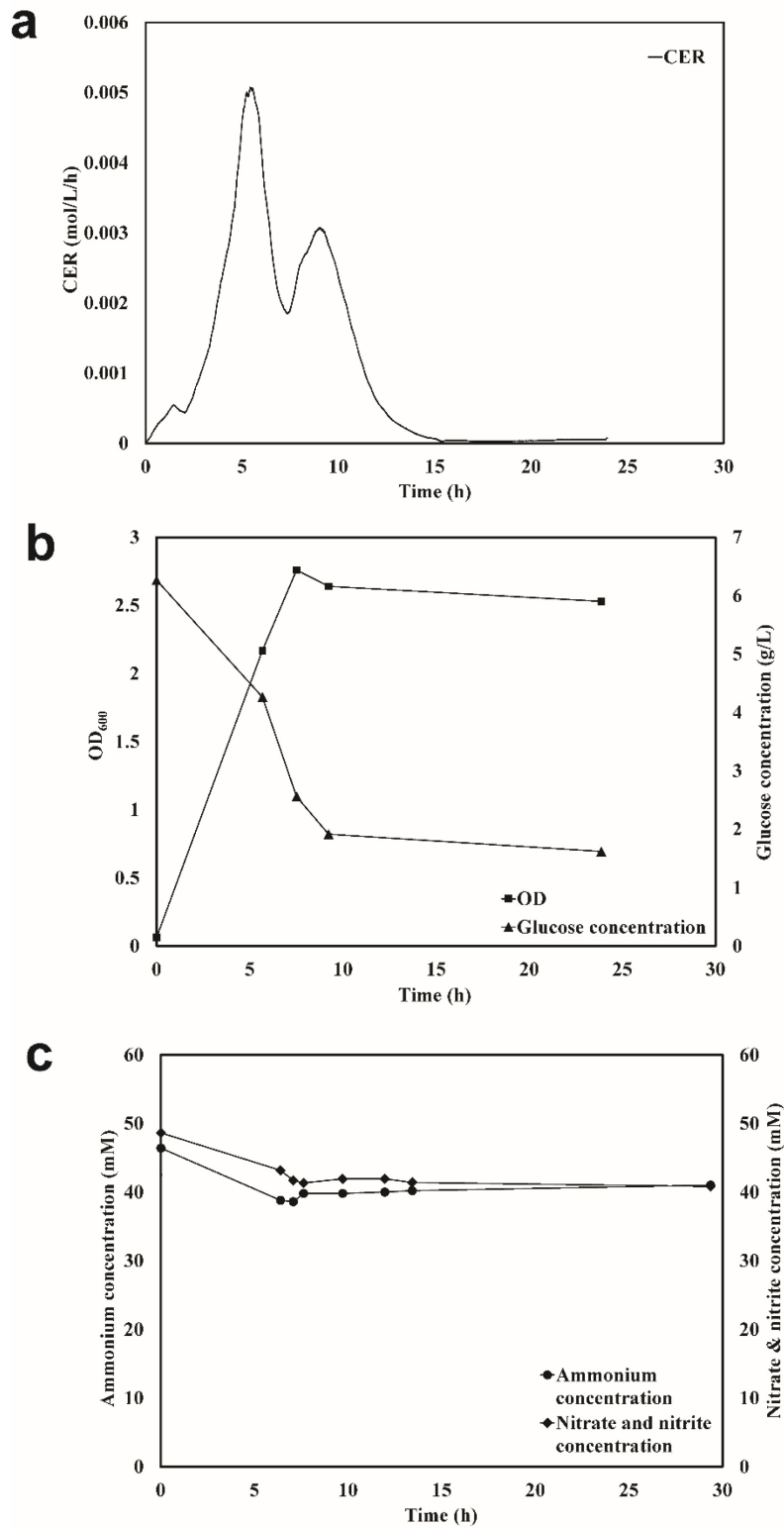


Figure 5.1 Growth of *E. coli* MG1655 in extended batch operation. A) Carbon dioxide evolution rate (CER). B) OD₆₀₀ and glucose concentration. C) Concentrations of ammonium, and combined nitrate and nitrite.

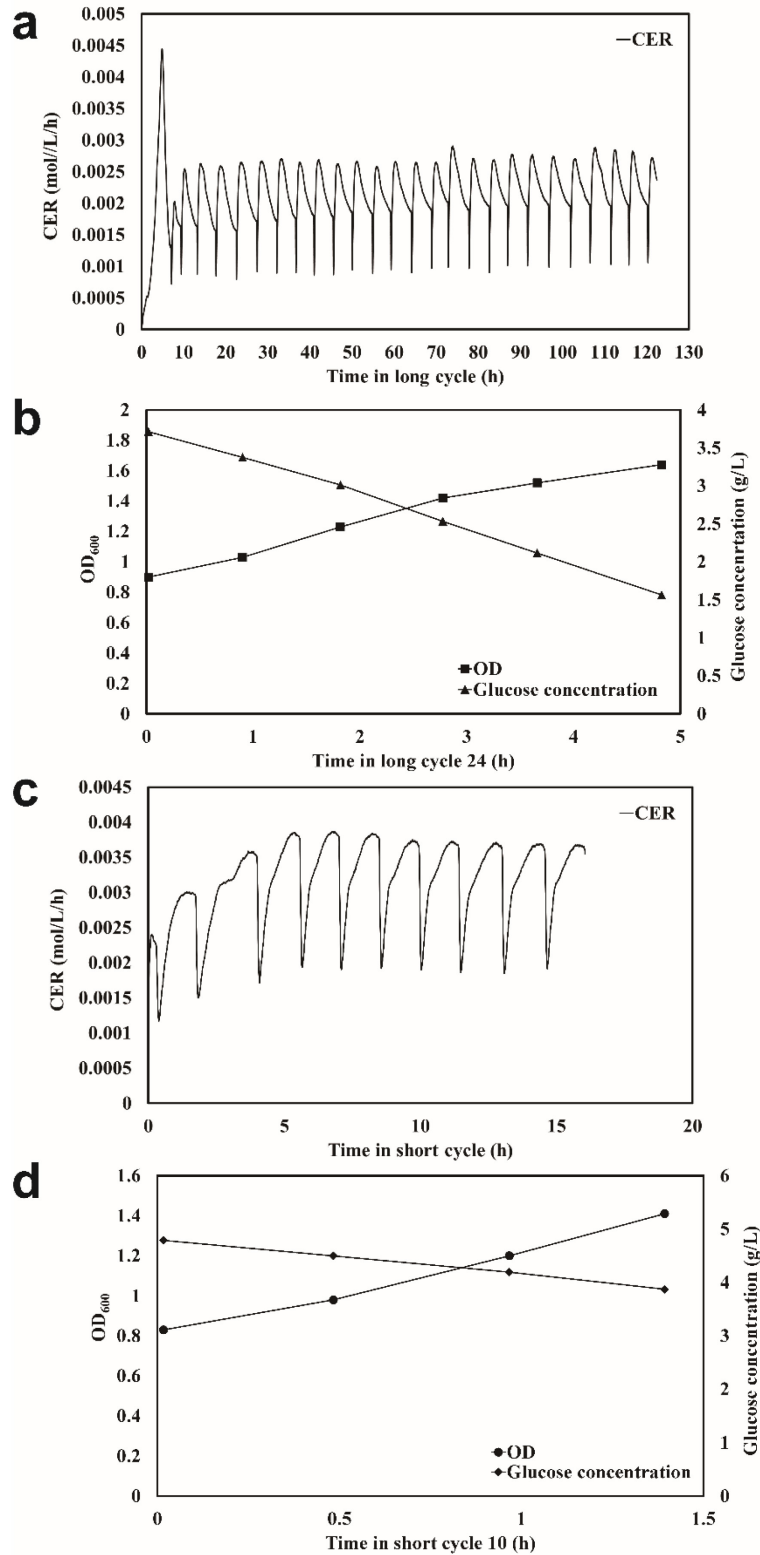


Figure 5.2 *E. coli* grown in SCF long cycle and short cycle schemes. A) CER during long cycle operation. B) Intracycle OD₆₀₀ and glucose concentration during long cycle 24. C) CER during short cycle operation. D) Intracycle OD₆₀₀ and glucose concentration during short cycle 10.

5.4.2 *S. cerevisiae* grown in SCF operation

Similarly to *E. coli*, *S. cerevisiae* was cultivated under SCF long cycle and short cycle schemes; the long cycle operation cycled when the decreasing CER flattened, whereas the short cycle scheme triggered cycling upon reaching a maximum in CER (Figures 5.3A and 5.3D). Both modes of operation were found to be highly stable and reproducible directly after their first cycles considering their CER profiles (Figures 5.3A and 5.3D), suggesting that *S. cerevisiae* cells completed one generation of cell proliferation within a long or short cycle time. However, similarly to *E. coli* experiments, there was a significant difference regarding the shapes of CER curves – no CER decrease was observed during short cycles. CER maxima increased from 0.009 mol/L/h to 0.011 mol/L/h between long and short cycle operation; the average CER (integrated CER per cycle time) also significantly increased (Figures 5.3A and 5.3D). Cycle times were significantly different, with an average cycle time of 12.11 ± 0.73 h for long cycles 2 to 16 and 3.80 ± 0.27 h for short cycles 2 to 20 (Figures 5.3A and 5.3D).

Figures 5.3B and 5.3C depict biomass accumulation and glucose consumption in cycles 1 and 10, respectively, of long cycle operation. The CER maximum in SCF long cycle 1 (Figure 5.3A) corresponded to a transition point between exponential phase and diauxic shift during BR growth (Figure 5.3B). Glucose, the limiting nutrient, was depleted at the end of the cycles, consistent with the co-occurrence of the flattening point of CER (cycling condition) and the exhaustion of the limiting nutrient. In contrast, during the short cycle scheme, although similar patterns in OD₆₀₀ and glucose concentration were observed in cycles 1 and 20 (Figures 5.3E and 5.3F, respectively), glucose was not exhausted by the end of the cycles. Consequently, the OD₆₀₀ at the end of each cycle was lower and increases in OD₆₀₀ were affected accordingly compared to the long cycle counterparts (Figures 5.3E and 5.3F). Nonetheless, volumetric productivity of *S. cerevisiae* cells was 0.17 1/h during long cycle 10 and 0.28 1/h during short cycle 20, a 1.6-fold increase (Figures 5.3C and 5.3F; Table 5.2). The glucose consumption rate was also found to be greater in short cycle 20 (Figures 5.3C and 5.3F). However, biomass yield was comparable between the long and short cycles – 0.22 and 0.21 L/g glucose, respectively (Figures 5.3C and 5.3F; Table 5.2). Additionally, the nitrogen source, ammonium, was always in excess and was not the limiting nutrient (data not shown).

5.4.3 Relative expression levels of selected cyclin genes in *S. cerevisiae*

Relative expression levels (fold changes) of *CLN1*, *CLN2*, *CLB3*, *CLB1*, and *CLB2*, were determined for *S. cerevisiae* growing in SCF short cycles 1 and 21 using qPCR (Figures 5.4A and 5.4B, respectively). Generally, fold changes of the cyclin genes during BR (short cycle 1) late-log phase were not significant: slight decreases in expression were found for *CLB1* and *CLB2*, and slight increases in expression were observed for *CLN1* and *CLN2* over the cycle (Figure 5.4A). In contrast, during short cycle 21 (with a cycle time of 3.7 h), the following observations were made: (1) *CLB1* and *CLB2* (paralog genes) were significantly up-regulated during the early stages of the short cycle up to a cycle time of 2.8 h, with peaks in expression at approximately 1.4 h; (2) the expression of *CLN1* and *CLN2* (paralog genes) was generally stable but showed significant up-regulation at 2.8 h; and (3) in comparison, *CLB3* transcription remained relatively steady throughout the short cycle (Figure 5.4B). Identical trends in relative expression levels of the cyclin genes were observed in replicated short cycle experiments (Supplementary Figures B2A and B2B for SCF short cycles 1 and 21, respectively).

Considering the significant sequential up-regulation of these cyclin genes, it can be established that some extent of synchrony was achieved during the short cycle operation, even though this could not be directly corroborated using cell counts due to flocculation of the yeast cells (data not shown). During a standard yeast cell cycle, *CLN1* and *CLN2* are up-regulated prior to *CLB1* and *CLB2*; *CLN1* and *CLN2* are expressed in G1 and S phases while *CLB1* and *CLB2* during M phase (Fitch et al. 1992; Futcher 1996; Cho et al. 1998; Feldmann 2012). However, here in the short cycle 21, the up-regulation of *CLB1* and *CLB2* was shown to be earlier than that of *CLN1* and *CLN2*. This indicated that partially synchronized (if not completely synchronized) cell replication started and ended in the middle of the short cycles, rather than being aligned with the SCF cycle progression.

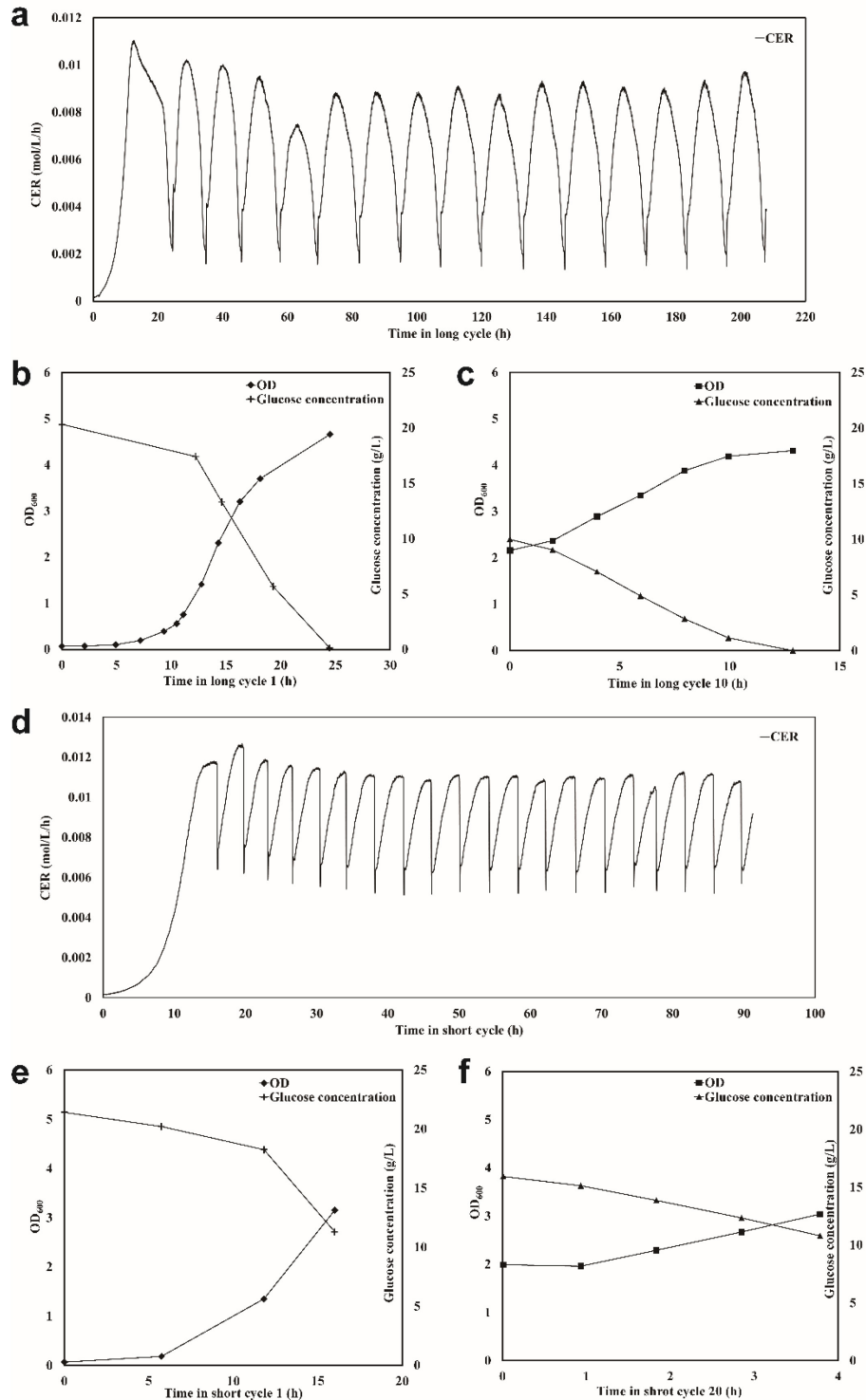


Figure 5.3 *S. cerevisiae* grown in SCF long and short cycle strategies. A) CER during long cycle operation. B) OD₆₀₀ and glucose concentration during long cycle 1 (BR). C) OD₆₀₀ and glucose concentration during long cycle 10. D) CER during short cycle operation. E) OD₆₀₀ and glucose concentration during short cycle 1 (BR). F) OD₆₀₀ and glucose concentration during short cycle 20.

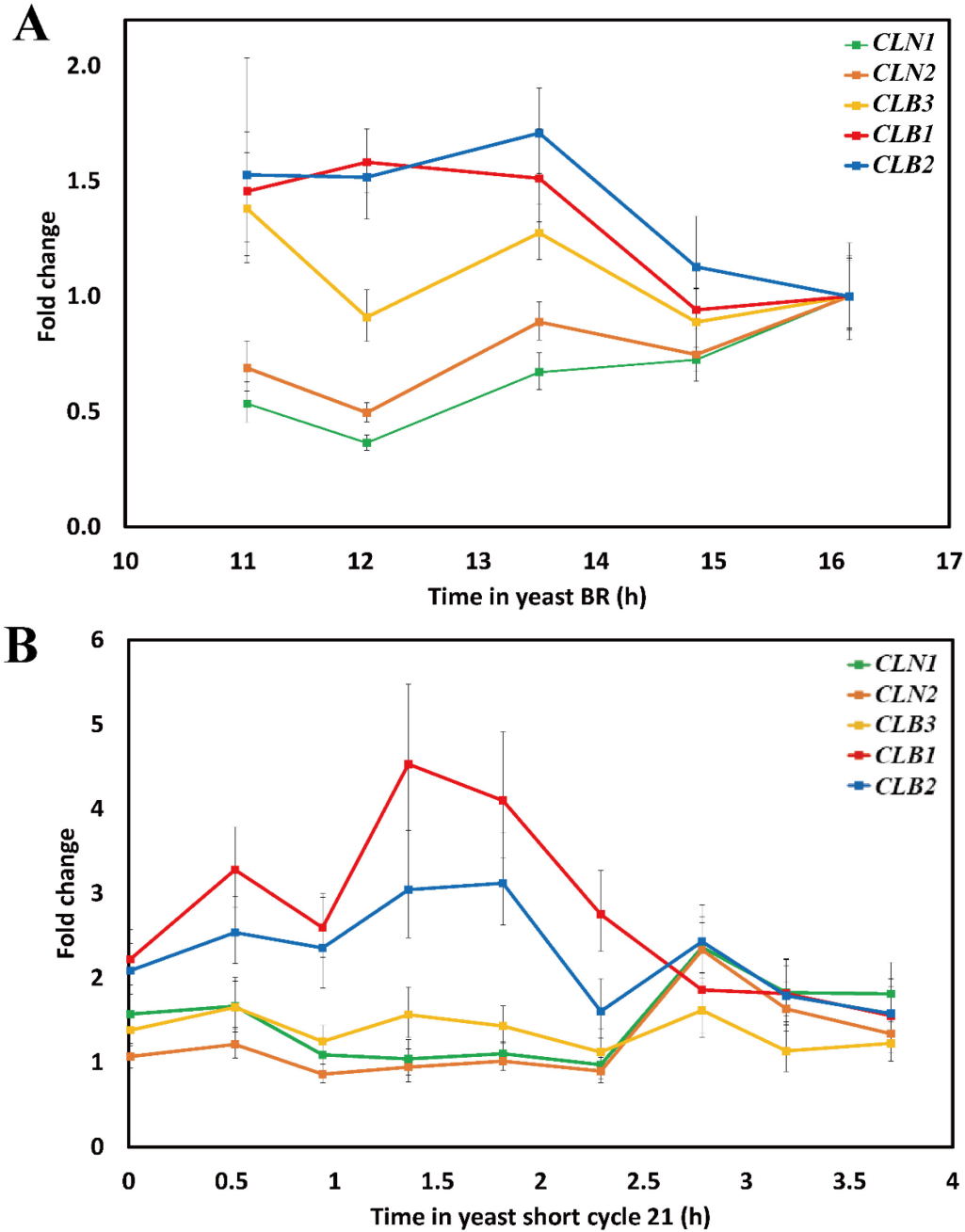


Figure 5.4 Relative expression levels of selected *S. cerevisiae* cyclin genes. A) fold changes of *CLN1*, *CLN2*, *CLB3*, *CLB1*, and *CLB2* during BR late-log phase. B) fold changes of the same cycling genes during SCF short cycle 21. *ACT1* and *ALG9* were used as reference genes, and a sample collected at 16.2 h during BR was used as the reference sample. Error bars show one standard deviations (n = 3).

5.5 Discussion

5.5.1 *E. coli* BR Operation

During *E. coli* BR operation, two major CER peaks could be observed (Figure 5.1A), which is consistent with a prior *E. coli* study (Sauvageau et al. 2010). During the current study, nitrogen, calcium, iron, and yeast extract were not shown to limit the growth. Little glucose was consumed during the late stages of BR and it was not depleted by the end of BR (Figure 5.1B). The restricted growth was most likely due to the accumulation of organic acids (e.g., acetic acid), resulting from bacterial Crabtree effect (Mustea and Muresian 1967), rather than the depletion of a limiting nutrient. Excessive organic acids might be produced from rapid growth in the early stages of BR, partly inhibiting the subsequent stages of growth and preventing the full consumption of glucose. Some future investigations can be carried out to identify the mechanisms of this inhibition and eliminate barriers towards complete consumption of glucose.

5.5.2 SCF Long Cycle and Short Cycle Operation

Much like the case for *E. coli* BR operation, *E. coli* SCF long cycles did not exhaust glucose when CER flattened (cycling condition) (Figure 5.2B). This was not the case for *S. cerevisiae* undergoing SCF operation, wherein glucose depletion was observed at the end of BR and long cycles (Figures 5.3B and 5.3C). As discussed earlier, the accumulation of organic acids might have an inhibitory effect on *E. coli* growth. Previous work investigating *E. coli* undergoing SCF long cycles (Sauvageau et al. 2010) found that glucose was totally consumed by the time CER stopped decreasing; however, while that study was performed with similar nutrient conditions, it used a different strain of *E. coli* (ATCC 11303) (Sauvageau et al. 2010).

The improvement in production of *E. coli* biomass was significant once SCF operation was adjusted to a short cycle scheme; 1.8-fold and 2.7-fold increases in yield and volumetric productivity, respectively (Table 5.2). In the previous study investigating SCF long cycles with *E. coli* ATCC 11303 (Sauvageau et al. 2010) the yield was found to be 0.23 L/g glucose, and the productivity of *E. coli* cells was 0.28 1/h (also shown in Table 5.2; calculated based on an original figure (Sauvageau et al. 2010) using Eq. 1 and 2). In comparison, the yield and volumetric productivity during the current short cycle operation also prevailed. As for *S. cerevisiae* cells

grown in SCF operation, short cycles led to a 1.6-fold increase in volumetric productivity while providing a similar yield to long cycles (Table 5.2). It was also noted that the average glucose consumption rate and average CER were enhanced during short cycles of both *E. coli* and *S. cerevisiae*, despite lower cell density (Figures 5.2 and 5.3) – meaning more glucose was consumed per cell and more CO₂ was released per cell. That is to say, cellular activity was generally more intense during SCF short cycles.

Table 5.2 Yield and volumetric productivity in cellular biomass production during SCF long and short cycle operation

SCF Operation	Yield of Cells (L/g glucose)	Volumetric Productivity of Cells (1/h)
<i>E. coli</i> long cycle operation (this study)	0.34	0.15
<i>E. coli</i> long cycle operation (2010) (Sauvageau et al. 2010)	0.23 ^a	0.28 ^a
<i>E. coli</i> short cycle operation (this study)	0.63	0.42
<i>S. cerevisiae</i> long cycle operation (this study)	0.22	0.17
<i>S. cerevisiae</i> short cycle operation (this study)	0.21	0.28

^aValues were calculated based on an original figure in (Sauvageau et al. 2010) using Eq. 1 and 2.

Significant improvements in yield, productivity, and metabolic activity highlight the advantages of the SCF short cycle scheme as compared to the long cycle counterpart. Yield and productivity would likely be further improved if the SCF short cycle strategy were used in the context of recent *E. coli* and *S. cerevisiae* SCF studies, such as *E. coli* biomass production (Sauvageau et al. 2010), bacteriophage production (Sauvageau and Cooper 2010; Storms et al. 2014), recombinant protein production (Storms et al. 2012), ethanol fermentation (Wang et al. 2017, 2020), and shikimic acid production (Agustin 2015). Instantaneous specific productivity of bacteriophage, recombinant protein, and shikimic acid was found to be optimal near the completion of synchronized cell replication (corresponding to a maximum in CER) during SCF long cycle operation (Storms et al. 2012, 2014; Agustin 2015).

In specific, the results observed in this study for *S. cerevisiae* SCF long cycle operation generally agree with a preceding study (Chapter 4). Growing the engineered yeast strain in SCF long cycles had substantially improved shikimic acid yield and productivity compared to BR (Chapter 4). Hence, it may be possible to further enhance shikimic acid production by implementing the SCF short cycle strategy. Based on the improved productivity of cellular biomass (Table 5.2), the production rate of the primary metabolite will highly likely be further reinforced in SCF short cycles.

The incomplete depletion of glucose during short cycles might be the only concern for the implementation of this SCF scheme. To address this, recycling of the carbon source might be considered in future studies.

A close link between CER maximum and the completion of synchronized cell division can be established. Firstly, the cycle time of short cycles – from start-of-cycle to CER maximum – allowed one generation of complete cell doubling. Considering the SCF cycling process is based on the replacement of exactly one-half of the working volume of the fermenter, if *E. coli* and *S. cerevisiae* cells had not completed one round of cell replication within each cycle, washout would have occurred and the CER profile would have been unrepeatable. The short cycles, however, were stable and repeatable. Secondly, during previous SCF studies based on long cycles with *E. coli* (ATCC 11303 (Sauvageau et al. 2010) and CY15050 (Storms et al. 2012)) and the engineered *S. cerevisiae* (CEN.PK 113-1A Matα (Agustin 2015)), step-wise doublings in cell count were observed at the CER maxima. This suggested that cell replication was in unison, and synchronized cell doubling was completed when CER reached its maximum. Thirdly, significant up-regulation of DNA replication-related genes and selected cyclin genes (*CLN1*, *CLN2*, *CLB3*, *CLB1*, and *CLB2*) were observed only during the first-half of *S. cerevisiae* SCF long cycles (Chapter 4). It is very likely that there was little replication activity after the maximum in CER. Fourthly, the cycle time of SCF long cycles was significantly longer than the expected doubling time in the same nutrient conditions. In contrast, the duration of short cycles was very close to those doubling times.

As to *S. cerevisiae* SCF short cycles, the expression profiles of the investigated cyclin genes provided valuable information (Figure 5.4). Firstly, the amplitudes and sequential changes in up-regulation suggested that a certain level of cell synchrony was established. Cyclical changes in glucose concentration established by the mode of operation provided a forcing function to

induce the entrainment effect required for cell synchrony; greater glucose availability early in the SCF cycles preferentially favored some stages of the cell cycle. It was also noted that, compared to SCF long cycles, a decrease in up-regulation amplitudes was observed during short cycles (Figure 5.4B and Chapter 4). This was likely due to the incomplete utilization of glucose, resulting in a tamer entrainment effect during short cycles. Secondly, the sequence of cyclin genes expression suggested that the replication of partially synchronized cells started from the middle of the short cycles and was completed at the same point in the subsequent cycle. *CLN1* and *CLN2* were expressed later than *CLB1* and *CLB2* during SCF short cycles (Figure 5.4B) – an inverse sequence compared to the standard yeast cell cycle (Fitch et al. 1992; Cho et al. 1998). This unexpected, distinct, cycle-spanning cell replication pattern in short cycles was likely caused by other driving forces apart from the oscillation of glucose concentration, as the nutrient cycle itself is expected to lead to an alignment between the starts of SCF and cell cycles.

This leads to another question – might synchronized yeast cell replication also present a cycle-spanning pattern during SCF long cycles, starting from the middle of a long cycle and ending at the same point in the succeeding long cycle? The answer should be no. One reason is that there was no significant expression of selected cyclin genes during the second-half of long cycles (Chapter 4). Hence, there was hardly any replication activity during the late stages of long cycles. Moreover, the onsets of SCF long cycles and the yeast cell cycle were aligned, as suggested by the congruent expression sequence of the cyclin genes during the first half of long cycles and the standard yeast cell cycle. Furthermore, the cycle time of long cycles was more than twice the doubling time of *S. cerevisiae* in the same nutrient conditions. It is unlikely that one round of cell replication occurred throughout the whole cycle time of long cycles.

Identical trends and amplitudes of cyclin gene expression during BR late-log phase were identified not only between replicate experiments in the present study (Figures 5.4A and B2A) but also amongst current qPCR results, previous qPCR results (Chapter 4), and previous RNA-Seq results (Chapter 4). This great alignment of the gene expression profiles across different studies and analytical techniques significantly increases confidence in the trends observed. Consequently, relative quantification results were considered to truly reflect transcriptional changes during SCF short cycles (Figure 5.4B).

5.5.3 An Overview of Characteristic Events in SCF

Significant differences in the occurrence of some SCF key events can be observed among SCF studies with different microorganisms implemented. These characteristic events include: (1) the time at which the limiting nutrient was depleted or reached a plateau, (2) the characteristic values of control parameters, and (3) the completion of one generation of synchronized cell division.

Nitrogen or carbon sources are frequently set as the limiting nutrients dictating the cycling of SCF operation. Control parameters used to establish cycling conditions have included dissolved oxygen (DO), carbon dioxide evolution rate (CER), or oxidation-reduction potential (ORP) (Brown 2001). Mass flow rate of the exit gas has also been used for SCF of *S. cerevisiae* Superstart™ producing ethanol (Wang et al. 2020) and was a direct reflection of CER under anaerobic conditions. In studies of phenol degradation using *Pseudomonas putida* ATCC 12633 (Hughes and Cooper 1996) and *Acinetobacter calcoaceticus* RAG-1 ATCC 31012 grown on hexadecane (van Walsum and Cooper 1993), CER patterns were found to mirror DO patterns, and CER maximum aligned with DO minimum. Under aerobic conditions, this relationship between CER and DO would generally be true (cautions on rare exceptions). In another study investigating toluene removal using *P. putida* ATCC 12633 undergoing SCF (Brown et al. 2000), the inflection point of ORP was observed near the concurrence of CER maximum and DO minimum. However, ORP patterns during SCF operation are generally more complex than other parameters. An increasing trend in ORP was observed in the toluene removal study using *P. putida* ATCC 12633 (Brown et al. 2000), while a decreasing trend was shown in the removal of oxidized nitrogen using *Pseudomonas denitrificans* ATCC 13867 (Brown et al. 1999). The presence and absence of oxygen in these two studies were likely responsible for these diverging patterns. In contrast, DO and CER generally present similar patterns amongst various studies and hence have been more often applied as the control parameter. Overall, it is illustrated that DO minimum would coincide with CER maximum during SCF operation, and the inflection point of ORP is likely close to this point. In the present study, the time at which this event occurs is referred to as the control parameters' "characteristic values" or "characteristic points".

In many SCF studies published before 2010, co-occurrence was always identified for the depletion of a limiting nutrient and the characteristic values of control parameters. SCF cycling

was triggered upon this concurrence unless an extended cycle strategy was applied. In antibiotic production using *Streptomyces aureofaciens* ATCC 12416c (Zenaitis and Cooper 1994), phenol degradation using *P. putida* ATCC 12633 (Hughes and Cooper 1996), and cultivating *Bacillus subtilis* ATCC 21332 (Sheppard and Cooper 1991), DO minimum occurred concomitantly with nitrogen depletion or the complete removal of phenol. Moreover, the co-occurrence of the completion of cell replication with the aforementioned two key events was observed in a wealth of SCF studies, and this is summarized as Trend A in Figure 5.5A. The first SCF upgrade from continuous phasing identified that the depletion of nitrogen, DO minimum, and the doubling endpoint of optical density (OD) took place at the same moment (Sheppard and Cooper 1990). In sophorolipid production using *Candida bombicola* ATCC 22214 (McCaffrey and Cooper 1995) and citric acid production using *Candida lipolytica* ATCC 20390 (Wentworth and Cooper 1996), cell count doubled within a narrow time window near the minimum in DO, concomitant with the exhaustion of the nitrogen source. In *A. calcoaceticus* RAG-1 ATCC 31012 grown on ethanol (Brown and Cooper 1991) and the degradation of aromatic compounds using *P. putida* ATCC 12633 (Sarkis and Cooper 1994), the completion of cell doubling co-occurred with carbon source exhaustion and DO minimum. Similarly, in oxidized nitrogen removal using *P. denitrificans* ATCC 13867 (Brown et al. 1999), the end of doubling of cell dry weight corresponded to the inflection point of ORP and nitrogen depletion.

The reliability of Trend A (Figure 5.5A) had been considered universal. For example, in studies tackling hydrocarbon degradation using *A. calcoaceticus* RAG-1 ATCC 31012 (Brown and Cooper 1992) and cultivating *B. subtilis* ATCC 21332 (Sheppard and Cooper 1991), the authors directly took the equivalence of SCF cycle time and cell doubling time as a default. However, this was only true when synchronized cell division was accomplished upon initiating SCF cycling. Also, it should be noted that the end point of the doubling of OD or dry weight does not necessarily represent the doubling endpoint of cell number. These can be decoupled and display different trends in synchronized populations – the cell count increases in a step-wise manner, while OD or dry weight present a continuous, near-linear increase regardless of the completion of synchronized cell division (Marchessault and Sheppard 1997; Storms et al. 2012).

Moreover, during polyhydroxybutyrate (PHB) production using *Alcaligenes eutrophus* DSM 545 (Marchessault and Sheppard 1997) and the growth of *B. subtilis* ATCC 10774 (Sheppard

1993), while the minimum in DO and the nitrogen source depletion coincided, synchronized cell replication was completed much earlier – in the middle of the SCF cycles. As the timing of the cell cycle end point showed a significant difference, these studies serve as representations for Trend B in Figure 5.5B. In summary, for most of the microbial systems used in earlier SCF studies, the depletion of a limiting nutrient and characteristic values of control parameters (DO minimum, CER maximum, or ORP inflection point) occurred concurrently at the end of each SCF cycle (Trends A and B in Figures 5.5A and 5.5B). One round of synchronous cell doubling was completed at the same time (Trend A in Figure 5.5A) or, in some instances, in the middle of the cycles (Trend B in Figure 5.5B).

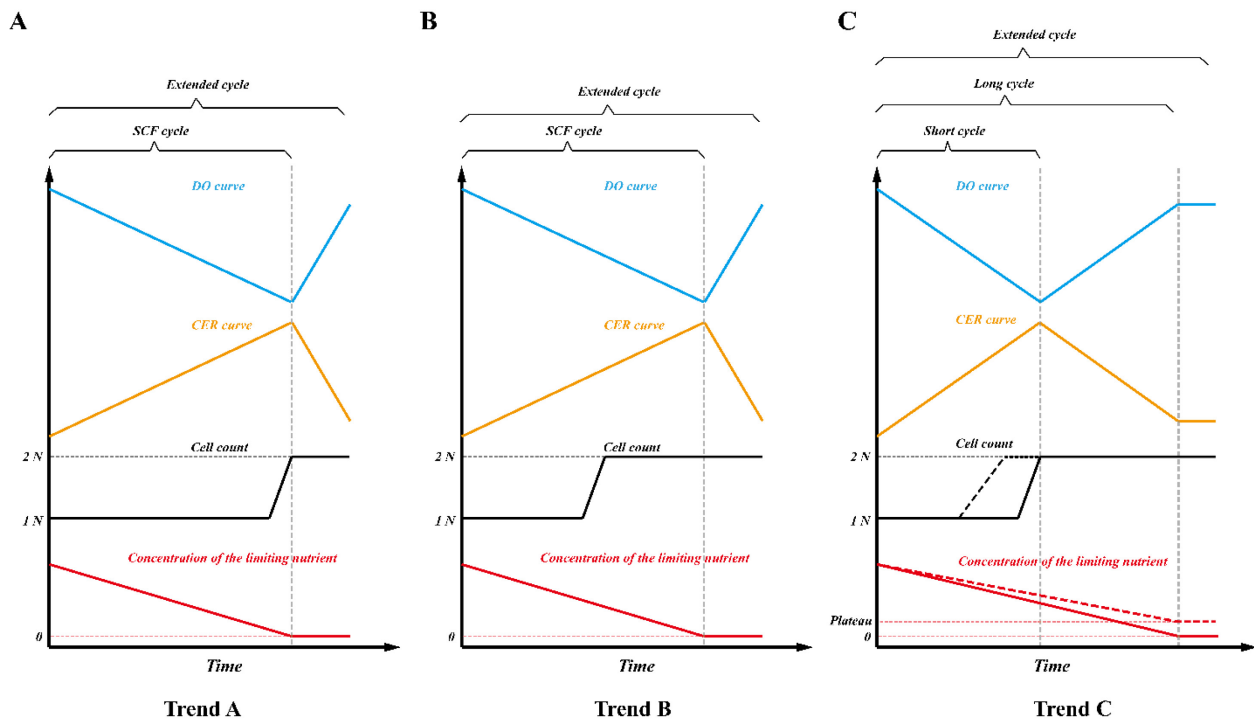


Figure 5.5 Schematic of the conceptual trends in characteristic events during SCF. DO curve is shown in blue, CER curve in orange, cell count in black, and concentration of the limiting nutrient in red. Straight lines are used to describe changes but do not necessarily represent linear changes. A) In Trend A, DO minimum or CER maximum, the end of synchronized cell replication, and the depletion of the limiting nutrient co-occur at the end of an SCF cycle. An extended cycle allows a delay in cycling. B) In Trend B, DO minimum or CER maximum, and the depletion of the limiting nutrient co-occur at the end of an SCF cycle, but synchronized cell replication ends in the middle of the cycle. An extended cycle allows a delay in cycling. C) In Trend C, the flattening of DO increase or CER decrease, and the depletion of the limiting nutrient (or a plateau, the red dashed

line) co-occur at the end of an SCF long cycle, but synchronized cell replication ends in the middle of the long cycle, corresponding to DO minimum or CER maximum. An SCF short cycle ends at DO minimum or CER maximum, but partially synchronized cell replication likely starts and ends in the middle of the short cycle (the black dashed line). The limiting nutrient is not depleted by the end of the short cycle. An extended cycle allows a delay in cycling beyond the end of a long cycle.

Compared to Trends A and B, the scenario observed in a study investigating biosurfactant production using *Corynebacterium alkanolyticum* ATCC 21511 growing on hexadecane in SCF (Crosman et al. 2002) was substantially different. DO minimum and the completion of synchronized cell division occurred concomitantly, but a considerable amount of carbon source was left over. Recent SCF works using *E. coli* ATCC 11303 (Sauvageau et al. 2010), *E. coli* CY15050 (Storms et al. 2012), and engineered *S. cerevisiae* CEN.PK 113-1A Mata (Agustin 2015) depicted an identical trend – cell count doubled step-wise at the maximum in CER (at the cycle midpoint), but glucose, the limiting nutrient, was only exhausted once the decrease in CER flattened (at the end of the cycles). In ethanol fermentation using *S. cerevisiae* Superstart™ undergoing SCF (Wang et al. 2020), glucose was depleted upon the time when CER flattened (reflected by exit gas mass flow rate in anaerobic conditions), though cell counts were not reported due to clumping of the yeast cells. As mentioned earlier, the same trend was observed in the present study when cultivating *E. coli* MG1655 or engineered *S. cerevisiae* CEN.PK 113-1A Mata (except that, for *E. coli* undergoing SCF long cycles, the end of cycle was due to an inhibitory effect rather than glucose depletion). Trend C in Figure 5.5C is used to describe the pattern observed in these studies.

Moreover, transcriptional evidence during *S. cerevisiae* SCF short cycles presented in this study revealed a likely cell replication pattern in short cycles – partially synchronized cell cycle starting and ending in the middle of short cycles. This cycle-spanning mode of cell replication is presented by the black dashed line in Figure 5.5C. Overall, in studies displaying Trend C, the flattening of CER decrease or DO increase coincided with the depletion or a plateau of the limiting nutrient at the end of SCF long cycles, but synchronized cell replication was completed in the middle of the long cycles, corresponding to CER maximum or DO minimum. SCF short cycles ended at CER maximum or DO minimum, but partially synchronized cell replication likely started

and ended in the middle of the short cycles. The limiting nutrients were not depleted by the end of the SCF short cycles.

The discrepancies amongst the three major trends in the characteristic events during SCF operation were likely derived from intrinsic differences in the microorganisms and nutrient environments used. *A. eutrophus* and *B. subtilis* ATCC 10774 following Trend B, and *C. alkanolyticum*, *E. coli*, and *S. cerevisiae* following Trend C likely sensed nutrient conditions more actively and adopted a feed-forward strategy (Levy and Barkai 2009) – in which cells proactively sensed external changes and regulated gene transcription and expression prior to the alteration of the growth rate (Levy and Barkai 2009). Completing one generation of the synchronized cell cycle but deciding not to continue the proliferation at the expense of the remaining limiting nutrient seemed to be the growth strategy of these microorganisms (Figures 5.5B and 5.5C). On the contrary, for a number of microorganisms following Trend A, all the available limiting nutrient was used in completing the cell doubling (Figure 5.5A). The difference between *A. eutrophus* and *B. subtilis* ATCC 10774 in Trend B, and *C. alkanolyticum*, *E. coli*, and *S. cerevisiae* in Trend C is expected to lie in the respiratory intensity between the end of the cell cycle and the time at which the limiting nutrient was depleted or reached a plateau. For the former group, the intensity of respiration increased even after synchronized cell replication. Therefore, the characteristic value of the control parameter (DO minimum) co-occurred with the exhaustion of the limiting nutrient but not with the end of cell doubling (Figure 5.5B). For microbes displaying Trend C, respiration slowed significantly after synchronized cell replication (during the consumption of residual limiting nutrient), and therefore CER maximum or DO minimum occurred at the completion of synchronized cell doubling but not at the depletion or a plateau of the limiting nutrient (Figure 5.5C).

Different nutrient conditions can lead to different physiologies and affect the trends in SCF. For example, implementing different types of limiting nutrients – nitrogen or carbon – in a continuous phased culture tremendously affected where synchronized cell replication of *Candida utilis* (Y-900) ended when the cycle time was set to 4, 6, 8, and 12 h (Müller and Dawson 1968). Further studies on this topic could lead to more in-depth understanding of the physiological patterns during SCF.

Limiting nutrient depletion has been one of the original premises of SCF, but a broader picture is emerging. The Trend C observed in some studies suggests a deviation from the original description of SCF – SCF does not necessarily require limiting nutrient depletion. Consequently, a novel description of SCF is proposed below, taking into consideration all SCF scenarios presented in Figure 5.5. This new SCF definition excludes the requirements of limiting nutrient depletion and joint occurrence of the key events.

SCF is a semi-continuous fermentation approach that allows the completion of one generation of microbial cell replication during each cycle. The cycling procedure comprises harvesting precisely one half of the working volume and then replenishing with the equivalent amount of fresh medium. Cycling is dictated by microbial growth and metabolism and is triggered automatically based on monitoring one or more growth- and/or metabolism-associated sensing elements (e.g., DO, CER, ORP, exit gas mass flow rate, etc.). SCF cycling takes place directly after the completion of one generation of cell proliferation or with a delay, depending on the microorganism, the initial nutrient conditions, and the control parameter conditions for cycling being implemented. SCF cycling is not necessarily related to the time at which the limiting nutrient is depleted or reaches a plateau. If limiting nutrient depletion or a plateau does not co-occur with the cell cycle completion, we identify SCF operation that cycles in advance of exhaustion or a plateau of the limiting nutrient as “short cycle”, and correspondingly, SCF operation that cycles upon depletion or a plateau of the limiting nutrient as “long cycle” (Figure 5.5). “Extended cycle” is generally referred to as SCF operation that cycles beyond exhaustion or a plateau of the limiting nutrient (Figure 5.5).

5.6 Conclusions

Previous SCF operation of *E. coli* and *S. cerevisiae* triggered cycling upon glucose depletion when the CER flattened. In the present study, SCF short cycle operation of *E. coli* and *S. cerevisiae* were cycled at the maximum in CER and led to stable and reproducible short cycles. Notably, compared to SCF long cycles, volumetric biomass productivity was significantly improved during SCF short cycles. Further transcriptional analysis for selected *S. cerevisiae* cyclin genes inferred a cycle-spanning mode of cell replication during SCF short cycles. Viable SCF

short cycles also helped identify the maximum in CER as the endpoint of cell replication during long cycles. Moreover, a thorough overview of previous SCF studies summarized the occurrence of three SCF characteristic events, (1) the completion of synchronized cell replication, (2) the depletion or a plateau of the limiting nutrient, and (3) the characteristic points of control parameters, into three typical trends. A novel description of SCF was then proposed to include all scenarios of SCF operation and clear definitions for SCF “short cycle”, “long cycle”, and “extended cycle”.

This work highlights a diversity in SCF operation and shows the potential of SCF as a research tool to explore microbial physiological properties – including nutrient use, proliferation strategies, and respiration intensity. It also demonstrates that short cycle schemes, in particular, can be used to improve performance of bioconversion. With trends in the key events summarized and the establishment of a clear definition of SCF, the present work consolidates and deepens our understanding of the SCF technique and its influences on microbial populations. Finally, it provides a solid framework to guide the further design and implementation of SCF-based processes.

5.7 Supplementary Materials

In this thesis, Supplementary Materials for Chapter 5 is incorporated as Appendix B, including schematic of the batch reactor configuration used for this study (Supplementary Figure B1) and relative expression levels of selected *S. cerevisiae* cyclin genes in replicated experiments (Supplementary Figure B2).

5.8 Acknowledgements

We would like to thank Prof. Vincent Martin from Concordia University for providing the engineered *S. cerevisiae* strain, Troy Locke at MBSU from the University of Alberta for the help in operating the Bioanalyzer, and Melissa Harrison for the help in manuscript editing.

This work was supported by Natural Sciences and Engineering Research Council of Canada (NSERC) Discovery Grant, the Canada First Research Excellence Fund – Future Energy

Systems, the Canada Foundation for Innovation – John R. Evans Leaders Fund, the Government of Alberta – Ministry of Economic Development and Trade Small Equipment Grant, and the University of Alberta Faculty of Engineering.

5.9 References

- Agustin RVC (2015) The Impact of Self-Cycling Fermentation on the Production of Shikimic Acid in Populations of Engineered *Saccharomyces cerevisiae*. University of Alberta
- Bollmann A, French E, Laanbroek HJ (2011) Isolation, cultivation, and characterization of ammonia-oxidizing bacteria and archaea adapted to low ammonium concentrations. In: Methods in Enzymology. Academic Press Inc., pp 55–88
- Brown WA (2001) The self-cycling fermentor – development, applications, and future opportunities. In: Recent Research and Developments in Biotechnology and Bioengineering. pp 4: 61-90
- Brown WA, Cooper DG (1991) Self-cycling fermentation applied to *Acinetobacter calcoaceticus* RAG-1. Appl Environ Microbiol 57:2901–2906. <https://doi.org/10.1128/aem.57.10.2901-2906.1991>
- Brown WA, Cooper DG (1992) Hydrocarbon degradation by *Acinetobacter calcoaceticus* RAG-1 using the self-cycling fermentation technique. Biotechnol Bioeng 40:797–805. <https://doi.org/10.1002/bit.260400707>
- Brown WA, Cooper DG, Liss SN (2000) Toluene removal in an automated cyclical bioreactor. Biotechnol Prog 16:378–384. <https://doi.org/10.1021/bp0000149>
- Brown WA, Cooper DG, Liss SN (1999) Adapting the self-cycling fermentor to anoxic conditions. Environ Sci Technol 33:1458–1463. <https://doi.org/10.1021/ES980856S>
- Cankorur-Cetinkaya A, Dereli E, Eraslan S, et al (2012) A novel strategy for selection and validation of reference genes in dynamic multidimensional experimental design in yeast. PLoS One 7:e38351. <https://doi.org/10.1371/journal.pone.0038351>
- Cho RJ, Campbell MJ, Winzeler EA, et al (1998) A genome-wide transcriptional analysis of the

- mitotic cell cycle. *Mol Cell* 2:65–73. [https://doi.org/10.1016/S1097-2765\(00\)80114-8](https://doi.org/10.1016/S1097-2765(00)80114-8)
- Crosman JT, Pinchuk RJ, Cooper DG (2002) Enhanced biosurfactant production by *Corynebacterium alkanolyticum* ATCC 21511 using self-cycling fermentation. *J Am Oil Chem Soc* 79:467–472. <https://doi.org/10.1007/s11746-002-0507-5>
- Davison SA, den Haan R, van Zyl WH (2016) Heterologous expression of cellulase genes in natural *Saccharomyces cerevisiae* strains. *Appl Microbiol Biotechnol* 100:8241–8254. <https://doi.org/10.1007/s00253-016-7735-x>
- Dawson PSS (1965) Continuous phased growth, with a modified chemostat. *Can J Microbiol* 11:893–903. <https://doi.org/10.1139/m65-119>
- Dawson PSS (1972) Continuously synchronised growth. *J Appl Chem Biotechnol* 22:79–103. <https://doi.org/10.1002/jctb.2720220112>
- Feldmann H (2012) *Yeast: Molecular and Cell Biology*. Wiley-Blackwell
- Fitch I, Dahmann C, Surana U, et al (1992) Characterization of four B-type cyclin genes of the budding yeast *Saccharomyces cerevisiae*. *Mol Biol Cell* 3:805–818. <https://doi.org/10.1091/mbc.3.7.805>
- Fritsch M, Starruß J, Loesche A, et al (2005) Cell cycle synchronization of *Cupriavidus necator* by continuous phasing measured via flow cytometry. *Biotechnol Bioeng* 92:635–642. <https://doi.org/10.1002/bit.20647>
- Futcher B (1996) Cyclins and the wiring of the yeast cell cycle. *Yeast* 12:1635–1646. [https://doi.org/10.1002/\(SICI\)1097-0061\(199612\)12:16<1635::AID-YEA83>3.0.CO;2-O](https://doi.org/10.1002/(SICI)1097-0061(199612)12:16<1635::AID-YEA83>3.0.CO;2-O)
- Hughes SM, Cooper DG (1996) Biodegradation of phenol using the self-cycling fermentation (SCF) process. *Biotechnol Bioeng* 51:112–119. [https://doi.org/10.1002/\(SICI\)1097-0290\(19960705\)51:1<112::AID-BIT13>3.0.CO;2-S](https://doi.org/10.1002/(SICI)1097-0290(19960705)51:1<112::AID-BIT13>3.0.CO;2-S)
- Levy S, Barkai N (2009) Coordination of gene expression with growth rate: A feedback or a feed-forward strategy? *FEBS Lett* 583:3974–3978. <https://doi.org/10.1016/j.febslet.2009.10.071>
- Livak KJ, Schmittgen TD (2001) Analysis of relative gene expression data using real-time quantitative PCR and the 2- $\Delta\Delta$ CT method. *Methods* 25:402–408.

<https://doi.org/10.1006/meth.2001.1262>

Marchessault P, Sheppard JD (1997) Application of self-cycling fermentation technique to the production of poly- β -hydroxybutyrate. *Biotechnol Bioeng* 55:815–820.

[https://doi.org/10.1002/\(SICI\)1097-0290\(19970905\)55:5<815::AID-BIT12>3.0.CO;2-A](https://doi.org/10.1002/(SICI)1097-0290(19970905)55:5<815::AID-BIT12>3.0.CO;2-A)

McCaffrey WC, Cooper DG (1995) Sophorolipids production by *Candida bombicola* using self-cycling fermentation. *J Ferment Bioeng* 79:146–151. [https://doi.org/10.1016/0922-338X\(95\)94082-3](https://doi.org/10.1016/0922-338X(95)94082-3)

Miller GL (1959) Use of dinitrosalicylic acid reagent for determination of reducing sugar. *Anal Chem* 31:426–428. <https://doi.org/10.1021/ac60147a030>

Mookerjee S (2016) Directing Precursor Flux to Optimize cis,cis-Muconic Acid Production in *Saccharomyces cerevisiae*. Concordia University

Müller J, Dawson PS (1968) The operational flexibility of the phased culture technique, as observed by changes in the cell cycle of *Candida utilis*. *Can J Microbiol* 14:1115–1126. <https://doi.org/10.1139/m68-187>

Mustea I, Muresian T (1967) Crabtree effect in some bacterial cultures. *Cancer* 20:1499–1501. [https://doi.org/10.1002/1097-0142\(196709\)20:9<1499::AID-CNCR2820200917>3.0.CO;2-Q](https://doi.org/10.1002/1097-0142(196709)20:9<1499::AID-CNCR2820200917>3.0.CO;2-Q)

Sarkis BE, Cooper DG (1994) Biodegradation of aromatic compounds in a self-cycling fermenter (SCF). *Can J Chem Eng* 72:874–880. <https://doi.org/10.1002/cjce.5450720514>

Sauvageau D, Cooper DG (2010) Two-stage, self-cycling process for the production of bacteriophages. *Microb Cell Fact* 9:1–10. <https://doi.org/10.1186/1475-2859-9-81>

Sauvageau D, Storms Z, Cooper DG (2010) Synchronized populations of *Escherichia coli* using simplified self-cycling fermentation. *J Biotechnol* 149:67–73. <https://doi.org/10.1016/J.JBIOTECH.2010.06.018>

Sheppard JD (1993) Improved volume control for self-cycling fermentations. *Can J Chem Eng* 71:426–430. <https://doi.org/10.1002/cjce.5450710312>

Sheppard JD, Cooper DG (1991) The response of *Bacillus subtilis* ATCC 21332 to manganese during continuous-phased growth. *Appl Microbiol Biotechnol* 35:72–76.

<https://doi.org/10.1007/BF00180639>

Sheppard JD, Cooper DG (1990) Development of computerized feedback control for the continuous phasing of *Bacillus subtilis*. *Biotechnol Bioeng* 36:539–545.

<https://doi.org/10.1002/bit.260360514>

Sheppard JD, Dawson PSS (1999) Cell synchrony and periodic behaviour in yeast populations. *Can J Chem Eng* 77:893–902. <https://doi.org/10.1002/cjce.5450770515>

Storms ZJ, Brown T, Cooper DG, et al (2014) Impact of the cell life-cycle on bacteriophage T4 infection. *FEMS Microbiol Lett* 353:63–68. <https://doi.org/10.1111/1574-6968.12402>

Storms ZJ, Brown T, Sauvageau D, Cooper DG (2012) Self-cycling operation increases productivity of recombinant protein in *Escherichia coli*. *Biotechnol Bioeng* 109:2262–2270. <https://doi.org/10.1002/bit.24492>

Teste MA, Duquenne M, François JM, Parrou JL (2009) Validation of reference genes for quantitative expression analysis by real-time RT-PCR in *Saccharomyces cerevisiae*. *BMC Mol Biol* 10:1–15. <https://doi.org/10.1186/1471-2199-10-99>

Untergasser A, Cutcutache I, Koressaar T, et al (2012) Primer3-new capabilities and interfaces. *Nucleic Acids Res* 40:1–12. <https://doi.org/10.1093/nar/gks596>

van Walsum GP, Cooper DG (1993) Self-cycling fermentation in a stirred tank reactor. *Biotechnol Bioeng* 42:1175–1180. <https://doi.org/10.1002/bit.260421007>

Wang J, Chae M, Beyene D, et al (2021) Co-production of ethanol and cellulose nanocrystals through self-cycling fermentation of wood pulp hydrolysate. *Bioresour Technol* 330:124969. <https://doi.org/https://doi.org/10.1016/j.biortech.2021.124969>

Wang J, Chae M, Bressler DC, Sauvageau D (2020) Improved bioethanol productivity through gas flow rate-driven self-cycling fermentation. *Biotechnol Biofuels* 13:1–14. <https://doi.org/10.1186/s13068-020-1658-6>

Wang J, Chae M, Sauvageau D, Bressler DC (2017) Improving ethanol productivity through self-cycling fermentation of yeast: a proof of concept. *Biotechnol Biofuels* 10:193. <https://doi.org/10.1186/s13068-017-0879-9>

Wentworth SD, Cooper DG (1996) Self-cycling fermentation of a citric acid producing strain of

Candida lipolytica. J Ferment Bioeng 81:400–405. [https://doi.org/10.1016/0922-338X\(96\)85140-3](https://doi.org/10.1016/0922-338X(96)85140-3)

Zenaitis MG, Cooper DG (1994) Antibiotic production by *Streptomyces aureofaciens* using self-cycling fermentation. Biotechnol Bioeng 44:1331–1336.
<https://doi.org/10.1002/bit.260441109>

6. Methanol Bioconversion in *Methylovimicrobium buryatense* 5GB1C through Self-cycling Fermentation

6.1 Abstract

Methanol is an abundant and low-cost next-generation carbon source. While many species of methanotrophic bacteria can convert methanol into valuable bioproducts in bioreactors, *Methylovimicrobium buryatense* 5GB1C stands out as one of the most promising strains for industrialization. It has a short doubling time compared to most methanotrophs, remarkable resilience against contamination, and a suite of tools enabling genetic engineering. When approaching industrial applications, growing *M. buryatense* 5GB1C on methanol using common batch reactor operation has important limitations. For example, the initial methanol concentration must be limited to avoid toxicity, which leads to mediocre biomass productivity. Herein, implementation of two advanced modes of operation led to: a 26-fold increase in biomass density under fed-batch operation, and 3-fold and 10-fold increases in volumetric biomass productivity based on different self-cycling fermentation schemes. These modes of operations thus greatly improved methanol bioconversion and demonstrated great potential towards efficient implementation in industrial fermentation.

6.2 Introduction

Methanol is an abundant, low-price non-food feedstock considered as a next-generation carbon source (Zhang et al. 2018). It can be produced from natural gas, coal, biomass, carbon dioxide (CO₂), etc. (Dalena et al. 2018). In fact, ~90 % industrial methanol is produced from natural gas-derived synthesis gas (Dalena et al. 2018). While many methanotrophic bacteria can be used to convert this low-value chemical into biomass and other valuable bioproducts, the Gammaproteobacterium *Methylovimicrobium buryatense* 5GB1C, previously known as “*Methylomicrobium buryatense*” 5GB1C (Orata et al. 2018), stands out as an industrially promising strain. It possesses many advantageous traits for bioproduction: it displays a relatively short doubling time; it is a haloalkaliphile – conferring it with great resilience to potential

contamination under high pH and high salinity conditions; and multiple tools enabling its genetic manipulation are readily available.

M. buryatense 5GB1C is a variant of *M. buryatense* 5GB1 that underwent intentional curing of its native plasmid, allowing conjugation with small vectors (Puri et al. 2015). Hence, *M. buryatense* 5GB1C maintains most properties of the 5GB1 strain while being more genetically tractable. Their common parental strain, *M. buryatense* 5G, was first isolated from a soda lake in the Transbaikal region of Russia (Kaluzhnaya et al. 2001). For this haloalkaliphile, high pH and salinity (Kaluzhnaya et al. 2001) can prevent the risks of contamination. It also shows great tolerance to heat, desiccation, and freeze-drying, and can be grown in a wide range of conditions (Kaluzhnaya et al. 2001; Puri et al. 2015). The specific growth rates of *M. buryatense* 5GB1 are appreciably high – e.g., $\sim 0.23 \text{ h}^{-1}$ when growing on methane in NMS2 medium and $\sim 0.17 \text{ h}^{-1}$ on methanol (Gilman et al. 2015) – facilitating its laboratory manipulations and industrial applications.

M. buryatense 5GB1C also displays many advantages towards genetic engineering: it has been sequenced and its genome is publicly available (NCBI Genome, ID 13071); small vectors and a sucrose counterselection system have been developed for conjugation-based genetic manipulations (Puri et al. 2015); electroporation-based genetic manipulation approaches have also been established, requiring fewer steps for gene insertions and deletions in the chromosome (Yan et al. 2016); and a stoichiometric flux balance model has been developed, with which a direct coupling of electron transfer between methane and methanol oxidation was confirmed (Torre et al. 2015). These tools were used to improve the production of lactate – by inserting a *Lactobacillus helveticus* L-lactate dehydrogenase (Henard et al. 2016), and to produce C4 carboxylic acids – by diverting carbon flux away from acetyl-CoA (Garg et al. 2018b).

While the simplicity of batch reactor (BR) operation makes it the most common bioconversion processing strategy, it is not appropriate for the conversion of methanol by *M. buryatense* 5GB1C. Because of its toxicity, the initial load of methanol in BR must be kept low to avoid inhibition, leading to mediocre biomass concentration and low productivity. Fed-batch operation, in which substrates are gradually added to the cultures, has been shown to be an efficient approach to overcome issues of substrate inhibition and achieve high biomass density and product density (Lim and Shin 2013). For instance, inhibition resulting from high concentrations of methanol (Çelik et al. 2009; Çalık et al. 2010) or glucose (Liu et al. 2008) has been overcome

through fed-batch strategies. Various products, such as microbial cells, vitamins, enzymes, amino acids, and antibiotics, have been produced through this mode of operation (Lim and Shin 2013). On the other hand, self-cycling fermentation (SCF), another advanced fermentation approach, is an automated semi-continuous system that exchanges half the reactor contents upon nutrient depletion (Sauvageau et al. 2010; Storms et al. 2012; Agustin 2015; Wang et al. 2017). It has been shown to significantly increase productivity during bioproduction in a wide variety of bacterial and yeast systems. Citric acid (Wentworth and Cooper 1996), recombinant proteins (Storms et al. 2012), bacteriophages (Sauvageau and Cooper 2010), bioethanol (Wang et al. 2020) and shikimic acid (Agustin 2015) are some examples of bioproducts produced through SCF. In the present study, fed-batch and SCF operation were implemented in cultivating *M. buryatense* 5GB1C growing on methanol, and their impact on biomass density and volumetric productivity was investigated, shedding light on the potential in producing single-cell proteins.

6.3 Methods and Materials

6.3.1 Strains and Media

M. buryatense 5GB1C was grown in NMS2 media (pH 9.5). 1.05 L NMS2 medium comprised 10 mL phosphate buffer, 40 mL carbonate solution, and 1 L 1X NMS2 medium. 1 L carbonate buffer contained 94.5 g sodium bicarbonate (all chemicals used were purchased from Fisher Scientific or Sigma Aldrich) and 13.2 g sodium carbonate. 0.5 L phosphate buffer (pH 6.8) contained 12.55 g sodium phosphate dibasic and 8.55 g potassium phosphate monobasic. 1 L 10X NMS2 contained 2 g magnesium sulfate heptahydrate, 0.134 g calcium chloride dihydrate, 10 g potassium nitrate, 75 g sodium chloride, 0.5 mL of 100 mM copper sulfate solution, and 10 mL trace element (TE) solution. 1 L TE solution had 5 g disodium ethylenediaminetetraacetate dihydrate, 2 g iron(II) sulfate heptahydrate, 0.3 g zinc sulfate heptahydrate, 0.03 g manganese(II) chloride tetrahydrate, 0.2 g cobalt(II) chloride hexahydrate, 0.3 g sodium tungstate dihydrate, 0.05 g nickel(II) chloride hexahydrate, 0.3 g sodium molybdate dihydrate, and 0.05 g boric acid. Methanol (HPLC grade) was added to NMS2 media as the main carbon source. Pre-cultures were grown in 100 mL of NMS2 medium containing 10 mM methanol in 250-mL serum bottles, which were incubated (Ecotron, Infors HT) at 30 °C and 150 rpm until reaching stationary phase.

During inhibition assessment experiments, when the bioreactor was not used, *M. buryatense* 5GB1C was grown using 100 mL of NMS2 media containing different concentrations of methanol in 250-mL Erlenmeyer flasks (with foam stoppers), and incubation (Ecotron, Infors HT) was performed at 30 °C and 150 rpm.

6.3.2 Bioreactor operation

A custom-made bioreactor system was used for fed-batch and SCF operation, the setup of which can be found in previous studies (Storms et al. 2012; Agustin 2015). For both processes, the working volume was kept at 1 L; the temperature was maintained at 30 °C; aeration at 150 mL/min; and agitation (Rushton impeller) at 200 rpm. A CO₂ gas sensor based on IR-spectrometry (Vernier Scientific) measured the carbon dioxide (CO₂) evolution rate (CER) based on exit gas concentration (Sauvageau et al. 2010).

Fed-batch operation was established by manually pulsing increasing amounts of methanol (5 mM, 10 mM, and 30 mM) into the reactor system once methanol was entirely consumed and optical density (OD₆₀₀, see section 6.3.3 below) reached a maximum. Antifoam SE-15 (Sigma-Aldrich) was added during the late stages of fed-batch fermentation to avoid foaming issues.

SCF operation was performed using reflectance (BugEye system, BugLab LLC; Figure 6.1) monitored in real-time as a proxy for culture cell density. SCF was established by harvesting one-half the working volume of the bioreactor once methanol was depleted and the reflectance unit reached a maximum, and then replenishing it with the same amount of fresh medium. For the first SCF strategy, cycle 1 was initiated with 10 mM methanol, and the succeeding cycles with 5 mM methanol. For the second SCF strategy, cycle 1 was initiated with 5 mM methanol, and the following cycles with 15 mM methanol. It should also be noted that the first cycle of SCF corresponded to BR operation.

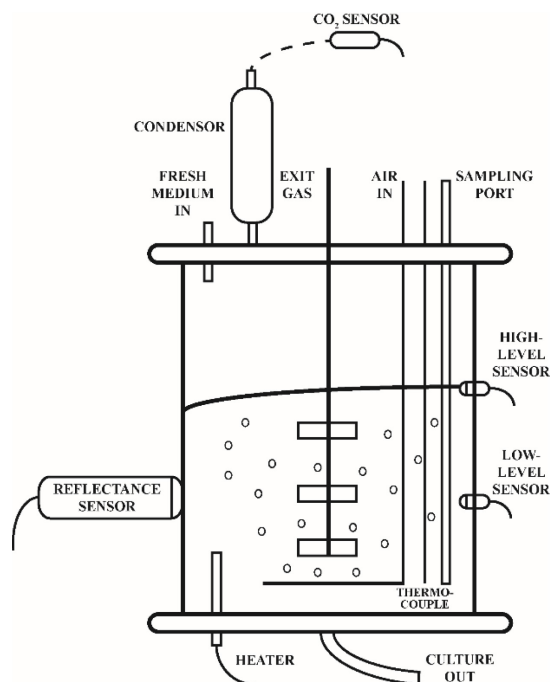


Figure 6.1 Simplified schematic of the bioreactor system incorporating a reflectance sensor for monitoring.

6.3.3 Cell density, pH, and methanol measurement

Cultures were assessed by measuring optical density at 600 nm (OD_{600}) using a spectrophotometer (Ultrospec 50, Biochrom). A Petroff-Hausser counting chamber (Hausser Scientific), a Laboval 4 light microscope (Carl Zeiss), and ImageJ software (Schneider et al. 2012) were used for cell count measurements. pH was measured using a pH meter and electrode (Denver Instruments Ultrabasic, Sartorius). Methanol concentration was measured using a Methanol Quantification Assay Kit (Sigma-Aldrich). A reaction mix containing two enzymes, a developer, and a probe was prepared and added to samples following the manufacturer's manual. After 15 min of incubation in the dark, samples were assessed by measuring fluorescence intensity at 535 nm (excitation)/590 nm (emission) using a Cytation 5 plate reader (BioTek Instruments). A standard curve was established (with a linear range from 0.5 to 10 nmol) and used for quantification. Methanol depletion was also confirmed by the lack of further growth of cultures transferred to a second-stage flask.

6.4 Results

6.4.1 Methanol Inhibition Assessment

Prior to fed-batch and SCF experiments, methanol inhibition was assessed by growing *M. buryatense* 5GB1C in batch cultures initiated at different methanol concentrations in the bioreactor and Erlenmeyer flasks. Table 6.1 summarizes the final OD₆₀₀ and further growth after additional methanol addition of 5 mM upon OD₆₀₀ reaching a plateau. The OD₆₀₀ was 0.19 when the initial methanol concentration was 5 mM, which reached 0.34 in the case of 10 mM methanol (Table 6.1). However, little improvement in final OD₆₀₀ was observed when batch cultures were initiated at higher concentrations of methanol (15-120 mM), and the disproportions between initial methanol input and final OD₆₀₀ inferred inhibition (Table 6.1). Notably, cultures initiated at 30 mM methanol in either the bioreactor or Erlenmeyer flasks resulted in congruent final OD₆₀₀.

Once OD₆₀₀ reached a plateau, additional methanol (equivalent to 5 mM) was pulsed to determine whether further growth could take place. Continued growth was observed for cultures previously grown on 5 mM and 10 mM methanol; delayed growth was found for cultures previously grown on 15 mM and 20 mM methanol (with the latter displaying a longer delay in growth); no significant growth was found for cultures initiated at 30 mM or more (Table 6.1). These results suggest that significant inhibition occurred when a batch culture was initiated at a concentration of methanol above 10 mM. Consequently, in order to avoid significant methanol inhibitory effects, fed-batch operation was initiated at 5 mM methanol. Two SCF schemes were developed: in the first, SCF operation was initiated at 10 mM methanol followed by pulses to 5 mM for the succeeding cycles; and in the second, the first cycle was initiated at 5 mM of methanol while methanol was pulsed to 15 mM for subsequent cycles.

Table 6.1 Final OD₆₀₀ and further growth after methanol addition of 5 mM for batch cultures that were initiated at different concentrations of methanol.

Vessel	Initial methanol concentration, mM	Final OD ₆₀₀	Growth after further methanol addition of 5 mM
Bioreactor	5	0.19	Continued Growth
Bioreactor	30	0.28	No Growth
Flasks	10	0.34	Continued Growth
Flasks	15	0.39	Delayed Growth
Flasks	20	0.39	Delayed Growth (Longer Delay)
Flasks	30	0.32	No Growth
Flasks	50	0.32	No Growth
Flasks	80	0.34	No Growth
Flasks	120	0.41	(Not Tested)

6.4.2 Fed-batch Operation

Growth of *M. buryatense* 5GB1C in fed-batch operation was initiated with 5 mM methanol. In this context, the initial growth step, which corresponded to a BR operation, led to an OD₆₀₀ of 0.206 within 42 h (Figure 6.2). Following this, methanol was added in a pulsing manner every time methanol was depleted; methanol was pulsed to increasing concentrations of 5 mM, 10 mM, and 30 mM over time as the cell concentration increased. This stepwise pulsing allowed the OD₆₀₀ to reach 5.56 – a 26-fold increase in final biomass density compared to BR (Figure 6.2) – at 246 h.

The depletion of methanol was confirmed by methanol quantification assay and by lack of further growth of cultures transferred to a second-stage flask. Upon methanol depletion, a slight decrease in OD₆₀₀ was observed, which was consistent with previous studies growing other methanotrophic bacteria using methanol (Zaldívar Carrillo et al. 2018; Tays et al. 2018). In addition, the decrease in OD₆₀₀ at 59.5 h was associated with replacing half the reactor contents with fresh medium.

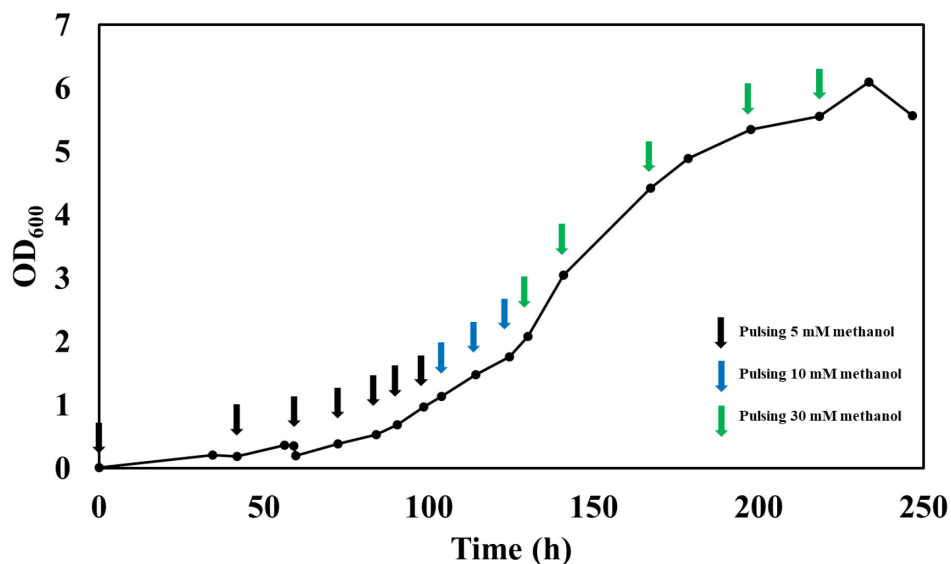


Figure 6.2 Optical density during fed-batch operation of *M. buryatense* 5GB1C growing on methanol. Arrows indicate time of methanol addition to 5 mM (black arrow), 10 mM (blue arrow), and 30 mM (green arrow).

6.4.3 First SCF Feeding Scheme

In the first SCF scheme, the first cycle, which corresponded to a BR, was initiated with 10 mM methanol, with each subsequent cycle (cycle 2 onwards) initiated at 5 mM methanol.

Using culture reflectance as the control parameter enabled the establishment of a stable SCF operation (Figure 6.3). Methanol quantification and lack of further growth confirmed complete methanol consumption at the end of each cycle. In the course of SCF operation, the patterns of reflectance (Figure 6.3A), CER (Figure 6.3B), cycle time (Figure 6.3C), OD_{600} and pH (Figure 6.3D) were reproducible. Within SCF cycles, reflectance, CER, and OD_{600} increased until reaching their maxima at the end of the cycles, while pH decreased slightly (Figures 6.3 and 6.4).

Some detailed observations in Figure 6.3 can be made. In cycle 1 (BR), a final OD_{600} of 0.247 was reached at 28.8 h. Cycle 2 had the longest cycle time at 29.7 h and presented a significant decrease in CER following its maximum; culture reflectance, however, increased continuously until the end of the cycle. After cycle 2, SCF operation gradually stabilized – cycle time decreased; intracycle increases in culture reflectance, CER, and OD_{600} were more significant; and end-of-cycle values of reflectance, CER, and OD_{600} increased. Stable patterns of the growth-associated

parameters were established after SCF cycle 11, which was an outlier – having a large cycle time (18.1 h) and a long-term decrease in CER following the CER maximum. Following this cycle, culture reflectance, CER, OD₆₀₀, and pH showed similar intra-cycle trends and comparable intra-cycle minima and maxima values. Cycle time for cycles 12 to 42 averaged 6.2 ± 0.6 h, indicative of operational stability. Cycles 33 and 34 were also considered outliers showing a slightly increased cycle time but a significant increase in reflectance signal due to a sudden change in reflectance baseline. However, it was noted that the intra-cycle increases in culture reflectance during cycles 33 and 34 were consistent with other cycles. Reflectance baseline returned after cycle 34.

Notably, once SCF operation stabilized after cycle 11, volumetric biomass productivity was 0.032 AU/h – a more than 3-fold increase compared to BR (cycle 1; 0.009 AU/h).

As one of the characteristic features of SCF, synchrony of the cell population (Brown and Cooper 1991; McCaffrey and Cooper 1995; Wentworth and Cooper 1996; Sauvageau et al. 2010) was investigated in cycles 32 and 40 of *M. buryatense* 5GB1C growing on methanol. Cell count and OD₆₀₀ increased in a continuous way during the cycles; a stepwise increase in cell count within a short time frame, typical of synchronized SCF cycles, was not seen (Figures 6.4). Based on these trends, it was concluded that synchrony was not established during SCF operation of *M. buryatense* 5GB1C. In addition, intra-cycle analysis showed that maxima in cell density and OD₆₀₀ occurred concomitantly with the maxima in reflectance and CER (Figures 6.4).

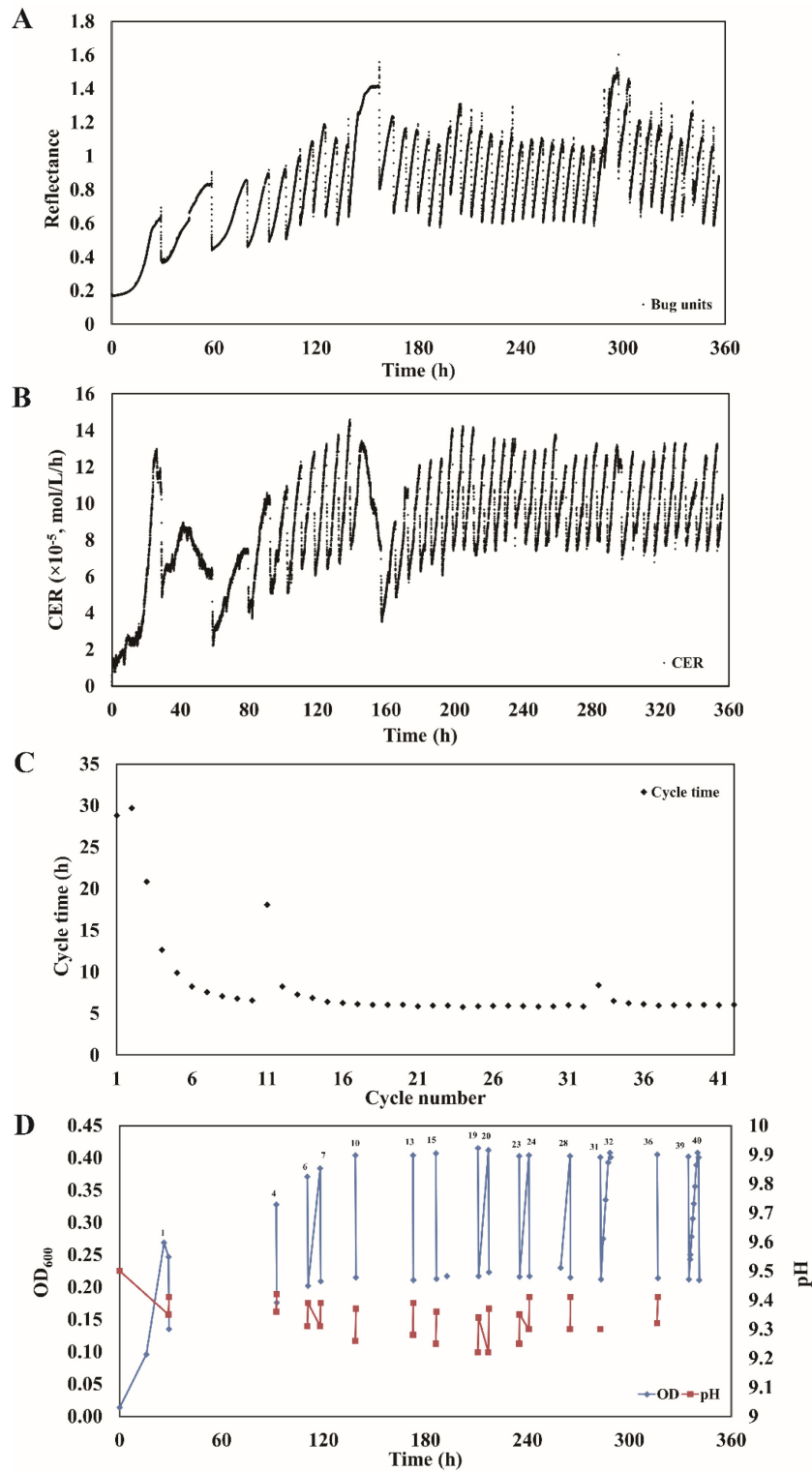


Figure 6.3 Monitored parameters during SCF operation of *M. buryatense* 5GB1C grown on methanol using the first feeding scheme. Cycle 1 was initiated with 10 mM methanol, and the succeeding cycles with 5 mM of methanol. A) Reflectance, B) carbon dioxide evolution rate (CER), C) cycle time, and D) OD₆₀₀ and pH.

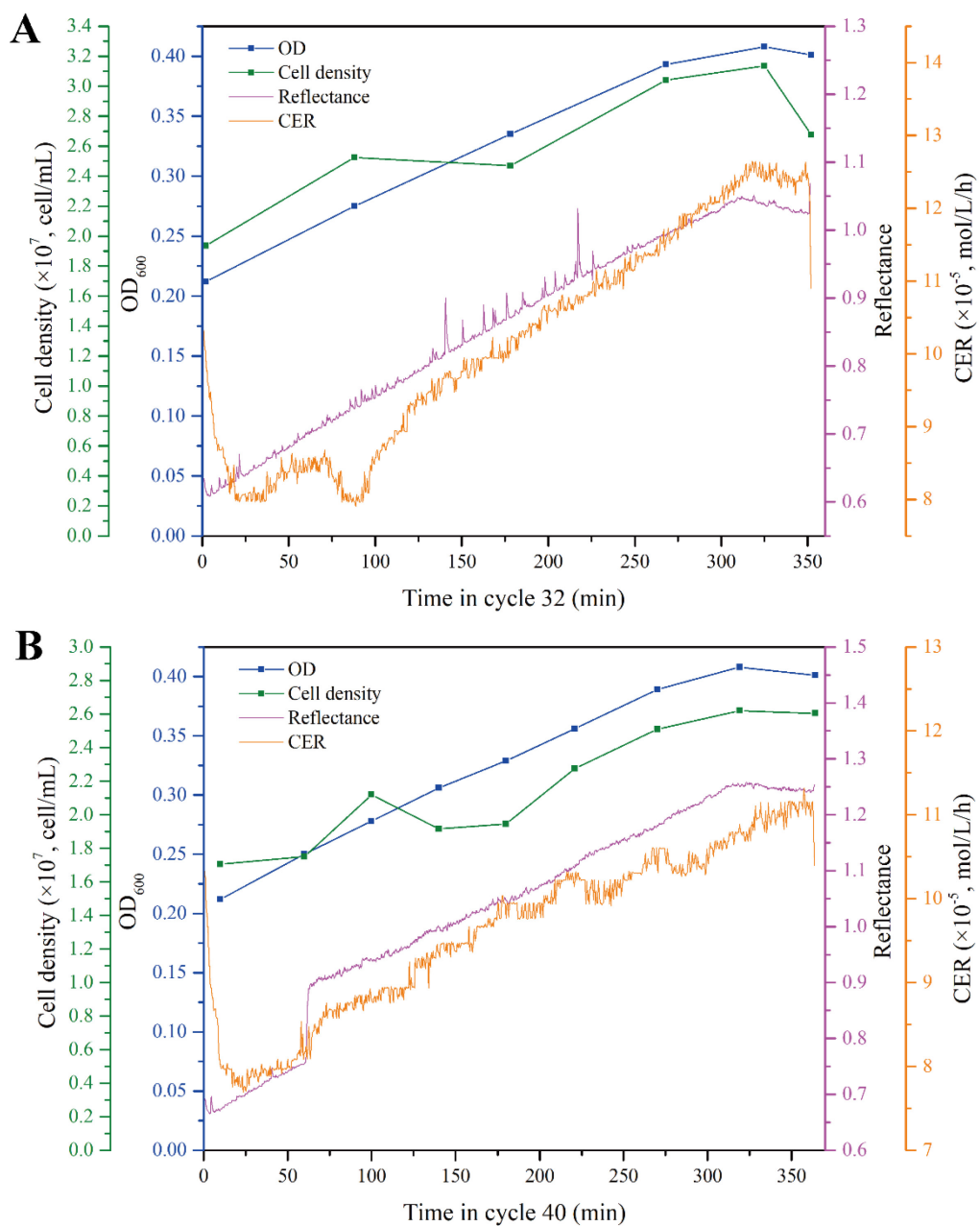


Figure 6.4 Intracycle cell count, OD₆₀₀, reflectance, and CER in SCF cycles 32 (A) and 40 (B) during SCF operation of *M. buryatense* 5GB1C growing on methanol using the first feeding scheme. These cycles were initiated with 5 mM of methanol.

6.4.4 Second SCF Feeding Scheme

The second SCF scheme consisted of initiating operation with 5 mM methanol and adding methanol to 15 mM for each subsequent SCF cycle (cycle 2 onwards). Similarly, cycling took place upon reaching a maximum in reflectance, corresponding to methanol depletion at the end of the cycles. The profiles of reflectance, CER, cycle time, OD₆₀₀ and pH are shown in Figures 6.5A-6.5D, respectively. Culture reflectance, CER and pH patterns became repeatable from cycle 6 onwards, and the cycle time averaged 6.9 ± 0.4 h for cycles 6 to 19. However, a stable pattern in OD₆₀₀ was only achieved from cycle 10 onwards. Remarkably, volumetric biomass productivity was improved 10-fold when comparing stable SCF cycles (cycles 10-19) to the BR (cycle 1). In addition, the increases in reflectance, CER and OD₆₀₀ (Figures 6.5A, 6.5B, and 6.5D) and the decrease in pH (Figure 6.5D) observed for each cycle were more significant than those observed with the first SCF feeding scheme, consistent with the greater availability of methanol. However, cycle times remained similar, regardless of the amount of methanol fed to the cycles (Figures 6.3C and 6.5C), suggesting a correlation between the doubling time of *M. buryatense* 5GB1C and the SCF cycle time.

Moreover, similarly to the first SCF scheme, cell density, OD₆₀₀, reflectance, and CER were increasing during the SCF cycles and reached their maxima at the end of the cycles (intracycle data for cycle 16 in Figure 6.6). While cell density and OD₆₀₀ doubled by the end of the cycles, clear patterns expected for synchrony (e.g., step-wise increase in cell density) were not observed (Figure 6.6). Furthermore, although reflectance and OD₆₀₀ patterns presented general correspondence during operation, it was noted that the overall trends diverged from each other during cycles 6 to 10 when undergoing the second SCF feeding scheme – end-of-cycle reflectance decreased while end-of-cycle OD₆₀₀ increased (Figures 6.5A and 6.5D).

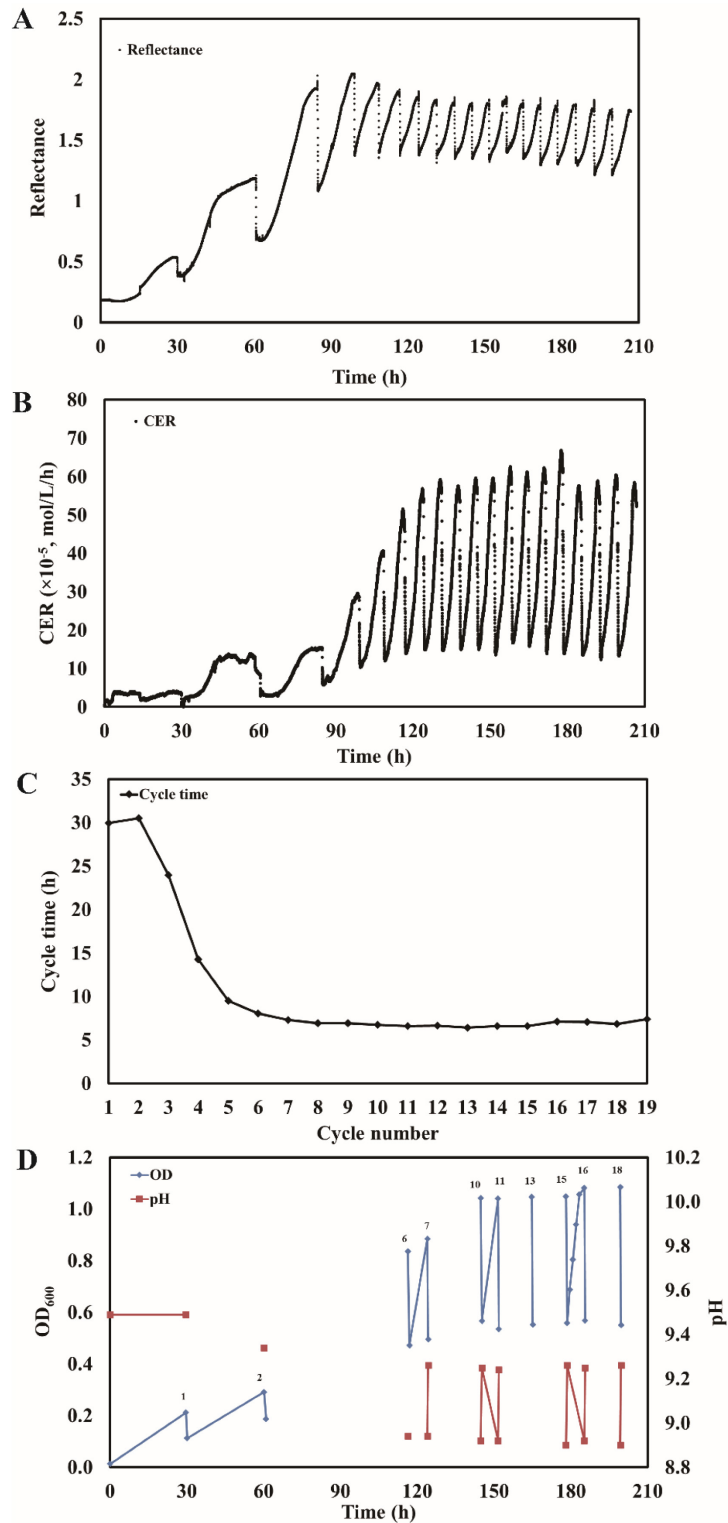


Figure 6.5 Monitored parameters during SCF operation of *M. buryatense* 5GB1C grown on methanol using the second feeding scheme. Cycle 1 was initiated with 5 mM methanol, and the following cycles with 15 mM methanol. A) Reflectance, B) carbon dioxide evolution rate (CER), C) cycle time, and D) OD₆₀₀ and pH.

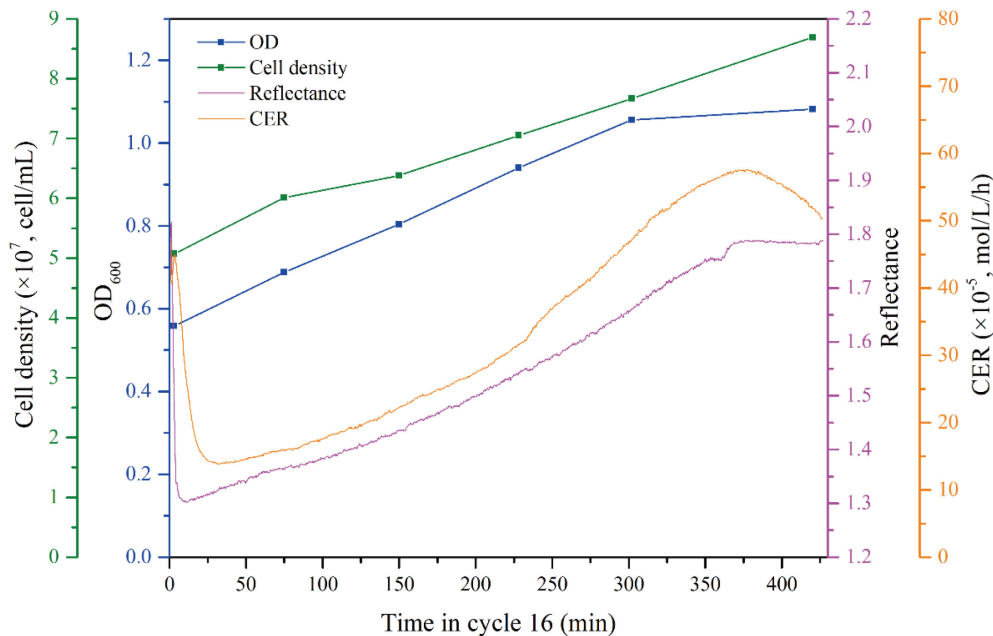


Figure 6.6 Intracycle cell count, OD₆₀₀, reflectance, and CER in cycle 16 during SCF operation of *M. buryatense* 5GB1C growing on methanol using the second feeding scheme. The cycle was initiated with 15 mM methanol.

6.5 Discussion

The low cost and high availability of methanol as a feedstock has attracted industrial interests for the production of high-value bioproducts (Zhang et al. 2018). Herein we investigated the implementation of two advanced modes of bioreactor operation to overcome methanol inhibition and achieve more efficient production of *M. buryatense* 5GB1C cells (compared to batch operation), showing potential for single-cell protein production.

As high concentrations of methanol inhibit cell growth, we first examined the impact of different methanol concentrations on *M. buryatense* 5GB1C in batch growth. Based on Table 6.1, 5 mM and 10 mM methanol resulted in relatively reasonable increases in OD₆₀₀ and continued growth once pulsing additional methanol, suggesting little inhibition at these lower concentrations. In contrast, strong inhibitory effects were observed (e.g., limited increases in OD₆₀₀ and impeded growth after pulsing additional methanol) when the initial concentration of methanol was set to 15

mM or above. Hence, it was established that inhibition of methanol became significant at concentrations between 10 mM and 15 mM.

In a previous study (He et al. 2019), *M. buryatense* 5GB1C was grown in a continuous reactor by feeding 1 g/L methanol (31 mM), and no significant inhibition was noted. It was likely due to the continuous approach having a much lower concentration of methanol at any one time inside the stirred-tank reactor. It is also noted that the parental strains 5GB1 and 5G have been cultivated using much higher concentrations of methanol to obtain elevated biomass density (e.g., 5GB1 strain with 124 mM methanol resulted in OD₆₀₀ over 3.5; 5G strain with 1.25 M methanol resulted in OD₆₀₀ over 4.8) (Kaluzhnaya et al. 2001; Eshinimaev et al. 2002; Gilman et al. 2015). Hence, future attention might be focused on whether curing of the native plasmid from the 5GB1 strain (i.e., the procedure used to obtain the 5GB1C strain (Puri et al. 2015)) resulted in a decrease in its methanol tolerance.

In order to minimize the effects of methanol inhibition, fed-batch operation was initiated with 5 mM methanol as were the SCF cycles in the first feeding scheme. Continued growth was observed after intermittent methanol additions during the fed-batch operation (Figure 6.2) and after the replacement of half the reactor contents (cycling) during SCF operation (Figure 6.3). Remarkably, as cell density increased during fed-batch operation, the increasing amounts of methanol pulsed, up to 30 mM, no longer presented significant inhibitory effects – cell growth quickly resumed upon methanol additions and increases in OD₆₀₀ were proportional to the amounts of methanol pulsed (Figure 6.2). Moreover, intermittent methanol additions in fed-batch operation enabled a significant increase in total methanol added, and as a result led to a 26-fold increase in biomass density compared to simple BR operation (Figure 6.2). On the other hand, the implementation of SCF operation had a significant impact on the rate of biomass production, leading to improvements in volumetric biomass productivity corresponding to a 3-fold increase when compared to BR (the first SCF feeding scheme; Figure 6.3). Overall, through these two advanced fermentation approaches, methanol inhibition was overcome, and production of *M. buryatense* 5GB1C cellular biomass was greatly improved in terms of the final biomass concentration and volumetric biomass productivity.

The second SCF feeding scheme (Figures 6.5 and 6.6) involved adding significantly greater amounts of methanol to the SCF cycles (cycle 2 onwards). As a result, volumetric biomass

productivity increased 10-fold compared to BR once stable operation was developed. This showed that, again, implementation of SCF operation can overcome methanol inhibition and enhance its bioconversion and that the feeding strategy of SCF operation can be conveniently adjusted. Additionally, the similarity in cycle times between SCF cycles with 5 mM and 15 mM methanol (6.3 h and 6.9 h, respectively; Figures 6.3C and 6.5C) and the fact that cell density doubled by the end of the cycles in both operations (Figures 6.4 and 6.6) indicate a strong coupling of the SCF cycle time and cell doubling time. The co-occurrence of CER maximum, the end of the doubling of cell density and OD₆₀₀, and methanol depletion in both feeding schemes suggested that SCF operation of *M. buryatense* 5GB1C growing on methanol followed SCF Trend A (see Chapter 5 for more details of the Trends); a trend observed in many earlier SCF studies (Sheppard and Cooper 1990; Brown and Cooper 1991; Sarkis and Cooper 1994; McCaffrey and Cooper 1995; Wentworth and Cooper 1996; Brown et al. 1999). Trend A depicts a clear contrast to the Trend C observed in recent *Escherichia coli* and *Saccharomyces cerevisiae* SCF studies (Chapters 4 and 5), where the depletion or a plateau of the limiting nutrient occurred much later than the concurrence of CER maximum and the completion of cell replication. This divergence infers that *M. buryatense* 5GB1C is different from *E. coli* and *S. cerevisiae* with regards to their nutrient utilization and proliferation strategies (Chapter 5).

Synchronized cell replication, observed in a number of SCF studies (Brown and Cooper 1991; McCaffrey and Cooper 1995; Wentworth and Cooper 1996; Sauvageau et al. 2010), is one of the characteristic features of SCF. For example, in Chapter 4, transcriptomic profiles of *S. cerevisiae* undergoing SCF were investigated, and synchrony of the yeast populations was confirmed. However, in the present study, replication of *M. buryatense* 5GB1C cells did not display the patterns typical of synchronization during SCF operation (in either scheme; Figures 6.4, 6.6). It is suggested that periodic availability of the carbon source did not provide an efficient entrainment effect (Sheppard and Dawson 1999) that was required to lead to cell synchronization in SCF. This was likely related to the metabolic mechanisms of methanol. The effects of methanol as the carbon source on transcriptomics and metabolomics of another gammaproteobacterial methanotroph, *Methylomicrobium album* BG8, were recently studied (Sugden et al. 2021). Additional ribosomes, higher abundances of stress-related transcripts, down-regulated central metabolic pathways, and more active GSH-dependent formaldehyde detoxification were all observed when methanol was used as the carbon source (at a non-inhibitory concentration)

(Sugden et al. 2021). Similar stress-related metabolism might take place in *M. buryatense* 5GB1C that interfere with the synchronization process, but this would need to be confirmed. In addition, significantly increased concentrations in formaldehyde, formate, and glycogen were identified when growing *M. buryatense* 5GB1 strain on methanol compared to methane (Fu et al., 2019). These metabolites likely accumulated in the 5GB1C cultures in the present study, potentially hindering synchronization in SCF.

Successful automated SCF cycling was established using two feeding strategies by incorporating culture reflectance as the control parameter (Figures 6.3 and 6.5). In addition, cycling was confirmed to take place upon the depletion of the limiting nutrient (methanol). Conventional optical density measurement using a spectrometer requires manual sampling and measurement and results in scattered data points. An optical density probe used inside the bioreactor systems to provide real-time cell density information is intrusive and prone to fouling. Culture reflectance, in comparison, provides a non-intrusive, automated, in-line measurement of culture density. Consistencies between culture reflectance and manually assessed optical density were generally observed in this work, and in particular the occurrence of maxima in reflectance and OD₆₀₀ coincided (Figures 6.4 and 6.6). There are, however, some limitations in using culture reflectance as the sensing element in SCF operation. Firstly, some metabolites and cell lysate may significantly modify light reflectance but not light scattering, resulting in a potential divergence between culture reflectance and cell growth. For example, though not often seen, an increase in reflectance along with a decrease in CER and a plateau in OD₆₀₀ during the late stages of cycle 2 during the first SCF operation (Figures 6.3A and 6.3B) may have resulted from an accumulation of metabolites that increased reflectance even without further cell growth. In addition, the disagreement between the general trends in reflectance and OD₆₀₀ during cycles 6 to 10 in the second SCF feeding scheme (Figures 6.5A and 6.5D) might be associated with more significant production of reflectance-increasing metabolites during the earlier SCF cycles. Secondly, the unexpected and sudden increase in reflectance baseline in cycles 33 and 34 during the first SCF feeding scheme revealed some potential issues regarding signaling stability of the instrument (Figure 6.3A).

As a future focus, other methanotrophic bacteria can be grown using the SCF technique on methanol or the potent greenhouse gas methane. Single-cell protein (Øverland et al. 2010; Ritala

et al. 2017; Zha et al. 2021), recombinant proteins, lipids (Fei et al. 2018), fatty acids (Dong et al. 2017), lactic acid (Garg et al. 2018a), and bioplastics (Strong et al. 2016; Zhang et al. 2017; Liu et al. 2020) are among the expected valuable products from methanotrophs undergoing SCF operation. Two-stage SCF operation (van Walsum and Cooper 1993; McCaffrey and Cooper 1995; Wentworth and Cooper 1996; Sauvageau and Cooper 2010; Storms et al. 2012) and the extended SCF cycle strategy (McCaffrey and Cooper 1995; Wentworth and Cooper 1996; Crosman et al. 2002) can be explored and incorporated if productivity and yield can be further improved.

6.6 Conclusions

In this study, an industrially promising methanotrophic bacterium, *M. buryatense* 5GB1C, has been grown in two types of advanced bioreactor platforms to overcome methanol inhibition and potentially for production of single-cell proteins. The fed-batch operation resulted in a 26-fold improvement in biomass cell density. The SCF operation led to substantial increases in volumetric biomass productivity (3-fold or 10-fold depending on the SCF scheme implemented). In addition, culture reflectance was demonstrated as a successful and convenient control parameter for SCF operation. These results serve as an important proof of concept for exploring efficient methanol bioconversion using methanotrophic bacteria.

6.7 Acknowledgement

We thank Les Dean for helping modify the data acquisition and control system.

This work was supported by the Natural Sciences and Engineering Research Council of Canada (NSERC) Discovery Grant program, the Canada First Research Excellence Fund – Future Energy Systems, the Canada Foundation for Innovation – John R. Evans Leaders Fund, the Government of Alberta – Ministry of Economic Development and Trade Small Equipment Grant, the Climate Change Innovation and Technology Framework (CCITF) – Clean Technology Development (CTD) program, and the University of Alberta Faculty of Engineering.

6.8 References

- Agustin RVC (2015) The Impact of Self-Cycling Fermentation on the Production of Shikimic Acid in Populations of Engineered *Saccharomyces cerevisiae*. University of Alberta
- Brown WA, Cooper DG (1991) Self-cycling fermentation applied to *Acinetobacter calcoaceticus* RAG-1. *Appl Environ Microbiol* 57:2901–2906. <https://doi.org/10.1128/aem.57.10.2901-2906.1991>
- Brown WA, Cooper DG, Liss SN (1999) Adapting the self-cycling fermentor to anoxic conditions. *Environ Sci Technol* 33:1458–1463. <https://doi.org/10.1021/ES980856S>
- Çalık P, İnankur B, Soyaslan EŞ, et al (2010) Fermentation and oxygen transfer characteristics in recombinant human growth hormone production by *Pichia pastoris* in sorbitol batch and methanol fed-batch operation. *J Chem Technol Biotechnol* 85:226–233. <https://doi.org/10.1002/JCTB.2292>
- Çelik E, Çalık P, Oliver SG (2009) Fed-batch methanol feeding strategy for recombinant protein production by *Pichia pastoris* in the presence of co-substrate sorbitol. *Yeast* 26:473–484. <https://doi.org/10.1002/YEA.1679>
- Crosman JT, Pinchuk RJ, Cooper DG (2002) Enhanced biosurfactant production by *Corynebacterium alkanolyticum* ATCC 21511 using self-cycling fermentation. *J Am Oil Chem Soc* 79:467–472. <https://doi.org/10.1007/s11746-002-0507-5>
- Dalena F, Senatore A, Marino A, et al (2018) Methanol Production and Applications: An Overview. *Methanol Sci Eng* 3–28. <https://doi.org/10.1016/B978-0-444-63903-5.00001-7>
- Dong T, Fei Q, Genelot M, et al (2017) A novel integrated biorefinery process for diesel fuel blendstock production using lipids from the methanotroph, *Methylomicrobium buryatense*. *Energy Convers Manag* 140:62–70. <https://doi.org/10.1016/J.ENCONMAN.2017.02.075>
- Eshinimaev BT, Khmelenina VN, Sakharovskii VG, et al (2002) Physiological, Biochemical, and Cytological Characteristics of a Haloalkalitolerant Methanotroph Grown on Methanol. *Microbiol* 2002 715 71:512–518. <https://doi.org/10.1023/A:1020594300166>
- Fei Q, Puri AW, Smith H, et al (2018) Enhanced biological fixation of methane for microbial lipid production by recombinant *Methylomicrobium buryatense*. *Biotechnol Biofuels* 11:1–

11. <https://doi.org/10.1186/S13068-018-1128-6>

Fu, Y., He, L., Reeve, J., Beck, D.A.C., Lidstrom, M.E., 2019. Core metabolism shifts during growth on methanol versus methane in the methanotroph *Methylobacterium buryatense* 5GB1. *MBio* 10. <https://doi.org/10.1128/mBio.00406-19>

Garg S, Clomburg JM, Gonzalez R (2018a) A modular approach for high-flux lactic acid production from methane in an industrial medium using engineered *Methylobacterium buryatense* 5GB1. *J Ind Microbiol Biotechnol* 45:379–391. <https://doi.org/10.1007/s10295-018-2035-3>

Garg S, Wu H, Clomburg JM, Bennett GN (2018b) Bioconversion of methane to C-4 carboxylic acids using carbon flux through acetyl-CoA in engineered *Methylobacterium buryatense* 5GB1C. *Metab Eng* 48:175–183. <https://doi.org/10.1016/j.ymben.2018.06.001>

Gilman A, Laurens LM, Puri AW, et al (2015) Bioreactor performance parameters for an industrially-promising methanotroph *Methylobacterium buryatense* 5GB1. *Microb Cell Fact* 14:182. <https://doi.org/10.1186/s12934-015-0372-8>

Hayden B, Canuel N, Shanse J (2013) What Was Brewing in the Natufian? An Archaeological Assessment of Brewing Technology in the Epipaleolithic. *J Archaeol Method Theory* 20:102–150. <https://doi.org/10.1007/S10816-011-9127-Y/FIGURES/3>

He L, Fu Y, Lidstrom ME (2019) Quantifying Methane and Methanol Metabolism of “*Methylobacterium buryatense*” 5GB1C under Substrate Limitation. *mSystems* 4:. <https://doi.org/10.1128/msystems.00748-19>

Henard CA, Smith H, Dowe N, et al (2016) Bioconversion of methane to lactate by an obligate methanotrophic bacterium. *Sci Rep* 6:1–9. <https://doi.org/10.1038/srep21585>

Kaluzhnaya M, Khmelenina V, Eshinimaev B, et al (2001) Taxonomic characterization of new alkaliphilic and alkalitolerant methanotrophs from soda lakes of the Southeastern Transbaikal region and description of *Methylobacterium buryatense* sp.nov. *Syst Appl Microbiol* 24:166–176. <https://doi.org/10.1078/0723-2020-00028>

Lim H, Shin H (2013) Fed-batch cultures: principles and applications of semi-batch bioreactors. Cambridge University Press

- Liu L-Y, Xie G-J, Xing D-F, et al (2020) Biological conversion of methane to polyhydroxyalkanoates: Current advances, challenges, and perspectives. *Environ Sci Ecotechnology* 2:100029. <https://doi.org/10.1016/J.ESE.2020.100029>
- Liu Y-P, Zheng P, Sun Z-H, et al (2008) Strategies of pH control and glucose-fed batch fermentation for production of succinic acid by *Actinobacillus succinogenes* CGMCC1593. *J Chem Technol Biotechnol* 83:722–729. <https://doi.org/10.1002/JCTB.1862>
- McCaffrey WC, Cooper DG (1995) Sphorolipids production by *Candida bombicola* using self-cycling fermentation. *J Ferment Bioeng* 79:146–151. [https://doi.org/10.1016/0922-338X\(95\)94082-3](https://doi.org/10.1016/0922-338X(95)94082-3)
- Orata FD, Meier-Kolthoff JP, Sauvageau D, Stein LY (2018) Phylogenomic analysis of the gammaproteobacterial methanotrophs (order methylococcales) calls for the reclassification of members at the genus and species levels. *Front Microbiol* 9:3162. <https://doi.org/10.3389/fmicb.2018.03162>
- Øverland M, Tauson A-H, Shearer K, Skrede A (2010) Evaluation of methane-utilising bacteria products as feed ingredients for monogastric animals. *Arch Anim Nutr* 64:171–189. <https://doi.org/10.1080/17450391003691534>
- Puri AW, Owen S, Chu F, et al (2015) Genetic tools for the industrially promising methanotroph *Methylomicrobium buryatense*. *Appl Environ Microbiol* 81:1775–1781. <https://doi.org/10.1128/AEM.03795-14>
- Ritala A, Häkkinen ST, Toivari M, Wiebe MG (2017) Single Cell Protein—State-of-the-Art, Industrial Landscape and Patents 2001–2016. *Front Microbiol* 0:2009. <https://doi.org/10.3389/FMICB.2017.02009>
- Sarkis BE, Cooper DG (1994) Biodegradation of aromatic compounds in a self-cycling fermenter (SCF). *Can J Chem Eng* 72:874–880. <https://doi.org/10.1002/cjce.5450720514>
- Sauvageau D, Cooper DG (2010) Two-stage, self-cycling process for the production of bacteriophages. *Microb Cell Fact* 9:1–10. <https://doi.org/10.1186/1475-2859-9-81>
- Sauvageau D, Storms Z, Cooper DG (2010) Synchronized populations of *Escherichia coli* using simplified self-cycling fermentation. *J Biotechnol* 149:67–73.

<https://doi.org/10.1016/J.JBIOTEC.2010.06.018>

- Schneider CA, Rasband WS, Eliceiri KW (2012) NIH Image to ImageJ: 25 years of image analysis. *Nat Methods* 2012 9:671–675. <https://doi.org/10.1038/nmeth.2089>
- Sheppard JD, Cooper DG (1990) Development of computerized feedback control for the continuous phasing of *Bacillus subtilis*. *Biotechnol Bioeng* 36:539–545. <https://doi.org/10.1002/bit.260360514>
- Sheppard JD, Dawson PSS (1999) Cell synchrony and periodic behaviour in yeast populations. *Can J Chem Eng* 77:893–902. <https://doi.org/10.1002/cjce.5450770515>
- Storms ZJ, Brown T, Sauvageau D, Cooper DG (2012) Self-cycling operation increases productivity of recombinant protein in *Escherichia coli*. *Biotechnol Bioeng* 109:2262–2270. <https://doi.org/10.1002/bit.24492>
- Strong PJ, Laycock B, Mahamud SNS, et al (2016) The Opportunity for High-Performance Biomaterials from Methane. *Microorganisms* 4:11. <https://doi.org/10.3390/MICROORGANISMS4010011>
- Sugden S, Lazic M, Sauvageau D, Stein LY (2021) Transcriptomic and Metabolomic Responses to Carbon and Nitrogen Sources in *Methylobacterium album* BG8. *Appl Environ Microbiol* 87:. <https://doi.org/10.1128/AEM.00385-21>
- Tays C, Guarnieri MT, Sauvageau D, Stein LY (2018) Combined Effects of Carbon and Nitrogen Source to Optimize Growth of Proteobacterial Methanotrophs. *Front Microbiol* 0:2239. <https://doi.org/10.3389/FMICB.2018.02239>
- Torre A, Metivier A, Chu F, et al (2015) Genome-scale metabolic reconstructions and theoretical investigation of methane conversion in *Methylobacterium buryatense* strain 5G(B1). *Microb Cell Fact* 14:188. <https://doi.org/10.1186/s12934-015-0377-3>
- van Walsum GP, Cooper DG (1993) Self-cycling fermentation in a stirred tank reactor. *Biotechnol Bioeng* 42:1175–1180. <https://doi.org/10.1002/bit.260421007>
- Wang J, Chae M, Bressler DC, Sauvageau D (2020) Improved bioethanol productivity through gas flow rate-driven self-cycling fermentation. *Biotechnol Biofuels* 13:1–14. <https://doi.org/10.1186/s13068-020-1658-6>

- Wang J, Chae M, Sauvageau D, Bressler DC (2017) Improving ethanol productivity through self-cycling fermentation of yeast: a proof of concept. *Biotechnol Biofuels* 10:193. <https://doi.org/10.1186/s13068-017-0879-9>
- Wentworth SD, Cooper DG (1996) Self-cycling fermentation of a citric acid producing strain of *Candida lipolytica*. *J Ferment Bioeng* 81:400–405. [https://doi.org/10.1016/0922-338X\(96\)85140-3](https://doi.org/10.1016/0922-338X(96)85140-3)
- Yan X, Chu F, Puri AW, et al (2016) Electroporation-based genetic manipulation in type I methanotrophs. *Appl Environ Microbiol* 82:2062–2069. <https://doi.org/10.1128/AEM.03724-15>
- Zaldívar Carrillo JA, Stein LY, Sauvageau D (2018) Defining Nutrient Combinations for Optimal Growth and Polyhydroxybutyrate Production by *Methylosinus trichosporium* OB3b Using Response Surface Methodology. *Front Microbiol* 0:1513. <https://doi.org/10.3389/FMICB.2018.01513>
- Zha X, Tsapekos P, Zhu X, et al (2021) Bioconversion of wastewater to single cell protein by methanotrophic bacteria. *Bioresour Technol* 320:124351. <https://doi.org/10.1016/J.BIORTECH.2020.124351>
- Zhang T, Zhou J, Wang X, Zhang Y (2017) Coupled effects of methane monooxygenase and nitrogen source on growth and poly- β -hydroxybutyrate (PHB) production of *Methylosinus trichosporium* OB3b. *J Environ Sci* 52:49–57. <https://doi.org/10.1016/J.JES.2016.03.001>
- Zhang W, Song M, Yang Q, et al (2018) Current advance in bioconversion of methanol to chemicals. *Biotechnol Biofuels* 2018 111 11:1–11. <https://doi.org/10.1186/S13068-018-1265-Y>
- Methylotuvimicrobium buryatense* (ID 13071) - Genome - NCBI. https://www.ncbi.nlm.nih.gov/genome/13071?genome_assembly_id=563816. Accessed 29 Jun 2021

7. Summary, Conclusion, and Future Directions

7.1 Summary and conclusion

This thesis explored SCF operation in three microbial systems – the yeast *S. cerevisiae* and the bacteria *E. coli* and *M. buryatense* 5GB1C. The focus was initially placed on an overview of yeast synchronization methods. Then, transcriptomic tools were used to elucidate the regulatory patterns taking place during SCF operation of an engineered, shikimic acid-producing *S. cerevisiae*. In addition, SCF short cycle schemes and their impact on physiological and processing parameters were investigated with cultures of *E. coli* and *S. cerevisiae*; and a thorough analysis of general trends in SCF key events followed. Finally, the methanotrophic bacterium *M. buryatense* 5GB1C was grown on methanol under SCF operation with the implementation of culture reflectance as a new control parameter. In specific, the following conclusions were established.

Chapter 3 summarized methods used to synchronize yeast cells, which includes SCF. Methods based on physical selection, physical induction, chemical blockage, nutrient deprivation, and nutrient cycle were introduced along with a summary of methods used to assess synchrony. SCF (Sheppard and Dawson 1999; Brown 2001) was highlighted in the nutrient cycle category. Considering the advantages and disadvantages of the different synchronization methods, a comparative analysis was then provided based on three factors: (i) perturbations to yeast cells, (ii) scalability, and (iii) requirements for expertise and equipment. Physical selection and nutrient cycling were generally considered superior as methods that introduce minimal perturbations to cells; but in turn, they require relatively sophisticated equipment and expertise. SCF and other nutrient cycling methods can produce larger volumes of synchronized cell populations, if compared to physical selection. Physical induction, chemical blockage, and nutrient deprivation were considered easy to operate, not requiring complicated apparatus, and scalable. These methods, however, tend to cause non-negligible perturbations to regular cell replication, and related artifacts have always been a concern.

In **Chapter 4**, shikimic acid was produced by cultivating an engineered *S. cerevisiae* strain using SCF; and related transcriptomic profiles were studied. Shikimic acid is a primary metabolite in the aromatic amino acid biosynthesis pathway that can be used as a precursor for a variety of

compounds and that is considered a valuable biocompound (Estevez and Estevez 2012; Rawat et al. 2013). SCF operation led to significant improvements in both the productivity and yield of shikimic acid – 4-fold increases as compared to BR (Agustin 2015). The stability of SCF operation was demonstrated through repeatable patterns in CER, optical density, and glucose concentration. The productivity of shikimic acid increased significantly during the first four cycles and nearly plateaued afterward until the end of operation (on a cycle-to-cycle basis). In contrast, the yield of shikimic acid on glucose was improved continuously throughout SCF operation. These indicated an increasing selectivity towards shikimic acid. Transcriptomic analyses, through RNA-Seq and qPCR techniques, were used to uncover transcriptional mechanisms leading to these improvements. Significant up-regulation of most genes associated with the citrate cycle, oxidative phosphorylation, and gluconeogenesis early and late into the SCF cycles suggested greater production of shikimic acid precursors and energy in those stages. Near the onset and end of the SCF cycles, phosphoenolpyruvate and D-erythrose 4-phosphate, the two main precursors for shikimic acid synthesis, were significantly accumulated based on ethanol, pyruvate, and beta-D-fructose 6-phosphate. High gluconeogenesis activity during SCF cycles, inferred by transcriptomic results, was supported by a consistent decrease in ethanol concentration and selectivity observed as cycle number increased. *ARO4_{br}*, a gene inserted to promote shikimic acid production, was overexpressed early in the SCF cycles, facilitating the conversion of the precursors that accumulated at the start and end of the cycles. Moreover, for the first time, synchrony, a characteristic feature of SCF, was verified and characterized through transcriptomic evidence. Most genes related to DNA replication and half the genes related to the yeast cell cycle were significantly up-regulated at the same time early in the SCF cycles; at the same time, all proteasome-related genes were substantially down-regulated. In addition, the expression sequence of selected cyclin genes in SCF cycles was congruent with that in standard yeast cell cycle progression. These findings highlight the features of SCF at the transcriptomic level, enhance our understanding of the corresponding cellular processes, and promote the implementation of this advanced semi-continuous approach in industrial fermentation. Meanwhile, transcriptomic profiles at four sampling points during BR provided a database for global gene expression during late-log phase and diauxic shift.

During SCF operation of *S. cerevisiae* for shikimic acid production, it was noticed that glucose depletion was not congruent with CER maximum – a trend not often seen in previous SCF

studies. A prior work growing *E. coli* under SCF operation also presented a misalignment of glucose depletion and CER maximum (Sauvageau et al. 2010). Thereby, in **Chapter 5**, a short cycle scheme of SCF operation with cycling initiated once CER reached a maximum was used to cultivate *E. coli* and *S. cerevisiae* cells. This was compared with an SCF long cycle strategy that cycled once the decreasing CER reached a plateau. The viability and stability of SCF short cycle operation implied that one round of cell replication was completed by the time a maximum in CER was reached. Taking into account prior evidence of *E. coli* and *S. cerevisiae* cultures – cell number doubled at CER maximum within a narrow time window during SCF long cycles (Sauvageau et al. 2010; Agustin 2015) – it was deduced that, when using the SCF long cycle scheme, the end of synchronized cell replication occurred at the time of CER maximum. However, during *S. cerevisiae* SCF short cycle operation, up-regulation of yeast cyclin genes was found in an inverse sequence and at attenuated intensity compared to observations in SCF long cycle operation (Chapter 4). This indicated the presence of an inter-cycle mode of partially synchronized cell doubling during the yeast SCF short cycle operation. Moreover, the SCF short cycle scheme further increased *E. coli* and *S. cerevisiae* biomass productivity compared to the long cycle operation, though residual glucose remained in the cultures.

Then, in the same Chapter, an overview of a large number of previous SCF studies led to the establishment of three major trends (A, B, and C) during SCF operation regarding (i) characteristic points of control parameters (e.g., CER maximum and DO minimum), (ii) completion of synchronized cell replication, and (iii) depletion or a plateau in the limiting nutrient. In trend A, CER maximum or DO minimum, the completion of synchronized cell replication, and the depletion of the limiting nutrient co-occur at the end of SCF cycles. In trend B, CER maximum or DO minimum and limiting nutrient depletion coincide at the end of SCF cycles, but synchronized cell replication ends in the middle of the cycle. In trend C, the flattening of CER decrease/DO increase and the depletion or plateau of the limiting nutrient co-occur at the end of SCF long cycles, but synchronized cell replication completes in the middle of the long cycles, corresponding to CER maximum or DO minimum. SCF short cycles ends at the time of CER maximum or DO minimum without limiting nutrient depletion; but the partially synchronized cell replication likely starts and ends in the middle of the short cycles (an inter-cycle mode). These diverse trends are expected to result from microbes having significant differences in nutrient use, proliferation strategy, and respiratory intensity. A new description of SCF was hence provided to

incorporate these SCF scenarios. These results and analyses have broadened operational strategies of SCF and significantly enhanced our understanding of this automated semi-continuous process. Also, they offered a more productive SCF scheme, the short cycle scheme, and highlighted the potential of SCF as a research tool in uncovering and comparing microbial physiological properties.

The enhanced understanding of regulatory patterns and trends in characteristic events during SCF helped in establishing SCF operation to a methanotrophic culture and validating the use of a new SCF control parameter. Methanotrophic bacteria can assimilate methane and methanol and convert them to valuable bioproducts, showing important industrial potential (Trotsenko and Murrell 2008). In **Chapter 6**, the growth of an industrially promising methanotroph strain, *M. buryatense* 5GB1C, was explored under SCF and fed-batch operation using methanol as the substrate. Firstly, methanol inhibitory effects were assessed, suggesting that concentrations equal to or below 10 mM methanol could be used as the initial input in BR to avoid significant inhibition. Then, as low levels of CER were observed, it was not considered as an effective monitoring parameter for *M. buryatense* 5GB1C undergoing SCF. Thus, culture reflectance was developed as the control parameter, leading to successful and stable SCF operation. SCF led to significant improvements in volumetric biomass productivity in comparison to BR (a 3-fold or 10-fold increase depending on the SCF scheme implemented). On the other hand, fed-batch operation resulted in a 26-fold increase in biomass density. These results highlight how the implementation of advanced fermentation approaches can help overcome methanol inhibition and enhance biomass production. Also, this work serves as a steppingstone for efficient methanotroph-mediated bioconversion of methanol – a wide range of further exploration can be established based on the results from this work.

Overall, Chapters 3-6 (1) provide a greatly enhanced understanding of SCF with regards to transcriptomic profiles, trends in characteristic events, and induced synchrony; (2) provide solid overviews focusing on yeast cell synchronization methods and on the relations of characteristic events in SCF; (3) demonstrate the applications of SCF during cultivation of one yeast strain and two bacterial strains; (4) establish a new SCF operational strategy – i.e., SCF short cycle scheme – and highlight its potential towards further improvements in productivity; (5) provide an instructive and inclusive redefinition of SCF; and (6) introduce a new monitoring parameter to the toolkits of SCF control parameters. These help researchers and bioprocessing engineers working

in both laboratory and industrial fermentation adopt and adapt SCF; hence contributing to the application of SCF in a broader context.

7.2 Future directions

Future directions, inspired by the findings found in this thesis, could focus on the following aspects. Some of these directions are specific, and others are more general.

- The reflectance signal monitored can be further stabilized (i.e., to achieve greater signaling stability), and its application as an SCF control parameter can be broadened.
- Automated fed-batch fermentation of *M. buryatense* 5GB1C growing on methanol can be established based on in-line monitoring culture reflectance. Different feeding strategies can also be explored.
- Many other methanotrophic bacteria (e.g., *Methylobacterium album* BG8 (Sugden et al. 2021)) can be grown on methanol or the potent greenhouse gas methane using the SCF technique. Biomass, single-cell protein (Banat et al. 1989; Øverland et al. 2010; Ritala et al. 2017; Rasouli et al. 2018; Zha et al. 2021), lipids (Fei et al. 2018), fatty acids (Dong et al. 2017), lactic acid (Garg et al. 2018), and bioplastics (Asenjo and Suk 1986; Kim et al. 1996; Strong et al. 2016; Zhang et al. 2017; Liu et al. 2020) are among the potential products from methanotrophs grown in SCF. Two-stage SCF operation (van Walsum and Cooper 1993; McCaffrey and Cooper 1995; Wentworth and Cooper 1996; Sauvageau and Cooper 2010; Storms et al. 2012) and extended SCF cycle strategy (McCaffrey and Cooper 1995; Wentworth and Cooper 1996; Crosman et al. 2002) can be explored to determine whether productivity and yield can be further improved.
- Other suitable monitoring parameters that fit different SCF scenarios can be implemented. For instance, methanol concentration measured by an in-line methanol probe would be a great control parameter in methanotroph-mediated methanol bioconversion.
- Mutant selection (e.g., through plasma treatment (Cui et al. 2018)) or culture adaptation (McDonald 2019) can be performed to improve methanol tolerance in methanotrophs. Growing on elevated methanol concentration should allow for more efficient methanol

bioconversion.

- A combination of fed-batch and SCF operation to grow microbes to a high OD before implementing SCF can be an ideal mode of operation to overcome substrate toxicity (e.g., methanol toxicity) and achieve exceptional bioproduction.
- Inhibitory effects observed during *E. coli* SCF long cycles can be further investigated. An elimination of growth inhibition could be achieved if the causes were clearly identified. A fed-batch strategy at the beginning of SCF may be helpful and considered.
- Shikimic acid yield and productivity during *S. cerevisiae* SCF short cycles can be determined and compared to those from the long cycle experiments (Agustin 2015). Similar analyses could be performed when SCF short cycle strategy is adopted to produce other valuable bioproducts.
- Cell replication patterns observed during SCF short cycles can be further studied with microbes exhibiting Trend C (see Chapter 5) through accurate cell count, transcriptional evidence, etc. Investigations could focus on whether other microbes present the same cell replication pattern as *S. cerevisiae* and whether there is a consensus pattern regarding the short-cycle cell cycle.
- Characterization of SCF synchronization effects through cell size distribution assessments and more accurate cell number counting methods might be worthwhile. Manual cell counting might bring biases and inconsistencies. Methods that deal with cell clumping issues need to be explored for yeast cultures specifically.
- It is also worthwhile to delve deeper into the fundamental mechanisms that entrain cells to synchrony during SCF. Although an entrainment effect has been proposed to describe the forcing function leading to cell population synchrony in SCF (Sheppard and Dawson 1999), basic interactions between periodic availability of nutrients and cell replication during the entrainment are still unclear. This can also help us understand cases in which synchrony was not observed during SCF (e.g., Chapter 6).
- A more systematic and comprehensive exploration of the trends in the characteristic events during SCF operation, which has been discussed in Chapter 5, can be the focus of further work. These trends are intriguing and inspiring. For instance, Chapter 6 has found that *M.*

buryatense 5GB1C presented Trend A (for more details on the trends, see Chapter 5), while in Chapters 4 and 5, *S. cerevisiae* and *E. coli* followed Trend C (Chapter 5). These results were generated by the same experimenter(s) and using the same experimental setups. However, the trends reflected in SCF characteristic events were very different.

- Further studies could focus on the effects of varying nutrient conditions on trends in the co-occurrence of the key events during SCF operation of the same microorganisms.
- Based on a clear understanding of the trends in SCF characteristic events, SCF can be used as a tool to study physiological properties, such as nutrient usage and respiratory intensity, for microorganisms of interest.
- A combination of synthetic biology and SCF can always be attractive. Metabolically engineered microorganisms grown with SCF can contribute to more efficient bioproduction and bioremediation. Good examples are engineered yeast producing shikimic acid (Agustin 2015) (as well as Chapter 4), engineered *E. coli* producing recombinant proteins (Storms et al. 2012), and TOL plasmid-containing *Pseudomonas putida* degrading toluene and p-xylene (Brown et al. 2000). Based on Chapter 4, metabolic engineering of the *S. cerevisiae* strain could be continued, aiming for greater performance in shikimic acid production.
- A comparison of SCF and continuous stirred tank reactor (CSTR) operations can be investigated, considering that SCF has predominantly been compared to BR. CSTR may offer greater productivity but lower yields, lower nutrient use efficiency, and lower product concentration.
- Microbial models would be involved in investigating overall kinetics in SCF, with which we could analyze intrinsic cellular mechanisms and predict growth and production for microbes undergoing SCF.
- Parameters, schemes, and strategies can be established to implement SCF in industrial settings. Work is required to determine the guiding parameters and principles to set processing conditions enabling efficient scale-up of SCF.

7.3 References

- Agustin RVC (2015) The Impact of Self-Cycling Fermentation on the Production of Shikimic Acid in Populations of Engineered *Saccharomyces cerevisiae*. University of Alberta
- Asenjo JA, Suk JS (1986) Microbial Conversion of Methane into poly- β -hydroxybutyrate (PHB): Growth and intracellular product accumulation in a type II methanotroph. *J Ferment Technol* 64:271–278. [https://doi.org/10.1016/0385-6380\(86\)90118-4](https://doi.org/10.1016/0385-6380(86)90118-4)
- Banat IM, Al-Awadhi N, Hamdan IY (1989) Physiological characteristics of four methylotrophic bacteria and their potential use in single-cell protein production. *MIRCEN J Appl Microbiol Biotechnol* 1989 52 5:149–159. <https://doi.org/10.1007/BF01741838>
- Brown WA (2001) The self-cycling fermentor: development, applications, and future opportunities. In: *Recent research developments in biotechnology and bioengineering*. Research Signpost, pp 61–90
- Brown WA, Cooper DG, Liss SN (2000) Toluene removal in an automated cyclical bioreactor. *Biotechnol Prog* 16:378–384. <https://doi.org/10.1021/bp0000149>
- Crosman JT, Pinchuk RJ, Cooper DG (2002) Enhanced biosurfactant production by *Corynebacterium alkanolyticum* ATCC 21511 using self-cycling fermentation. *J Am Oil Chem Soc* 79:467–472. <https://doi.org/10.1007/s11746-002-0507-5>
- Cui L-Y, Wang S-S, Guan C-G, et al (2018) Breeding of Methanol-Tolerant *Methylobacterium extorquens* AM1 by Atmospheric and Room Temperature Plasma Mutagenesis Combined With Adaptive Laboratory Evolution. *Biotechnol J* 13:1700679. <https://doi.org/10.1002/BIOT.201700679>
- Dong T, Fei Q, Genelot M, et al (2017) A novel integrated biorefinery process for diesel fuel blendstock production using lipids from the methanotroph, *Methylomicrobium buryatense*. *Energy Convers Manag* 140:62–70. <https://doi.org/10.1016/J.ENCONMAN.2017.02.075>
- Estevez AM, Estevez RJ (2012) A short overview on the medicinal chemistry of (—)-shikimic acid. *Mini-Reviews Med Chem* 12:1443–1454. <https://doi.org/10.2174/138955712803832735>
- Fei Q, Puri AW, Smith H, et al (2018) Enhanced biological fixation of methane for microbial

- lipid production by recombinant *Methylobacterium buryatense*. *Biotechnol Biofuels* 11:1–11. <https://doi.org/10.1186/S13068-018-1128-6>
- Garg S, Clomburg JM, Gonzalez R (2018) A modular approach for high-flux lactic acid production from methane in an industrial medium using engineered *Methylobacterium buryatense* 5GB1. *J Ind Microbiol Biotechnol* 45:379–391. <https://doi.org/10.1007/s10295-018-2035-3>
- Kim SW, Kim P, Lee HS, Kim JH (1996) High production of Poly- β -hydroxybutyrate (PHB) from *Methylobacterium organophilum* under potassium limitation. *Biotechnol Lett* 1996 181 18:25–30. <https://doi.org/10.1007/BF00137805>
- Liu L-Y, Xie G-J, Xing D-F, et al (2020) Biological conversion of methane to polyhydroxyalkanoates: Current advances, challenges, and perspectives. *Environ Sci Ecotechnology* 2:100029. <https://doi.org/10.1016/J.ESE.2020.100029>
- McCaffrey WC, Cooper DG (1995) Sophorolipids production by *Candida bombicola* using self-cycling fermentation. *J Ferment Bioeng* 79:146–151. [https://doi.org/10.1016/0922-338X\(95\)94082-3](https://doi.org/10.1016/0922-338X(95)94082-3)
- Øverland M, Tauson A-H, Shearer K, Skrede A (2010) Evaluation of methane-utilising bacteria products as feed ingredients for monogastric animals. *Arch Anim Nutr* 64:171–189. <https://doi.org/10.1080/17450391003691534>
- Rasouli Z, Valverde-Pérez B, D'Este M, et al (2018) Nutrient recovery from industrial wastewater as single cell protein by a co-culture of green microalgae and methanotrophs. *Biochem Eng J* 134:129–135. <https://doi.org/10.1016/J.BEJ.2018.03.010>
- Rawat G, Tripathi P, Saxena RK (2013) Expanding horizons of shikimic acid: Recent progresses in production and its endless frontiers in application and market trends. *Appl Microbiol Biotechnol* 97:4277–4287. <https://doi.org/10.1007/s00253-013-4840-y>
- Ritala A, Häkkinen ST, Toivari M, Wiebe MG (2017) Single Cell Protein—State-of-the-Art, Industrial Landscape and Patents 2001–2016. *Front Microbiol* 0:2009. <https://doi.org/10.3389/FMICB.2017.02009>
- Sauvageau D, Cooper DG (2010) Two-stage, self-cycling process for the production of

- bacteriophages. *Microb Cell Fact* 9:1–10. <https://doi.org/10.1186/1475-2859-9-81>
- Sauvageau D, Storms Z, Cooper DG (2010) Synchronized populations of *Escherichia coli* using simplified self-cycling fermentation. *J Biotechnol* 149:67–73. <https://doi.org/10.1016/J.JBIOTECH.2010.06.018>
- Sheppard JD, Dawson PSS (1999) Cell synchrony and periodic behaviour in yeast populations. *Can J Chem Eng* 77:893–902. <https://doi.org/10.1002/cjce.5450770515>
- Storms ZJ, Brown T, Sauvageau D, Cooper DG (2012) Self-cycling operation increases productivity of recombinant protein in *Escherichia coli*. *Biotechnol Bioeng* 109:2262–2270. <https://doi.org/10.1002/bit.24492>
- Strong PJ, Laycock B, Mahamud SNS, et al (2016) The Opportunity for High-Performance Biomaterials from Methane. *Microorganisms* 4:11. <https://doi.org/10.3390/MICROORGANISMS4010011>
- Sugden S, Lazic M, Sauvageau D, Stein LY (2021) Transcriptomic and Metabolomic Responses to Carbon and Nitrogen Sources in *Methylobacterium album* BG8. *Appl Environ Microbiol* 87:. <https://doi.org/10.1128/AEM.00385-21>
- Trotsenko YA, Murrell JC (2008) Metabolic Aspects of Aerobic Obligate Methanotrophy {star, open}. *Adv Appl Microbiol* 63:183–229. [https://doi.org/10.1016/S0065-2164\(07\)00005-6](https://doi.org/10.1016/S0065-2164(07)00005-6)
- van Walsum GP, Cooper DG (1993) Self-cycling fermentation in a stirred tank reactor. *Biotechnol Bioeng* 42:1175–1180. <https://doi.org/10.1002/bit.260421007>
- Wentworth SD, Cooper DG (1996) Self-cycling fermentation of a citric acid producing strain of *Candida lipolytica*. *J Ferment Bioeng* 81:400–405. [https://doi.org/10.1016/0922-338X\(96\)85140-3](https://doi.org/10.1016/0922-338X(96)85140-3)
- Zha X, Tsapekos P, Zhu X, et al (2021) Bioconversion of wastewater to single cell protein by methanotrophic bacteria. *Bioresour Technol* 320:124351. <https://doi.org/10.1016/J.BIORTECH.2020.124351>
- Zhang T, Zhou J, Wang X, Zhang Y (2017) Coupled effects of methane monooxygenase and nitrogen source on growth and poly- β -hydroxybutyrate (PHB) production of *Methylosinus trichosporium* OB3b. *J Environ Sci* 52:49–57. <https://doi.org/10.1016/J.JES.2016.03.001>

Unified Bibliography

- Abeliovich H (2011) Stationary-phase mitophagy in respiring *Saccharomyces cerevisiae*. *Antioxid Redox Signal* 14:2003–2011. <https://doi.org/10.1089/ars.2010.3807>
- Afgan E, Baker D, Batut B, et al (2018) The Galaxy platform for accessible, reproducible and collaborative biomedical analyses: 2018 update. *Nucleic Acids Res* 46:537–544. <https://doi.org/10.1093/nar/gky379>
- Agustin RVC (2015) The Impact of Self-Cycling Fermentation on the Production of Shikimic Acid in Populations of Engineered *Saccharomyces cerevisiae*. University of Alberta
- Amon A (2002) Synchronization procedures. In: *Methods in Enzymology*. Academic Press Inc., pp 457–467
- Anders S (2010) Babraham Bioinformatics - FastQC A Quality Control tool for High Throughput Sequence Data. <https://www.bioinformatics.babraham.ac.uk/projects/fastqc/>. Accessed 1 Nov 2021
- Anders S, Pyl PT, Huber W (2015) HTSeq--a Python framework to work with high-throughput sequencing data. *Bioinformatics* 31:166–169. <https://doi.org/10.1093/bioinformatics/btu638>
- Angeles Juanes M (2017) Methods of synchronization of yeast cells for the analysis of cell cycle progression. In: *Methods in Molecular Biology*. Humana Press Inc., pp 19–34
- Asenjo JA, Suk JS (1986) Microbial Conversion of Methane into poly- β -hydroxybutyrate (PHB): Growth and intracellular product accumulation in a type II methanotroph. *J Ferment Technol* 64:271–278. [https://doi.org/10.1016/0385-6380\(86\)90118-4](https://doi.org/10.1016/0385-6380(86)90118-4)
- Ashburner M, Ball CA, Blake JA, et al (2000) Gene ontology: Tool for the unification of biology. *Nat Genet* 25:25–29. <https://doi.org/10.1038/75556>
- Askree SH, Yehuda T, Smolikov S, et al (2004) A genome-wide screen for *Saccharomyces cerevisiae* deletion mutants that affect telomere length. *Proc Natl Acad Sci U S A* 101:8658–8663. <https://doi.org/10.1073/pnas.0401263101>
- Banat IM, Al-Awadhi N, Hamdan IY (1989) Physiological characteristics of four methylotrophic bacteria and their potential use in single-cell protein production. *MIRCEN J Appl Microbiol*

- Biotechnol 1989 52 5:149–159. <https://doi.org/10.1007/BF01741838>
- Baneyx F (1999) Recombinant protein expression in *Escherichia coli*. *Curr Opin Biotechnol* 10:411–421. [https://doi.org/10.1016/S0958-1669\(99\)00003-8](https://doi.org/10.1016/S0958-1669(99)00003-8)
- Bates D, Epstein J, Boye E, et al (2005) The *Escherichia coli* baby cell column: a novel cell synchronization method provides new insight into the bacterial cell cycle. *Mol Microbiol* 57:380–391. <https://doi.org/10.1111/j.1365-2958.2005.04693.x>
- Bean JM, Siggia ED, Cross FR (2006) Coherence and timing of cell cycle start examined at single-cell resolution. *Mol Cell* 21:3–14. <https://doi.org/10.1016/j.molcel.2005.10.035>
- Bertani G (1951) Studies on lysogenesis. I. The mode of phage liberation by lysogenic *Escherichia coli*. *J Bacteriol* 62:293–300. <https://doi.org/10.1128/JB.62.3.293-300.1951>
- Blankenberg D, Hillman-Jackson J (2014) Analysis of next-generation sequencing data using galaxy. *Methods Mol Biol* 1150:21–43. https://doi.org/10.1007/978-1-4939-0512-6_2
- Blattner FR, Plunkett G, Bloch CA, et al (1997) The complete genome sequence of *Escherichia coli* K-12. *Science* (80-) 277:1453–1462. <https://doi.org/10.1126/science.277.5331.1453>
- Blumenthal LK, Zahler SA (1962) Index for measurement of synchronization of cell populations. *Science* (80-) 135:724. <https://doi.org/10.1126/science.135.3505.724.a>
- Boiteux S, Jinks-Robertson S (2013) DNA repair mechanisms and the bypass of DNA damage in *Saccharomyces cerevisiae*. *Genetics* 193:1025–1064. <https://doi.org/10.1534/genetics.112.145219>
- Bolger AM, Lohse M, Usadel B (2014) Trimmomatic: A flexible trimmer for Illumina sequence data. *Bioinformatics* 30:2114–2120. <https://doi.org/10.1093/bioinformatics/btu170>
- Bollmann A, French E, Laanbroek HJ (2011) Isolation, cultivation, and characterization of ammonia-oxidizing bacteria and archaea adapted to low ammonium concentrations. In: *Methods in Enzymology*. Academic Press Inc., pp 55–88
- Bonten M, Johnson JR, van den Biggelaar AHJ, et al (2020) Epidemiology of *Escherichia coli* bacteremia: A systematic literature review. *Clin Infect Dis*. <https://doi.org/10.1093/cid/ciaa210>

- Boom R, Sol CJA, Salimans MMM, et al (1990) Rapid and simple method for purification of nucleic acids. *J Clin Microbiol* 28:495–503. <https://doi.org/10.1128/jcm.28.3.495-503.1990>
- Breeden LL (1997) α -Factor synchronization of budding yeast. In: *Methods in Enzymology*. Academic Press Inc., pp 332–342
- Brown WA (2001) The self-cycling fermentor – development, applications, and future opportunities. In: *Recent Research and Developments in Biotechnology and Bioengineering*. pp 4: 61-90
- Brown WA, Cooper DG (1991) Self-cycling fermentation applied to *Acinetobacter calcoaceticus* RAG-1. *Appl Environ Microbiol* 57:2901–2906. <https://doi.org/10.1128/aem.57.10.2901-2906.1991>
- Brown WA, Cooper DG (1992) Hydrocarbon degradation by *Acinetobacter calcoaceticus* RAG-1 using the self-cycling fermentation technique. *Biotechnol Bioeng* 40:797–805. <https://doi.org/10.1002/bit.260400707>
- Brown WA, Cooper DG, Liss SN (1999) Adapting the self-cycling fermentor to anoxic conditions. *Environ Sci Technol* 33:1458–1463. <https://doi.org/10.1021/es980856s>
- Brown WA, Cooper DG, Liss SN (2000) Toluene removal in an automated cyclical bioreactor. *Biotechnol Prog* 16:378–384. <https://doi.org/10.1021/bp0000149>
- Brüssow H (2005) Phage therapy: the *Escherichia coli* experience. *Microbiology* 151:2133–2140. <https://doi.org/10.1099/MIC.0.27849-0>
- Bruttin A, Brüssow H (2005) Human volunteers receiving *Escherichia coli* phage T4 orally: A safety test of phage therapy. *Antimicrob Agents Chemother* 49:2874–2878. <https://doi.org/10.1128/AAC.49.7.2874-2878.2005>
- Bubnov DM, Yuzbashev T V., Vybornaya T V., et al (2018) Development of new versatile plasmid-based systems for λ Red-mediated *Escherichia coli* genome engineering. *J Microbiol Methods* 151:48–56. <https://doi.org/10.1016/J.MIMET.2018.06.001>
- Bustin SA, Benes V, Garson JA, et al (2009) The MIQE guidelines: minimum information for publication of quantitative real-time PCR experiments. *Clin Chem* 55:611–22. <https://doi.org/10.1373/clinchem.2008.112797>

- Bustin SA, Benes V, Nolan T, Pfaffl MW (2005) Quantitative real-time RT-PCR--a perspective. *J Mol Endocrinol* 34:597–601. <https://doi.org/10.1677/jme.1.01755>
- Çalık P, İnankur B, Soyaslan EŞ, et al (2010) Fermentation and oxygen transfer characteristics in recombinant human growth hormone production by *Pichia pastoris* in sorbitol batch and methanol fed-batch operation. *J Chem Technol Biotechnol* 85:226–233. <https://doi.org/10.1002/JCTB.2292>
- Cankorur-Cetinkaya A, Dereli E, Eraslan S, et al (2012) A novel strategy for selection and validation of reference genes in dynamic multidimensional experimental design in yeast. *PLoS One* 7:e38351. <https://doi.org/10.1371/journal.pone.0038351>
- Carmona-Saez P, Chagoyen M, Tirado F, et al (2007) GENECODIS: a web-based tool for finding significant concurrent annotations in gene lists. *Genome Biol* 8:R3. <https://doi.org/10.1186/gb-2007-8-1-r3>
- Çelik E, Çalık P (2012) Production of recombinant proteins by yeast cells. *Biotechnol Adv* 30:1108–1118. <https://doi.org/10.1016/j.biotechadv.2011.09.011>
- Çelik E, Çalık P, Oliver SG (2009) Fed-batch methanol feeding strategy for recombinant protein production by *Pichia pastoris* in the presence of co-substrate sorbitol. *Yeast* 26:473–484. <https://doi.org/10.1002/YEA.1679>
- Chan K-Y, Cheng CY (1977) Synchronization of cell division in marine bacteria by amino acid starvation. *FEMS Microbiol Lett* 2:177–180. <https://doi.org/10.1111/j.1574-6968.1977.tb00934.x>
- Cho RJ, Campbell MJ, Winzeler EA, et al (1998) A genome-wide transcriptional analysis of the mitotic cell cycle. *Mol Cell* 2:65–73. [https://doi.org/10.1016/S1097-2765\(00\)80114-8](https://doi.org/10.1016/S1097-2765(00)80114-8)
- Chomczynski P, Sacchi N (1987) Single-step method of RNA isolation by acid guanidinium thiocyanate-phenol-chloroform extraction. *Anal Biochem* 162:156–159. [https://doi.org/10.1016/0003-2697\(87\)90021-2](https://doi.org/10.1016/0003-2697(87)90021-2)
- Chu D, Barnes DJ (2016) The lag-phase during diauxic growth is a trade-off between fast adaptation and high growth rate. *Sci Rep* 6:1–15. <https://doi.org/10.1038/srep25191>
- Chu Y, Corey DR (2012) RNA sequencing: platform selection, experimental design, and data

- interpretation. *Nucleic Acid Ther* 22:271–4. <https://doi.org/10.1089/nat.2012.0367>
- Clomburg JM, Gonzalez R (2010) Biofuel production in *Escherichia coli*: The role of metabolic engineering and synthetic biology. *Appl Microbiol Biotechnol* 86:419–434. <https://doi.org/10.1007/s00253-010-2446-1>
- Conesa A, Madrigal P, Tarazona S, et al (2016) A survey of best practices for RNA-seq data analysis. *Genome Biol* 17:13. <https://doi.org/10.1186/s13059-016-0881-8>
- Cooper S (2002) Minimally disturbed, multicycle, and reproducible synchrony using a eukaryotic “baby machine.” *BioEssays* 24:499–501. <https://doi.org/10.1002/bies.10108>
- Costa-Silva J, Domingues D, Lopes FM (2017) RNA-Seq differential expression analysis: An extended review and a software tool. *PLoS One* 12:e0190152. <https://doi.org/10.1371/journal.pone.0190152>
- Costello G, Rodgers L, Beach D (1986) Fission yeast enters the stationary phase G0 state from either mitotic G1 or G2. *Curr Genet* 11:119–125. <https://doi.org/10.1007/BF00378203>
- Crabtree HG (1929) Observations on the carbohydrate metabolism of tumours. *Biochem J* 23:536–545. <https://doi.org/10.1042/bj0230536>
- Creanor J, Mitchison JM (1979) Reduction of perturbations in leucine incorporation in synchronous cultures of *Schizosaccharomyces pombe* made by elutriation. *J Gen Microbiol* 112:385–388. <https://doi.org/10.1099/00221287-112-2-385>
- Crosman JT, Pinchuk RJ, Cooper DG (2002) Enhanced biosurfactant production by *Corynebacterium alkanolyticum* ATCC 21511 using self-cycling fermentation. *J Am Oil Chem Soc* 79:467–472. <https://doi.org/10.1007/s11746-002-0507-5>
- Cui L-Y, Wang S-S, Guan C-G, et al (2018) Breeding of Methanol-Tolerant *Methylobacterium extorquens* AM1 by Atmospheric and Room Temperature Plasma Mutagenesis Combined With Adaptive Laboratory Evolution. *Biotechnol J* 13:1700679. <https://doi.org/10.1002/BIOT.201700679>
- Cunningham F, Achuthan P, Akanni W, et al (2019) Ensembl 2019. *Nucleic Acids Res* 47:D745–D751. <https://doi.org/10.1093/nar/gky1113>
- Currie A, Honish L, Cutler J, et al (2019) Outbreak of *Escherichia coli* O157:H7 Infections

- Linked to Mechanically Tenderized Beef and the Largest Beef Recall in Canada, 2012. *J Food Prot* 82:1532–1538. <https://doi.org/10.4315/0362-028X.JFP-19-005>
- Dalena F, Senatore A, Marino A, et al (2018) Methanol Production and Applications: An Overview. *Methanol Sci Eng* 3–28. <https://doi.org/10.1016/B978-0-444-63903-5.00001-7>
- Danø S, Danø S, Hynne F, et al (2001) Synchronization of glycolytic oscillations in a yeast cell population. *Faraday Discuss* 120:261–276. <https://doi.org/10.1039/b103238k>
- Davison SA, den Haan R, van Zyl WH (2016) Heterologous expression of cellulase genes in natural *Saccharomyces cerevisiae* strains. *Appl Microbiol Biotechnol* 100:8241–8254. <https://doi.org/10.1007/s00253-016-7735-x>
- Dawson PSS (1985) Growth, cell cultivation, cell metabolism, and the cell cycle of *Candida utilis* as explored by continuous phased culture. *Can J Microbiol* 31:183–189. <https://doi.org/10.1139/m85-036>
- Dawson PSS (1965) Continuous phased growth, with a modified chemostat. *Can J Microbiol* 11:893–903. <https://doi.org/10.1139/m65-119>
- Dawson PSS (1972) Continuously synchronised growth. *J Appl Chem Biotechnol* 22:79–103. <https://doi.org/10.1002/jctb.2720220112>
- Dawson PSS (1970) Cell cycle and post cycle changes during continuous phased growth of *Candida utilis*. *Can J Microbiol* 16:783–795. <https://doi.org/10.1139/m70-132>
- Dell KA, Frost JW (1993) Identification and Removal of Impediments to Biocatalytic Synthesis of Aromatics from D-Glucose: Rate-Limiting Enzymes in the Common Pathway of Aromatic Amino Acid Biosynthesis. *J Am Chem Soc* 115:11581–11589. <https://doi.org/10.1021/ja00077a065>
- Demidenko A, Akberdin IR, Allemann M, et al (2017) Fatty Acid Biosynthesis Pathways in *Methylomicrobium buryatense* 5G(B1). *Front Microbiol* 0:2167. <https://doi.org/10.3389/FMICB.2016.02167>
- DeRisi JL, Iyer VR, Brown PO (1997) Exploring the metabolic and genetic control of gene expression on a genomic scale. *Science* (80-) 278:680–686. <https://doi.org/10.1126/science.278.5338.680>

- Di Talia S, Skotheim JM, Bean JM, et al (2007) The effects of molecular noise and size control on variability in the budding yeast cell cycle. *Nature* 448:947–951.
<https://doi.org/10.1038/nature06072>
- Didenko V V (2001) DNA probes using fluorescence resonance energy transfer (fret): Designs and applications. *Biotechniques* 31:1106–1121. <https://doi.org/10.2144/01315rv02>
- Dobin A, Davis CA, Schlesinger F, et al (2013) STAR: ultrafast universal RNA-seq aligner. *Bioinformatics* 29:15–21. <https://doi.org/10.1093/bioinformatics/bts635>
- Dong T, Fei Q, Genelot M, et al (2017) A novel integrated biorefinery process for diesel fuel blendstock production using lipids from the methanotroph, *Methylomicrobium buryatense*. *Energy Convers Manag* 140:62–70. <https://doi.org/10.1016/J.ENCONMAN.2017.02.075>
- Eijkman JF (1885) Sur les principes constituants de l'Illicium religiosum (Sieb.) (Shikimi-no-ki en japonais). *Recl des Trav Chim des Pays-Bas* 4:32–54.
<https://doi.org/10.1002/recl.18850040202>
- Enrich LB, Scheuermann ML, Mohadjer A, et al (2008) *Liquidambar styraciflua*: a renewable source of shikimic acid. *Tetrahedron Lett* 49:2503–2505.
<https://doi.org/10.1016/j.tetlet.2008.02.140>
- Escherich T, Bettelheim KS (1888) The intestinal bacteria of the neonate and breast-fed infant. *Rev Infect Dis* 10:1220–1225. <https://doi.org/10.2307/4454681>
- Eshinimaev BT, Khmelenina VN, Sakharovskii VG, et al (2002) Physiological, Biochemical, and Cytological Characteristics of a Haloalkalitolerant Methanotroph Grown on Methanol. *Microbiol* 2002 715 71:512–518. <https://doi.org/10.1023/A:1020594300166>
- Estevez AM, Estevez RJ (2012) A short overview on the medicinal chemistry of (—)-shikimic acid. *Mini-Reviews Med Chem* 12:1443–1454.
<https://doi.org/10.2174/138955712803832735>
- Fairman JW, Noinaj N, Buchanan SK (2011) The structural biology of β -barrel membrane proteins: a summary of recent reports. *Curr Opin Struct Biol* 21:523–531.
<https://doi.org/10.1016/J.SBI.2011.05.005>
- Fei Q, Puri AW, Smith H, et al (2018) Enhanced biological fixation of methane for microbial

- lipid production by recombinant *Methylobacterium buryatense*. *Biotechnol Biofuels* 11:1–11. <https://doi.org/10.1186/S13068-018-1128-6>
- Feldmann H (2012) *Yeast: Molecular and Cell Biology*. Wiley-Blackwell
- Ferullo DJ, Cooper DL, Moore HR, Lovett ST (2009) Cell cycle synchronization of *Escherichia coli* using the stringent response, with fluorescence labeling assays for DNA content and replication. *Methods* 48:8–13. <https://doi.org/10.1016/j.ymeth.2009.02.010>
- Fitch I, Dahmann C, Surana U, et al (1992) Characterization of four B-type cyclin genes of the budding yeast *Saccharomyces cerevisiae*. *Mol Biol Cell* 3:805–818. <https://doi.org/10.1091/mbc.3.7.805>
- Foltman M, Molist I, Sanchez-Diaz A (2016) Synchronization of the budding yeast: *Saccharomyces cerevisiae*. In: *Methods in Molecular Biology*. Humana Press Inc., pp 279–291
- Forsburg SL (1999) The best yeast? *Trends Genet* 15:340–344. [https://doi.org/10.1016/S0168-9525\(99\)01798-9](https://doi.org/10.1016/S0168-9525(99)01798-9)
- Forsburg SL (2005) The yeasts *Saccharomyces cerevisiae* and *Schizosaccharomyces pombe*: models for cell biology research. *Gravitational Sp Biol* 18(2):3–10
- Forsburg SL, Nurse P (1991) Cell cycle regulation in the yeasts *Saccharomyces cerevisiae* and *Schizosaccharomyces pombe*. *Annu Rev Cell Biol* 7:227–256. <https://doi.org/10.1146/annurev.cb.07.110191.001303>
- Foury F (1997) Human genetic diseases: A cross-talk between man and yeast. *Gene* 195:1–10. [https://doi.org/10.1016/S0378-1119\(97\)00140-6](https://doi.org/10.1016/S0378-1119(97)00140-6)
- Fritsch M, Starruß J, Loesche A, et al (2005) Cell cycle synchronization of *Cupriavidus necator* by continuous phasing measured via flow cytometry. *Biotechnol Bioeng* 92:635–642. <https://doi.org/10.1002/bit.20647>
- Fu Y, He L, Reeve J, et al (2019) Core metabolism shifts during growth on methanol versus methane in the methanotroph *Methylobacterium buryatense* 5GB1. *MBio* 10:. <https://doi.org/10.1128/mBio.00406-19>
- Fu Y, Li Y, Lidstrom M (2017) The oxidative TCA cycle operates during methanotrophic

- growth of the Type I methanotroph *Methylomicrobium buryatense* 5GB1. *Metab Eng* 42:43–51. <https://doi.org/10.1016/j.ymben.2017.05.003>
- Futcher B (1999) Cell cycle synchronization. *Methods Cell Sci* 21:79–86. <https://doi.org/10.1023/A:1009872403440>
- Futcher B (1996) Cyclins and the wiring of the yeast cell cycle. *Yeast* 12:1635–1646. [https://doi.org/10.1002/\(SICI\)1097-0061\(199612\)12:16<1635::AID-YEA83>3.0.CO;2-O](https://doi.org/10.1002/(SICI)1097-0061(199612)12:16<1635::AID-YEA83>3.0.CO;2-O)
- Gao M, Cao M, Suástegui M, et al (2017) Innovating a nonconventional yeast platform for producing shikimate as the building block of high-value aromatics. *ACS Synth Biol* 6:29–38. <https://doi.org/10.1021/acssynbio.6b00132>
- Garg S, Clomburg JM, Gonzalez R (2018a) A modular approach for high-flux lactic acid production from methane in an industrial medium using engineered *Methylomicrobium buryatense* 5GB1. *J Ind Microbiol Biotechnol* 45:379–391. <https://doi.org/10.1007/s10295-018-2035-3>
- Garg S, Wu H, Clomburg JM, Bennett GN (2018b) Bioconversion of methane to C-4 carboxylic acids using carbon flux through acetyl-CoA in engineered *Methylomicrobium buryatense* 5GB1C. *Metab Eng* 48:175–183. <https://doi.org/10.1016/j.ymben.2018.06.001>
- Ghosh S, Chisti Y, Banerjee UC (2012) Production of shikimic acid. *Biotechnol Adv* 30:1425–1431. <https://doi.org/10.1016/j.biotechadv.2012.03.001>
- Gilman A, Laurens LM, Puri AW, et al (2015) Bioreactor performance parameters for an industrially-promising methanotroph *Methylomicrobium buryatense* 5GB1. *Microb Cell Fact* 14:182. <https://doi.org/10.1186/s12934-015-0372-8>
- Girard PM, Boiteux S (1997) Repair of oxidized DNA bases in the yeast *Saccharomyces cerevisiae*. *Biochimie* 79:559–566. [https://doi.org/10.1016/S0300-9084\(97\)82004-4](https://doi.org/10.1016/S0300-9084(97)82004-4)
- Goecks J, Nekrutenko A, Taylor J, Galaxy Team T (2010) Galaxy: a comprehensive approach for supporting accessible, reproducible, and transparent computational research in the life sciences. *Genome Biol* 11:R86. <https://doi.org/10.1186/gb-2010-11-8-r86>
- Goffeau A, Barrell G, Bussey H, et al (1996) Life with 6000 genes. *Science* (80-) 274:546–567. <https://doi.org/10.1126/science.274.5287.546>

- Gómez EB, Forsburg SL (2004) Analysis of the fission yeast *Schizosaccharomyces pombe* cell cycle. In: Methods in Molecular Biology. Humana Press, New Jersey, pp 93–111
- Guo J, Suástegui M, Sakimoto KK, et al (2018) Light-driven fine chemical production in yeast biohybrids. Science (80-) 362:813–816. <https://doi.org/10.1126/science.aat9777>
- Gushima H, Miya T, Murata K, Kimura A (1983) Construction of glutathione-producing strains of *Escherichia coli* B by recombinant DNA techniques. J Appl Biochem 5:43–52
- Hagman A, Säll T, Compagno C, Piskur J (2013) Yeast “make-accumulate-consume” life strategy evolved as a multi-step process that predates the whole genome duplication. PLoS One 8:e68734. <https://doi.org/10.1371/journal.pone.0068734>
- Hartmann M, Schneider TR, Pfeil A, et al (2003) Evolution of feedback-inhibited β/α barrel isoenzymes by gene duplication and a single mutation. Proc Natl Acad Sci U S A 100:862–867. <https://doi.org/10.1073/pnas.0337566100>
- Hartwell LH, Culotti J, Pringle JR, Reid BJ (1974) Genetic control of the cell division cycle in yeast. Science (80-). 183:46–51
- Hartwell LH, Unger MW (1977) Unequal division in *Saccharomyces cerevisiae* and its implications for the control of cell division. J Cell Biol 75:422–435. <https://doi.org/10.1083/JCB.75.2.422>
- He L, Fu Y, Lidstrom ME (2019) Quantifying Methane and Methanol Metabolism of “*Methylovimicrobium buryatense*” 5GB1C under Substrate Limitation. mSystems 4:. <https://doi.org/10.1128/msystems.00748-19>
- He L, Groom JD, Lidstrom ME (2020) The Entner-Doudoroff Pathway Is an Essential Metabolic Route for *Methylovimicrobium Buryatense* 5GB1C. Appl Environ Microbiol 87:1–11. <https://doi.org/10.1128/AEM.02481-20>
- Heid CA, Stevens J, Livak KJ, Williams PM (1996) Real time quantitative PCR. Genome Res 6:986–994. <https://doi.org/10.1101/GR.6.10.986>
- Heitmann M, Zannini E, Arendt E (2018) Impact of *Saccharomyces cerevisiae* metabolites produced during fermentation on bread quality parameters: A review. Crit Rev Food Sci Nutr 58:1152–1164. <https://doi.org/10.1080/10408398.2016.1244153>

- Henard CA, Smith H, Dowe N, et al (2016) Bioconversion of methane to lactate by an obligate methanotrophic bacterium. *Sci Rep* 6:1–9. <https://doi.org/10.1038/srep21585>
- Henard CA, Smith HK, Guarnieri MT (2017) Phosphoketolase overexpression increases biomass and lipid yield from methane in an obligate methanotrophic biocatalyst. *Metab Eng* 41:152–158. <https://doi.org/10.1016/J.YMBEN.2017.03.007>
- Hennecke H, Günther I, Binder F (1982) A novel cloning vector for the direct selection of recombinant DNA in *E. coli*. *Gene* 19:231–234. [https://doi.org/10.1016/0378-1119\(82\)90011-7](https://doi.org/10.1016/0378-1119(82)90011-7)
- Herskowitz I (1988) Life cycle of the budding yeast *Saccharomyces cerevisiae*. *Microbiol Rev* 52:536–553. <https://doi.org/10.1128/membr.52.4.536-553.1988>
- Hiraoka Y, Toda T, Yanagida M (1984) The NDA3 gene of fission yeast encodes β -tubulin: A cold-sensitive *nda3* mutation reversibly blocks spindle formation and chromosome movement in mitosis. *Cell* 39:349–358. [https://doi.org/10.1016/0092-8674\(84\)90013-8](https://doi.org/10.1016/0092-8674(84)90013-8)
- Hirsch I, Vondrejs V (1971) Division of *Escherichia coli* 15 TAU cells synchronized by arginine and uracil starvation. *Folia Microbiol (Praha)* 16:137–141. <https://doi.org/10.1007/BF02887484>
- Hoebeke J, Van Nijen G, De Brabander M (1976) Interaction of oncodazole (R 17934), a new anti-tumoral drug, with rat brain tubulin. *Biochem Biophys Res Commun* 69:319–324. [https://doi.org/10.1016/0006-291X\(76\)90524-6](https://doi.org/10.1016/0006-291X(76)90524-6)
- Hossain N, Zaini JH, Mahlia TMI (2017) A review of bioethanol production from plant-based waste biomass by yeast fermentation. *Int J Technol* 8:5–18. <https://doi.org/10.14716/ijtech.v8i1.3948>
- Huang W-P, Klionsky DJ (2002) Autophagy in yeast: A review of the molecular machinery. *Cell Struct Funct* 27:409–420. <https://doi.org/10.1247/csf.27.409>
- Hudault S, Guignot J, Servin AL (2001) *Escherichia coli* strains colonising the gastrointestinal tract protect germfree mice against *Salmonella typhimurium* infection. *Gut* 49:47–55. <https://doi.org/10.1136/gut.49.1.47>
- Huffer S, Roche CM, Blanch HW, Clark DS (2012) *Escherichia coli* for biofuel production:

- bridging the gap from promise to practice. *Trends Biotechnol* 30:538–545.
<https://doi.org/10.1016/J.TIBTECH.2012.07.002>
- Hughes SM, Cooper DG (1996) Biodegradation of phenol using the self-cycling fermentation (SCF) process. *Biotechnol Bioeng* 51:112–119. [https://doi.org/10.1002/\(SICI\)1097-0290\(19960705\)51:1<112::AID-BIT13>3.0.CO;2-S](https://doi.org/10.1002/(SICI)1097-0290(19960705)51:1<112::AID-BIT13>3.0.CO;2-S)
- Hur JY, Park MC, Suh KY, Park SH (2011) Synchronization of cell cycle of *Saccharomyces cerevisiae* by using a cell chip platform. *Mol Cells* 32:483–488.
<https://doi.org/10.1007/s10059-011-0174-8>
- Ihssen J, Kowarik M, Dilettoso S, et al (2010) Production of glycoprotein vaccines in *Escherichia coli*. *Microb Cell Factories* 2010 9:1–13. <https://doi.org/10.1186/1475-2859-9-61>
- Ishii T (2014) Transcriptome Analysis of Adrenocortical Cells in Health and Disease. In: *Cellular Endocrinology in Health and Disease*. Elsevier, pp 169–192
- Jacobs CW, Adams AE, Szanislo PJ, Pringle JR (1988) Functions of microtubules in the *Saccharomyces cerevisiae* cell cycle. *J Cell Biol* 107:1409–1426.
<https://doi.org/10.1083/jcb.107.4.1409>
- Johnston GC, Pringle JR, Hartwell LH (1977) Coordination of growth with cell division in the yeast *Saccharomyces cerevisiae*. *Exp Cell Res* 105:79–98. [https://doi.org/10.1016/0014-4827\(77\)90154-9](https://doi.org/10.1016/0014-4827(77)90154-9)
- Johnston LH, Johnson AL (1997) Elutriation of budding yeast. In: *Methods in Enzymology*. Academic Press Inc., pp 342–350
- Ju Q, Warner JR (1994) Ribosome synthesis during the growth cycle of *Saccharomyces cerevisiae*. *Yeast* 10:151–157. <https://doi.org/10.1002/yea.320100203>
- Kaluzhnaya M, Khmelenina V, Eshinimaev B, et al (2001) Taxonomic characterization of new alkaliphilic and alkalitolerant methanotrophs from soda lakes of the Southeastern Transbaikal region and description of *Methylomicrobium buryatense* sp.nov. *Syst Appl Microbiol* 24:166–176. <https://doi.org/10.1078/0723-2020-00028>
- Kanehisa M, Goto S (2000) KEGG: Kyoto Encyclopedia of Genes and Genomes. *Nucleic Acids*

Res 28:27–30. <https://doi.org/10.1093/nar/28.1.27>

Kasarjian JKA, Iida M, Ryu J (2003) New restriction enzymes discovered from *Escherichia coli* clinical strains using a plasmid transformation method. *Nucleic Acids Res* 31:e22–e22.

<https://doi.org/10.1093/NAR/GNG022>

Khmelenina VN, Colin Murrell J, Smith TJ, Trotsenko YA (2018) Physiology and Biochemistry of the Aerobic Methanotrophs. In: *Aerobic Utilization of Hydrocarbons, Oils and Lipids*. Springer International Publishing, pp 1–25

Kim D, Langmead B, Salzberg SL (2015) HISAT: A fast spliced aligner with low memory requirements. *Nat Methods* 12:357–360. <https://doi.org/10.1038/nmeth.3317>

Kim D, Pertea G, Trapnell C, et al (2013) TopHat2: Accurate alignment of transcriptomes in the presence of insertions, deletions and gene fusions. *Genome Biol* 14:R36.

<https://doi.org/10.1186/gb-2013-14-4-r36>

Kim SW, Kim P, Lee HS, Kim JH (1996) High production of Poly- β -hydroxybutyrate (PHB) from *Methylobacterium organophilum* under potassium limitation. *Biotechnol Lett* 1996 181 18:25–30. <https://doi.org/10.1007/BF00137805>

Knop DR, Draths KM, Chandran SS, et al (2001) Hydroaromatic equilibration during biosynthesis of shikimic acid. *J Am Chem Soc* 123:10173–10182.

<https://doi.org/10.1021/ja0109444>

Knutsen J, Rein ID, Rothe C, et al (2011) Cell-cycle analysis of fission yeast cells by flow cytometry. *PLoS One* 6:17175. <https://doi.org/10.1371/journal.pone.0017175>

Koç A, Wheeler LJ, Mathews CK, Merrill GF (2004) Hydroxyurea Arrests DNA Replication by a Mechanism that Preserves Basal dNTP Pools. *J Biol Chem* 279:223–230.

<https://doi.org/10.1074/jbc.M303952200>

Korf IHE, Meier-Kolthoff JP, Adriaenssens EM, et al (2019) Still Something to Discover: Novel Insights into *Escherichia coli* Phage Diversity and Taxonomy. *Viruses* 2019, Vol 11, Page 454 11:454. <https://doi.org/10.3390/V11050454>

Kramhøft B, Zeuthen E (1975) Chapter 18 synchronization of the fission yeast

Schizosaccharomyces pombe using heat shocks. In: *Methods in Cell Biology*. Academic

Press, pp 373–380

Krueger F (2017) Babraham Bioinformatics - Trim Galore! In: Version 0.4.4.

https://www.bioinformatics.babraham.ac.uk/projects/trim_galore/. Accessed 1 Nov 2021

Lagunas R (1981) Is *Saccharomyces cerevisiae* a typical facultative anaerobe? Trends Biochem Sci 6:201–203. [https://doi.org/10.1016/0968-0004\(81\)90073-6](https://doi.org/10.1016/0968-0004(81)90073-6)

Langmead B, Salzberg SL (2012) Fast gapped-read alignment with Bowtie 2. Nat Methods 9:357–359. <https://doi.org/10.1038/nmeth.1923>

Lautenberger JA, Linn S (1972) The deoxyribonucleic acid modification and restriction enzymes of *Escherichia coli* B. I. Purification, subunit structure, and catalytic properties of the modification methylase. J Biol Chem 247:6176–6182. [https://doi.org/10.1016/S0021-9258\(19\)44779-0](https://doi.org/10.1016/S0021-9258(19)44779-0)

Levy S, Barkai N (2009) Coordination of gene expression with growth rate: A feedback or a feed-forward strategy? FEBS Lett 583:3974–3978. <https://doi.org/10.1016/j.febslet.2009.10.071>

Liao Y, Smyth GK, Shi W (2014) featureCounts: an efficient general purpose program for assigning sequence reads to genomic features. Bioinformatics 30:923–930. <https://doi.org/10.1093/bioinformatics/btt656>

Lim H, Shin H (2013) Fed-batch cultures: principles and applications of semi-batch bioreactors. Cambridge University Press

Lindstedt BA, Finton MD, Porcellato D, Brandal LT (2018) High frequency of hybrid *Escherichia coli* strains with combined Intestinal Pathogenic *Escherichia coli* (IPEC) and Extraintestinal Pathogenic *Escherichia coli* (ExPEC) virulence factors isolated from human faecal samples. BMC Infect Dis 18:. <https://doi.org/10.1186/s12879-018-3449-2>

Liu DF, Ai GM, Zheng QX, et al (2014) Metabolic flux responses to genetic modification for shikimic acid production by *Bacillus subtilis* strains. Microb Cell Fact 13:1–11. <https://doi.org/10.1186/1475-2859-13-40>

Liu L, Wang J, Rosenberg D, et al (2019) Response to comments on archaeological reconstruction of 13,000-y old Natufian beer making at Raqefet Cave, Israel. J Archaeol Sci

- Reports 28:101914. <https://doi.org/10.1016/J.JASREP.2019.101914>
- Liu L-Y, Xie G-J, Xing D-F, et al (2020) Biological conversion of methane to polyhydroxyalkanoates: Current advances, challenges, and perspectives. *Environ Sci Ecotechnology* 2:100029. <https://doi.org/10.1016/J.ESE.2020.100029>
- Liu S (2017) Batch Reactor. In: *Bioprocess Engineering*. Elsevier, pp 139–178
- Liu T, Khosla C (2010) Genetic engineering of *Escherichia coli* for biofuel production. *Annu. Rev. Genet.* 44:53–69
- Liu Y-P, Zheng P, Sun Z-H, et al (2008) Strategies of pH control and glucose-fed batch fermentation for production of succinic acid by *Actinobacillus succinogenes* CGMCC1593. *J Chem Technol Biotechnol* 83:722–729. <https://doi.org/10.1002/JCTB.1862>
- Livak KJ, Schmittgen TD (2001) Analysis of relative gene expression data using real-time quantitative PCR and the $2^{-\Delta\Delta CT}$ method. *Methods* 25:402–408. <https://doi.org/10.1006/METH.2001.1262>
- Lord PG, Wheals AE (1981) Variability in individual cell cycles of *Saccharomyces cerevisiae*. *J Cell Sci* 50:361–376. <https://doi.org/10.1242/JCS.50.1.361>
- Love MI, Huber W, Anders S (2014) Moderated estimation of fold change and dispersion for RNA-seq data with DESeq2. *Genome Biol* 15:550. <https://doi.org/10.1186/s13059-014-0550-8>
- Luche DD, Forsburg SL (2009) Cell-cycle synchrony for analysis of *S. pombe* DNA replication. *Methods Mol Biol* 521:437–448. https://doi.org/10.1007/978-1-60327-815-7_24
- Manukyan A, Abraham L, Dugrawala H, Schneider BL (2011) Synchronization of yeast. In: *Methods in Molecular Biology*. Humana Press, pp 173–200
- Marchessault P, Sheppard JD (1997) Application of self-cycling fermentation technique to the production of poly- β -hydroxybutyrate. *Biotechnol Bioeng* 55:815–820. [https://doi.org/10.1002/\(SICI\)1097-0290\(19970905\)55:5<815::AID-BIT12>3.0.CO;2-A](https://doi.org/10.1002/(SICI)1097-0290(19970905)55:5<815::AID-BIT12>3.0.CO;2-A)
- Marcus S, Caldwell GA, Miller D, et al (1991) Significance of C-terminal cysteine modifications to the biological activity of the *Saccharomyces cerevisiae* a-factor mating pheromone. *Mol Cell Biol* 11:3603–3612. <https://doi.org/10.1128/mcb.11.7.3603>

- Markham KA, Alper HS (2015) Synthetic Biology for Specialty Chemicals. *Annu Rev Chem Biomol Eng* 6:35–52. <https://doi.org/10.1146/annurev-chembioeng-061114-123303>
- Martínez JA, Bolívar F, Escalante A (2015) Shikimic acid production in *Escherichia coli*: From classical metabolic engineering strategies to omics applied to improve its production. *Front Bioeng Biotechnol* 3:145. <https://doi.org/10.3389/fbioe.2015.00145>
- Mazodier P, Petter R, Thompson C (1989) Intergeneric conjugation between *Escherichia coli* and *Streptomyces* species. *J Bacteriol* 171:3583–3585. <https://doi.org/10.1128/JB.171.6.3583-3585.1989>
- McCaffrey WC, Cooper DG (1995) Sophorolipids production by *Candida bombicola* using self-cycling fermentation. *J Ferment Bioeng* 79:146–151. [https://doi.org/10.1016/0922-338X\(95\)94082-3](https://doi.org/10.1016/0922-338X(95)94082-3)
- McClellan K, Perry CM (2001) Oseltamivir: A review of its use in influenza. *Drugs* 61:263–283. <https://doi.org/10.2165/00003495-200161020-00011>
- McDonald K (2019) Adaptation of *Methylobacterium album* BG8 to growth at low pH. University of Alberta
- Metsalu T, Vilo J (2015) ClustVis: A web tool for visualizing clustering of multivariate data using Principal Component Analysis and heatmap. *Nucleic Acids Res* 43:W566–W570. <https://doi.org/10.1093/nar/gkv468>
- Miller C, Schwalb B, Maier K, et al (2011) Dynamic transcriptome analysis measures rates of mRNA synthesis and decay in yeast. *Mol Syst Biol* 7:458. <https://doi.org/10.1038/msb.2010.112>
- Miller GL (1959) Use of dinitrosalicylic acid reagent for determination of reducing sugar. *Anal Chem* 31:426–428. <https://doi.org/10.1021/ac60147a030>
- Miller SA, Dykes DD, Polesky HF (1988) A simple salting out procedure for extracting DNA from human nucleated cells. *Nucleic Acids Res* 16:1215. <https://doi.org/10.1093/nar/16.3.1215>
- Mitchison JM, Vincent WS (1965) Preparation of synchronous cell cultures by sedimentation. *Nature* 205:987–989. <https://doi.org/10.1038/205987a0>

- Mohd Azhar SH, Abdulla R, Jambo SA, et al (2017) Yeasts in sustainable bioethanol production: A review. *Biochem Biophys Reports* 10:52–61. <https://doi.org/10.1016/j.bbrep.2017.03.003>
- Mookerjee S (2016) Directing Precursor Flux to Optimize cis,cis-Muconic Acid Production in *Saccharomyces cerevisiae*. Concordia University
- Müller J, Dawson PS (1968) The operational flexibility of the phased culture technique, as observed by changes in the cell cycle of *Candida utilis*. *Can J Microbiol* 14:1115–1126. <https://doi.org/10.1139/m68-187>
- Müller M, Lu K, Reichert AS (2015) Mitophagy and mitochondrial dynamics in *Saccharomyces cerevisiae*. *Biochim Biophys Acta - Mol Cell Res* 1853:2766–2774. <https://doi.org/10.1016/j.bbamcr.2015.02.024>
- Münch T, Sonnleitner B, Fiechter A (1992) New insights into the synchronization mechanism with forced synchronous cultures of *Saccharomyces cerevisiae*. *J Biotechnol* 24:299–314. [https://doi.org/10.1016/0168-1656\(92\)90039-C](https://doi.org/10.1016/0168-1656(92)90039-C)
- Murphy JP, Stepanova E, Everley RA, et al (2015) Comprehensive temporal protein dynamics during the diauxic shift in *Saccharomyces cerevisiae*. *Mol Cell Proteomics* 14:2454–2465. <https://doi.org/10.1074/mcp.M114.045849>
- Mustea I, Muresian T (1967) Crabtree effect in some bacterial cultures. *Cancer* 20:1499–1501. [https://doi.org/10.1002/1097-0142\(196709\)20:9<1499::AID-CNCR2820200917>3.0.CO;2-Q](https://doi.org/10.1002/1097-0142(196709)20:9<1499::AID-CNCR2820200917>3.0.CO;2-Q)
- Oliva A, Rosebrock A, Ferrezuelo F, et al (2005) The cell cycle-regulated genes of *Schizosaccharomyces pombe*. *PLOS Biol* 3:1239–1260. <https://doi.org/10.1371/journal.pbio.0030225>
- Orata FD, Meier-Kolthoff JP, Sauvageau D, Stein LY (2018) Phylogenomic analysis of the gammaproteobacterial methanotrophs (order methylococcales) calls for the reclassification of members at the genus and species levels. *Front Microbiol* 9:3162. <https://doi.org/10.3389/fmicb.2018.03162>
- Otterstedt K, Larsson C, Bill RM, et al (2004) Switching the mode of metabolism in the yeast *Saccharomyces cerevisiae*. *EMBO Rep* 5:532–537.

<https://doi.org/10.1038/sj.embor.7400132>

Øverland M, Tauson A-H, Shearer K, Skrede A (2010) Evaluation of methane-utilising bacteria products as feed ingredients for monogastric animals. *Arch Anim Nutr* 64:171–189.

<https://doi.org/10.1080/17450391003691534>

Pelechano V, Pérez-Ortín JE (2010) There is a steady-state transcriptome in exponentially growing yeast cells. *Yeast* 27:413–422. <https://doi.org/10.1002/yea.1768>

Pertea M, Kim D, Pertea GM, et al (2016) Transcript-level expression analysis of RNA-seq experiments with HISAT, StringTie and Ballgown. *Nat Protoc* 11:1650–1667.

<https://doi.org/10.1038/nprot.2016.095>

Phornphisutthimas S, Thamchaipenet A, Panijpan B (2007) Conjugation in *Escherichia coli*. *Biochem Mol Biol Educ* 35:440–445. <https://doi.org/10.1002/BMB.113>

Pinchuk RJ, Brown WA, Hughes SM, Cooper DG (2000) Modeling of biological processes using self-cycling fermentation and genetic algorithms. *Biotechnol Bioeng* 67:19–24.

[https://doi.org/10.1002/\(SICI\)1097-0290\(20000105\)67:1<19::AID-BIT3>3.0.CO;2-C](https://doi.org/10.1002/(SICI)1097-0290(20000105)67:1<19::AID-BIT3>3.0.CO;2-C)

Ponchel F, Toomes C, Bransfield K, et al (2003) Real-time PCR based on SYBR-Green I fluorescence: An alternative to the TaqMan assay for a relative quantification of gene rearrangements, gene amplifications and micro gene deletions. *BMC Biotechnol* 3:18.

<https://doi.org/10.1186/1472-6750-3-18>

Poolman JT (2016) *Escherichia coli*. In: International Encyclopedia of Public Health. Elsevier Inc., pp 585–593

Poolman JT, Wacker M (2016) Extraintestinal pathogenic *Escherichia coli*, a common human pathogen: challenges for vaccine development and progress in the field. *J Infect Dis* 213:6–

13. <https://doi.org/10.1093/infdis/jiv429>

Porro D, Gasser B, Fossati T, et al (2011) Production of recombinant proteins and metabolites in yeasts. *Appl Microbiol Biotechnol* 89:939–948. <https://doi.org/10.1007/s00253-010-3019-z>

Postma E, Verduyn C, Scheffers WA, Van Dijken JP (1989) Enzymic analysis of the crabtree effect in glucose-limited chemostat cultures of *Saccharomyces cerevisiae*. *Appl Environ Microbiol* 55:468–477. <https://doi.org/10.1128/aem.55.2.468-477.1989>

- Pringle JR, Adams AEM, Drubin DG, Haarer BK (1991) Immunofluorescence methods for yeast. In: *Methods in Enzymology*. pp 565–602
- Puri AW, Owen S, Chu F, et al (2015) Genetic tools for the industrially promising methanotroph *Methylomicrobium buryatense*. *Appl Environ Microbiol* 81:1775–1781.
<https://doi.org/10.1128/AEM.03795-14>
- Radonjic M, Andrau JC, Lijnzaad P, et al (2005) Genome-wide analyses reveal RNA polymerase II located upstream of genes poised for rapid response upon *S. cerevisiae* stationary phase exit. *Mol Cell* 18:171–183. <https://doi.org/10.1016/j.molcel.2005.03.010>
- Rasouli Z, Valverde-Pérez B, D’Este M, et al (2018) Nutrient recovery from industrial wastewater as single cell protein by a co-culture of green microalgae and methanotrophs. *Biochem Eng J* 134:129–135. <https://doi.org/10.1016/J.BEJ.2018.03.010>
- Rawat G, Tripathi P, Jahan F, Saxena RK (2013a) A natural isolate producing shikimic acid: isolation, identification, and culture condition optimization. *Appl Microbiol Biotechnol* 169:2290–2302. <https://doi.org/10.1007/s12010-013-0150-1>
- Rawat G, Tripathi P, Saxena RK (2013b) Expanding horizons of shikimic acid: Recent progresses in production and its endless frontiers in application and market trends. *Appl Microbiol Biotechnol* 97:4277–4287. <https://doi.org/10.1007/s00253-013-4840-y>
- Richardson HE, Wittenberg C, Cross F, Reed SI (1989) An essential G1 function for cyclin-like proteins in yeast. *Cell* 59:1127–1133. [https://doi.org/10.1016/0092-8674\(89\)90768-X](https://doi.org/10.1016/0092-8674(89)90768-X)
- Ritala A, Häkkinen ST, Toivari M, Wiebe MG (2017) Single Cell Protein—State-of-the-Art, Industrial Landscape and Patents 2001–2016. *Front Microbiol* 0:2009.
<https://doi.org/10.3389/FMICB.2017.02009>
- Roberts RJ (1990) Restriction enzymes and their isoschizomers. *Nucleic Acids Res* 18:2331.
<https://doi.org/10.1093/NAR/18.SUPPL.2331>
- Robinson MD, McCarthy DJ, Smyth GK (2010) edgeR: a Bioconductor package for differential expression analysis of digital gene expression data. *Bioinformatics* 26:139–140.
<https://doi.org/10.1093/bioinformatics/btp616>
- Rosebrock AP (2017a) Methods for synchronization and analysis of the budding yeast cell cycle.

- Cold Spring Harb Protoc 2017:5–7. <https://doi.org/10.1101/pdb.top080630>
- Rosebrock AP (2017b) Synchronization of budding yeast by centrifugal elutriation. Cold Spring Harb Protoc 2017:53–62. <https://doi.org/10.1101/pdb.prot088732>
- Sarkis BE, Cooper DG (1994) Biodegradation of aromatic compounds in a self-cycling fermenter (SCF). Can J Chem Eng 72:874–880. <https://doi.org/10.1002/cjce.5450720514>
- Sauvageau D, Cooper DG (2010) Two-stage, self-cycling process for the production of bacteriophages. Microb Cell Fact 9:1–10. <https://doi.org/10.1186/1475-2859-9-81>
- Sauvageau D, Storms Z, Cooper DG (2010) Synchronized populations of *Escherichia coli* using simplified self-cycling fermentation. J Biotechnol 149:67–73. <https://doi.org/10.1016/J.JBIOTECH.2010.06.018>
- Schneider BL, Zhang J, Markwardt J, et al (2004) Growth rate and cell size modulate the synthesis of, and requirement for, G1-phase cyclins at Start. Mol Cell Biol 24:10802–10813. <https://doi.org/10.1128/MCB.24.24.10802-10813.2004>
- Schneider CA, Rasband WS, Eliceiri KW (2012) NIH Image to ImageJ: 25 years of image analysis. Nat Methods 2012 9:671–675. <https://doi.org/10.1038/nmeth.2089>
- Syednasrollah F, Laiho A, Elo LL (2015) Comparison of software packages for detecting differential expression in RNA-seq studies. Brief Bioinform 16:59–70. <https://doi.org/10.1093/bib/bbt086>
- Sheppard JD (1993) Improved volume control for self-cycling fermentations. Can J Chem Eng 71:426–430. <https://doi.org/10.1002/cjce.5450710312>
- Sheppard JD, Cooper DG (1990) Development of computerized feedback control for the continuous phasing of *Bacillus subtilis*. Biotechnol Bioeng 36:539–545. <https://doi.org/10.1002/bit.260360514>
- Sheppard JD, Cooper DG (1991) The response of *Bacillus subtilis* ATCC 21332 to manganese during continuous-phased growth. Appl Microbiol Biotechnol 35:72–76. <https://doi.org/10.1007/BF00180639>
- Sheppard JD, Dawson PSS (1999) Cell synchrony and periodic behaviour in yeast populations. Can J Chem Eng 77:893–902. <https://doi.org/10.1002/cjce.5450770515>

- Smith J, Manukyan A, Hua H, et al (2016) Synchronization of yeast. In: *Methods in Molecular Biology*. Humana Press Inc., pp 215–242
- Spellman PT, Sherlock G, Zhang MQ, et al (1998) Comprehensive identification of cell cycle-regulated genes of the yeast *Saccharomyces cerevisiae* by microarray hybridization. *Mol Biol Cell* 9:3273–3297. <https://doi.org/10.1091/mbc.9.12.3273>
- Stabb E V., Ruby EG (2002) RP4-based plasmids for conjugation between *Escherichia coli* and members of the Vibrionaceae. *Methods Enzymol* 358:413–426. [https://doi.org/10.1016/S0076-6879\(02\)58106-4](https://doi.org/10.1016/S0076-6879(02)58106-4)
- Stone KA, Hilliard M V., He QP, Wang J (2017) A mini review on bioreactor configurations and gas transfer enhancements for biochemical methane conversion. *Biochem Eng J* 128:83–92. <https://doi.org/10.1016/j.bej.2017.09.003>
- Storms ZJ, Brown T, Cooper DG, et al (2014) Impact of the cell life-cycle on bacteriophage T4 infection. *FEMS Microbiol Lett* 353:63–68. <https://doi.org/10.1111/1574-6968.12402>
- Storms ZJ, Brown T, Sauvageau D, Cooper DG (2012) Self-cycling operation increases productivity of recombinant protein in *Escherichia coli*. *Biotechnol Bioeng* 109:2262–2270. <https://doi.org/10.1002/bit.24492>
- Strogatz SH (1997) Spontaneous synchronization in nature. In: *IEEE International Frequency Control Symposium*. pp 2–4
- Strong PJ, Laycock B, Mahamud SNS, et al (2016) The Opportunity for High-Performance Biomaterials from Methane. *Microorganisms* 4:11. <https://doi.org/10.3390/MICROORGANISMS4010011>
- Suástegui M, Guo W, Feng X, Shao Z (2016) Investigating strain dependency in the production of aromatic compounds in *Saccharomyces cerevisiae*. *Biotechnol Bioeng* 113:2676–2685. <https://doi.org/10.1002/bit.26037>
- Suástegui M, Shao Z (2016) Yeast factories for the production of aromatic compounds: from building blocks to plant secondary metabolites. *J Ind Microbiol Biotechnol* 43:1611–1624. <https://doi.org/10.1007/s10295-016-1824-9>
- Suástegui M, Yu Ng C, Chowdhury A, et al (2017) Multilevel engineering of the upstream

- module of aromatic amino acid biosynthesis in *Saccharomyces cerevisiae* for high production of polymer and drug precursors. *Metab Eng* 42:134–144.
<https://doi.org/10.1016/j.ymben.2017.06.008>
- Sugden S, Lazic M, Sauvageau D, Stein LY (2021) Transcriptomic and Metabolomic Responses to Carbon and Nitrogen Sources in *Methylomicrobium album* BG8. *Appl Environ Microbiol* 87:. <https://doi.org/10.1128/AEM.00385-21>
- Sui R (2008) Separation of shikimic acid from pine needles. *Chem Eng Technol* 31:469–473.
<https://doi.org/10.1002/ceat.200700413>
- Suzuki K, Ohsumi Y (2007) Molecular machinery of autophagosome formation in yeast, *Saccharomyces cerevisiae*. *FEBS Lett* 581:2156–2161.
[https://doi.org/10.1016/J.FEBSLET.2007.01.096@10.1002/\(ISSN\)1873-3468.NOBELPRIZEAUTOPHAGY](https://doi.org/10.1016/J.FEBSLET.2007.01.096@10.1002/(ISSN)1873-3468.NOBELPRIZEAUTOPHAGY)
- Tan Y, Agustin RVC, Stein LY, Sauvageau D (2021) Transcriptomic analysis of synchrony and productivity in self-cycling fermentation of engineered yeast producing shikimic acid. *Biotechnol Reports* 32:e00691. <https://doi.org/10.1016/j.btre.2021.e00691>
- Tays C, Guarnieri MT, Sauvageau D, Stein LY (2018) Combined Effects of Carbon and Nitrogen Source to Optimize Growth of Proteobacterial Methanotrophs. *Front Microbiol* 0:2239. <https://doi.org/10.3389/FMICB.2018.02239>
- Tenaillon O, Skurnik D, Picard B, Denamur E (2010) The population genetics of commensal *Escherichia coli*. *Nat Rev Microbiol* 8:207–217. <https://doi.org/10.1038/nrmicro2298>
- Teng S-C, Zakian VA (1999) Telomere-telomere recombination is an efficient bypass pathway for telomere maintenance in *Saccharomyces cerevisiae*. *Mol Cell Biol* 19:8083–8093.
<https://doi.org/10.1128/mcb.19.12.8083>
- Teste MA, Duquenne M, François JM, Parrou JL (2009) Validation of reference genes for quantitative expression analysis by real-time RT-PCR in *Saccharomyces cerevisiae*. *BMC Mol Biol* 10:1–15. <https://doi.org/10.1186/1471-2199-10-99>
- ThermoFisher Scientific (2019) Basic Principles of RT-qPCR | Thermo Fisher Scientific.
<https://www.thermofisher.com/ca/en/home/brands/thermo-scientific/molecular->

biology/molecular-biology-learning-center/molecular-biology-resource-library/spotlight-articles/basic-principles-rt-qpcr.html. Accessed 22 Jul 2021

- Thornton M, Eward KL, Helmstetter CE (2002) Production of minimally disturbed synchronous cultures of hematopoietic cells. *Biotechniques* 32:1098–1105.
<https://doi.org/10.2144/02325rr05>
- Tian Y, Luo C, Lu Y, et al (2012) Cell cycle synchronization by nutrient modulation. *Integr Biol (Camb)* 4:328–334. <https://doi.org/10.1039/c2ib00083k>
- Tian Y, Luo C, Ouyang Q (2013) A microfluidic synchronizer for fission yeast cells. *Lab Chip* 13:4071–4077. <https://doi.org/10.1039/c3lc50639h>
- Toda T, Umesono K, Hirata A, Yanagida M (1983) Cold-sensitive nuclear division arrest mutants of the fission yeast *Schizosaccharomyces pombe*. *J Mol Biol* 168:251–270.
[https://doi.org/10.1016/S0022-2836\(83\)80017-5](https://doi.org/10.1016/S0022-2836(83)80017-5)
- Tormos-Pérez M, Pérez-Hidalgo L, Moreno S (2016) Fission yeast cell cycle synchronization methods. In: *Methods in Molecular Biology*. Humana Press Inc., pp 293–308
- Torre A, Metivier A, Chu F, et al (2015) Genome-scale metabolic reconstructions and theoretical investigation of methane conversion in *Methylomicrobium buryatense* strain 5G(B1). *Microb Cell Fact* 14:188. <https://doi.org/10.1186/s12934-015-0377-3>
- Trapnell C, Pachter L, Salzberg SL (2009) TopHat: discovering splice junctions with RNA-Seq. *Bioinformatics* 25:1105–1111. <https://doi.org/10.1093/bioinformatics/btp120>
- Trapnell C, Roberts A, Goff L, et al (2012) Differential gene and transcript expression analysis of RNA-seq experiments with TopHat and Cufflinks. *Nat Protoc* 7:562–578.
<https://doi.org/10.1038/nprot.2012.016>
- Trapnell C, Williams BA, Pertea G, et al (2010) Transcript assembly and quantification by RNA-Seq reveals unannotated transcripts and isoform switching during cell differentiation. *Nat Biotechnol* 28:511–515. <https://doi.org/10.1038/nbt.1621>
- Trieu-Cuot P, Carlier C, Martin P, Courvalin P (1987) Plasmid transfer by conjugation from *Escherichia coli* to Gram-positive bacteria. *FEMS Microbiol Lett* 48:289–294.
<https://doi.org/10.1111/J.1574-6968.1987.TB02558.X>

- Tripathi P, Rawat G, Yadav S, Saxena RK (2013) Fermentative production of shikimic acid: A paradigm shift of production concept from plant route to microbial route. *Bioprocess Biosyst Eng* 36:1665–1673. <https://doi.org/10.1007/s00449-013-0940-4>
- Trotsenko YA, Murrell JC (2008) Metabolic Aspects of Aerobic Obligate Methanotrophy {star, open}. *Adv Appl Microbiol* 63:183–229. [https://doi.org/10.1016/S0065-2164\(07\)00005-6](https://doi.org/10.1016/S0065-2164(07)00005-6)
- Untergasser A, Cutcutache I, Koressaar T, et al (2012) Primer3-new capabilities and interfaces. *Nucleic Acids Res* 40:1–12. <https://doi.org/10.1093/nar/gks596>
- van Walsum GP, Cooper DG (1993) Self-cycling fermentation in a stirred tank reactor. *Biotechnol Bioeng* 42:1175–1180. <https://doi.org/10.1002/bit.260421007>
- Verma S, Kuila A (2019) Bioremediation of heavy metals by microbial process. *Environ Technol Innov* 14:100369. <https://doi.org/10.1016/J.ETI.2019.100369>
- Vidal L, Pinsach J, Striedner G, et al (2008) Development of an antibiotic-free plasmid selection system based on glycine auxotrophy for recombinant protein overproduction in *Escherichia coli*. *J Biotechnol* 134:127–136. <https://doi.org/10.1016/J.JBIOTEC.2008.01.011>
- Vogel C, Marcotte EM (2012) Insights into the regulation of protein abundance from proteomic and transcriptomic analyses. *Nat Rev Genet* 13:227–232. <https://doi.org/10.1038/nrg3185>
- Vogt RL, Dippold L (2005) *Escherichia coli* O157:H7 outbreak associated with consumption of ground beef, June–July 2002. *Public Health Rep* 120:174–178. <https://doi.org/10.1177/003335490512000211>
- Wacker M, Wang L, Kowarik M, et al (2014) Prevention of *Staphylococcus aureus* Infections by Glycoprotein Vaccines Synthesized in *Escherichia coli*. *J Infect Dis* 209:1551–1561. <https://doi.org/10.1093/INFDIS/JIT800>
- Walker GM (1999) Synchronization of yeast cell populations. *Methods Cell Sci* 21:87–93. <https://doi.org/10.1023/A:1009824520278>
- Walker GM, Duffus JH (1980) Magnesium ions and the control of the cell cycle in yeast. *J Cell Sci VOL*.42:329–356. <https://doi.org/10.1242/jcs.42.1.329>
- Wang J, Chae M, Beyene D, et al (2021) Co-production of ethanol and cellulose nanocrystals through self-cycling fermentation of wood pulp hydrolysate. *Bioresour Technol*

330:124969. <https://doi.org/https://doi.org/10.1016/j.biortech.2021.124969>

Wang J, Chae M, Bressler DC, Sauvageau D (2020) Improved bioethanol productivity through gas flow rate-driven self-cycling fermentation. *Biotechnol Biofuels* 13:1–14.

<https://doi.org/10.1186/s13068-020-1658-6>

Wang J, Chae M, Sauvageau D, Bressler DC (2017) Improving ethanol productivity through self-cycling fermentation of yeast: a proof of concept. *Biotechnol Biofuels* 10:193.

<https://doi.org/10.1186/s13068-017-0879-9>

Wang W, Jiang F, Wu F, et al (2019) Biodetection and bioremediation of copper ions in environmental water samples using a temperature-controlled, dual-functional *Escherichia coli* cell. *Appl Microbiol Biotechnol* 2019 10316 103:6797–6807.

<https://doi.org/10.1007/S00253-019-09984-9>

Wang Z, Gerstein M, Snyder M (2009) RNA-Seq: a revolutionary tool for transcriptomics. *Nat Rev Genet* 10:57–63. <https://doi.org/10.1038/nrg2484>

Wellinger RJ, Zakian VA (2012) Everything you ever wanted to know about *Saccharomyces cerevisiae* telomeres: Beginning to end. *Genetics* 191:1073–1105.

<https://doi.org/10.1534/genetics.111.137851>

Wentworth SD, Cooper DG (1996) Self-cycling fermentation of a citric acid producing strain of *Candida lipolytica*. *J Ferment Bioeng* 81:400–405. [https://doi.org/10.1016/0922-338X\(96\)85140-3](https://doi.org/10.1016/0922-338X(96)85140-3)

Wincure BM, Cooper DG, Rey A (1995) Mathematical model of self-cycling fermentation. *Biotechnol Bioeng* 46:180–183. <https://doi.org/10.1002/bit.260460212>

Yan N (2015) Structural Biology of the Major Facilitator Superfamily Transporters. *Annu Rev Biophys* 44:257–283. <https://doi.org/10.1146/annurev-biophys-060414-033901>

Yan X, Chu F, Puri AW, et al (2016) Electroporation-based genetic manipulation in type I methanotrophs. *Appl Environ Microbiol* 82:2062–2069.

<https://doi.org/10.1128/AEM.03724-15>

Yang J, Dungrawala H, Hua H, et al (2011) Cell size and growth rate are major determinants of replicative lifespan. *Cell Cycle* 10:144–155. <https://doi.org/10.4161/cc.10.1.14455>

- Yu L, Guo N, Yang Y, et al (2010) Microarray analysis of p-anisaldehyde-induced transcriptome of *Saccharomyces cerevisiae*. *J Ind Microbiol Biotechnol* 37:313–322.
<https://doi.org/10.1007/S10295-009-0676-Y>
- Zaldívar Carrillo JA, Stein LY, Sauvageau D (2018) Defining Nutrient Combinations for Optimal Growth and Polyhydroxybutyrate Production by *Methylosinus trichosporium* OB3b Using Response Surface Methodology. *Front Microbiol* 0:1513.
<https://doi.org/10.3389/FMICB.2018.01513>
- Zalewska-Piątek B, Piątek R (2020) Phage Therapy as a Novel Strategy in the Treatment of Urinary Tract Infections Caused by *E. Coli*. *Antibiot* 2020, Vol 9, Page 304 9:304.
<https://doi.org/10.3390/ANTIBIOTICS9060304>
- Zenaitis MG, Cooper DG (1994) Antibiotic production by *Streptomyces aureofaciens* using self-cycling fermentation. *Biotechnol Bioeng* 44:1331–1336.
<https://doi.org/10.1002/bit.260441109>
- Zha X, Tsapekos P, Zhu X, et al (2021) Bioconversion of wastewater to single cell protein by methanotrophic bacteria. *Bioresour Technol* 320:124351.
<https://doi.org/10.1016/J.BIORTECH.2020.124351>
- Zhang B, Liu ZQ, Liu C, Zheng YG (2016) Application of CRISPRi in *Corynebacterium glutamicum* for shikimic acid production. *Biotechnol Lett* 38:2153–2161.
<https://doi.org/10.1007/s10529-016-2207-z>
- Zhang T, Zhou J, Wang X, Zhang Y (2017) Coupled effects of methane monooxygenase and nitrogen source on growth and poly- β -hydroxybutyrate (PHB) production of *Methylosinus trichosporium* OB3b. *J Environ Sci* 52:49–57. <https://doi.org/10.1016/J.JES.2016.03.001>
- Zhang W, Song M, Yang Q, et al (2018) Current advance in bioconversion of methanol to chemicals. *Biotechnol Biofuels* 2018 11:1–11. <https://doi.org/10.1186/S13068-018-1265-Y>
- Zhu X, Zou S, Li Y, Liang Y (2017) Transcriptomic analysis of *Saccharomyces cerevisiae* upon honokiol treatment. *Res Microbiol* 168:626–635.
<https://doi.org/10.1016/J.RESMIC.2017.04.007>

(2021) Global Bioproduct Market Size, Share & Growth Analysis Report. In: Jan.

<https://www.bccresearch.com/market-research/energy-and-resources/biorefinery-products-markets-report.html>. Accessed 31 Oct 2021

Methylovimicrobium buryatense (ID 13071) - Genome - NCBI.

https://www.ncbi.nlm.nih.gov/genome/13071?genome_assembly_id=563816. Accessed 29 Jun 2021

Appendix A. Supplementary Materials for Chapter 4

A.1 Continued Discussion

With regard to the pathways discussed in Figures 4.4-4.8, differential expression was not as pronounced between BR sampling points (BR₁₋₄, across late-log phase and diauxic shift) as between SCF sampling points; likely due to the fact that synchrony obtained by the SCF cycle could magnify differential expression levels through the entire population and gluconeogenesis activity was enhanced for the SCF cycle. However, the change in expression levels between BR sampling points did reflect the influence of different stages during late-log phase and diauxic shift. Growth-related pathways – taking the ribosome, ribosome biogenesis, and RNA polymerase as examples – were down-regulated during late-log phase and diauxic shift (Figures A12, A13, and A14). Pathways associated with proteolysis were up-regulated at the end of log phase (ubiquitin-mediated proteolysis in Figure A15). Gluconeogenesis-related pathways, including gluconeogenesis, the citrate cycle, and oxidative phosphorylation (except for ATPase-related genes), presented greater transcript abundance during the diauxic shift (upper cluster in Figure A16; Figure A17; and lower cluster in Figure A18). These findings agree with previous studies (DeRisi et al. 1997; Radonjic et al. 2005; Murphy et al. 2015) which used microarray-based transcriptomics and proteomics. Although this part of the analyses was not a focus in the current study, this concordance strongly increased the confidence in the transcriptomic analyses conducted. Moreover, greater expression levels of many genes related to RNA polymerase (Figure A19), ribosome (Figure A6), ribosome biogenesis (Figure A7), glycolysis (lower cluster in Figure A8), pentose phosphate pathway (upper cluster in Figure A20), and aromatic amino acids biosynthesis (Figure A21) observed at the earliest BR sampling point (BR₁) implied greater activity in biomass synthesis, even compared to SCF sampling points. The reduced availability of nutrients (e.g. glucose, Figure 4.2E) and the stress from a more acidic environment in SCF cycles may have been the causes of

the lower expression for those growth-associated genes in the SCF cycle. The synchronized cell replication could have also played a role in this.

As for oxidative phosphorylation, ATPase-related genes displayed an inverse trend in expression compared to the other genes involved, and this during both BR (upper cluster in Figure A18) and SCF cycle 23 (upper cluster in Figure 4.8). When cell rapidly grew in the BR log phase and when the synchronized cell population replicated during the SCF cycle, more resources were allocated to ATP hydrolysis in order to efficiently utilize the energy molecules for rapid biomass accumulation. Moreover, it is interesting to observe greater ATP synthesis from the citrate cycle and oxidative phosphorylation during the BR diauxic shift (Figure A17 and lower cluster in Figure A18) and late stages of SCF cycle 23 (Figure 4.7 and lower cluster in Figure 4.8), when glycolysis activity was attenuated (lower clusters in Figures A16 and A8). These trends during the BR diauxic shift have also been shown in previous microarray-based transcriptomics and proteomics data (DeRisi et al. 1997; Murphy et al. 2015). Ethanol production and, later, consumption seem to be the cause of misalignment of glycolysis and the citrate cycle. As can be seen in Figure A9, during extended BR, almost half the glucose was first converted to ethanol even in aerobic conditions; and following glucose depletion, ethanol started to be consumed (“make-accumulate-consume” life strategy (Hagman et al. 2013)). Most likely, during the BR log phase, the significant ethanol production led to a relatively lower amount of carbon being assimilated into the citrate cycle. In contrast, during diauxic shift, previously accumulated ethanol started to be metabolized and the activation of gluconeogenesis channeled more carbon into the citrate cycle. Oxidative phosphorylation (except for ATPase-related genes) was up-regulated concomitantly, converting other energy molecules into ATP. Similarly, in SCF operation, glucose was depleted near the end of the cycle (Figure A3) when the diauxic shift took place. Genes related to glycolysis were up-regulated in the middle of the SCF cycle (lower cluster in Figure A8), while transcripts related to gluconeogenesis, the citrate cycle, and oxidative phosphorylation (except for ATPase-related genes) significantly accumulated mostly during the late stages and at the start of the cycle (upper cluster

in Figure A8; Figure 4.7; and lower cluster in Figure 4.8) when mitochondrial ribosomal proteins were also greatly expressed (upper cluster in Figure A6).

Many previous SCF studies (Sheppard and Cooper 1991; Brown and Cooper 1991, 1992; Sheppard 1993; van Walsum and Cooper 1993; Sarkis and Cooper 1994; Zenaitis and Cooper 1994; McCaffrey and Cooper 1995; Wentworth and Cooper 1996; Brown et al. 1999) posited the equivalence of cycle time and doubling time of the microbes investigated when SCF cycling was triggered upon the depletion of a limiting nutrient. In this work, as well as in recent *E. coli* SCF studies (Sauvageau et al. 2010; Storms et al. 2012), a sharp increase in cell concentration (that is, synchronized cell segregation) was observed near the midpoint of SCF cycles, even if SCF cycling corresponded to the depletion of the main carbon source. This discrepancy, likely derived from the intrinsic differences in the implemented microorganisms and the diversity of the corresponding environments, will be explored further in upcoming work.

qPCR experiments have shown that SCF cycle 2 (the cycle immediately following BR) presented similar trends in regulation of the selected cyclin genes as seen in cycle 21 (data not shown). This suggests the synchronization process was most likely initiated directly after BR. The partially synchronized population in cycle 2 resulted in much higher shikimic acid yield, productivity, and specific productivity compared to the asynchronous population in BR (Figures 4.3A and 4.3B). As the cycle number increased, the extent of synchrony was enhanced and so were the yield, productivity, and specific productivity (Figures 4.3A and 4.3B). This implied positive correlation between synchrony and shikimic acid production could be further investigated.

As SCF operation proceeded beyond 25 cycles, a slight decrease in shikimic acid concentration was observed, likely due to slight attenuation in plasmid retention. Nevertheless, a greater shikimic acid concentration was observed for cycle 37 compared to cycle 11 (data not shown).

Table A1 Sampling time points in BR and SCF cycle 23 for RNA-Seq analyses.

Sampling point	Time [min]	OD ₆₀₀
BR ₁	666	0.75
BR ₂	872	2.04
BR ₃	993	2.78
BR ₄	1200	3.62
SCF ₁	0.3	2.37
SCF ₂	46	2.37
SCF ₃	116	2.59
SCF ₄	204	3.02
SCF ₅	280	3.28
SCF ₆	595	3.99

Table A2 Sampling time points in SCF cycle 21 for qPCR experiments.

Sampling point for Figure A1B	Normalized Cycle Time	Sampling point for Figure A1C	Normalized Cycle Time
1	0.003	1	0.001
2	0.052	2	0.059
3	0.098	3	0.121
4	0.157	4	0.189
5	0.214	5	0.256
6	0.259	6	0.325
7	0.314	7	0.405
8	0.362	8	0.480
9	0.414	9	0.555
10	0.469	10	0.630
11	0.526	11	0.705
12	0.578	12	0.780
13	0.631	13	0.855
14	0.679	14	0.931
15	0.731	15	1.000
16	0.791		
17	0.857		
18	0.914		
19	1.000		

Table A3 Information about the plasmid used by the engineered yeast strain in this study

Origin Vector	Auxotrophy	Description	Reference
pYES2	<i>URA3</i>	<i>TEF1_p – ARO4 K229L – PGI_{ter}; PGK_p – E. coli ARO_B – ADH1_{ter}; and TDH3_p – E. coli AROD – ADH2_{ter}</i>	(Mookerjee 2016)

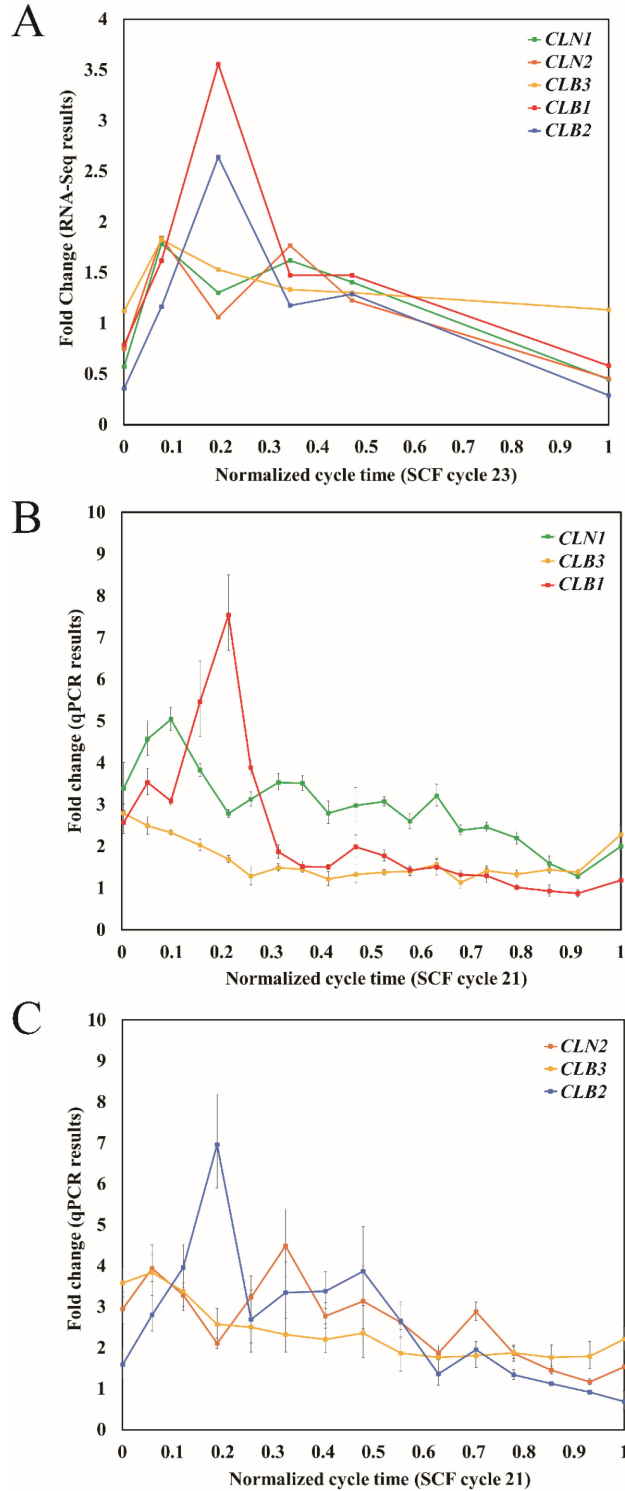


Figure A1 Relative expression levels (fold changes) of selected cyclin genes during SCF cycles 21 and 23. A) The relative expression levels (fold change, with statistical significance) of *CLN1*, *CLN2*, *CLB3*, *CLB1*, and *CLB2* within cycle 23, assessed from RNA-Seq results using BR3 as the reference sampling point. B) The relative expression levels of *CLN1*, *CLB3*, and *CLB1* during SCF

cycle 21 based on qPCR results using *ACT1* as the reference gene and a BR₃ sample as the reference sample. C) The relative expression levels of *CLN2*, *CLB3*, and *CLB2* during cycle 21 based on qPCR results using *ACT1* and *ALG9* as the reference genes and a BR₃ sample as the reference sample. Relative expression levels are reported as a function of normalized cycle time (in-cycle time over total cycle time) so that a complete cycle has a normalized time of 1. Error bars in B) and C) show one standard deviation (n = 3).

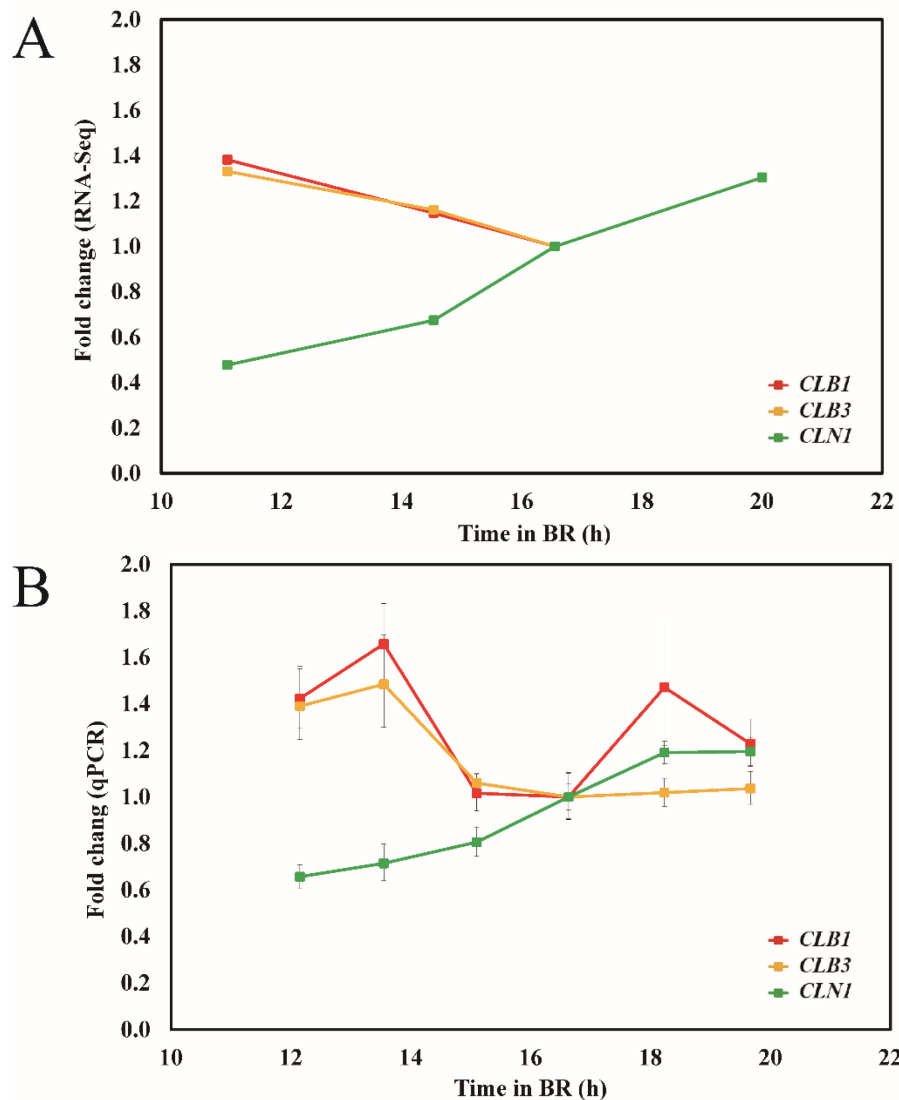


Figure A2 Relative expression levels (fold changes) for *CLB1*, *CLB3*, and *CLN1* during BR late-log phase and diauxic shift. A) RNA-Seq results using BR₃ as the reference sampling point. The expression levels for *CLB1* and *CLB3* at the last sampling point BR₄ are not shown due to lack of statistical significance. B) qPCR results using *ACT1* and *ALG9* as the reference genes and a BR₃ sample as the reference sample. Error bars show one standard deviation (n = 3).

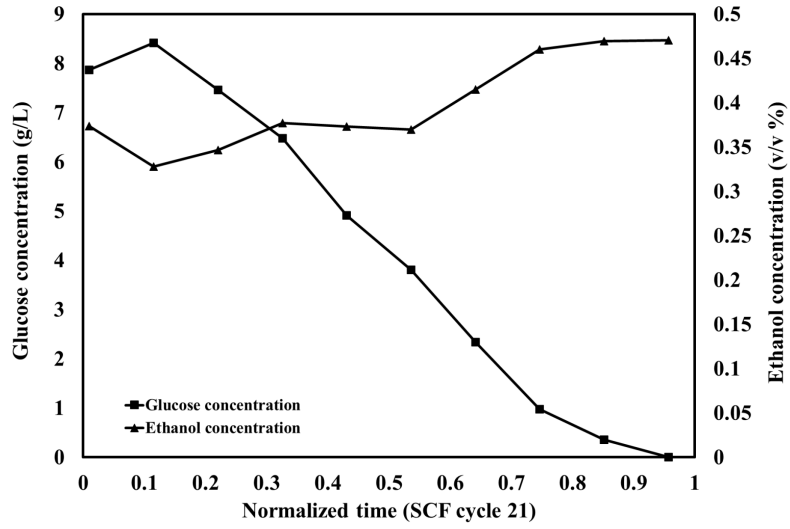


Figure A3 Glucose and ethanol concentration during SCF cycle 21. Concentrations are reported as a function of normalized cycle time (in-cycle time over total cycle time).

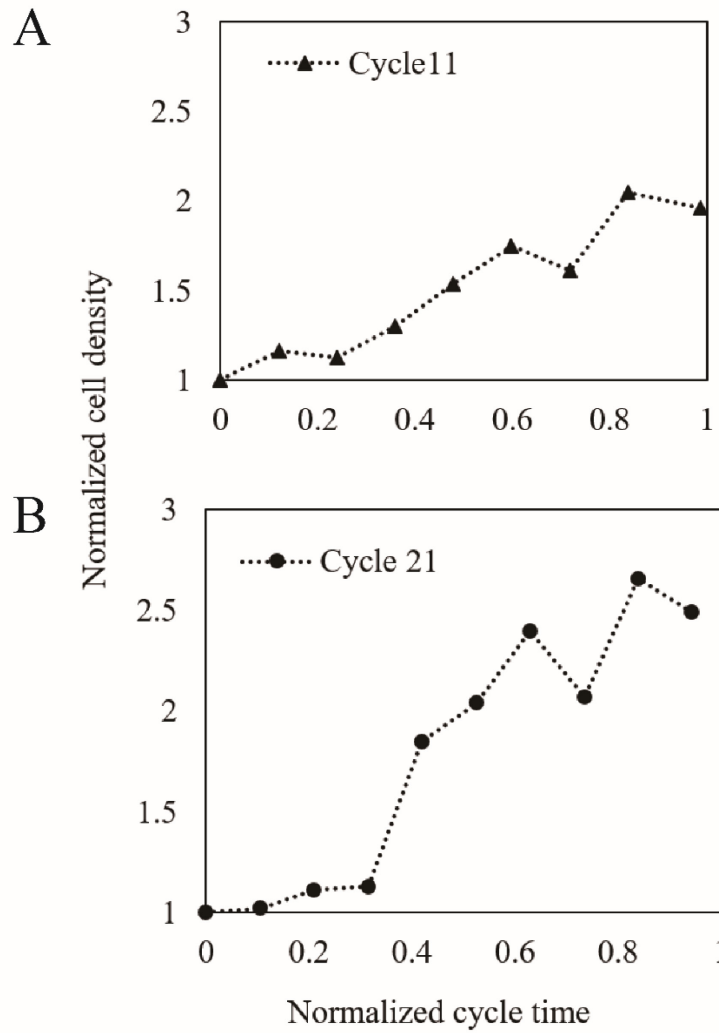


Figure A4 Intra-cycle normalized cell density during SCF cycles 11 (A) and 21 (B). Relative cell densities are reported as a function of normalized cycle time (in-cycle time over total cycle time).

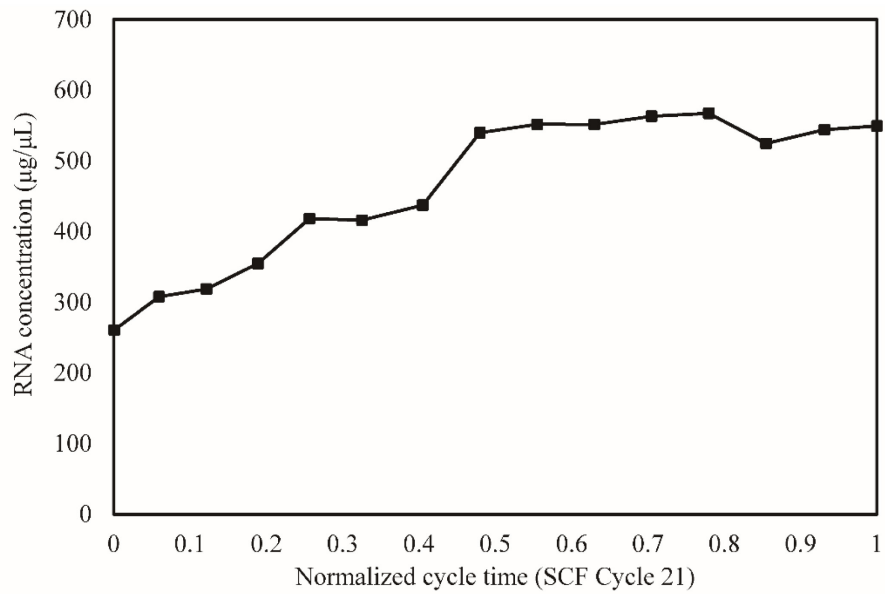


Figure A5 Total RNA concentration (after extraction) during SCF cycle 21. Total RNA was extracted from equivalent volume of cell samples and dissolved in the same amount of water. Total RNA concentrations are reported as a function of normalized cycle time (in-cycle time over total cycle time).

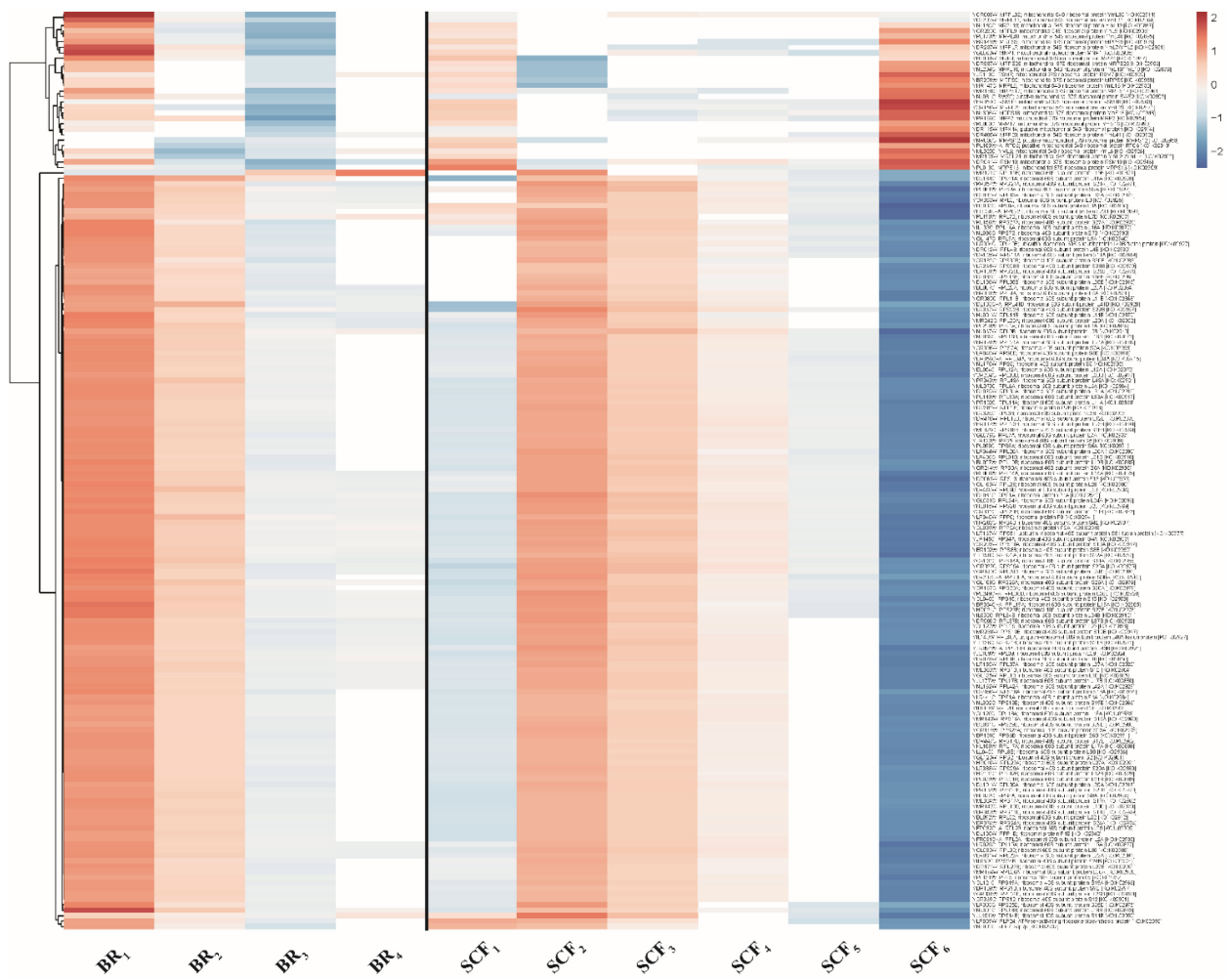


Figure A6 Relative expression levels ($\log_2(\text{FC})$) of genes related to the ribosome at different time points during BR and SCF cycle 23. The names, descriptions, and affiliations of genes related to the ribosome were retrieved from KEGG. Each column illustrates $\log_2(\text{FC})$ (with statistical significance) from DESeq2 comparison using BR₃ as reference. Normalization within each row and clustering for rows were employed. Red to white to blue represents a decreasing trend of relative expression level. Data points without statistically significant differences are colored in pure white.



Figure A7 Relative expression levels (log₂(FC)) of genes related to ribosome biogenesis at different time points during BR and SCF cycle 23. The names, descriptions, and affiliations of genes related to ribosome biogenesis were retrieved from KEGG. Each column illustrates log₂(FC) (with statistical significance) from DESeq2 comparison using BR₃ as reference. Normalization within each row and clustering for rows were employed. Red to white to blue represents a decreasing trend of relative expression level. Data points without statistically significant differences are colored in pure white.

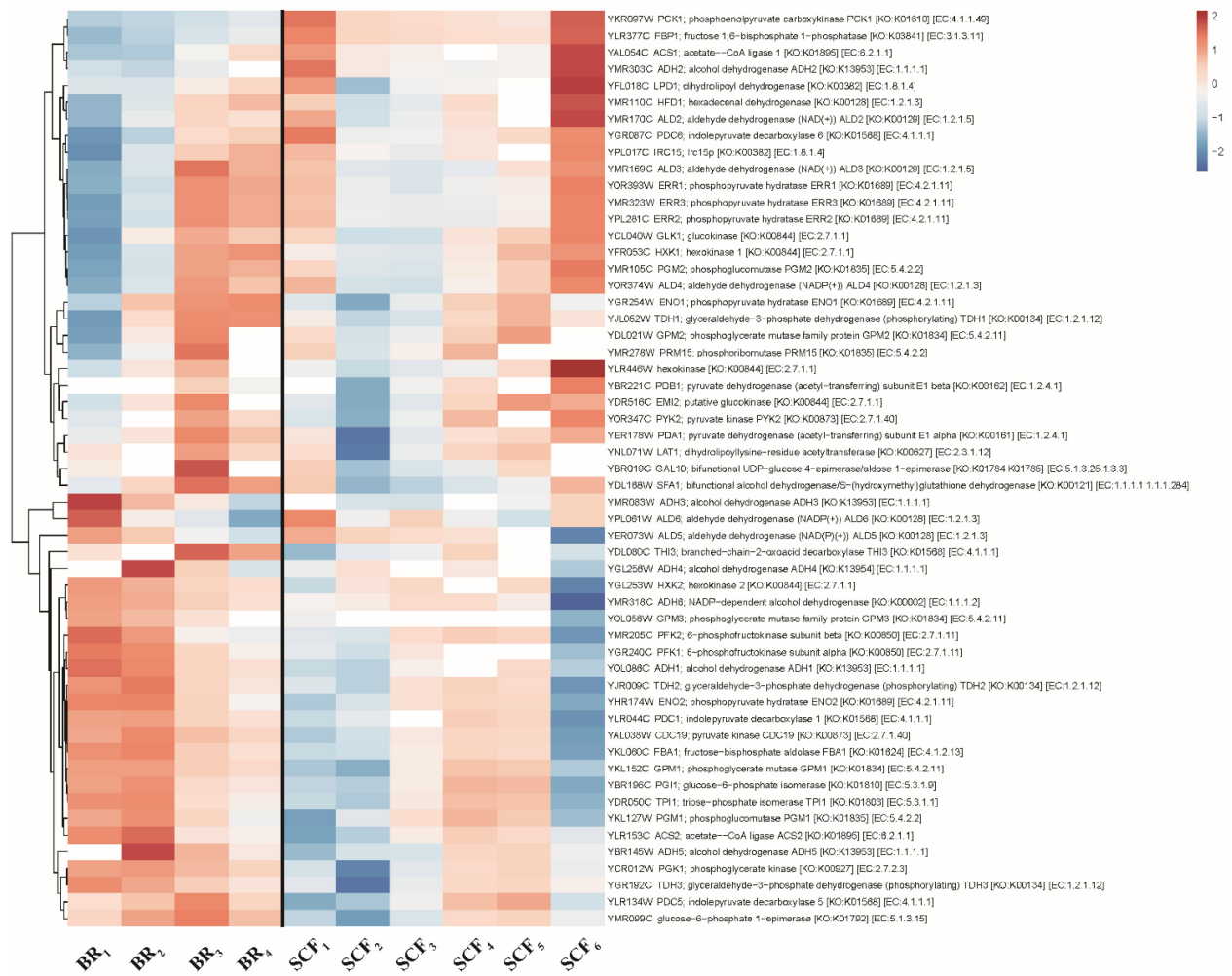


Figure A8 Relative expression levels ($\log_2(\text{FC})$) of genes related to glycolysis and gluconeogenesis at different time points during BR and SCF cycle 23. The names, descriptions, and affiliations of genes related to glycolysis and gluconeogenesis were retrieved from KEGG. Each column illustrates $\log_2(\text{FC})$ (with statistical significance) from DESeq2 comparison using BR₃ as reference. Normalization within each row and clustering for rows were employed. Red to white to blue represents a decreasing trend of relative expression level. Data points without statistically significant differences are colored in pure white.

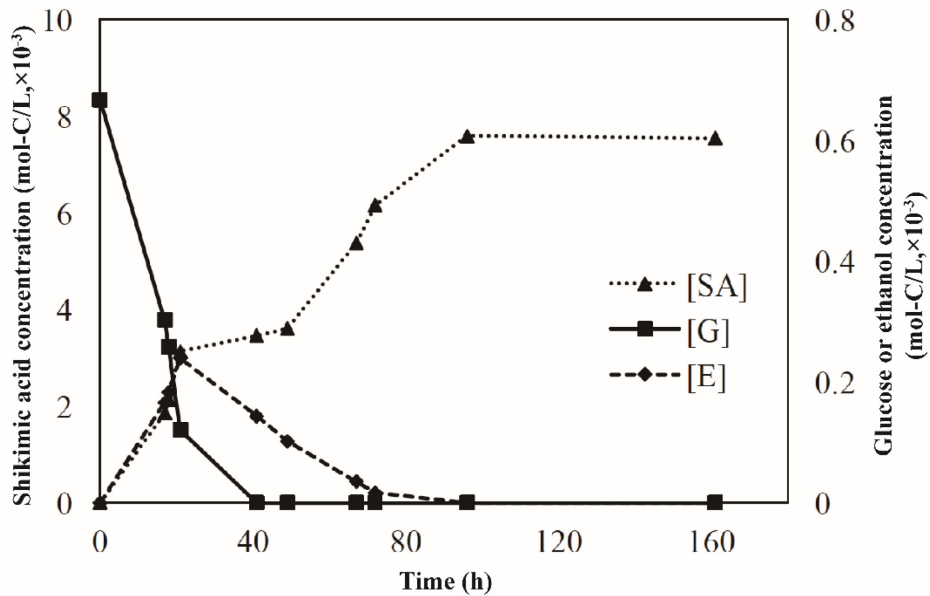


Figure A9 Shikimic acid, glucose, and ethanol concentration during extended BR operation. Concentrations are all presented in mol carbon per liter.

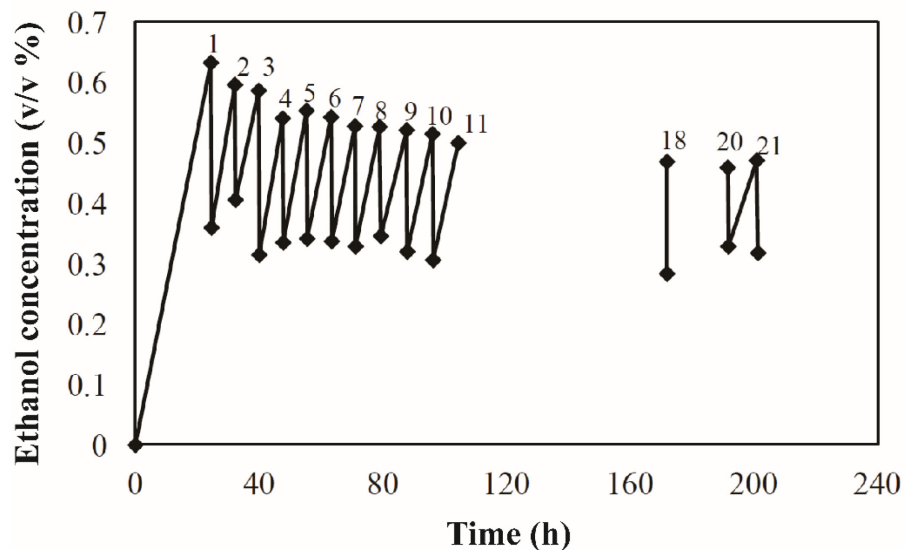


Figure A10 Ethanol concentration measured at the start and the end of the cycles during SCF operation. Cycle numbers are shown by the end of each cycle.

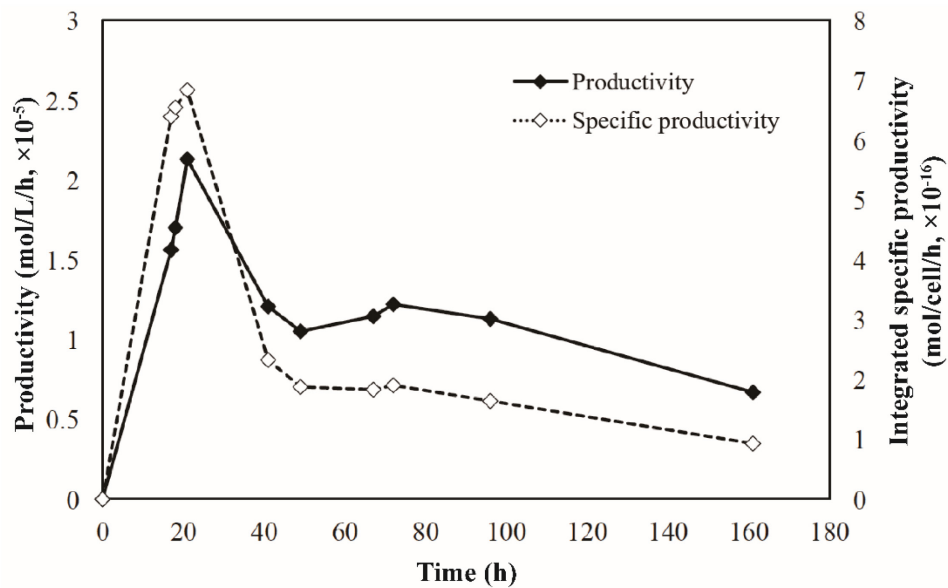


Figure A11 Productivity and integrated specific productivity of shikimic acid during extended BR operation.

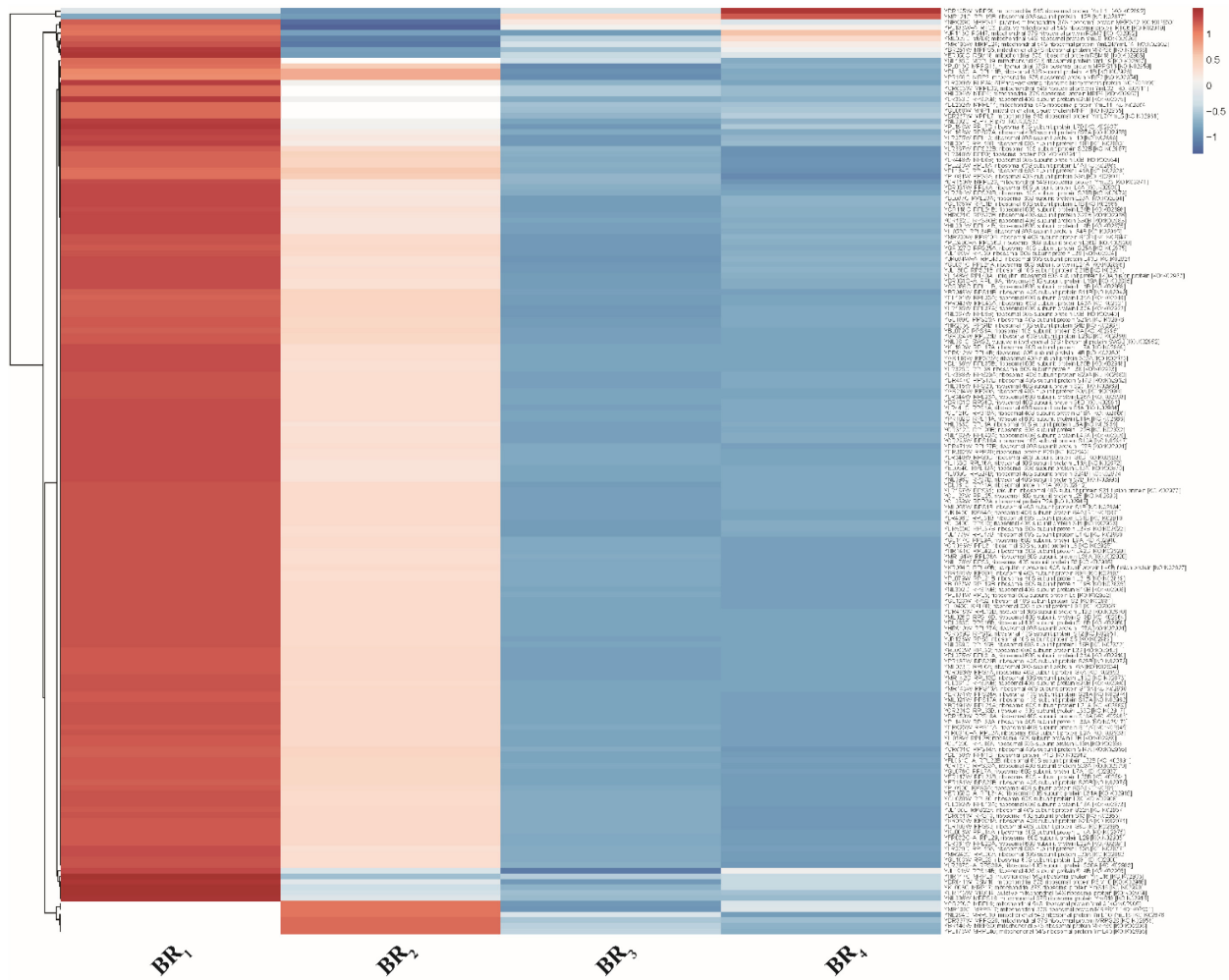


Figure A12 Relative expression levels ($\log_2(\text{FC})$) for genes related to the ribosome at different time points during late-log phase and diauxic shift in BR. The names, descriptions, and affiliations of genes related to the ribosome were retrieved from KEGG. Each column illustrates $\log_2(\text{FC})$ (with statistical significance) from DESeq2 comparison using an external sampling point SCF₆ as reference. Normalization within each row and clustering for rows were employed. Red to white to blue represents a decreasing trend of relative expression level. Data points without statistically significant differences are colored in pure white.

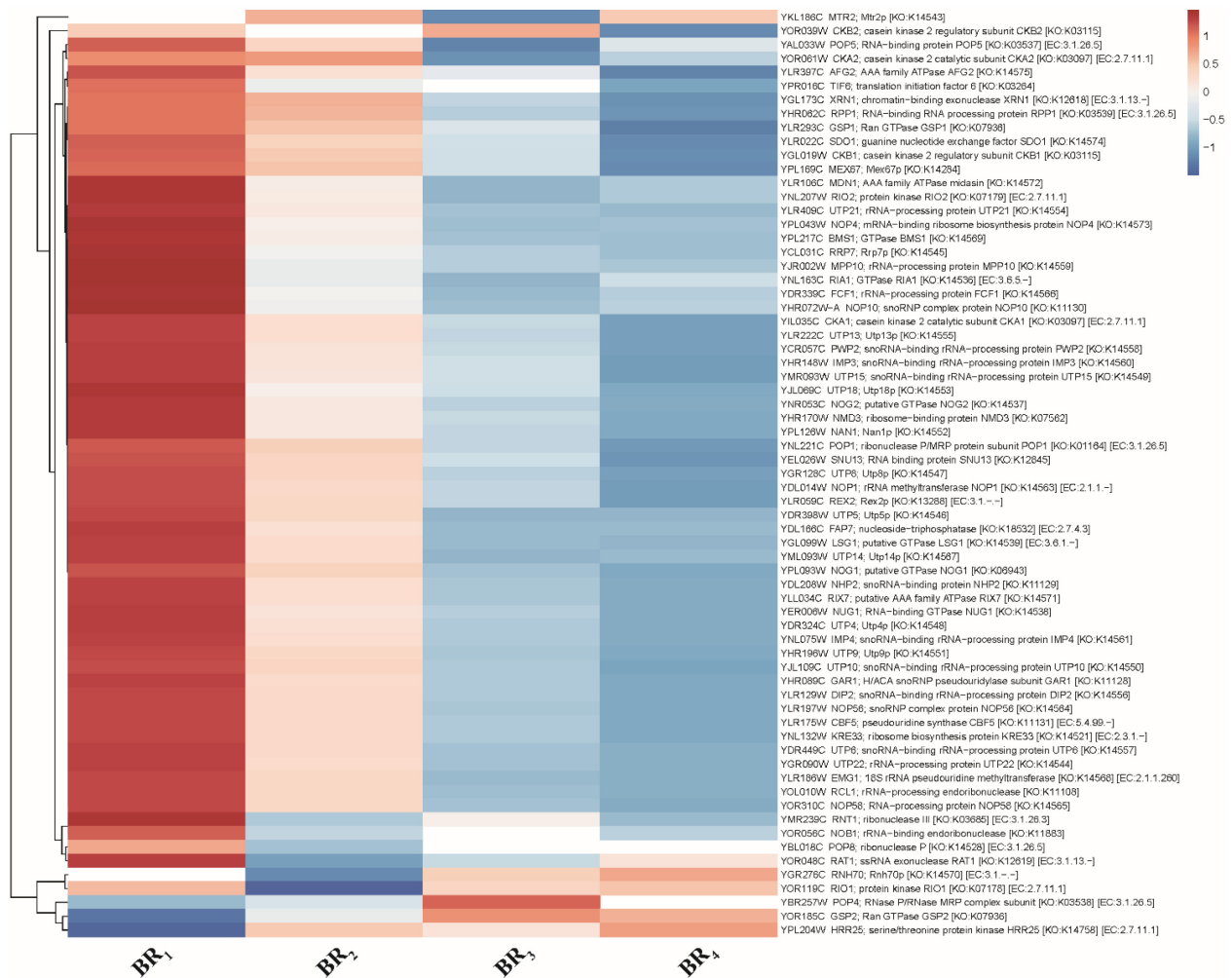


Figure A13 Relative expression levels ($\log_2(\text{FC})$) for genes related to ribosome biogenesis at different time points during late-log phase and diauxic shift in BR. The names, descriptions, and affiliations of genes related to ribosome biogenesis were retrieved from KEGG. Each column illustrates $\log_2(\text{FC})$ (with statistical significance) from DESeq2 comparison using an external sampling point SCF₆ as reference. Normalization within each row and clustering for rows were employed. Red to white to blue represents a decreasing trend of relative expression level. Data points without statistically significant differences are colored in pure white.

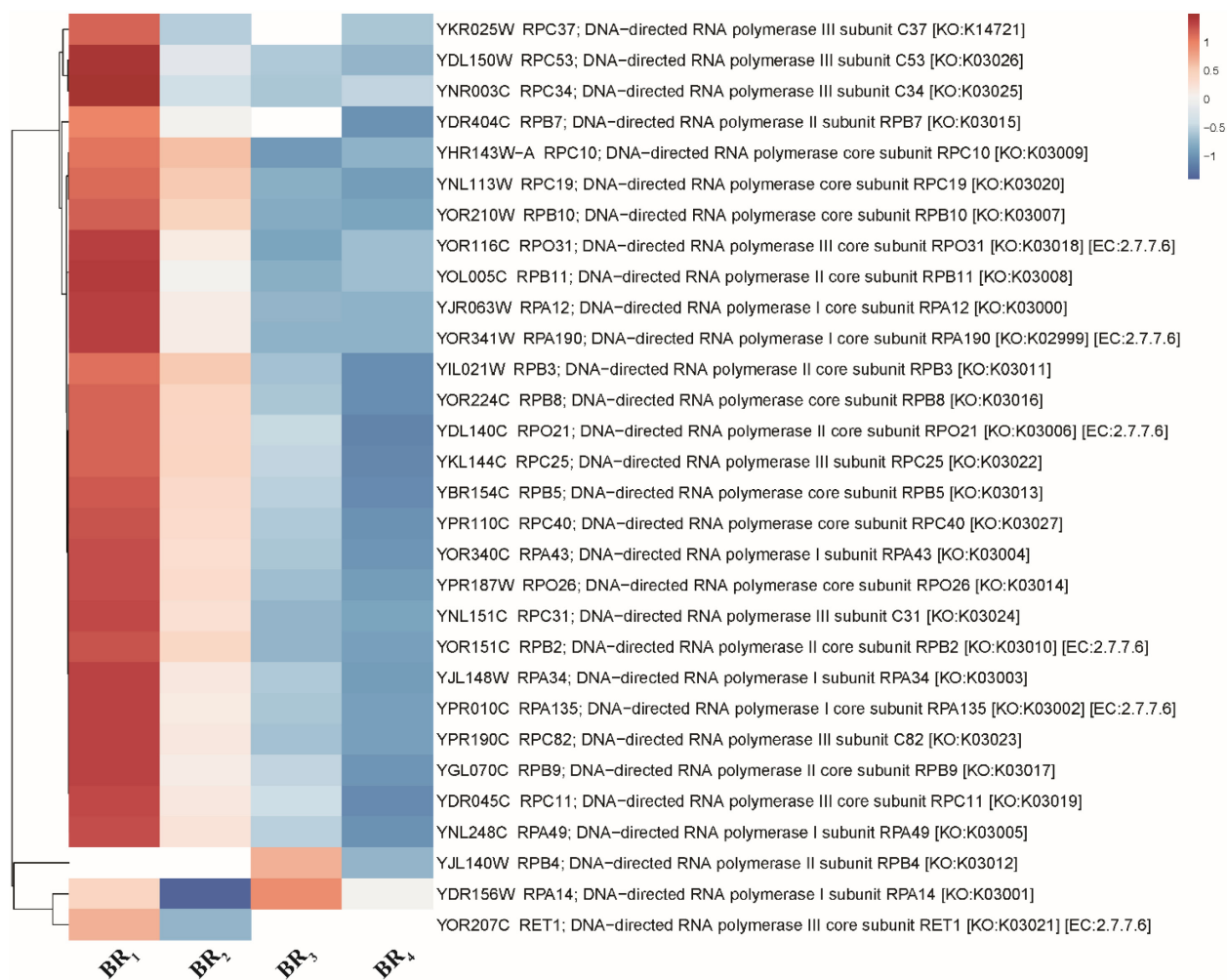


Figure A14 Relative expression levels ($\log_2(\text{FC})$) for genes related to RNA polymerase at different time points during late-log phase and diauxic shift in BR. The names, descriptions, and affiliations of genes related to RNA polymerase were retrieved from KEGG. Each column illustrates $\log_2(\text{FC})$ (with statistical significance) from DESeq2 comparison using an external sampling point SCF_6 as reference. Normalization within each row and clustering for rows were employed. Red to white to blue represents a decreasing trend of relative expression level. Data points without statistically significant differences are colored in pure white.

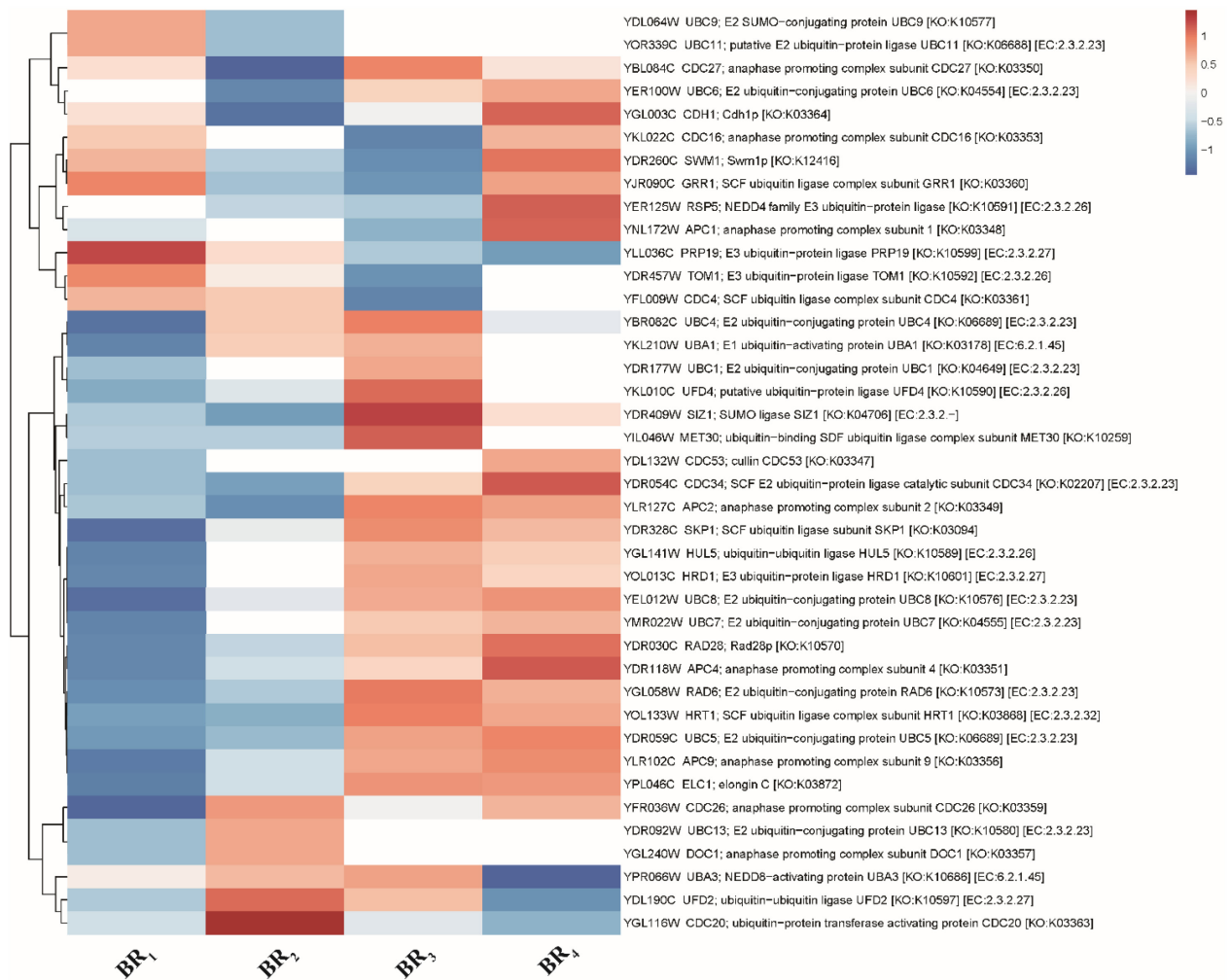


Figure A15 Relative expression levels ($\log_2(\text{FC})$) for genes related to ubiquitin-mediated proteolysis at different time points during late-log phase and diauxic shift in BR. The names, descriptions, and affiliations of genes related to ubiquitin-mediated proteolysis were retrieved from KEGG. Each column illustrates $\log_2(\text{FC})$ (with statistical significance) from DESeq2 comparison using an external sampling point SCF₆ as reference. Normalization within each row and clustering for rows were employed. Red to white to blue represents a decreasing trend of relative expression level. Data points without statistically significant differences are colored in pure white.

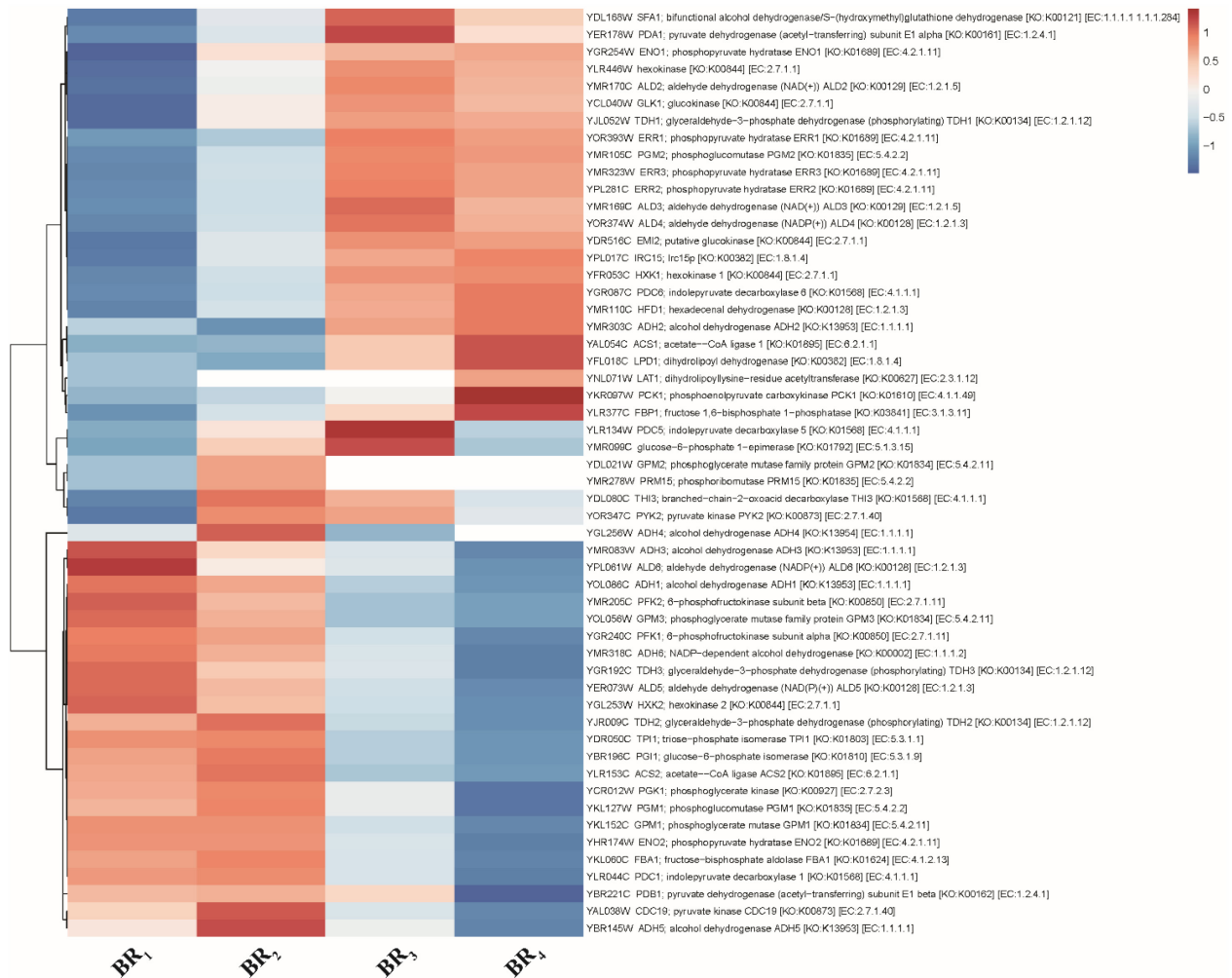


Figure A16 Relative expression levels ($\log_2(\text{FC})$) for genes related to glycolysis and gluconeogenesis at different time points during late-log phase and diauxic shift in BR. The names, descriptions, and affiliations of genes related to glycolysis and gluconeogenesis were retrieved from KEGG. Each column illustrates $\log_2(\text{FC})$ (with statistical significance) from DESeq2 comparison using an external sampling point SCF₆ as reference. Normalization within each row and clustering for rows were employed. Red to white to blue represents a decreasing trend of relative expression level. Data points without statistically significant differences are colored in pure white.

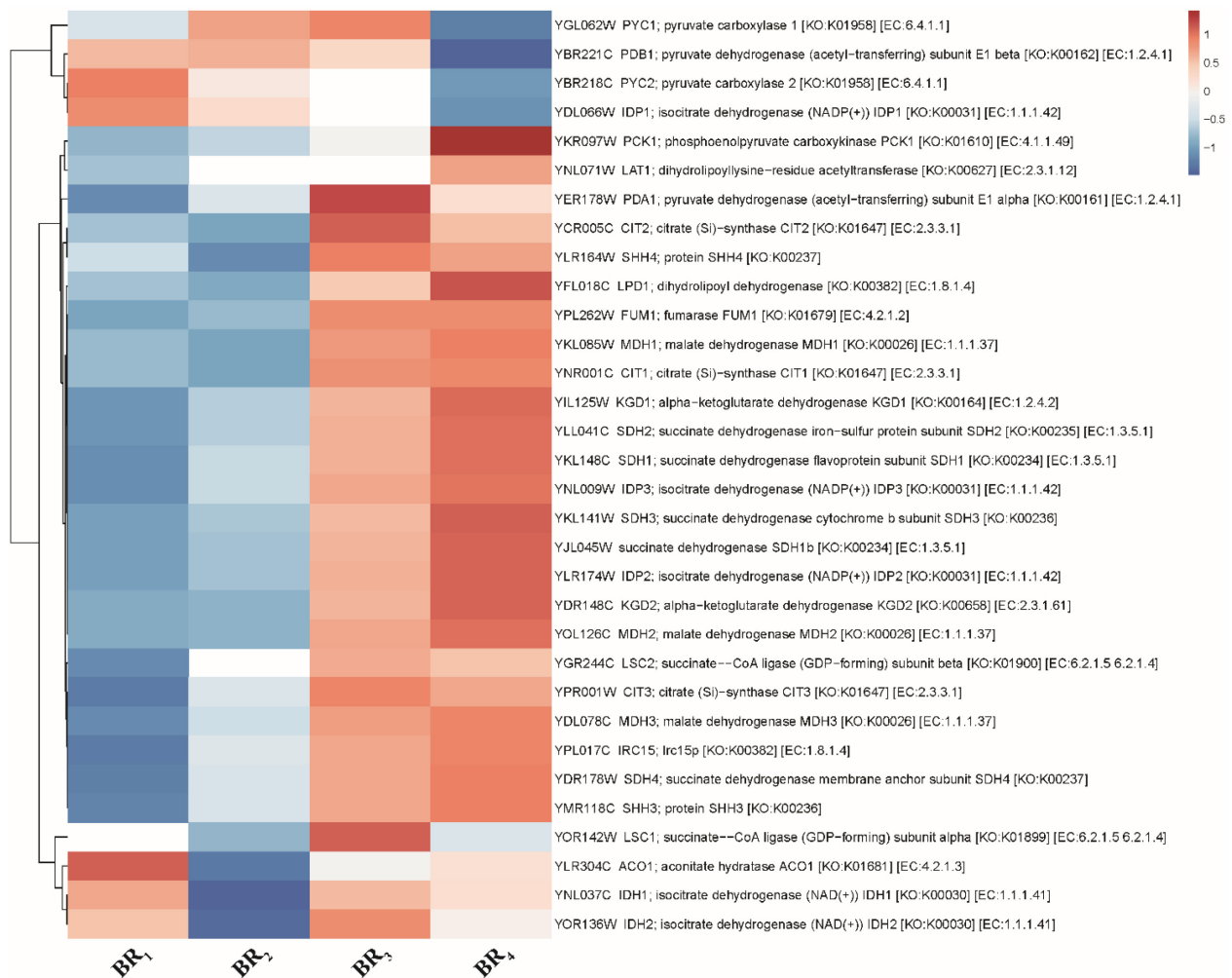


Figure A17 Relative expression levels (log₂(FC)) for genes related to the citrate cycle at different time points during late-log phase and diauxic shift in BR. The names, descriptions, and affiliations of genes related to the citrate cycle were retrieved from KEGG. Each column illustrates log₂(FC) (with statistical significance) from DESeq2 comparison using an external sampling point SCF₆ as reference. Normalization within each row and clustering for rows were employed. Red to white to blue represents a decreasing trend of relative expression level. Data points without statistically significant differences are colored in pure white.

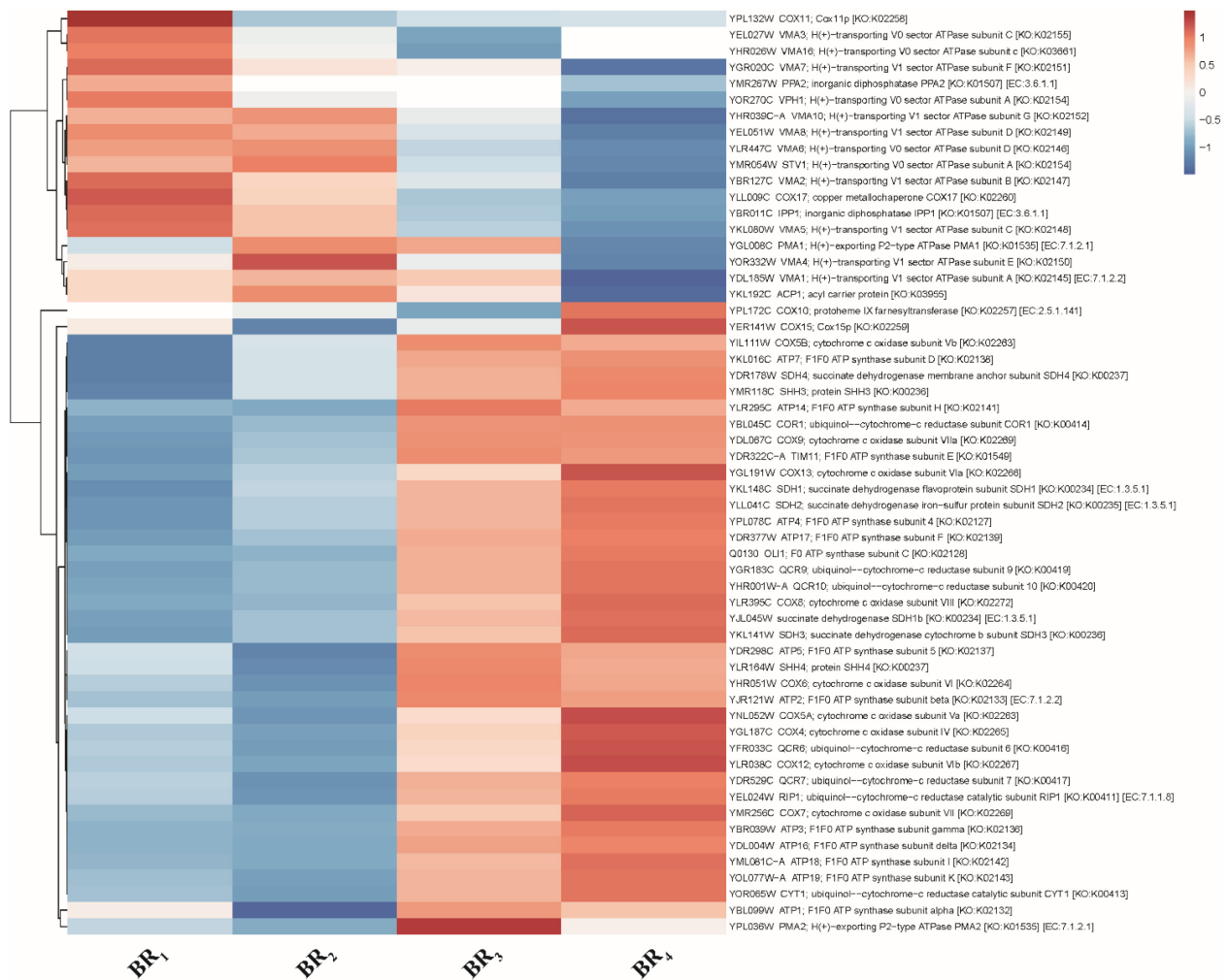


Figure A18 Relative expression levels ($\log_2(\text{FC})$) for genes related to oxidative phosphorylation at different time points during late-log phase and diauxic shift in BR. The names, descriptions, and affiliations of genes related to oxidative phosphorylation were retrieved from KEGG. Each column illustrates $\log_2(\text{FC})$ (with statistical significance) from DESeq2 comparison using an external sampling point SCF₆ as reference. Normalization within each row and clustering for rows were employed. Red to white to blue represents a decreasing trend of relative expression level. Data points without statistically significant differences are colored in pure white.

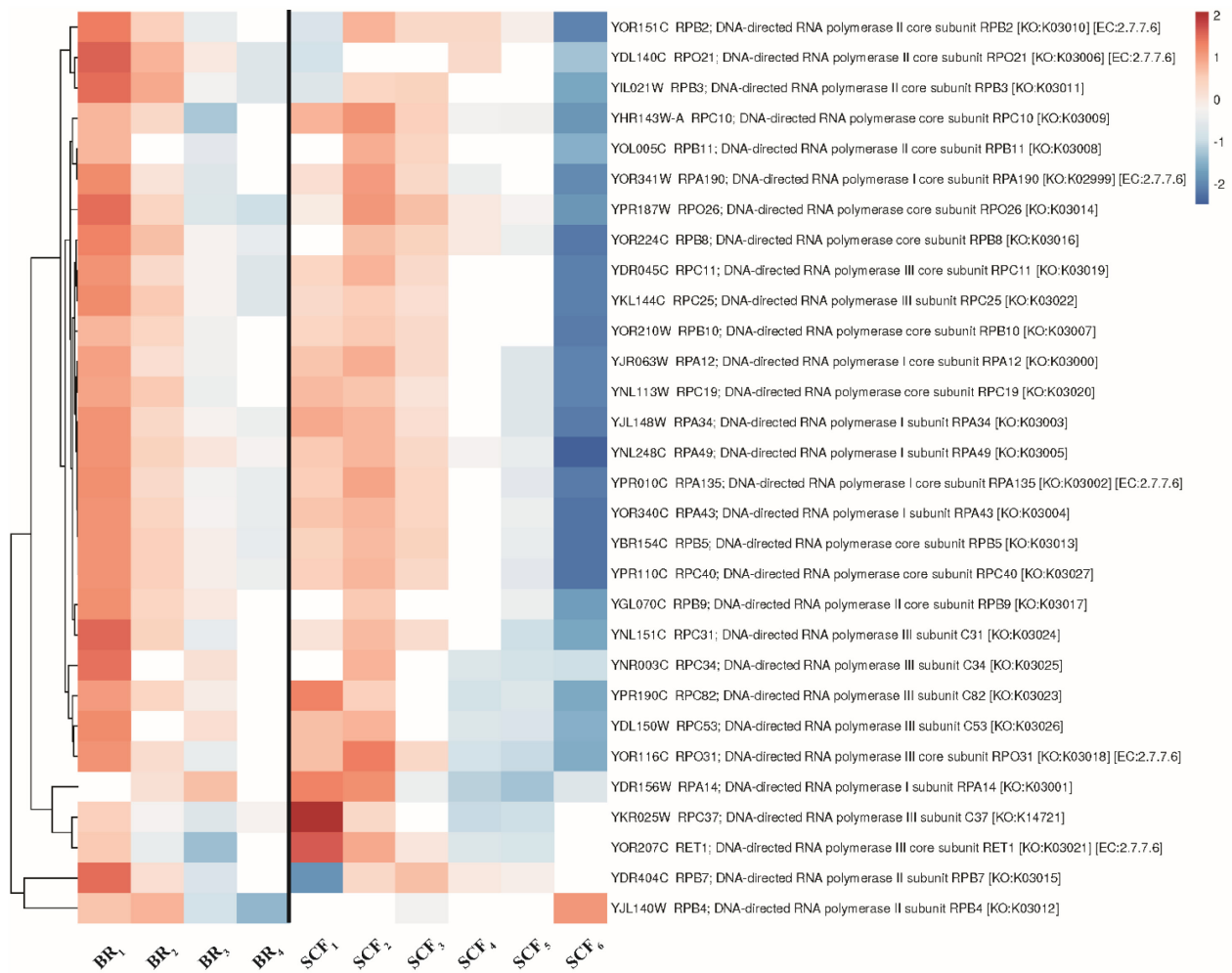


Figure A19 Relative expression levels ($\log_2(\text{FC})$) of genes related to RNA polymerase at different time points during BR and SCF cycle 23. The names, descriptions, and affiliations of genes related to RNA polymerase were retrieved from KEGG. Each column illustrates $\log_2(\text{FC})$ (with statistical significance) from DESeq2 comparison using BR₃ as reference. Normalization within each row and clustering for rows were employed. Red to white to blue represents a decreasing trend of relative expression level. Data points without statistically significant differences are colored in pure white.

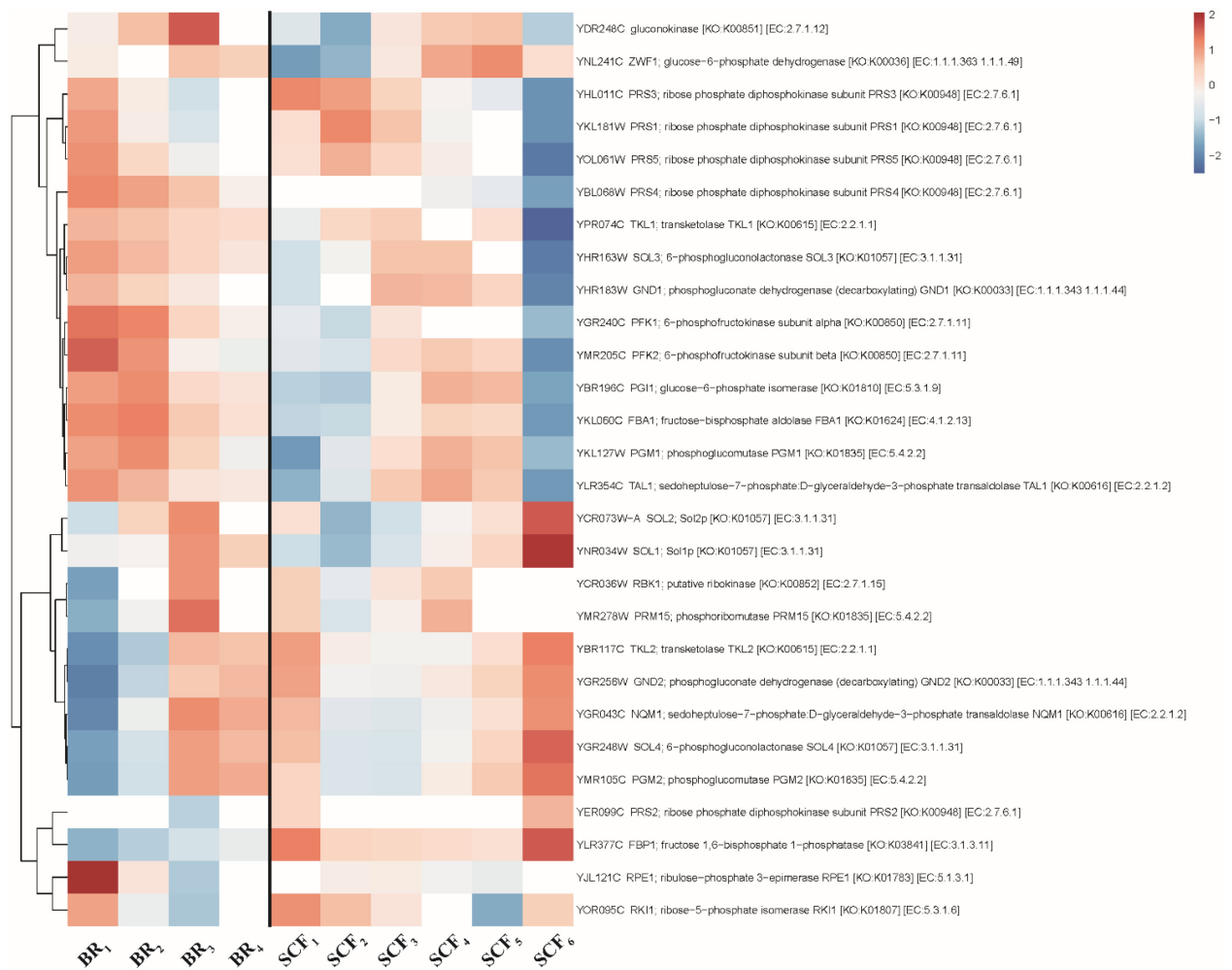


Figure A20 Relative expression levels ($\log_2(\text{FC})$) of genes related to pentose phosphate pathway at different time points during BR and SCF cycle 23. The names, descriptions, and affiliations of genes related to pentose phosphate pathway were retrieved from KEGG. Each column illustrates $\log_2(\text{FC})$ (with statistical significance) from DESeq2 comparison using BR₃ as reference. Normalization within each row and clustering for rows were employed. Red to white to blue represents a decreasing trend of relative expression level. Data points without statistically significant differences are colored in pure white.

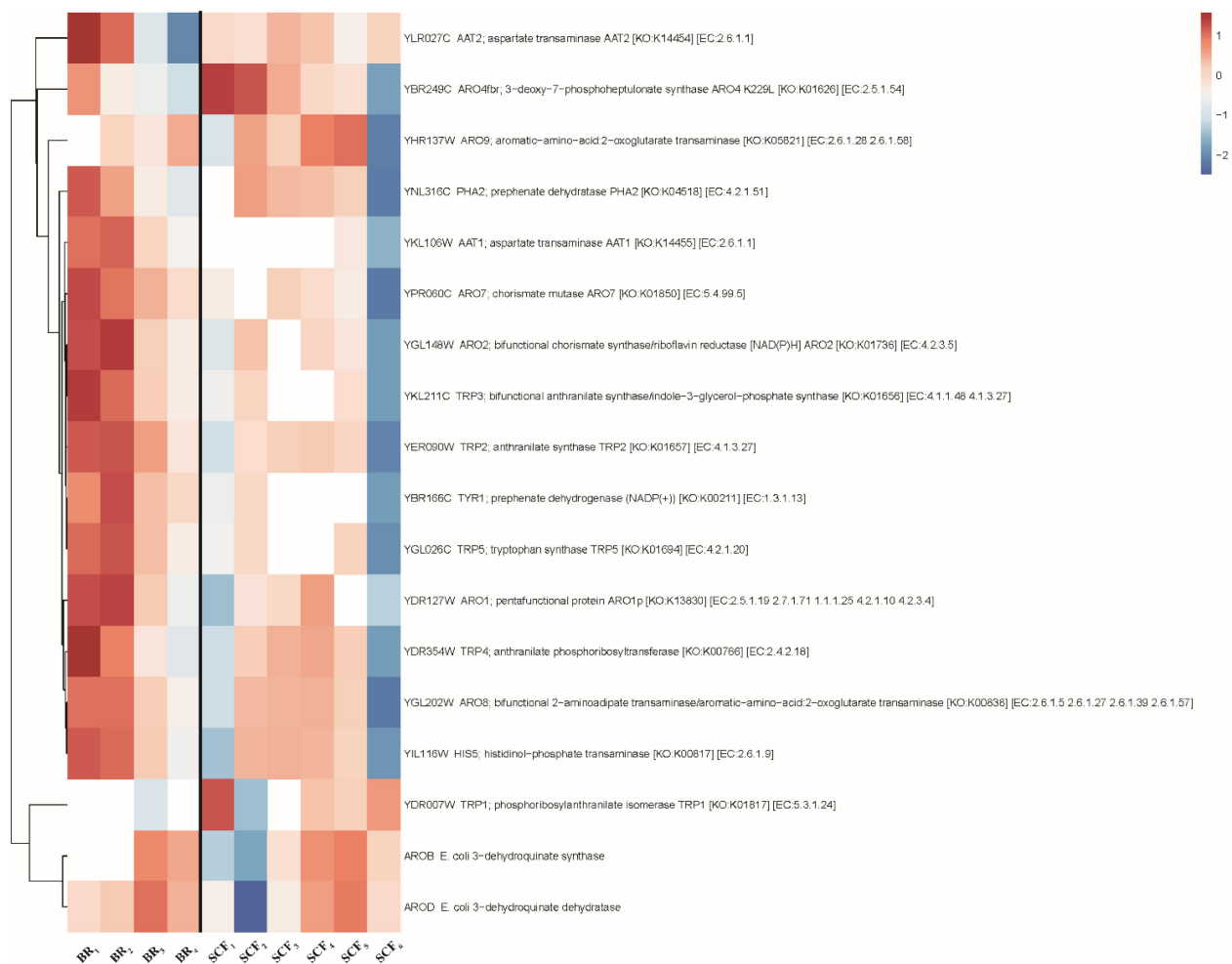


Figure A21 Relative expression levels ($\log_2(\text{FC})$) of genes related to phenylalanine, tyrosine, and tryptophan biosynthesis at different time points during BR and SCF cycle 23. The names, descriptions, and affiliations of genes related to phenylalanine, tyrosine, and tryptophan biosynthesis were retrieved from KEGG. Each column illustrates $\log_2(\text{FC})$ (with statistical significance) from DESeq2 comparison using BR₃ as reference. Normalization within each row and clustering for rows were employed. Red to white to blue represents a decreasing trend of relative expression level. Data points without statistically significant differences are colored in pure white.

A.2 References for Appendix A

Brown WA, Cooper DG (1991) Self-cycling fermentation applied to *Acinetobacter calcoaceticus* RAG-1. Appl Environ Microbiol 57:2901–2906. <https://doi.org/10.1128/aem.57.10.2901-2906.1991>

- Brown WA, Cooper DG (1992) Hydrocarbon degradation by *Acinetobacter calcoaceticus* RAG-1 using the self-cycling fermentation technique. *Biotechnol Bioeng* 40:797–805.
<https://doi.org/10.1002/bit.260400707>
- Brown WA, Cooper DG, Liss SN (1999) Adapting the self-cycling fermentor to anoxic conditions. *Environ Sci Technol* 33:1458–1463. <https://doi.org/10.1021/es980856s>
- DeRisi JL, Iyer VR, Brown PO (1997) Exploring the metabolic and genetic control of gene expression on a genomic scale. *Science* (80-) 278:680–686.
<https://doi.org/10.1126/science.278.5338.680>
- Hagman A, Säll T, Compagno C, Piskur J (2013) Yeast “make-accumulate-consume” life strategy evolved as a multi-step process that predates the whole genome duplication. *PLoS One* 8:e68734. <https://doi.org/10.1371/journal.pone.0068734>
- McCaffrey WC, Cooper DG (1995) Sophorolipids production by *Candida bombicola* using self-cycling fermentation. *J Ferment Bioeng* 79:146–151. [https://doi.org/10.1016/0922-338X\(95\)94082-3](https://doi.org/10.1016/0922-338X(95)94082-3)
- Mookerjee S (2016) Directing Precursor Flux to Optimize cis,cis-Muconic Acid Production in *Saccharomyces cerevisiae*. Concordia University
- Murphy JP, Stepanova E, Everley RA, et al (2015) Comprehensive temporal protein dynamics during the diauxic shift in *Saccharomyces cerevisiae*. *Mol Cell Proteomics* 14:2454–2465.
<https://doi.org/10.1074/mcp.M114.045849>
- Radonjic M, Andrau JC, Lijnzaad P, et al (2005) Genome-wide analyses reveal RNA polymerase II located upstream of genes poised for rapid response upon *S. cerevisiae* stationary phase exit. *Mol Cell* 18:171–183. <https://doi.org/10.1016/j.molcel.2005.03.010>
- Sarkis BE, Cooper DG (1994) Biodegradation of aromatic compounds in a self-cycling fermenter (SCF). *Can J Chem Eng* 72:874–880. <https://doi.org/10.1002/cjce.5450720514>
- Sauvageau D, Storms Z, Cooper DG (2010) Synchronized populations of *Escherichia coli* using simplified self-cycling fermentation. *J Biotechnol* 149:67–73.
<https://doi.org/10.1016/j.jbiotec.2010.06.018>
- Sheppard JD (1993) Improved volume control for self-cycling fermentations. *Can J Chem Eng*

71:426–430. <https://doi.org/10.1002/cjce.5450710312>

Sheppard JD, Cooper DG (1991) The response of *Bacillus subtilis* ATCC 21332 to manganese during continuous-phased growth. *Appl Microbiol Biotechnol* 35:72–76.
<https://doi.org/10.1007/BF00180639>

Storms ZJ, Brown T, Sauvageau D, Cooper DG (2012) Self-cycling operation increases productivity of recombinant protein in *Escherichia coli*. *Biotechnol Bioeng* 109:2262–2270.
<https://doi.org/10.1002/bit.24492>

van Walsum GP, Cooper DG (1993) Self-cycling fermentation in a stirred tank reactor. *Biotechnol Bioeng* 42:1175–1180. <https://doi.org/10.1002/bit.260421007>

Wentworth SD, Cooper DG (1996) Self-cycling fermentation of a citric acid producing strain of *Candida lipolytica*. *J Ferment Bioeng* 81:400–405. [https://doi.org/10.1016/0922-338X\(96\)85140-3](https://doi.org/10.1016/0922-338X(96)85140-3)

Zenaitis MG, Cooper DG (1994) Antibiotic production by *Streptomyces aureofaciens* using self-cycling fermentation. *Biotechnol Bioeng* 44:1331–1336.
<https://doi.org/10.1002/bit.260441109>

Appendix B Supplementary Materials for Chapter 5

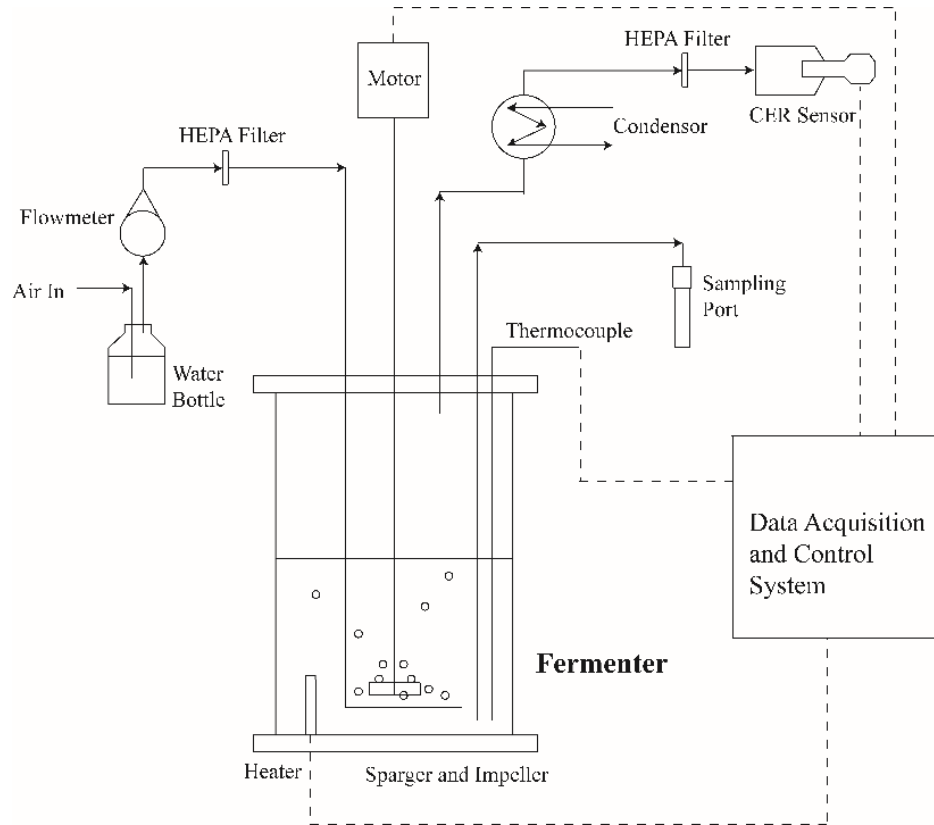


Figure B1 Schematic of the batch reactor configuration used for this study.

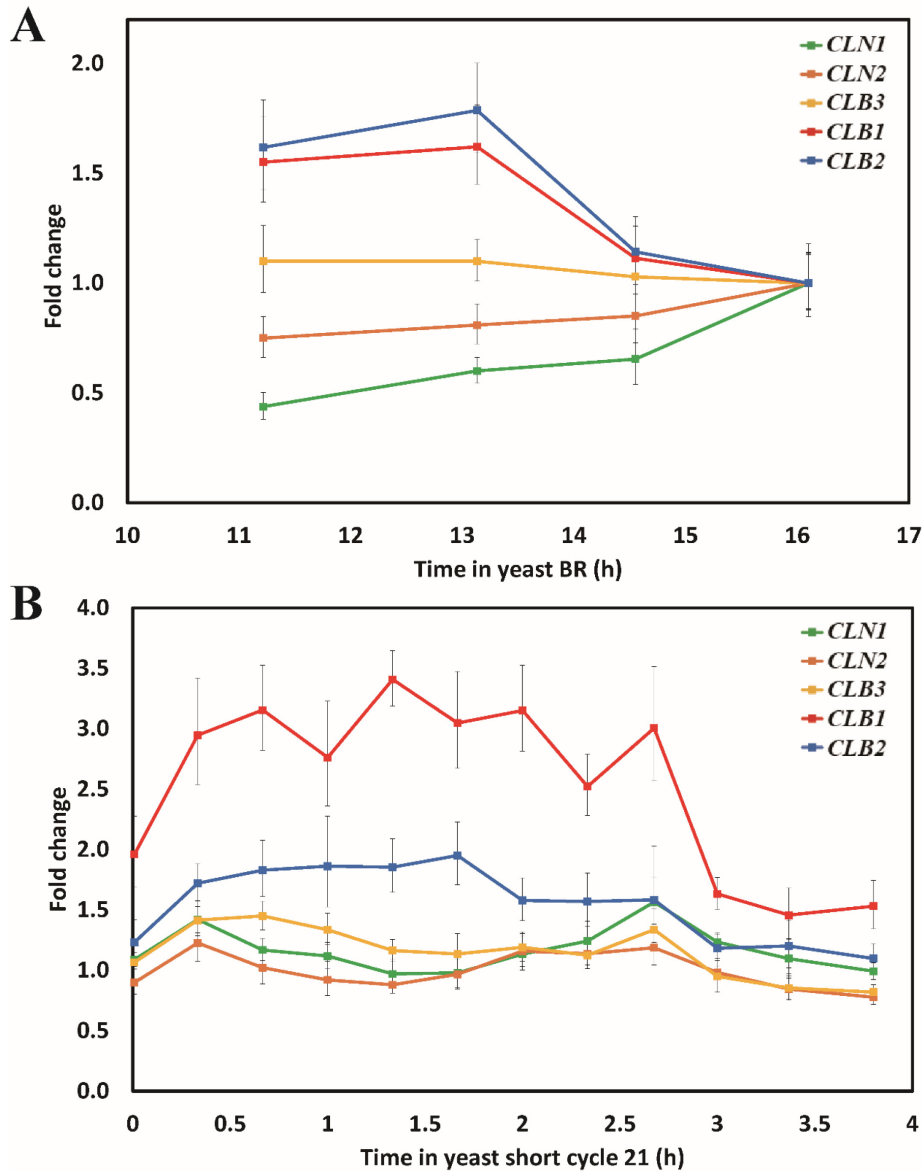


Figure B2 Relative expression levels of selected *S. cerevisiae* cyclin genes in replicated experiments. A) fold changes of *CLN1*, *CLN2*, *CLB3*, *CLB1*, and *CLB2* during BR late-log phase. B) fold changes of the same cycling genes during SCF short cycle 21. *ACT1* and *ALG9* were used as reference genes, and a sample collected at 16.2 h during BR was used as the reference sample. Error bars show one standard deviations (n = 3).